NASA Tech Briefs

National Aeronautics and Space Administration

Spring 1985
Volume 9 Number 1

Harnessing the Power of Space Technology for Life on Earth

What it takes to first factory

Experience.

Turning America's first permanent space station into a producing space station will take a special kind of commitment and know-how.

How can we produce purer metals, stronger alloys, create new kinds of crystals?

How do we manage five production lines and twenty experiments at the same time? And without having one project compromise another?

How do we handle and store volatile products, or products which measure 1/2500 of an inch in diameter?

These are the very questions General Electric has been working on, some of them for as long as we've been in business.

Here's a brief look at our experience, and what we can do to make America's first space station a success.

Processing metals: the new "space furnaces."

Over one hundred years of GE experimentation with electromagnetics has proved invaluable in our work with NASA.

The success of automated electromagnetic induction melting and levitation apparatus for the NASA sounding rocket program is the basis for our current work — an electromagnetic "furnace" GE is helping to prepare for a series of planned space shuttle flights in 1985.

Essentially, the shuttle experiments will involve the melting and solidification of metals and alloys

run America's in space:

by electromagnetic containerless undercooling. This has been demonstrated on earth with a sphere of molten tungsten (melting point: 6,170°F). But we've discovered in GE research labs, the electromagnetic power needed to position spheres of molten metals on earth makes their manufacturing cost prohibitive. In space, microgravity solves that problem.

What we learn in future shuttle flights will be the basis for work on the first permanent space station. We hope by then to be planning actual production of purer metals, stronger alloys, new crystals.

Growing gallium arsenide: a gold mine in space.

The benefits of gallium arsenide production in space — a potential 7,000% increase in yield, for example — are clearly astronomical. And the possibility of increasing computer chip capacities one hundredfold (and of making similar improvements in microwave and laser technologies) long ago led GE into gallium arsenide microelectronics research.

GE has prepared a concept study for NASA on automating production of gallium arsenide ingots in space. That study also addresses the feasibility of automating production of the ingots into finished and tested computer chips ready for use when they arrive on earth.

Manufacturing products in space for use on earth.

The part GE has already played in making it possible to manufacture space-made products for use on earth is similar to the part we will play on the "producing" end of the permanent space station.

In 1978, we began basic development of the apparatus for manufacturing latex microspheres 1/2500 of an inch in diameter — the most perfectly uniform spheres ever made, and impossible to make on earth (18,000 microspheres can fit on the head of a pin).

The apparatus GE designed and built worked successfully on all four 1982 and 1983 shuttle flights.

NASA has turned the latex microspheres over to the Bureau of Standards for packaging and sale.

So far, a university and various businesses in health and microscopy are interested in the first products manufactured in space.

Improving life on earth by manufacturing in space.

By creating a space station designed to produce a diversity of products such as purer vaccines, new drugs, stronger self-lubricating metals, new alloys which cannot be made on earth (400 have been identified so far), NASA will be helping to improve our life on earth. The value of such work to all of us is incalculable.

General Electric has both experience and commitment. As one of the world's largest diversified manufacturers, with an annual R&D budget larger than those of many countries, we will build on GE experience with all the technology, ingenuity, and determination we have to make America's first permanent space station a productive national asset.

Space Systems Division, Valley Forge, PA.

Leading from the start ... and working on the future.

Circle Reader Action No. 9

A registered trademark of General Electric Company.
162-110

Excellence

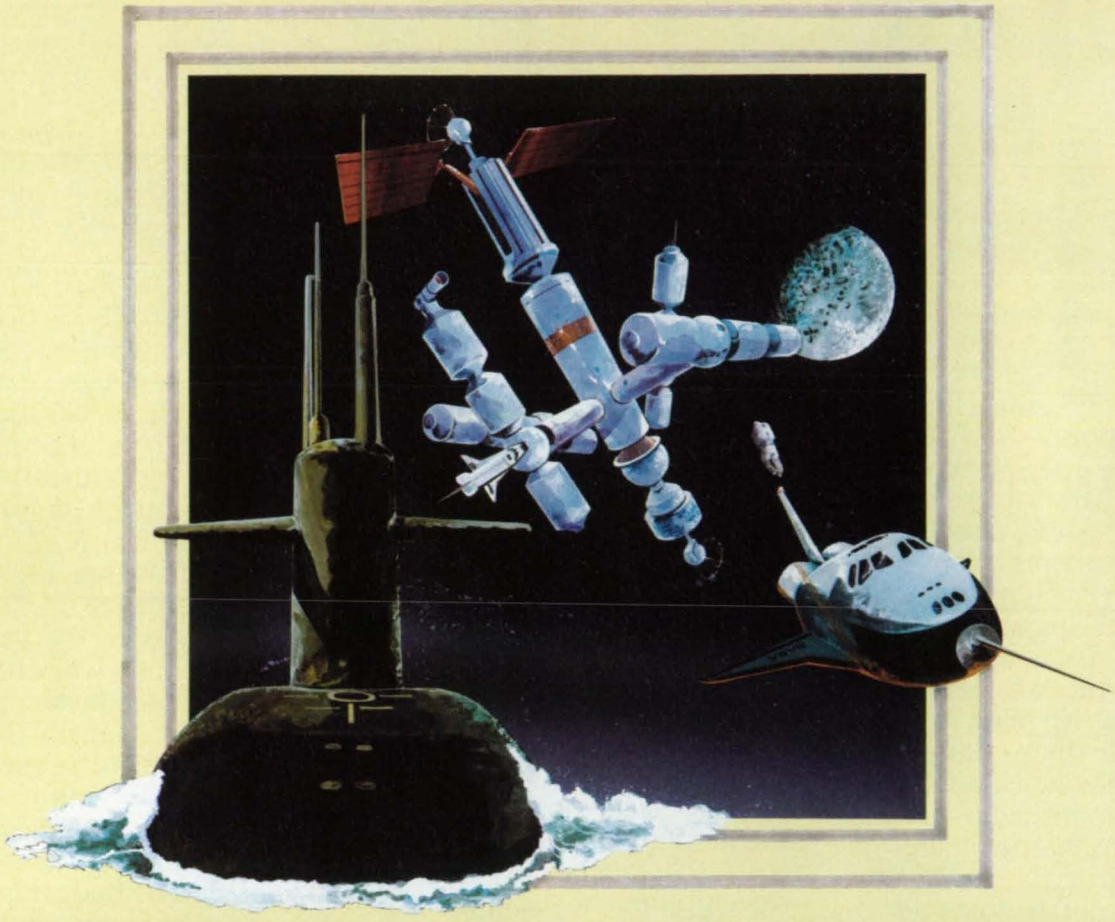

What do Space Stations and Submarines Have in Common?

Space stations will be required to be self-sufficient for long periods . . . just like submarines. Vitro Corporation has long ensured the sustained on-station operation of the submarine fleet.

How does Vitro make this happen?

Full Support - Vitro provides the logistics support, maintainability support, and systems engineering necessary to keep a submarine on patrol for extended periods.

Long Experience - Vitro support capability is founded upon over 35 years of systems engineering experience. Our engineers are well-versed in the techniques that ensure optimum systems operation in a demanding environment. With over 6,200 employees, Vitro provides mission support analysis, quality assurance, software, and modern management information systems to ensure system operability.

Extensive Resources - Yes, a space station orbiting our planet and a submarine patrolling our oceans have many needs in common. Vitro has and will continue to meet those needs. Our combination of experience, technical capability, and resources is unmatched.

This capability is available to you. Vitro Corporation stands ready now to work with you to ensure a long and successful Space Station Program . . . to continue a tradition of excellence.

Vitro

CORPORATION

14000 Georgia Avenue, Silver Spring, Maryland 20910
For information call our Marketing Manager, (301) 231-1300

Circle Reader Action No. 19

NASA Tech Briefs

National Aeronautics and Space Administration

SPRING 1985
Volume 9
Number 1

NASA Tech Briefs:

Published by:
Associated Business Publications
Editor-in-Chief/Publisher: **Bill Schnirring**
Managing Editor: **Rita Nothaft**
Assistant Editors: **Judith Mann, Gina Brandt**
Creative Director: **Virginia Ferrara**
Associate Art Director: **Michael Binkley**
Production Manager: **Joy Larios Hickey**
Traffic Manager: **Jack Doxey**
Circulation Manager: **Anita Weissman**
Fulfillment Manager: **Elizabeth Kuzio**
Controller: **Neil B. Rose**

Technical Staff:
Briefs prepared for National Aeronautics and Space Administration by **Logical Technical Services Corp.**:
Technical Editor: **Jay Kirschenbaum**
Art Director: **Ernest Gillespie**
Managing Editors: **Jerome Rosen, Ted Selinsky**
Administrator: **Agnes Chastain**
Chief Copy Editor: **Melanie Tarka**
Staff Editors: **James Boyd, Larry Grunberger, Paul Johnson, Jordan Randjelovich, George Watson**
Graphics: **Andrew Abramoske, Luis Martinez, Huburn Profitt**
Editorial & Production: **Camille McQueen, Trudy Cavallo, Sabrina Gibson, Henry Lai, Frank Ponce, Joe Renzler, Elizabeth Texeira**

NASA:
NASA Tech Briefs are provided by the National Aeronautics and Space Administration, Technology Transfer Division, Washington, DC:
Administrator: **James M. Beggs**
Assistant Administrator for Commercial Programs: **Isaac T. Gillam IV**
Deputy Administrator for Commercial Programs: **L.J. Evans, Jr.**
Publications Manager: **Leonard A. Ault.**

Advertising: (212) 490-3999
Vice President—Sales: **Wayne Pierce**
Sales Manager: **Robin DuCharme**
Account Executive: **Robert Bruder.**

Associated Business Publications
41 East 42nd Street, Suite 921
New York, NY 10017-5391
(212) 490-3999
President: **Bill Schnirring**
Executive Vice President: **Frank Nothaft**
Vice President—Sales: **Wayne Pierce**
Vice President: **Patricia Neri**

Charter Issue
Special Features and Departments

Editorial Notebook 7

The Space Age – An Era Of Technical Change 10
by **James M. Beggs,** NASA Administrator

Encouraging the Commercial Use of Space and NASA's Office of Commercial Programs 14
by **Isaac T. Gillam, IV** Assistant Administrator for Commercial Programs

The NASA Technology Utilization Program 20
by **Len Ault,** Deputy Director Technology Utilization Division

Langley – A Bridge in Time 22

Letters 164

Mission Accomplished 165

About This Publication 166

Classified Advertising 167

Advertising Index 167

ON THE FRONT COVER:

The seventh launch of the Space Shuttle, and the second lift-off of the Orbiter Challenger, took place at Kennedy Space Center on July 18, 1983. The crew included Commander Robert Crippen, the first two-time Shuttle astronaut, and Dr. Sally Ride, NASA's first woman astronaut assigned to a space mission. To protect it from the searing heat of re-entry, the shuttle is covered with heat-shield tiles, which were developed in collaboration with private industry. A re-application of tile research and development in the private sector is featured in Mission Accomplished, page 165, this issue.

Technical Section Thumb Index

NASA TU Services 28

New Product Ideas 31

Electronic Components and Circuits 36

Electronic Systems 58

Physical Sciences 72

Materials 90

Life Sciences 112

Mechanics 114

Machinery 126

Fabrication Technology 144

Mathematics and Information Sciences 154

Subject Index 160

This document was prepared under the sponsorship of the National Aeronautics and Space Administration. Neither Associated Business Publications, Inc., nor anyone acting on behalf of Associated Business Publications, Inc., nor the United States Government nor any person acting on behalf of the United States Government assumes any liability resulting from the use of the information contained in this document, or warrants that such use will be free from privately owned rights. The U. S. Government does not endorse any commercial product, process, or activity identified in this publication.

NASA Tech Briefs, copyright © 1985 in U.S., is published quarterly by Associated Business Publications, Inc. The copyrighted information does not include the individual Tech Briefs which are supplied by NASA. Editorial, sales, production and circulation offices at 41 E. 42nd Street, New York, NY 10017-5391. Subscriptions for non-qualified subscribers in the U.S., Panama Canal Zone, and Puerto Rico, $50.00 for 1 year; $100.00 for 2 years; $150 for 3 years. Single copies $15.00. Remit by check, draft, postal or express orders. Other remittances at sender's risk. Address all communications for subscriptions or circulation to NASA Tech Briefs, 41 E. 42nd Street, New York, NY 10017-5391. Application to mail at second-class postage rates is pending at New York, NY 10017 and additional mailing offices.

POSTMASTER: please send address changes to 41 E. 42nd Street, Suite 921, New York, NY 10017-5391.

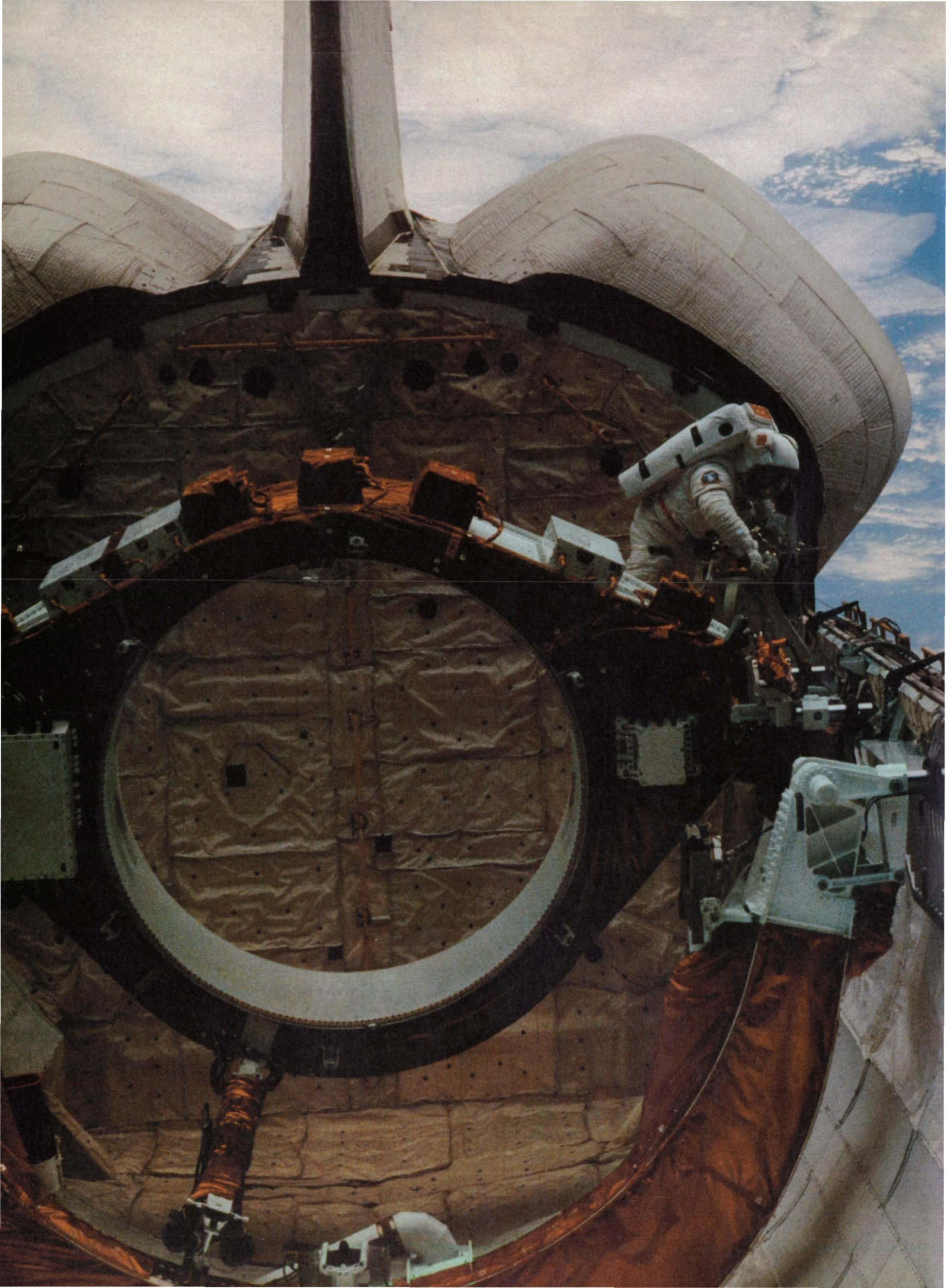

Rockwell International know-how: It goes into the Space Shuttle. It's in everything we do.

Rockwell International is NASA's prime contractor for development and production of the Space Shuttle Orbiters and for their Rocketdyne main engines.

With the know-how to combine advanced technology with outstanding engineering and management skills, we led the way in creating an entirely new capability for America's space program: providing regular access to space. Now, we're putting that proven know-how to work on the next logical step in space, NASA's earth-orbiting space station.

The space station will be used for commercial and government scientific research and development; commercial manufacture of critical materials and pharmaceuticals not available on earth; assembly, service and repair of satellites and other large structures in space; and research focused on extending man's stay time in space. It is a first step toward an even more ambitious manned space program.

The know-how that makes us leaders in America's space program goes into everything we do at Rockwell.

In electronics: where virtually every jetliner in the free world relies on one or more of our Collins avionics systems for navigation, communications, instrumentation or flight control.

In the automotive industry: where we are addressing our customers' operating need for lower cost per mile. This includes application of state-of-the-art technology in such areas as materials, manufacturing and quality control processes and innovative systems designs for both truck and trailer axles, brakes, drivelines and a wide range of components for heavy and light vehicles.

In general industries: where advancements such as electronic press controls and total production systems have made our Goss presses a world leader in offset newspaper printing.

We're a $9 billion company where science gets down to business in four diverse areas. And that diversity has helped us achieve nine consecutive years of increased earnings and impressive growth.

If you are interested in any of our products or want to learn more about us, write: Rockwell International, Department 815NT-11, 600 Grant Street, Pittsburgh, PA 15219.

Rockwell International

...where science gets down to business

Aerospace/Electronics
Automotive/General Industries

Circle Reader Action No. 18

THE HEREAFTER NAMED SUBSIDIARIES OF

CELLULAR RADIO SYSTEMS, INC.

SUITE 3120, 11100 E. BETHANY DR., AURORA, CO 80014
Propose to register with the
Securities and Exchange Commission

a Public Offering of $6,613,200
on Form S-1
of 1002 Jumbo Units @ $6,600 per unit
Each Jumbo Unit consisting of 6 Mini-Units,
Each Mini-Unit consisting of 1000 Shares of Common Stock, Par value $.001, 1000 Class A Warrants, 1000 Class B Warrants and one $1000 subordinated, convertible debenture.

THE OFFERING WILL BE MADE ONLY BY MEANS OF A PROSPECTUS

ANTICIPATED TIME OF OFFERING
APRIL 15, 1985

ZERO GRAVITY ENTERPRISES, INC.

The purpose of the Offering is to capitalize the Company to conduct the business of developing commercial products based on existing and future technology derived from space programs and to develop new technology under weightless environments.

Circle Reader Action No. 30

SPACE METALURGY, INC.

The purpose of the Offering is to capitalize the Company to conduct the business of commercializing existing metalurgical technology and developing new metals technology related to international aerospace activities.

Circle Reader Action No. 31

OUTER SPACE LABORATORIES, INC.

The purpose of the Offering is to capitalize the Company to conduct the business of developing products and services which can be used in governmental and private space environments and to contract for private, commercial experimentation related to space programs.

Circle Reader Action No. 32

SPACE GENETICS RESEARCH CORPORATION

The purpose of the Offering is to capitalize the Company to conduct the business of experimentation and productivity in the fields of human, animal and plant life relating to bacteriological, geobiology, aging, gene splicing, disease control, chemo-remedial chemistry and waste control.

Circle Reader Action No. 33

SPACE SHUTTLE CARGO CORPORATION

The purpose of the Offering is to capitalize the Company to conduct the business of providing international transportation systems and services related to aerospace research and development activities with governmental and private entities.

Circle Reader Action No. 34

INTERSTELLAR COMMUNICATIONS CORPORATION

The purpose of the Offering is to capitalize the Company to conduct the business of commercializing existing technology from past governmental space programs and to develop new technologies of international earth and space communications.

Circle Reader Action No. 35

Editorial Notebook

About The New NASA Tech Briefs

Thomas Hobson was the 17th century English liveryman who gave his customers the choice of renting any horse they wanted, as long as it was the horse nearest the door. Hence the term "Hobson's choice"...no choice at all. Essentially, this was The National Aeronautics and Space Administration's position as it sought to extend the dissemination of *NASA Tech Briefs* while cutting costs.

The recommendations of the President's Commission on Cost Control, better known as the Grace Commission, underscored the problem and reinforced NASA's position: smack on the horns of a dilemma.

One of the commission's cost-cutting suggestions was to charge subscriptions for appropriate government publications...among which was *NASA Tech Briefs*. When NASA surveyed you, the reader, projections showed that converting *NASA Tech Briefs* to paid subscriptions would decimate the circulation of the publication.

While NASA was and is in favor of cutting costs, one of Congress' original mandates to NASA was the widest possible dissemination of information and technology gained in the space exploration process. *NASA Tech Briefs* has been the primary medium for this dissemination, called technology transfer. Clearly, charting a course of paid subscriptions to *NASA Tech Briefs* would be inconsistent with NASA's charter.

You're holding the answer to the problem. It's the new *NASA Tech Briefs*...a joint venture between The National Aeronautics and Space Administration and Associated Business Publications, Inc. This is the first periodical partnership, if you will, between a government agency and a private sector publishing company. It's certainly appropriate that it was initiated by the organization that represents the spirit of the pioneer of the ultimate frontier...The National Aeronautics and Space Administration. We're proud to have been chosen by NASA as the partner in this launch.

In the past there has been an OMB-imposed cap of 75,000 on the *NASA Tech Briefs* mailing list, which has resulted in a waiting list that has reached as high as 12,000. I'm delighted to be able to doff that cap. Now all United States citizens qualified to make use of the technology described in *NASA Tech Briefs* are entitled to free subscriptions. Engineers, researchers, and management in small and large American businesses are among those qualified to receive *NASA Tech Briefs* free. Further qualification information is on the subscription card in the back of this and all issues of *NASA Tech Briefs*. To receive a free subscription, all you need do is fill in the card completely and drop it in the mail. Even the postage is free.

Several more benefits will result from our joint endeavour, not the least of which will be a $2,000,000 plus savings over the next five years. The reader response to NTB has been excellent over the years, but heretofore the format has not allowed for a forum in which to exchange ideas. Therefore, effective with this issue, we're instituting just that, a reader's forum in each issue where ideas, comments and suggestions will be found. Please send me yours.

We'd also like to acknowledge more of the success stories that have come about due to *NASA Tech Briefs*. While NASA publishes the annual Spinoffs every year, we feel there is room for an ongoing section in *NASA Tech Briefs* that highlights products and processes which have been developed and commercialized. NASA has published New Product Ideas for some time, and we plan to expand on the section. We'd like to hear in detail from readers who've used the new product ideas and other technologies published in *NASA Tech Briefs*.

Another of our objectives is to shed a little more light on NASA, its goals and accomplishments. As part of this process, we'll be featuring each of the ten field centers operated by NASA. We feel that with this charter commercial issue of *NASA Tech Briefs*, it is fitting to begin with the primogenitor, Langley Research Center in Hampton, Virginia.

We plan other feature articles on NASA, Space Law, Finance and the Commercialization of Space. However, with all of these additions, let me assure you that the core of the book, the briefs themselves, will not change. We will continue to publish as many and more tech briefs as before on a regular quarterly basis.

The two other changes you'll have noticed by now are the coated paper and the addition of advertising. The coated paper is part of our upgrade of the presentation of the material in NTB, and the advertising is what provides the wherewithal for all of the above.

I'd like to take a moment to discuss the advertising in *NASA Tech Briefs* with you. Certainly it's a radical departure from the previous format, and some may be surprised by its appearance. Some have questioned the appropriateness of advertising in a government periodical. I'm indebted to Robert Heinlein for "Taanstaffel," the one word answer that translates into, "There is no free lunch."

There are only four ways to fund *NASA Tech Briefs:* 1. Paid subscriptions. 2. Government subsidy. 3. Advertising. 4. A combination of two or more of the above. (I have rejected charity as a pragmatic alternative.)

A company invests a dollar in advertising to get ten back, to reach people and companies who can make use of the products or services advertised most efficiently, with the end result being the reduction in cost...for everyone's benefit. When the medium, in our case *NASA Tech Briefs*, does this efficiently and well, the advertisers repeat and we all—reader, advertiser and publication—prosper. If it doesn't, they don't and we don't. It's that simple.

Just as NASA is the symbol of the 21st century pioneer, the advertisers in this issue are pioneers. For the first time, American industry is promoting the NASA technology transfer process. These companies are not only supporting NASA's Technology Utilization program... they're part of it as they advertise their technology for dissemination to the readers of *NASA Tech Briefs*. Just as those early pioneers to The New World became the founding fathers of America, both our advertisers in this issue and you, the reader, are in a very real sense among the founding fathers of NASA's commercialization efforts. Together we are all exploring new territory and expanding existing frontiers. Please write me with your comments on our current effort and ideas for future exploration.

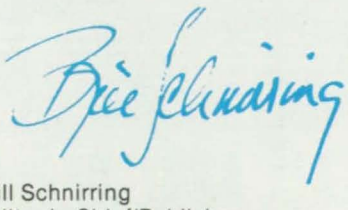

Bill Schnirring
Editor-in-Chief/Publisher

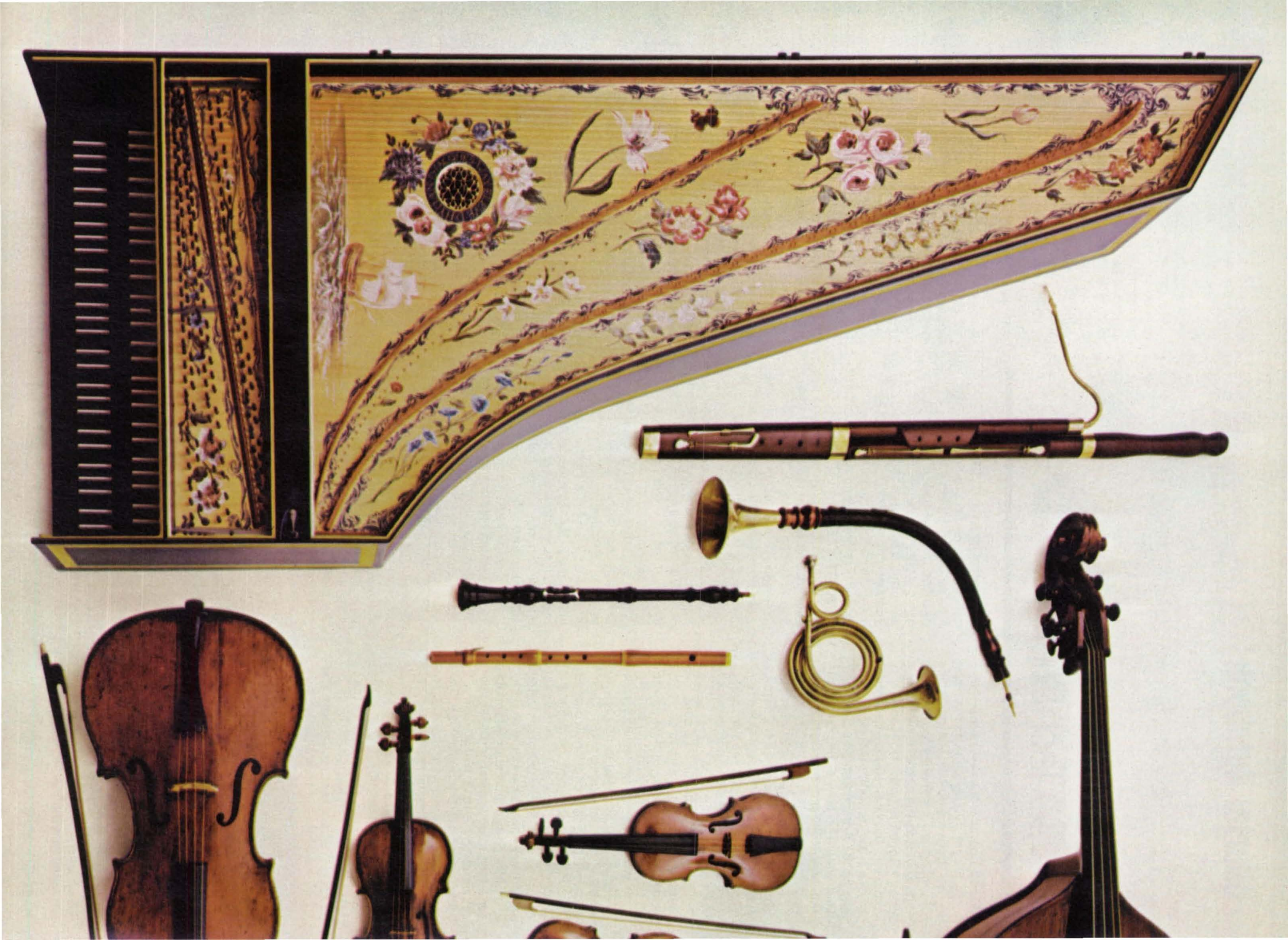

For years baroque music was composed without major change, until J.S. Bach put these instruments together in a way that set him apart.

All the baroque composers were faced with the same restrictions, the same notes, the same instruments, and the same musical forms. Yet today, we remember J.S. Bach above them all. Simply because he was able to arrange scores of music in a way no one had ever seen ... or heard before.

At IBM Federal Systems Division we know that it takes the same degree of ingenuity to design and manage within the dimensions of today's complex systems programs. It's a special ability to combine a broad range of technology — and make it work together in harmony.

And we're doing exactly that for the National Aeronautics and Space Administration's Space Shuttle program.

We've orchestrated the operations of the most sophisticated flying vehicle ever built with a team of on-board computers. And we compose software that can be tuned for each mission to make space a more available resource.

In every project we undertake, we start with a myriad of individual parts, as separate as the notes of a scale. And put them into play—together. It isn't easy. But the more complex the task, the more we manage to make it happen.

IBM®

Federal Systems Division

Circle Reader Action No. 10

The Space Age—An Era of

Not long ago, I stopped at an airport newsstand and was nearly bowled over by what I saw There were more magazines on the shelves devoted to computers and high technology than there were to cars. Could it be, I wondered, that the American love affair with the automobile has taken a back seat to a new national romance with technology? If this is true, it should not surprise us, because rapid technological change has become the hallmark of our society. We can see its effects clearly when we think about how technolgy has transformed our lives in recent time. Change is, indeed, one of the few constants in our society, and it is bound to continue to accelerate in the future.

But, as Alvin Toffler once wrote: "The problem...is not to suppress change, but to manage it." And this is the real challenge that faces us all. If technological advancements are to be productive, they must somehow be used to create new products, new processes and new jobs. This requires participation not only by the creators of the technology, but by those who can most effectively put that technology to work.

Since its inception 26 years ago, the National Aeronautics and Space Administration has vigorously pursued the goal, set forth by Congress, of realizing "the potential benefits to be gained from its aeronautical and space activities." The results of these efforts have been impressive.

Lift-off at the Kennedy Space Center, Fla., of the 51-A Space Shuttle mission. Objectives included retrieving and deploying two satellites. In addition the 3M Company's DMOS experiment (Diffusive Mixing of Organic Solutions) was installed on Discovery's mid-deck.

Technological Change

By James M. Beggs, Administrator
National Aeronautics and Space Administration

Two decades ago, NASA pioneered the technology that enabled operation of satellites in geostationary orbit, thereby building a foundation for the space communications networks that followed. Today, more than two-thirds of all overseas communication traffic is relayed by satellite and there are, additionally, a number of domestic communication satellite systems in operation. The commercial space communications industry does more than $3 billion worth of business annually and employes, directly and indirectly, more than one million people—most Americans.

The development of space-relayed communications was the first effort to commercialize space and it is, so far, the most economically successful. In coming years, however, we can expect to see much broader pursuit of commercial space opportunities.

Three areas hold great promise for the commercial use of space. The first is operating satellites for communications or for a variety of other practical applications involving observation of Earth from orbit. The second is providing services to satellite operators—building space systems, launching them, or processing and analyzing the data they supply. The third—and perhaps the most exciting—is manufacturing in orbit products that cannot be made on Earth, products that promise societal and economic benefits of immense order.

President Reagan's initiative to build a permanently manned orbital station significantly advances the prospects for space commercialization. It is a plan that builds upon the highly successful policies of earlier years, when the nation expanded and strengthened its economy through publicly-funded development of highways, railroads and airports. Initial Congressional approval of the Space Station program, now in its preliminary phases, has assured the U.S. industrial community that the government will create the foundation essential to private sector investment in space. When the Space Station is in operation in the early 1990's, it will enable government and industry to forge a new partnership toward realizing the commercial potential of the space realm.

The Space Station, however, will be much more than a place to pursue practical applications. It will be an orbital laboratory for advanced scientific and technological research; a base for more efficient operation and servicing of unmanned space systems; a facility for assembling future structures too large to be launched from Earth; and a staging area for the dramatic space ventures contemplated for tomorrow. Most importantly, it will be a symbol of American dedication to maintaining leadership in space.

Although no one can predict the future with precision, there are certain assumptions we can make about our future in space through the end of the century.

The first is that the rapid rate of technological change will result in unprecedented progress in every facet of space technology and operations.

Second, we can anticipate that the Shuttle, the permanently manned Space Station we are developing, and their related technologies will be the key to our major space operations in the scientific, commercial and industrial areas.

And third, just as advances in space technology will continue to drive our quest for knowledge in space, they will continue to benefit our lives on Earth, both directly and indirectly.

One of the greatest benefits of the space program, overall, I believe, is that it continues to push advances in science and technology on Earth. The technology we push enables us to continue to advance in such areas as computer science, solid state electronics, medical electronics and in many other fields that contribute to our individual well-being and national economic growth. As these areas and industries expand, they continue to spur the innovation, new products, new jobs and greater productivity. All of this enables us to maintain our high standard of living, to compete internationally and to build for the future.

Broad dissemination and transfer of new aerospace advances, however, is prerequisite to their effective use in the industrial marketplace. I congratulate the publisher of *NASA Tech Briefs*—Associated Business Publications, Inc.—on having been selected to assist NASA to carry on this vital function. ABP's foresight and willingness to participate at its own risk in this partnership venture is, in my view, a measure of the importance of this task and its value to industry nationwide. For only by sharing the fruits of technological achievement will we be able to stay abreast of technological change and assure maximum benefit from such endeavors.

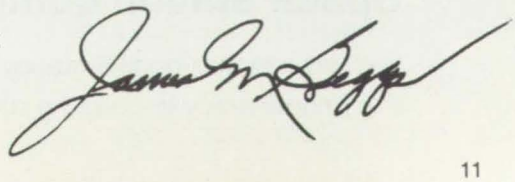

Space station communications by Motorola.

We've been making technology work reliably in space communications systems for 28 years. We're now ready to build the communications systems for NASA's new Space Station.

MOTOROLA INC.

Government Electronics Group

602/897-4623 • P.O. Box 2606. Scottsdale. AZ 85252

Circle Reader Action No. 14

Encouraging the and NASA's

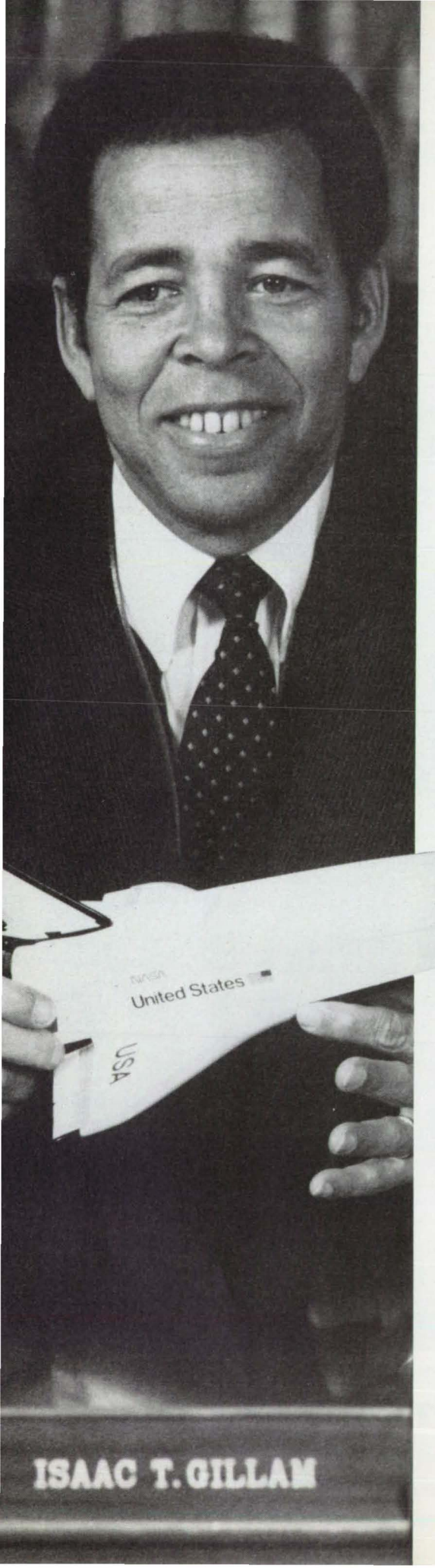

The Office of Commercial Programs serves as the focus for a NASA-wide program that is designed to reduce the technical, financial, and institutional risks of doing business in space.

In announcing the establishment of the Commercial Programs Office this past September, NASA Administrator James Beggs stated that the office "will provide a focus for efforts within NASA to expand U.S. private sector investment and involvement in civil space-related activities." The creation of the Office of Commercial Programs and the issuance of NASA's Commercial Use of Space Policy has demonstrated the agency's commitment to support the President's initiative to open the next frontier, space, to private enterprise.

Our Office is taking an active role in supporting three categories of commercial space endeavors: new commercial high technology ventures, new, applications of existing technology, and the unsubsidized transfer of existing space programs to the private sector.

A key focus of the Office of Commercial Programs is NASA support for a broad program of basic research to establish a broader and firmer foundation for commercial space ventures. This research program has been underway with the on-going NASA program in materials sciences, but more effort is needed. Our office expects to augment this effort by providing NASA assistance, in partnership with industry and the university community, to establish new research activities and programs. The basic knowledge which is the expected result of these efforts will provide the understanding of what can be done in space that cannot be done at all or as well on earth. It will also provide a better understanding of processes which can lead to improvements in earth based manufacturing processes.

We believe that the knowledge and understanding which will result from these basic research activities will be a catalyst for new ideas with increased attention being given to potential commercial uses of space. In addition, an outreach program directed at non-aerospace companies will help NASA to establish a dialogue and new relationships with those companies that may never have considered involvement in a commercial space venture.

The following are some examples of commercial space initiatives that are being managed by the Office of Commercial Programs:

• Centers for the Commercial Development of Space:

Assuring the competitiveness of U.S. companies pursuing commercial space ventures has required the science and research communities to look at accelerating the process of moving ideas developed by basic research into the marketplace. One such model for facilitating the movement of technology from the laboratory to the marketplace involves a partnership of industry, government, and universities in the establishment of joint research centers.

NASA plans to provide seed funding for three to six Centers for the Commercial Development of Space at a rate of $500K to $1M per center. At a "discussion conference" recently held at NASA Headquarters, we explained to over 200 participants from industry, universities, and other government agencies, that they serve as the foundation for strong university and industrial participation in this program.

Potential technology areas to be examined by the Centers for the Commercial Development of Space include: electronic materials, metallic alloys, glasses and ceramics, biological materials, and fluid dynamics.

• Increasing the Availability of NASA Facilities:

Perhaps the greatest barrier to undertaking a commercial space venture is the large capital costs

Commercial Use of Space
Office of Commercial Programs

by Isaac T. Gillam IV,
Assistant Administrator for Commercial Programs

associated with doing the basic and applied research. And of those capital costs, the greatest driver is the use and acquisition of NASA facilities and equiment. NASA plans to further open wider its doors to industry and university researchers seeking access to NASA's unique facilities, equipment, and personnel and expand the availability of facilities such as furnaces, drop tubes, optical fiber production devices, and automated crystal growth devices. These steps should enable industry and university researchers to consider space flight experimentation without major investments in highly specialized equipment.

One of the key NASA barometers of private sector interests in new high technology commercial space ventures is the number of existing and proposed agreements submitted by private companies interested in pursuing commercial space endeavors. NASA mechanisms such as the Joint Endeavor Agreement have been used to facilitate the demonstration of commercial applications in space technology through a NASA-Industry partnership. In processing and negotiating these agreements, the Office of Commercial Programs will take every step to avoid stifling private sector innovation and creativity by an overly cumbersome approach to proposal evaluation.

By helping to develop NASA policies which encourage the commercial use of space and by providing a single point of contact for companies interested in pursuing commercial space endeavors, we in the Office of Commercial Programs, and NASA, can help our nation realize the promise a competitive U.S. commercial space industry holds.

Inquiries or expressions of interest concerning NASA's Commercial Use of Space Program may be addressed to the Commercial Development Division (Code 1C), Office of Commercial Programs, NASA Headquarters, Washington, D.C. 20546

WHAT'S YOUR HIGH "Q"?

In precision electronic components, GAF Carbonyl Iron Powders show the outstanding performance characteristics necessary to the design of cores with high Q-values, excellent permeability, low loss factors and superior resistance to magnetic shock and temperature.

GAF Carbonyl Iron Powders also perform well in alloy production and powder metallurgy, magnetic fluid systems, inductive heating and chemical reactions (as catalysts).

GAF is the sole domestic manufacturer of Carbonyl Iron Powders in North America. For more detailed information, contact GAF Corporation, Chemical Division, 1361 Alps Road, Wayne, NJ 07470, 201 628-3000.

GAF® CARBONYL IRON POWDERS

Circle Reader Action No. 8

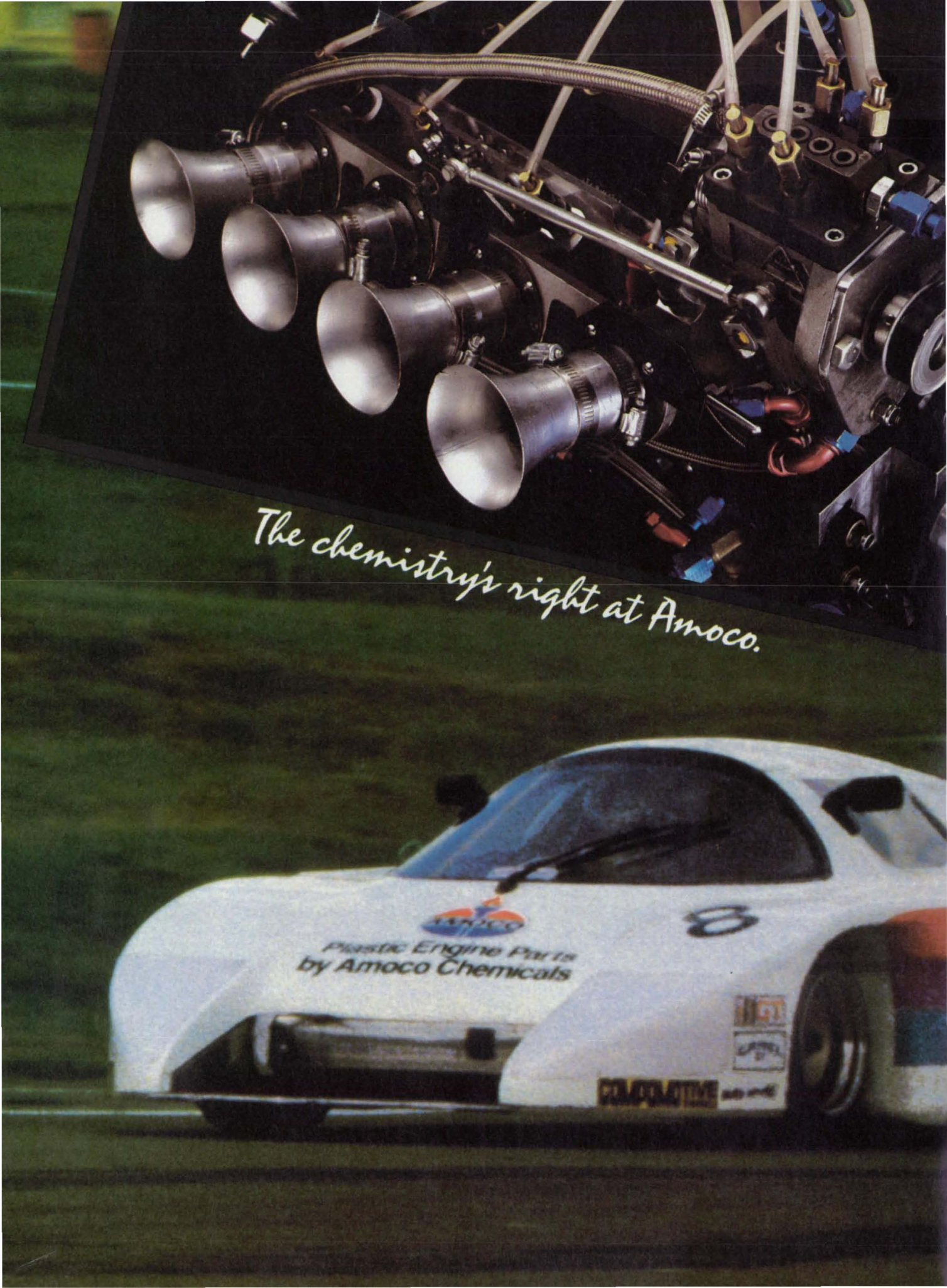
The chemistry's right at Amoco.
Plastic Engine Parts
by Amoco Chemicals

INCREDIBLE. NOW THERE'S A CAR ENGINE MADE OF PLASTIC.

The future has arrived. In the form of a plastic engine built by Polimotor, Fair Lawn, New Jersey. It weighs about half of an ordinary steel engine, develops 318 horsepower at 9,500 rpm—a 2.0 liter, dual overhead cam, fuel injected plastic engine. More importantly, it opens the door to a whole new level of engine performance.

And it's proving itself on the IMSA GT racing circuit in a Lola T-616 chassis at places such as Watkins Glen and Elkhart Lake.

Amoco's Torlon high strength engineering polymer is used for critical engine parts. It handles temperatures to 500° and can be injection molded at costs competitive to metal.

Torlon, polypropylene, polystyrene, polyethylene and petroleum additives and intermediates for advanced composites are part of the storehouse of materials Amoco Chemicals provides the automotive market. With a dedication to quality, dependable follow-through and technical skill.

At Amoco, the chemistry is right.

AMOCO

Amoco Chemicals Corporation

Circle Reader Action No. 1

For more information write to Amoco Chemicals, MC 4002, Dept. 672, 200 E. Randolph Drive, Chicago, IL 60601.

© 1985 Amoco Chemicals Corporation

The NASA Technology Utilization Program

By Leonard A. Ault,
Deputy Director Technology Utilization Division

NASA transfers new knowledge and innovative technology resulting from its aeronautical and space R&D programs to industry, medicine, and other important public sector areas such as transportation, environment, urban development, and public safety. Resultant secondary uses of this technology provides an additional return to the public for the investment in aeronautics and space research.

NASA Tech Briefs is but one of many mechanisms designed to promote and encourage the effective use of aerospace technology in the U.S. industrial marketplace. New advancements across a diverse spectrum of aerospace endeavor, embracing virtually every scientific and technological discipline, are published periodically for the secondary benefit and use of industrial scientists, engineers and businessmen nationwide.

Carefully planned and organized efforts, such as the NASA Technology Utilization Program, accelerates the technology transfer process and broadens user participation. Over the past 26 years, thousands of aerospace-derived technologies have spun off to the public and private sectors of the economy. The steady stream of technological innovations and advancements has already entered nearly every facet of our lives—home and automotive design, fire prevention and protection for firefighters, medical diagnostic instrumentation, bridge construction, food processing equipment, farm machinery, computerized banking, industrial and highway safety, microelectronic products, energy systems, and manufacturing processes of almost every description.

By Congressional mandate, NASA is charged with stimulating the widest possible use of aeronautics and space research results. As part of these efforts, technology transfer mechanisms, such as *NASA Tech Briefs*, provide a link between the creators of advanced technology and those who are able to apply such technologies productively. NASA's aim is to broaden and accelerate the technology transfer process to create new products, new processes and new jobs, and thus gain substantial dividends on governmental funds invested in aerospace research. It should be stressed, however, that technology transfer is a two-way street, requiring that the potential user or beneficiary be as aggressive as the originator in seeking productive and tangible uses of aerospace-derived advances.

The horizontal transfer of technologies developed for one purpose into areas of dissimilar application and use is, however, a major challange. . . and one that does not always come easily. But it is just such cross-fertilization of ideas and technological resources that yield the most rewarding dividends. In recognition of this challenge, NASA sponsors a nationwide university-based network of dissemination centers to assist industry in seeking out the most appropriate technologies to match its needs. The NASA Industrial Applications Centers, listed on page 29, use as their principle resource a vast storehouse of accumulated technical knowledge, computerized for ready retrieval. Through these centers, industrial clients have access to more than 70 million documents gathered worldwide. . . a veritable "department store" of technology.

In addition to information services, these centers provide problem-solving assistance and referral services to government laboratory experts engaged in research and development activities which may relate directly to the technological needs of industry. This latter service aids industry in staying abreast of ongoing technological advances long before they appear in the open literature. Moreover, such access aids in accelerating downstream uses of these advances throughout U.S. industry. We encourage our readers to make use of these facilities. They exist to help you—American industry.

For those industrial firms interested in adapting or applying computer software to their needs, NASA operates the Computer Software Management and Information Center (COSMIC) located at the University of Georgia. COSMIC collects, screens and stores computer programs developed by NASA and other government agencies. Many of these programs are directly applicable to secondary uses with little or no modification, and can be adapted for special purposes at far less cost to the user than that of developing a new program from scratch. The Center's library contains more than 1,300 programs which perform such tasks as structural analysis, design of fluid systems, electronic circuit design, chemical analysis and a variety of other functions. COSMIC, listed on page 28, offers these programs at a fraction of their original costs and can provide a detailed catalog or available programs upon request.

NASA programs, by their challenging nature, are particularly demanding of technological advance and the technologies they generate are exceptionally diverse. Thus, the large storehouse of technology built over more than a quarter century of aeronautical and space research activity constitutes a national resource, a bank of knowledge available for new uses. Alternative applications of technology rarely occur naturally, however, without the active participation and effort of the user. Thus, readers of *NASA Tech Briefs* are encouraged to get involved. Where applicable to your needs, order additional information from NASA on new advances announced in this journal, or explore other technology transfer programs available through the NASA Technology Utilization Program. Your efforts may yield significant dividends for you and your organization.

For additional information, either use the cards found in the back of this or any other issue, or contact your local TU Officer.

My associates in the Technology Utilization Network and I are also listed on page 29 in this issue. Any and all of us are ready to help you get the information you need from NASA. Helping you is what we're all about.

Repeat Ability!

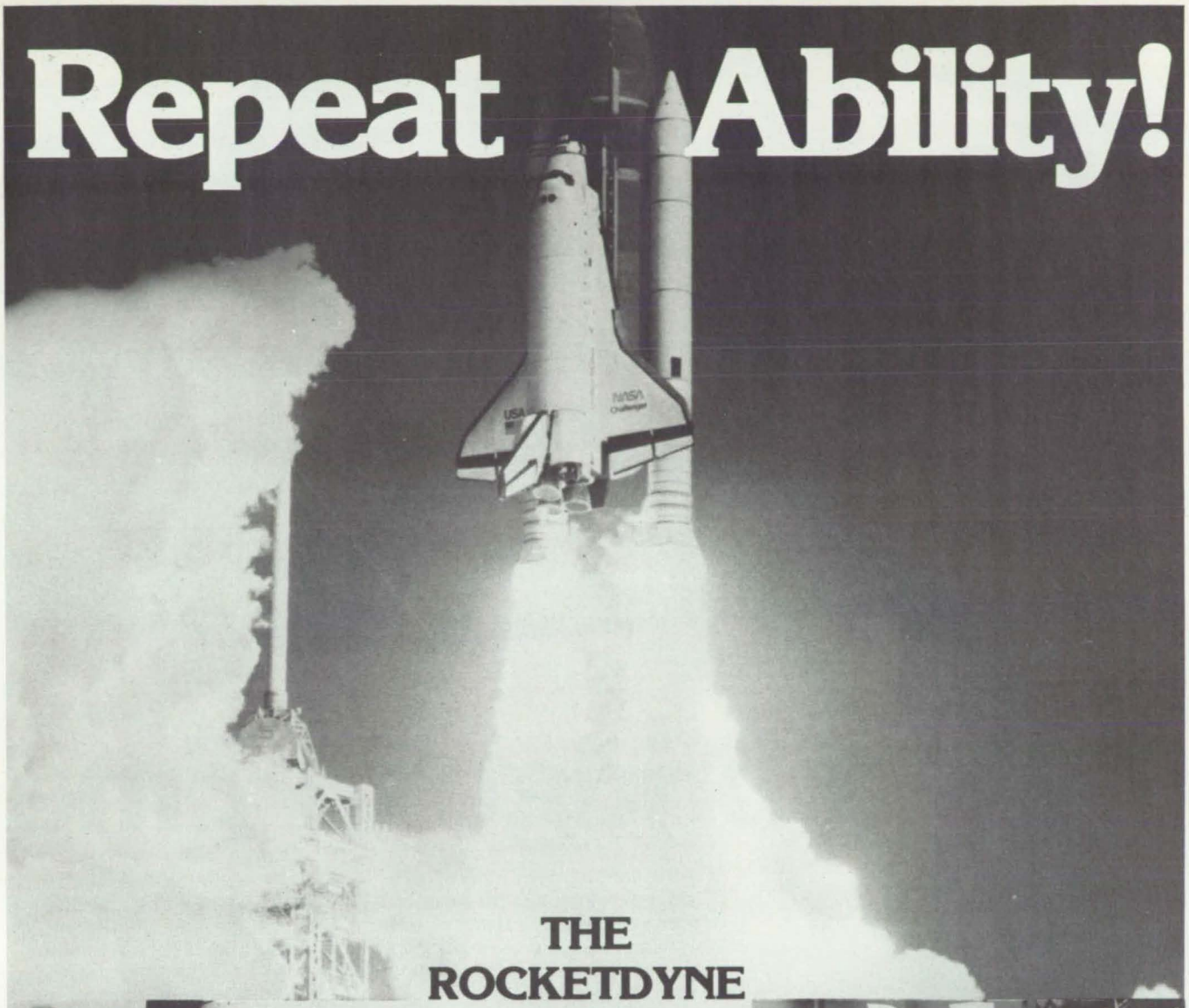

THE ROCKETDYNE TEAM SCORES AGAIN!

America's Shuttles have made many spectacular flights into space and back.

The Rockwell-built Shuttles are the latest in the long list of space vehicles powered by rocket engines designed, built, tested, and proven by the Rocketdyne team—for almost 30 years, the world's leader in space propulsion.

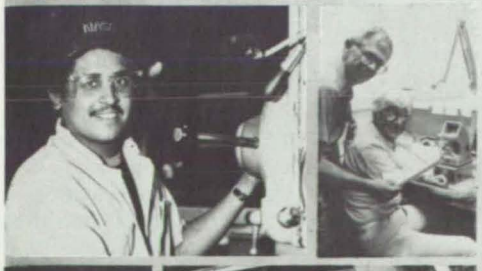

Rockwell International

...where science gets down to business

Aerospace/Electronics
Automotive/General Industries

Circle Reader Action No. 29

Langley—

a bridge in time

In the waning days of WWI, the ground was broken for America's first aeronautical research laboratory, Langley Field. America had dissipated the technological lead in aeronautics bequeathed by the Wright Brothers, and was lagging far behind Europe in the field. Aviation in America had become the province of a few wealthy daredevils, while in Europe men like Gustave Eiffel were pioneering the wind tunnel.

Two years before, in March 1915, President Woodrow Wilson had signed the National Advisory Committee for Aeronautics (NACA) into being and funded it with $5,000. Originally conceived as a nucleus around which the scattered particles of American aeronautical research, both within the government and the private sector, could be arranged and coordinated, NACA was forced to establish itself independently when the realities of WWI intervened, and both the Army and the Navy pursued their own courses elsewhere.

Construction began on July 17, 1917, and on August 7, the facility was formally designated Langley Field, in honor of Samuel Pierpont Langley, an aeronautical pioneer whose steam-powered airplane just missed beating the Wright Brothers into the air by three months. By the time the first wind tunnel was dedicated in 1920, Langley had died and the NACA facility became Langley Memorial Aeronautical Laboratory. In 1948, "Memorial" was dropped and, in 1958, when the National Aeronautics and Space Administration acquired NACA as its foundation, the name it bears today, Langley Research Center, was adopted.

Langley, then, is the elder statesman of NASA's ten centers, the place where it all began. As such the history of Langley is the history of American aeronautical research.

While we can't, in these few pages, delineate a detailed history of Langley, we do hope to give you some flavor of the center, a feeling for its evolution and the role it has played and continues to play in the history of the world. Melodramatic as it may sound, the beginning of the twentieth century, not the 17th, can be argued to mark the real emergence from the dark ages. At the very least, the age of flight, to say nothing of space travel, is the beginning of a new era in human history. The work done at Langley has helped shape this history.

In the early days at Langley the aerodynamics of birds were studied for aircraft adaptation . . .

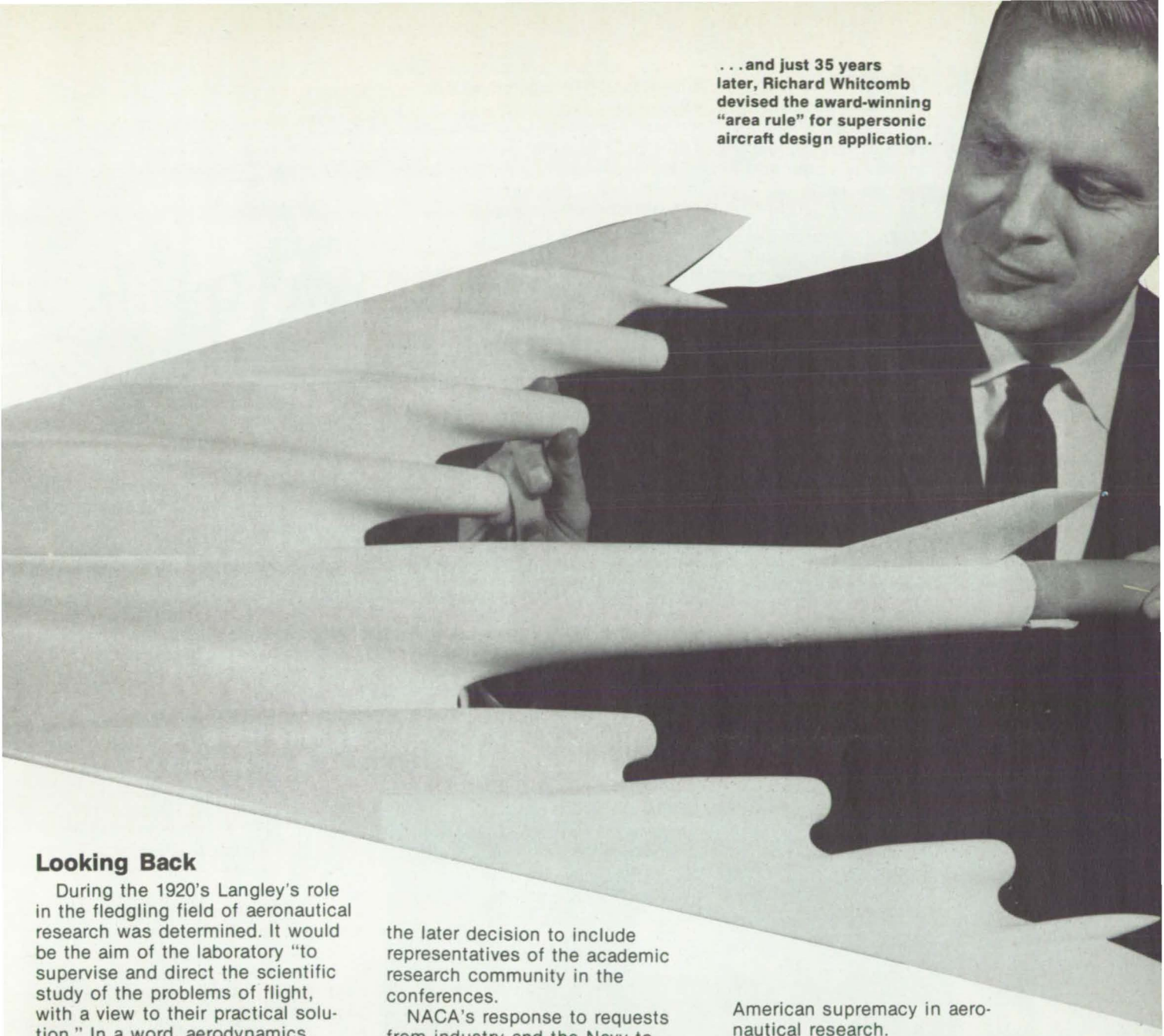

. . . and just 35 years later, Richard Whitcomb devised the award-winning "area rule" for supersonic aircraft design application.

Looking Back

During the 1920's Langley's role in the fledgling field of aeronautical research was determined. It would be the aim of the laboratory "to supervise and direct the scientific study of the problems of flight, with a view to their practical solution." In a word, aerodynamics.

Wind tunnel tests measuring the aerodynamic characteristics of existing aircraft components led to design revisions and improved performance. Facilities expansion began almost immediately. Within a year, a second wind tunnel was constructed.

Simultaneously, Langley's role expanded to carry out the NACA's original purpose—that of a clearinghouse for aeronautical research information. In May 1926, Langley hosted NACA's first joint conference with aircraft manufacturers' representatives and operators, which provided participants with the opportunity to criticize current research and suggest modifications or alternatives. This interchange of information between industry and NACA was to become a major factor in determining the course of future research, as was the later decision to include representatives of the academic research community in the conferences.

NACA's response to requests from industry and the Navy to reduce aircraft drag capped the achievements of Langley's first decade. Using results from tests conducted in Langley's newly constructed "full-scale" propeller research tunnel, NACA researchers designed and developed a streamlined cowling which, when fitted around aircraft engines, provided a significant reduction in drag, allowed for increased aircraft speed and increased efficiency of air-cooling systems. The device became an aircraft design standard and its designers at Langley were awarded the prestigious Collier Trophy in 1929 for their outstanding contribution to American aviation.

By the end of the decade, the Langley staff numbered 181. In just 10 years, they had already made vital and internationally recognized contributions to the study of aerodynamics and firmly established American supremacy in aeronautical research.

More importantly, perhaps, these first years provided opportunities for organizational development, facilities expansion and systematic surveys of existing aircraft, which defined priorities for the years ahead.

Early Achievements

The success of the Langley-designed engine cowling prompted additional drag reduction research. The results indicated that fixed landing gear, engine positions and airfoil sections all needed design improvement. An aircraft design revolution occurred. By the late 1930's, both military and commercial aircraft had adopted Langley recommendations for cowled engines positioned on wing edges, wing flaps and retractable landing gear.

Meanwhile, developments in European aeronautical research had

Langley—

again diminished America's technological lead. NACA's 1937 Annual Report to Congress urged the construction of additional facilities.

Just prior to the outbreak of WWII, Congress authorized NACA's second research laboratory at Moffett Field in Mountain View, California. The Ames Aeronautical Laboratory, named for Dr. Joseph S. Ames, NACA chairman for 12 years, drew on Langley personnel for its staff nucleus.

In mid-1940, at the behest of a special committee headed by Charles A. Lindbergh, Congress authorized a new engine research facility at a site near the Cleveland, Ohio, municipal airport. Again, personnel from Langley were called upon to staff the new facility, even while the purchase of additional acreage at Langley was expanding that facility's personnel needs.

In 1941, the United States entered the war, and the demands on its aeronautical research facilities, primarily Langley, increased enormously. "Quick fixes" for the structural, engine and aerodynamic problems of existing aircraft, not original research, were the tasks at hand.

Under wartime pressure, airplane after airplane—models and full-sized—went through the Langley tunnels and a wealth of information came out, much of which remained in designers' notebooks until after the war, when theoretical and applied research programs were resumed.

Aeronautics Comes of Age

The aeronautical engineering done by the Germans in the latter stages of WWII had developed not only plans but prototypes for jet-propelled aircraft. When the war ended, Langley researchers shifted gear and attacked the problem of breaking the sound barrier.

Langley scientists and researchers presented a study for the design of transonic aircraft at a joint seminar of Army, Air Force, Navy and NACA personnel. It was unanimously approved, and NACA and the military proceeded to develop a joint stable of reserve aircraft in a program that culminated in Air Force Captain Charles E. Yeager's historic flight beyond the speed of sound on October 14, 1947. In the process, yet another Collier Trophy Trophy was won by Langley scientists.

Fast on the heels of this breakthrough came Richard Whitcomb's "area rule" concept, which defined the optimum balance between wing and fuselage volume. This piece of research not only won a Collier Trophy, but was a military aircraft design benchmark.

John Samos, Langley's TU officer, and Richard A. "Pete" Petersen, Langley's fifth Director.

NACA and the military's joint achievements in transonic flight spawned further collaboration, and researchers at Langley developed programs in ballistic and guided missile research.

Beyond the Blue . . . The Birth of NASA

Out of the depths of the Cold War, Russia launched Sputnik I in October, 1957. The dramatic failure of the first American attempt to launch a satellite in December, 1957 ignited a chain of political events which formally established the American space program.

The National Aeronautics and Space Act, signed into law by President Dwight Eisenhower on July 29, 1958, drew heavily on NACA's long-term, scientifically based proposal for aeronautic and space research, to the point of absorbing that organization as the nucleus of the National Aeronautics and Space Administration. The 43-year history of NACA research, its three laboratories and annual budget were transferred to NASA on October 1, 1958.

From the outset, Langley's role in the space program was pivotal. Project Mercury, America's first manned spaceflight program, was born there out of the "Little Joe" test vehicle concept and managed by Langley's Space Task Group. The original seven astronauts trained at the Center.

Project Mercury, designed to accomplish a manned orbit of the

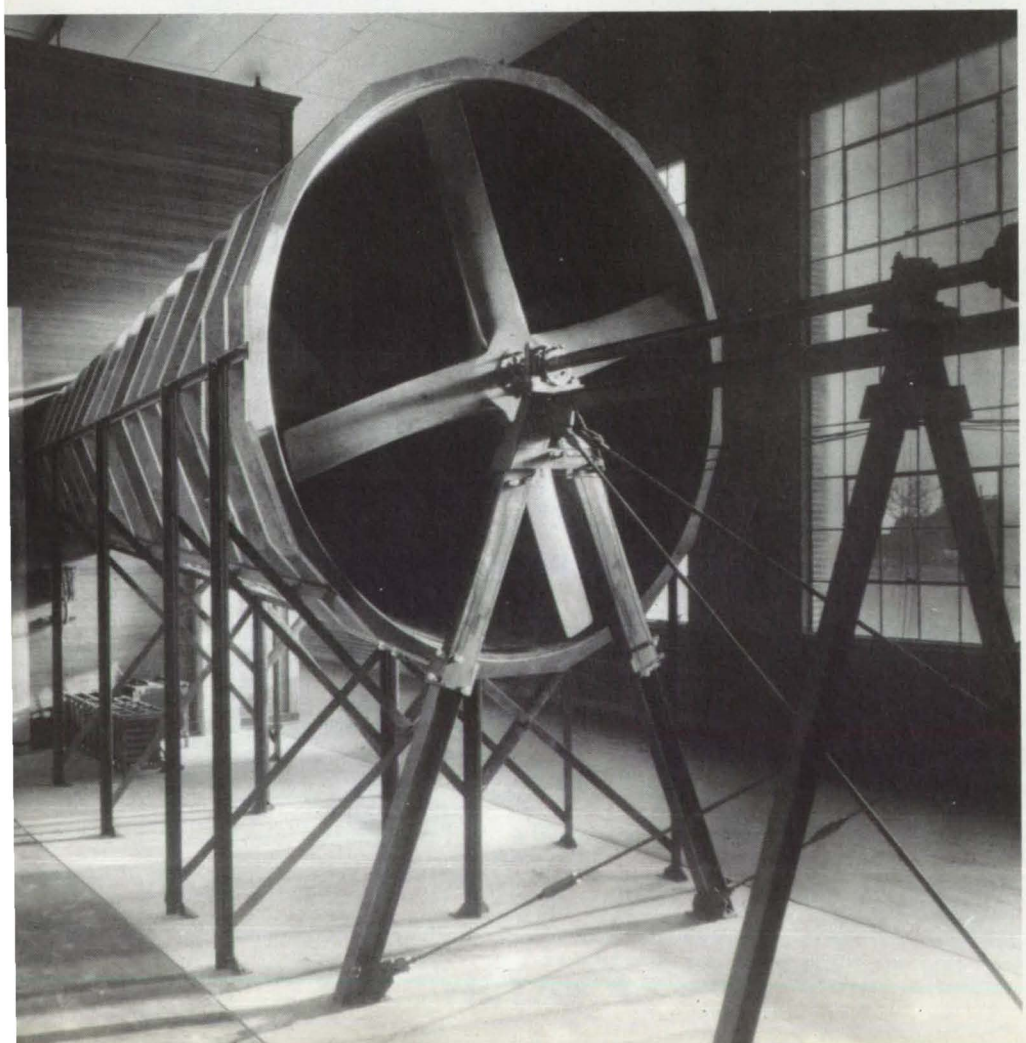

Langley's first wind tunnel, completed in 1920, was designed to measure the aerodynamic characteristics of existing aircraft components.

We're specialists when it comes to advanced fluid control technology. Our products have appeared on every major space program since the X-15 and they have set new standards for compactness, light weight and reliability. In proprietary products from the Space Shuttle Prevalve, which combines the sealing characteristics of a poppet with the free flow path of a ball, to the MX 4th stage pressure regulator which has an accuracy of ±2%, Fairchild Control Systems Company has successfully met the most demanding challenges.

But, we're more than just component specialists. We're system specialists too. Our knowledge and experience in specialized advanced fluid control systems spans more than 25 years.

- Fluid & Propulsion Control Products
  - Pressure Regulators
  - Couplings/Disconnects
  - Fill & Drain Valves
  - Isolation Valves
  - Thrusters

Fairchild Control Systems Company... a company fully committed to meeting the challenges of today's and tomorrow's aerospace/defense industry.

Fairchild Control Systems Company
Dept. AF-3
1800 Rosecrans Ave.
Manhattan Beach
California 90266
Tel.: (213) 643-9222
Telex: 910-325-6216

We're more than fluid control component specialists.

FAIRCHILD
CONTROL SYSTEMS COMPANY

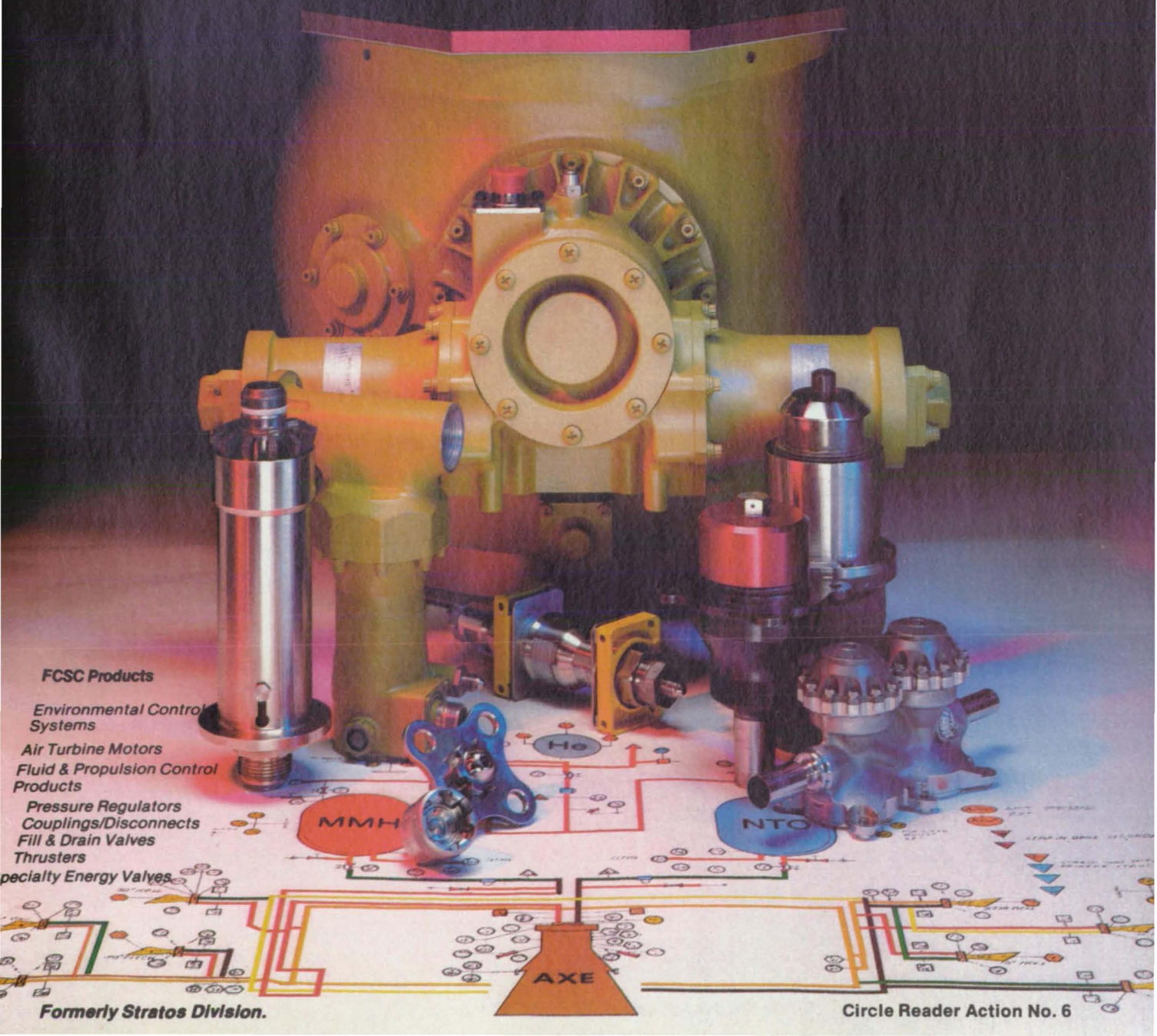

FCSC Products

- Environmental Control Systems
- Air Turbine Motors
- Fluid & Propulsion Control Products
  - Pressure Regulators
  - Couplings/Disconnects
  - Fill & Drain Valves
  - Thrusters
- Specialty Energy Valves

Formerly Stratos Division.

Circle Reader Action No. 6

Langley—

earth, expanded into Project Apollo, the aim of which was a manned lunar landing. Both aims were accomplished in the space of seven years, and the United States posted an historic victory in the "space race."

Langley has provided support for all of the manned space programs through spacecraft design and testing, flight concept development and mission planning. The Center also developed unmanned space programs, including the Echo communications satellites, air density/drag measurement Explorer spacecraft and the Lunar Orbiter. The Viking Project, which landed two automated laboratories on Mars, was also managed by Langley.

Today's Research . . . and Tomorrow's

Today Langley employs nearly 3,000 people in facilities worth over one billion dollars located on almost 800 acres of government land. Just as Langley was, in the early days, in the forefront of aeronautics, so today the Center is and has been one of the pioneers in astronautics as well. Beginning with Project Mercury, America's first manned space project, and extending through Gemini, Apollo, Skylab, Viking and the Space Shuttle. Langley continues to support NASA and America with ongoing research in the design of experiments, sensors, communications equipment and data handling systems. Langley researchers participate in programs that investigate various effects on space vehicles, such as heat, vacuum, noise and meteroid impacts. Advanced composites and thermal control systems, plus improved technology for many kinds of electronic systems, are also being investigated.

Langley is heavily involved in atmospheric science research, developing improved techniques for remotely monitoring atmospheric constituents and processes and determining the earth's radiation budget. A variety of sensors and specialized instruments are already field-proven and in use in aircraft and spacecraft, while others are being developed or tested in preparation for specific applications in the future.

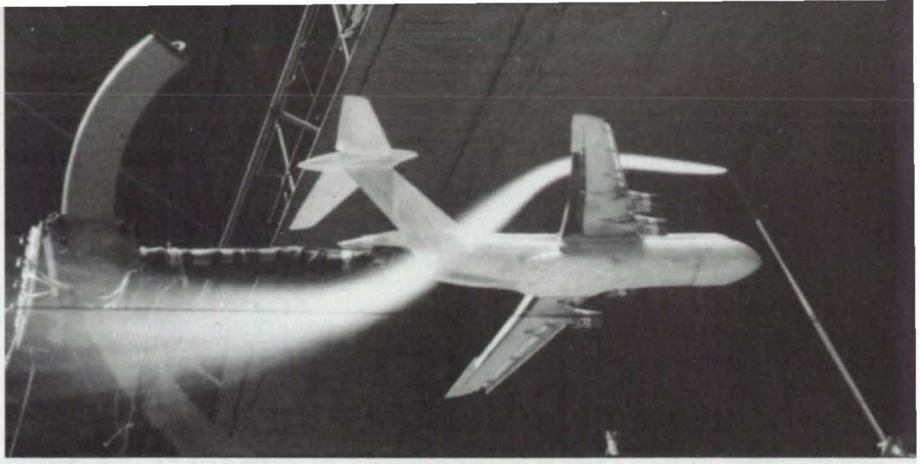

Tests in Langley's full-scale propeller research tunnel led to the development of the streamlined cowling.

On February 2, 1985, Richard A. ("Pete") Petersen became Langley's fifth Director. Under his direction, Langley can be expected to continue its aeronautics research emphasis and further its space research efforts.

As Langley expands and continues its research, the Technology Utilization Office helps transfer the knowledge gained in the process to scientists and engineers throughout American industry. Head of the Office of Technology Utilization and Applications Programs at Langley is John Samos. He and his staff are not only responsible for the transfer of ideas to private industry, but are also responsible for the identification of those ideas worthy of consideration for *NASA Tech Briefs*. Contractor and in-house generated technology is continually assessed and evaluated. It was at Langley, for example, that NASA's advanced technology demonstration house was designed, constructed, and demonstrated to the public. It was featured in *Popular Mechanics* as "NASA's Far Out House."

Currently, under NASA's Technology Utilization Applications Program, Langley researchers are collaborating with their counterparts in other agencies and institutions to foster industrial and biomedical spinoffs incorporating a wide range of aerospace-developed technologies.

From 1917, as the United States' first aeronautical laboratory, to today's multi-faceted research center, Langley has made history, ameliorated the quality of life on earth and, in the process, helped shape the world.

PSI PRESSURE SCANNERS MAKE TURBINE TESTING A BREEZE.

For fast, accurate and reliable pressure measurement, you can't beat the 780B, today's state of the art in pressure scanning systems.

The 780B gives you faster data acquisition rates. Improved accuracy, with repeatable results. And computer compatability that offers a friendly interface to nearly any system.

Call or write today for more information on the 780B from PSI...the leaders in digital pressure measurement technology.

- 20,000 measurements per second ± 0.10% F.S. worst case inaccuracy
- ± 1.0 psid to 500 psid ranges
- Automatic on-line calibration
- IEEE-488 compatability

PSI PRESSURE SYSTEMS

15 Research Drive, Hampton, VA 23666
(804) 865-1243

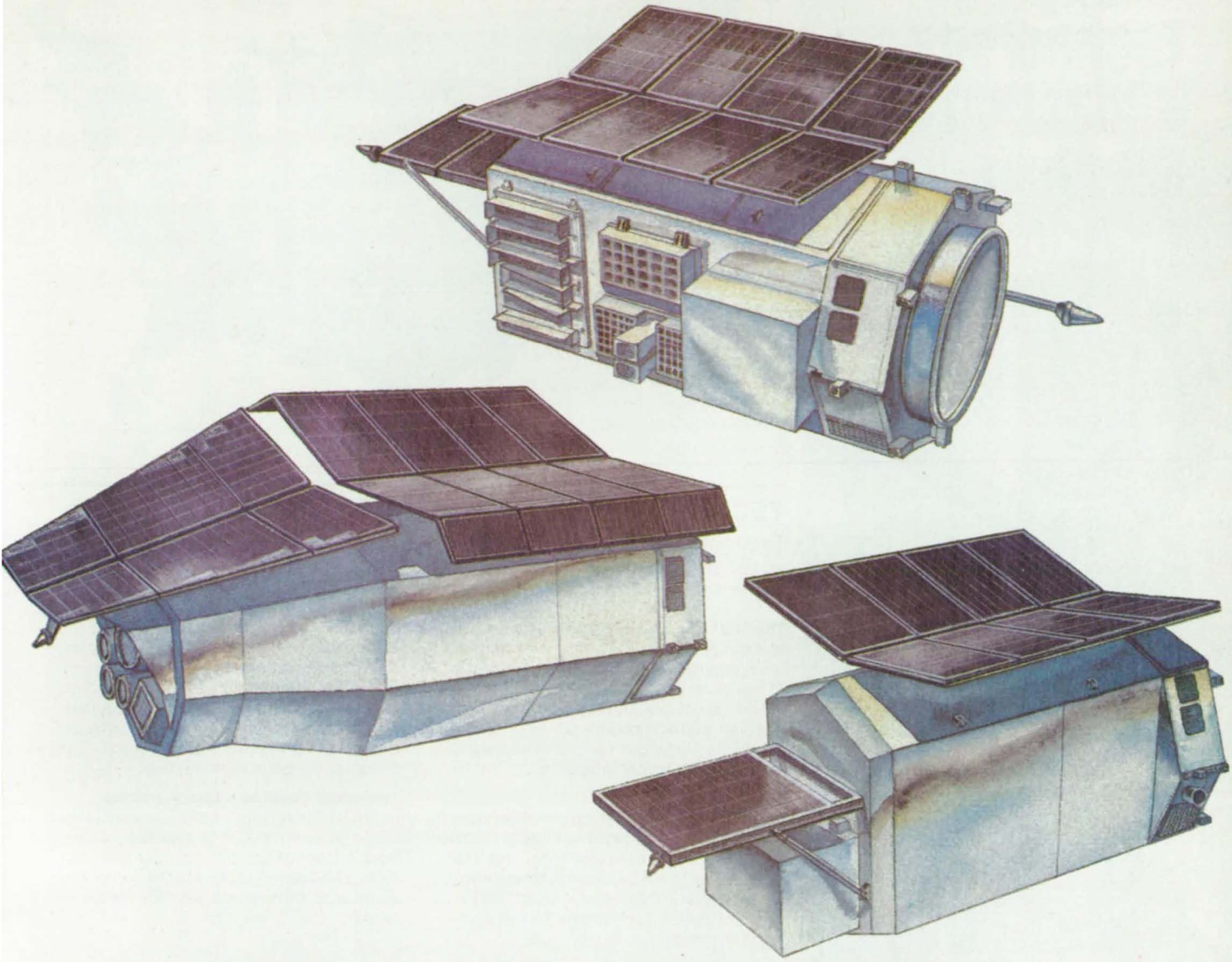

THE RIGHT ATTITUDE

It was NASA's goal to measure, with a pointing accuracy of 1 arc minute, X-ray sources in outer space. So Control Data's 469R² micro-miniature computer was selected for the High Energy Astronomical Observatory (HEAO) satellites to keep critical instruments right on target.

The 469R², with large-scale integrated circuits, is specially designed to operate in the rigorous environment of space; the 'R²,' in fact, stands for rugged and reliable—so reliable that this computer's meantime-to-failure is calculated to exceed 200,000 hours.

Other applications to which 469R² computers have been delivered include the Teal Ruby experiment, an infrared sensor satellite which will be launched from the space shuttle.

Find out how Control Data's spaceborne technology and capabilities can help meet your needs. Get more information, along with a print of the spacecraft above, by calling 612/853-5000. Or write Government Systems Resource Center, Control Data Corporation, P.O. Box 609, Minneapolis, MN 55440.

CONTROL DATA

Circle Reader Action No. 4

NASA Technology Utilization Services

TECHNOLOGY UTILIZATION OFFICERS

Technology transfer experts can help you apply the innovations in NASA Tech Briefs.

The Technology Utilization Officer at each NASA Field Center is an applications engineer who can help you make use of new technology developed at his center. He brings you NASA Tech Briefs and other special publications, sponsors conferences, and arranges for expert assistance in solving technical problems.

Technical assistance, in the form of further information about NASA innovations and technology, is one of the services available from the TUO. Together with NASA scientists and engineers, he can often help you find and implement NASA technology to meet your specific needs.

Technical Support Packages (TSP's) are prepared by the center TUO's. They provide further technical details for articles in NASA Tech Briefs. This additional material can help you evaluate and use NASA technology. You may receive most TSP's free of charge by using the TSP Request Card found at the back of this issue.

Technical questions about articles *in NASA Tech Briefs are answered in the TSP's. When no TSP is available, or you have further questions, contact the Technology Utilization Officer at the center that sponsored the research [see facing page for details].*

COSMIC®

An economical source of computer programs developed by NASA and other government agencies.

A vast software library is maintained by COSMIC—the Computer Software Management and Information Center. COSMIC gives you access to approximately 1,600 computer programs developed for NASA and the Department of Defense and selected programs for other government agencies. Programs and documentation are available at reasonable cost.

Available programs range from management (PERT scheduling) to information science (retrieval systems) and computer operations (hardware and software). Hundreds of engineering programs perform such tasks as structural analysis, electronic circuit design, chemical analysis, and the design of fluid systems. Others determine building energy requirements and optimize mineral exploration.

COSMIC services go beyond the collection and storage of software packages. Programs are checked for completeness; special announcements and an indexed software catalog are prepared; and programs are reproduced for distribution. Customers are helped to identify their software needs; and COSMIC follows up to determine the successes and problems and to provide updates and error corrections. In some cases, NASA engineers can offer guidance to users in installing or running a program.

Information about programs *descibed in NASA Tech Briefs articles can be obtained by completing the COSMIC Request Card at the back of this issue. Just circle the letters that correspond to the programs in which you are interested.*

★ TECHNOLOGY UTILIZATION OFFICERS

Stanley A. Miller
Ames Research Center
Mail Code 234-2
Moffett Field, CA 94035
(415) 694-6471

Donald S. Friedman
Goddard Space Flight Center
Mail Code 702.1
Greenbelt, MD 20771
(301) 344-6242

William Chmylak
Lyndon B. Johnson Space Center
Mail Code AL32
Houston, TX 77058
(713) 483-3809

U. Reed Barnett
John F. Kennedy Space Center
Mail Code PT-TPO
Mail Stop: PT-TPO-A
Kennedy Space Center, FL 32899
(305) 867-3017

John Samos
Langley Research Center
Mail Stop 139A
Hampton, VA 23665
(804) 865-3281

S.F. Felder
Lewis Research Center
Mail Stop 7-3
21000 Brookpark Road
Cleveland, OH 44135
(216) 433-4000, Ext. 422

Ismail Akbay
George C. Marshall Space Flight Center
Code AT01
Marshall Space Flight Center, AL 35812
(205) 453-2223

Leonard A. Ault
NASA Headquarters
Code IU
Washington, DC 20546
(202) 453-8415

James T. English
NASA Resident Office
Jet Propulsion Laboratory
Mail Stop 201-110
4800 Oak Grove Drive
Pasadena, CA 91109
(818) 354-2240

Robert M. Barlow
National Space Technology Laboratories
Code GA-10
NSTL Station, MS 39529
(601) 688-1929

● INDUSTRIAL APPLICATIONS CENTERS

Aerospace Research Applications Center (ARAC)
Indianapolis Center for Advanced Research
611 N. Capital Avenue
Indianapolis, IN 46204
John M. Ulrich, Director
(317) 264-4644

Kerr Industrial Applications Center (KIAC)
Southeastern Oklahoma State University
Station A, Box 2584
Durant, OK 74701
Tom J. McRorey, Director
(405) 924-6822

NASA Industrial Applications Center
823 William Pitt Union
University of Pittsburgh
Pittsburgh, PA 15260
Paul A. McWilliams, Executive Director
(412) 624-5211

New England Research Application Center (NERAC)
Mansfield Professional Park
Storrs, CT 06268
Daniel U. Wilde, Director
(203) 486-4533

North Carolina Science and Technology Research Center (NC/STRC)
Post Office Box 12235
Research Triangle Park, NC 27709
James E. Vann, Director
(919) 549-0671

Technology Application Center (TAC)
University of New Mexico
Albuquerque, NM 87131
Stanley A. Morain, Director
(505) 277-3622

NASA Industrial Applications Center (WESRAC)
University of Southern California
Research Annex
3716 South Hope Street
Room 200
Los Angeles, CA 90007
Radford G. King, Executive Director
(213) 743-8988

◆ PATENT COUNSELS

Robert F. Kempf, Asst. Gen. Counsel for Patent Matters
NASA Headquarters
Code GP
Washington, DC 20546
(202) 453-2424

Darrell G. Brekke
Ames Research Center
Mail Code: 200-11A
Moffett Field, CA 94035
(415) 694-5104

John O. Tresansky
Goddard Space Flight Center
Mail Code: 204
Greenbelt, MD 20771
(301) 344-7351

Marvin F. Matthews
Lyndon B. Johnson Space Center
Mail Code: AL-3
Houston, TX 77058
(713) 483-4871

James O. Harrell
John F. Kennedy Space Center
Mail Code: PT-PAT
Kennedy Space Center, FL 32899
(305) 867-2544

Howard J. Osborn
Langley Research Center
Mail Code: 279
Hampton, VA 23665
(804) 827-3725

Norman T. Musial
Lewis Research Center
Mail Code: 500-318
21000 Brookpark Road
Cleveland, OH 44135
(216) 433-4000, Ext. 346

Leon D. Wofford, Jr.
George C. Marshall Space Flight Center
Mail Code: CC01
Marshall Space Flight Center, AL 35812
(205) 453-0020

Paul F. McCaul
NASA Resident Office-JPL
Mail Code: 180-801
4800 Oak Grove Drive
Pasadena, CA 91103
(818) 354-2700

■ STATE TECHNOLOGY APPLICATIONS CENTERS

NASA/Florida State Technology Applications Center
State University System of Florida
307 Weil Hall
Gainesville, FL 32611
J. Ronald Thornton, Director
(904) 392-6626

NASA/UK Technology Applications Program
University of Kentucky
109 Kinkead Hall
Lexington, KY 40506-0057
William R. Strong, Program Director
(606) 257-6322

▲ APPLICATION TEAM

Technology Application Team
Research Triangle Institute
Post Office Box 12194
Research Triangle Park, NC 27709
Doris Rouse, Director
(919) 541-6980

● COMPUTER SOFTWARE MANAGEMENT & INFORMATION CENTER

COSMIC®
112 Barrow Hall
University of Georgia
Athens, GA 30602
John A. Gibson, Director
(404) 542-3265

STATE TECHNOLOGY APPLICATIONS CENTERS

Technical information services for industry and state and local government agencies

Government and private industry in Florida and Kentucky can utilize the services of NASA's State Technology Applications Centers (STAC's). The STAC's differ from the Industrial Applications Centers described on page 30, primarily in that they are integrated into existing state technical assistance programs and serve only the host state, whereas the IAC's serve multistate regions.

Many data bases, including the NASA base and several commercial bases, are available for automatic data retrieval through the STAC's. Other services such as document retrieval and special searches are also provided. (Like the IAC's, the STAC's normally charge a fee for their services.)

To obtain information *about the services offered, write or call the STAC in your state [see above].*

NASA INVENTIONS AVAILABLE FOR LICENSING

Over 3,500 NASA inventions are available for licensing in the United States—both exclusive and nonexclusive.

Nonexclusive licenses
for commerical use of NASA inventions are encouraged to promote competition and to achieve the widest use of inventions. They must be used by a negotiated target date.

Exclusive licenses
may be granted to encourage early commercial development of NASA inventions, especially when considerable private investment is required. These are generally for 5 to 10 years and usually require royalties based on sales or use.

Additional licenses available
include those of NASA-owned foreign patents. In addition to inventions described in NASA Tech Briefs, *"NASA Patent Abstract Bibliography"* (PAB), containing abstracts of all NASA inventions, can be purchased from National Technical Information Service, Springfield, VA 22161. The PAB is updated semiannually.

Patent licenses for Tech Briefs
are frequently available. Many of the inventions reported in NASA Tech Briefs are patented or are under consideration for a patent at the time they are published. The current patent status is described at the end of the article; otherwise, there is no statement about patents. If you want to know more about the patent program or are interested in licensing a particular invention, contact the Patent Counsel at the NASA Field Center that sponsored the research [see page 29]. Be sure to refer to the NASA reference number at the end of the Tech Brief.

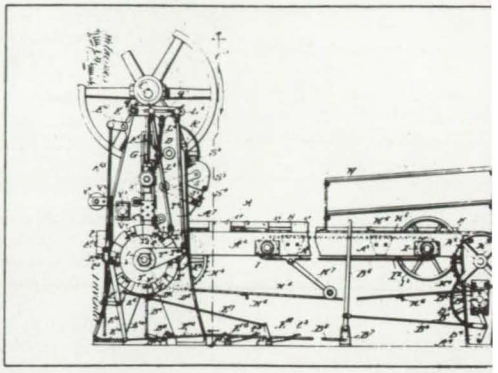

INDUSTRIAL APPLICATIONS CENTERS

Computerized access to over 10 million documents worldwide

Computerized information retrieval
from one of the world's largest banks of technical data is available from NASA's network of industrial Applications Centers (IAC's). The IAC's give you access to 1,800,000 technical reports in the NASA data base and to more than 10 times that many reports and articles found in nearly 200 other computerized data bases.

The major sources include:
- *750,000 NASA Technical Reports*
- *Selected Water Resources Abstracts*
- *NASA Scientific and Technical Aerospace Reports*
- *Air Pollution Technical Information Center*
- *NASA International Aerospace Abstracts*
- *Chem Abstracts Condensates*
- *Engineering Index*
- *Energy Research Abstracts*
- *NASA Tech Briefs*
- *Government Reports*
- *Announcements*

and many other specialized files on food technology, textile technology, metallurgy, medicine, business, economics, social sciences, and physical science.

The IAC services
range from tailored literature searches through expert technical assistance:
- *Retrospective Searches:* Published or unpublished literature is screened and documents are identified according to your interest profile. AIC engineers tailor results to your specific needs and furnish abstracts considered the most pertinent. Complete reports are available upon request.
- *Current-Awareness Searchs:* IAC engineers will help design a program to suit your needs. You will receive selected monthly or quarterly abstracts on new developments in your area of interest.
- *Technical Assistance:* IAC engineers will help you evaluate the results of your literature searches. They can help find answers to your technical problems and put you in touch with scientists and engineers at appropriate NASA Field Centers.

Prospective clients
can obtain more information about these services by contacting the nearest IAC [see page 29]. User fees are charged for IAC information services.

APPLICATION TEAMS

Technology-matching and problem-solving assistance to public sector organizations

Application engineering projects
are conducted by NASA to help solve public-sector problems in such areas as safety, health, transportation, and environmental protection. Some application teams specialize in biomedical disciplines; others, in engineering and scientific problems. Staffed by professionals from various disciplines, these teams work with other Federal agencies and health organizations to identify critical problems amenable to solution by the application of existing NASA technology.

Public-sector organization
representatives can learn more about application teams by contacting a nearby NASA Field Center Technology Utilization Office [see page 29].

Tiltmeter Indicates Sense of Slope

A tiltmeter that indicates the sense as well as the magnitude of a slope can be used in locations where the incline is not visible to the operator. The measurement relies on varying resistance between electrodes as they are tilted with respect to each other in an electrolyte. Power for the instrument is furnished by two "AA" electrochemical cells. An operational amplifier provides an adjustable, regulated low voltage to a measuring bridge.

(See page 40.)

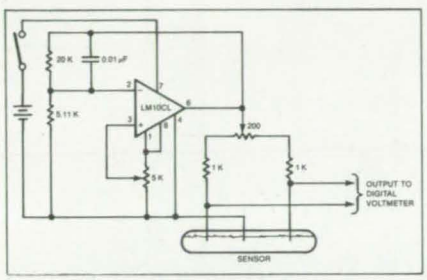

Continuous Laminar-Smoke Generator

A continuous laminar-smoke generator produces a single filament of smoke for visualizing flow details in low-speed wind-tunnel tests. The smoke exit hole is a drilled hole in the side of a small-diameter feed tube. The local flow speed is kept low enough to prevent eddy shedding. By placing the tube in the low-speed part of the wind tunnel (just ahead of the contraction), the technician can make the actual test speed much higher than the local speed around the smoke generator.

(See page 116.)

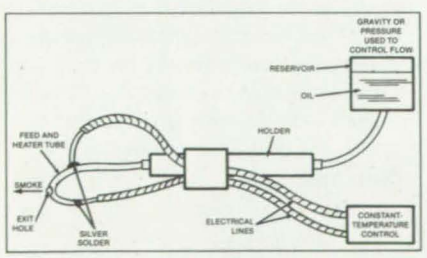

Static-Suppressing Optical Paint

An electrically conductive flat black paint adheres well to magnesium, aluminum, fiberglass, and other materials. The paint absorbs stray light in optical instruments while preventing the buildup of electrostatic fields and arcing. It consists of a primer and a topcoat, both containing electrically-conductive carbon-black powder. The primer has a two-part epoxy base, and the topcoat has a polyurethane base.

(See page 107.)

Nonyellowing Polycarbonate for Outdoor Use

A two-step photochemical process prevents the yellowing of polycarbonate plastics. The use of polycarbonate plastics is growing in windows, aircraft glazing, and streetlight globes. However, outdoor exposure of originally-clear polycarbonate causes yellowing, often within a few days. The new photochemical process creates stabilizers that become bound to the polymer chains and therefore cannot be leached out.

(See page 99.)

Long-Life Cryogenic Cooler

A Stirling cycle cryogenic cooler would operate unattended at 65 K for more than 3 years to cool infrared detectors and other scientific instruments. The new cooler, which uses magnetic bearings, small piston/cylinder clearance seals, and linear motors, consists of compression and expansion sections connected end to end. The compression section houses a reciprocating hollow piston driven by a linear motor.

(See page 140.)

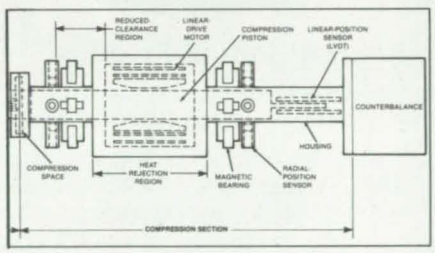

Copyboard Quickly Makes Clean Printing Plates

A vacuum copyboard for printing shops keeps a camera-ready original clean and in the proper position for making plates. The copyboard is intended for use on an electrostatic platemaker consisting of a lighttight plate container, processing tank and dryer, lamps to illuminate the copyboard, and a camera lens focused on the copyboard. The copyboard allows the camera-ready original to be properly positioned, then holds it for photography. A bleed valve allows the vacuum in the copyboard box to be adjusted for small or large originals.

(See page 152.)

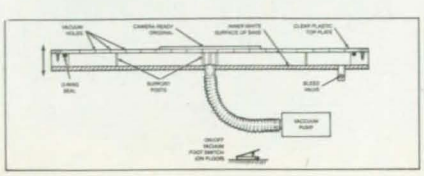

New Product Ideas

New Product Ideas are just a few of the many innovations described in this issue of *NASA Tech Briefs* and having promising commercial applications. Each is discussed further on the referenced page in the appropriate section in this issue. If you are interested in developing a product from these or other NASA innovations, you can receive further technical information by requesting the TSP referenced at the end of the full-length article or by writing the Technology Utilization Office of the sponsoring NASA center (see page 29). NASA's patent-licensing program to encourage commercial development is described on page 30.

Aircraft Canopy Lock

A lock for an aircraft canopy can be operated from both inside and outside the cockpit but is unlikely to be actuated by accidental pilot movements or aerodynamic forces during flight. To unlock the latch from the inside, the pilot pulls a knob out from the cockpit wall to disengage a pull pin from a recess. Once the pin is disengaged, the arm on which the knob is mounted can be rotated. The motion of the arm is transmitted by a pair of linked rods to a pair of hooks, thus causing the hooks to disengage from a pair of pins on the canopy. The canopy is then free to open upward.

(See page 114.)

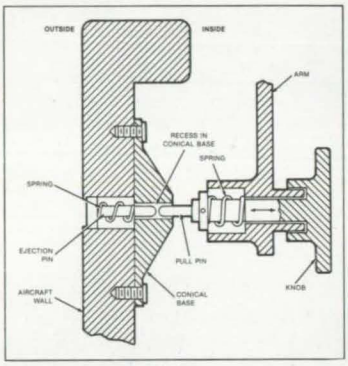

Air Bearing for Small Planar Vibrations

An air bearing allows small linear displacements in any direction in a horizontal plane as well as rotation about a vertical axis. It can support a large mass at the end of a long arm, yet it transmits no microphonic or other vibrations to the mass. The bearing includes a movable Y-shaped slide sandwiched between two fixed support plates. The slide supports an object to be oscillated linearly or rotationally in a plane. Pressurized air forms a cushion above and below the plate. The bearing was originally developed for stirring crystal-growth liquids in containers.

(See page 132.)

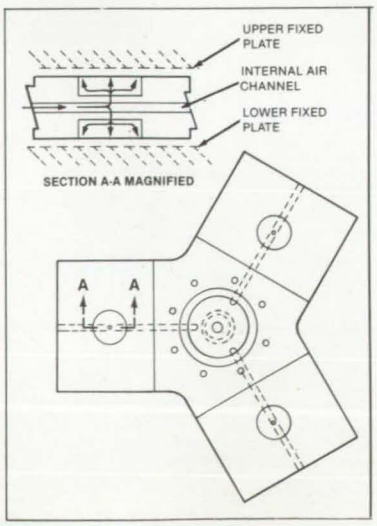

Fastening Parts Having Mismatched Thermal Coefficients

A new fastener minimizes thermal stresses and maintains a snug fit between materials with different thermal-expansion coefficients. It is particularly useful in joining carbon/carbon composite materials to metals or other composites. A conical-head bolt and metal washer are the main components of the fastener which does not become looser or tighter as the temperature changes.

(See page 137.)

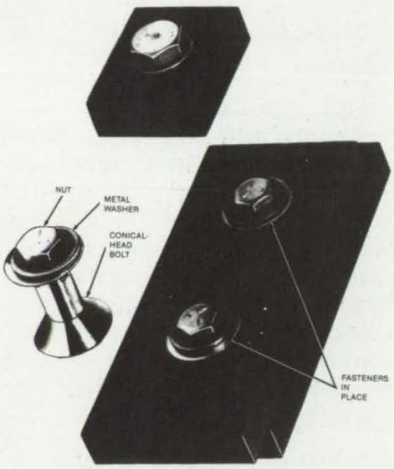

Aircraft Control-Position Indicator

The maintenance-free aircraft control-position indicator is a cockpit-mounted instrument that displays the positions of the elevator and the ailerons to the pilot. The display, which is mounted in a standard flight instrument case, is a cruciform array of lights: A horizontal row of amber lights and a vertical row of green lights represent aileron and elevator positions, respectively. All indicators are electronically driven by instantly acting transducers and an integrated circuit that senses the analog voltage level, providing a zero-lag display and easy readability under all light conditions.

(See page 54.)

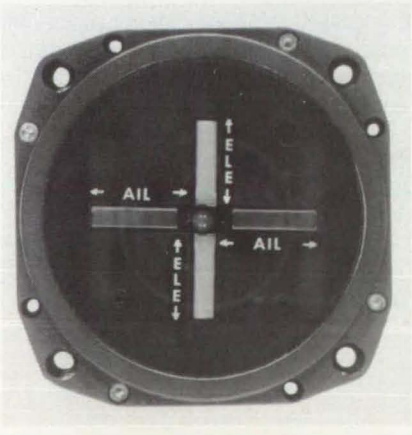

Wide-Grasp Latching Mechanism

A latching mechanism grasps a bar located within a relatively wide envelope of possible positions, retains the object, and releases it on command. The large acceptance envelope reduces the accuracy with which the object must be positioned for capture by the latch. A rack and pinion drive the fingers. A worm/spur gear, powered by a worm gear at a 90° angle, drives the rack and pinion. The movement of the fingers can be halted at any point in the latching and unlatching sequence.

(See page 141.)

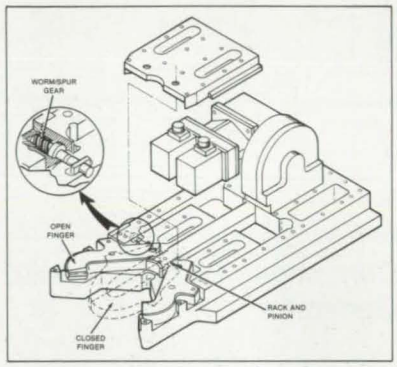

Microprocessor-Controlled Laser Balancing System

A microprocessor-controlled laser balancing system has been developed for automatic dynamic balancing of rotating components. This system provides complete and accurate balancing in a single load-and-spinup cycle. It computes all balance plane corrections simultaneously and then uses a pulsed laser for precise material removal, even from parts that may be inaccessible for installation of conventional correction weights. Since the unbalance correction is performed by the laser under microprocessor supervision as the part rotates, human error and rejected workpieces are virtually eliminated.

(See page 118.)

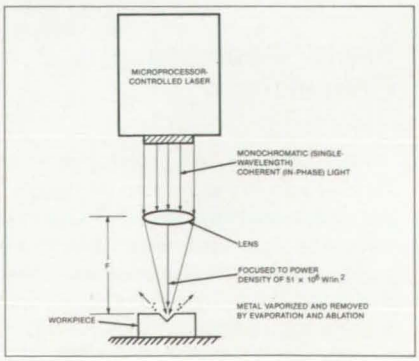

BREAKTHROUGH: TAKE THE HEADACHES OUT OF HIGH ALTITUDES.

Planes going a long distance fly at high altitudes to conserve fuel. But at those altitudes, some oxygen atoms cluster together in threes to form ozone that can give passengers headaches and respiratory problems.

Our engineers reasoned that it is easier to pull the ozone apart than to build heavy filters to keep it out. A concept was developed using catalytic screens in the air ducts to attract the ozone for an instant as it passes, allowing the atoms to reform as oxygen and literally turning a noxious gas into a breath of fresh air.

We're creating breakthroughs not only in airline travel, but in space manufacturing, information systems, and helicopter design and production.

We're McDonnell Douglas.

Material used is Deoxo® catalyst substrate ozone abater manufactured by Englehard Corporation Specialty Chemicals Division.

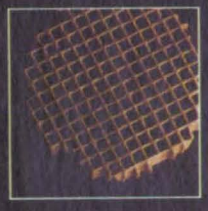

MCDONNELL DOUGLAS

© 1984 McDonnell Douglas Corporation

Circle Reader Action No. 23

UNMATCHED LINEAR MOTION PRECISION

MODEL MR 50

$170. per axis

1 Micron Accuracy

- 400 Series Stainless Steel Bodies With Hardened Steel Guides Exceeding Rockwell 60.
- Minimal Differential Thermal Expansion.
- Won't Creep . . . Won't Bind . . . Long Term Stability.
- Trajectory to ±1 Micron Over Travel Range.
- Pre-loaded Carriage Provides Zero Backlash.
- High Load Carrying Capacities.
- Modular Design Permits X-Y and X-Y-Z Positioning.
- Easy Mounting To Any Standard Optical Table With 1" Hole Centers.
- Full Compatibility With Klinger Micropositioners And Most Others.

FREE! NEW MICROPOSITIONING GUIDE. Send for Catalog 584.

KLINGER SCIENTIFIC

110-20 Jamaica Avenue
Richmond Hill, NY 11418
(718) 846-3700

Circle Reader Action No. 11

Spill-Detector-and-Shutoff Device

A new device rapidly detects and stops overflow in liquid chromatography systems. The spill-detector-and-shutoff device incorporates a liquid sensor. When liquid is spilled on the liquid sensor, the device automatically stops the pumping action and causes a pliable flow tube to be pinched. The tube is pinched with a plunger actuated by a solenoid.

(See page 129.)

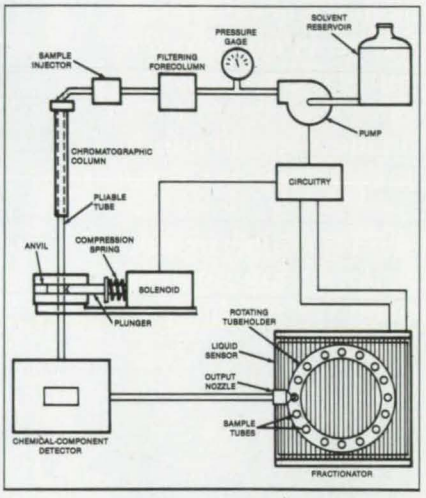

Foam Insulation for Cryogenic Flowlines

Welded stainless-steel vacuum jackets on cryogenic ducts can be replaced by plastic foam-insulation jackets that weigh 12 percent less. The new insulation, which is easier to install than the vacuum jacket, has layers of material that protect, hold, and bond the foam. Moreover, the foam is less sensitive to damage and requires minimal maintenance. It resists vibration and is expected to have a service life of at least 10 years.

(See page 96.)

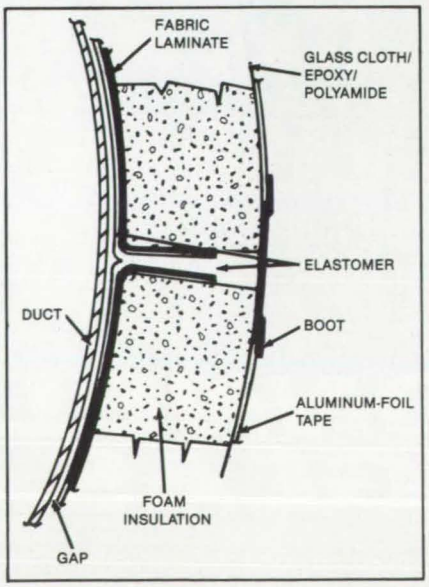

Thermosetting Phthalocyanine Polymers

A group of phthalocyanine polymers made either of two classes of monomers resist thermal degradation up to 500° C. One class consists of bisphthalonitriles with imide linkages. The other monomer class consists of bisphthalonitriles with ester-imide linkages. A monomer is polymerized by heating in the presence of cuprous chloride and an inert atmosphere. The principal application of the new polymers would be in molded or laminated parts that have to withstand high temperatures.

(See page 91.)

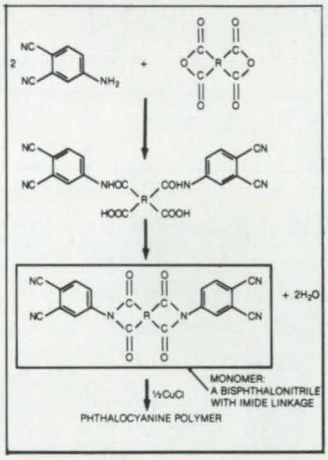

Contact Heat Exchanger

A segmented interface moved by fluid pressure controls the amount of heat transferred between a heat pipe and a circulating heat exchanger. The device consists of split cylindrical heat-exchanger sections made of soft-aluminum tubing with small flow tubes brazed on the outside. Gas or hydraulic pressure applied across a flexible metal diaphragm forces these cylindrical heat-exchanger sections into contact with matching sections of the heat pipe evaporator.

(See page 117.)

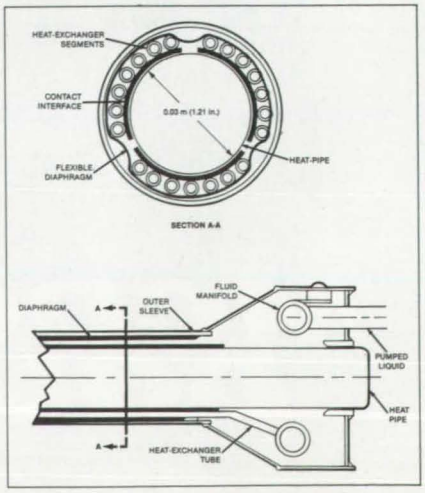

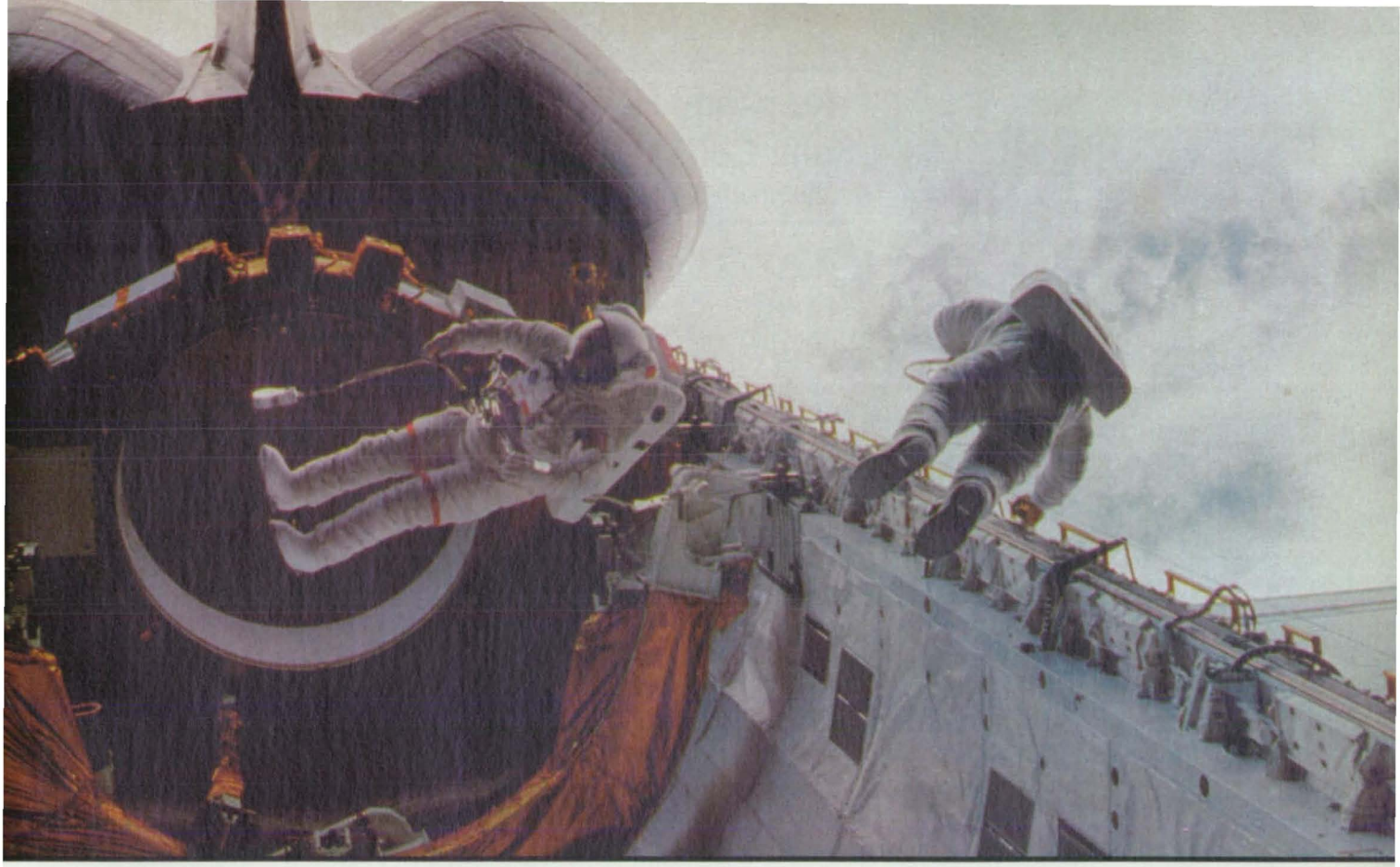

WYLE WORKS IN SPACE...

The commercialization of space represents the biggest marketing opportunity in decades. Research in a weightless environment is taking place in areas from microbiology to macro-defense systems.

Wyle Laboratories has been a pioneer in the development of commercial applications for space. We've been supporting the NASA Space Commercialization Task Force and we're participating in space station definition requirements and NASA/industry sponsored workshops.

Wyle is supporting definition of Space Station architecture, missions and payloads, data base development, and definition of industrial requirements under NASA's Space Commercialization Program.

We also support industry. For example, Wyle has helped to qualify the unique McDonnell Douglas electrophoresis systems hardware under their joint endeavor program with NASA.

Wyle can support you in these key areas:

- Systems Concept Design and Definition Studies
- Technical and Economic Feasibility Studies
- Hardware Qualification, Verification and Safety Analysis
- Management Information Systems
- Experiment Data and Hardware Performance Analysis
- Interface Support Between Industry and NASA

Wyle Laboratories serves both industry and government. To find out how you can benefit from our experience, contact Dave Christensen or Bill Vardaman at 205/837-4411.

WYLE LABORATORIES SCIENTIFIC SERVICES & SYSTEMS GROUP

The nation's leading independent testing laboratory.

Huntsville, AL
Lanham, MD
Arlington, VA
El Segundo, CA
Norco, CA
Hampton, VA

Circle Reader Action No. 20

Electronic Components and Circuits

Hardware, Techniques, and Processes

36 Measuring Recombination Velocities in Solar Cells
38 Hybrid Fiber-Optic/CCD Chip
39 Digital High-Current Monitor
39 Improved Thick Dichroic Reflector for Microwave Feeds
40 Tiltmeter Indicates Sense of Slope
42 Dual-Mode Horn Antenna for Millimeter Wavelengths
43 FLux Coupling for Wheelchair Battery Chargers
43 Signal Processor for Multirate PSK Signals
44 SAW-Modulated Image Device
45 Damping Relaxation Oscillations in Laser Diodes
46 Protective Cover for IC Packages
47 Recovering Energy From Relays
47 Resistive Fine Tuning of Resonant Circuit
48 Telephone Instrument for the Deaf
49 Double Light-Emitting Diode
49 Fast-Recovery, High-Voltage Power Diode
51 Complementary-Logic Fault Detector
52 High-Voltage Isolation Transformer
53 Fast Clock Recovery for Digital Communications
54 Aircraft Control-Position Indicator
55 Solar Cells With Multiple Small Junctions
55 Lowering Ammeter Input Impedance
56 Infrared Linear Imaging Array

Books and Reports

57 Power-Factor Controllers:How Safe?
57 Photovoltaics in Japan

Measuring Recombination Velocities in Solar Cells

A scanning-electron-microscope beam would probe BSF cells.

NASA's Jet Propulsion Laboratory, Pasadena, California

An electron-beam scanning method has been suggested for determining the back-surface recombination velocity, S_B, of a back-surface-field (BSF) solar photovoltaic cell. The recombination velocity is important because a smaller value is correlated with smaller saturation current and therefore higher cell efficiency. The method involves analyzing the short-circuit current measured while an electron beam is scanned along an edge of the cell.

Figure 1 gives a cross section (not to scale) of a BSF cell and the measurement geometry. The electric field of the p/p^+ junction confines the minority carriers (the electrons) to the bulk p region away from the ohmic back contact. The minority carriers therefore experience a considerably lower recombination velocity at the back surface than they do in cells with simple ohmic back contacts. While S_B is infinite for an ohmic back contact, it would ideally be zero for

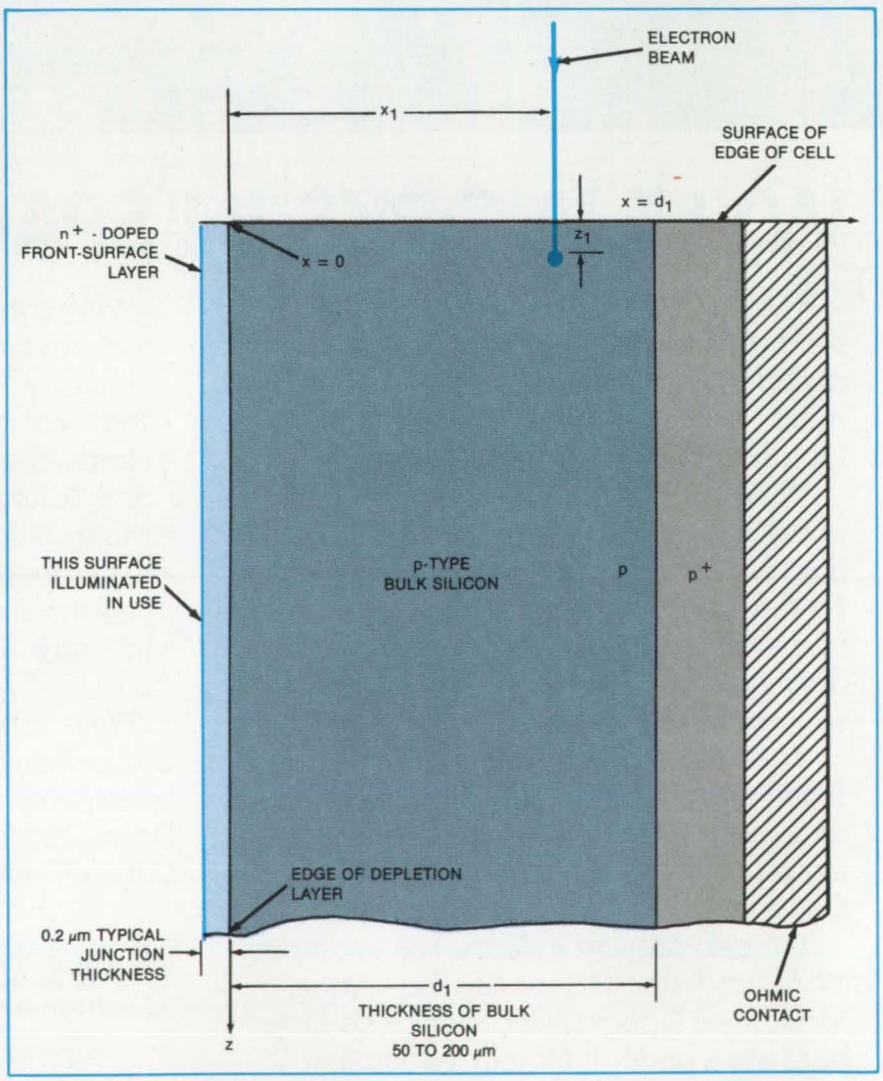

Figure 1. A **Back-Surface-Field Silicon Solar Cell** is probed by an electron beam that lies in a plane parallel to the faces and strikes the edge of the cell at depth x_1. The electron beam is conveniently generated by a scanning electron microscope.

a "perfect" BSF cell: In practice, S_B of a typical BSF cell lies between a few hundred and a thousand cm/s.

The theory of the method assumes a 30-keV electron beam, for which the radius of the volume of interaction with the bulk silicon of the cell is about 4 μm. In contrast, typical diffusion lengths are around 100 μm, and the bulk thickness, d_1, is at least 50 μm. Therefore, the interaction volume may be considered a point source of electron/hole pairs to simplify the theoretical diffusion analysis. Based on this assumption, an equation has been derived for the relative short-circuit cell current I_N as a function of the beam position x_1, the diffusion length L, the diffusion constant D, the interaction depth z_1, the recombination velocity S_T at the surface struck by the beam, and the previously defined quantities d_1 and S_B.

A sample plot of I_N vs. x_1 for various values of S_B is shown in Figure 2. One "brute-force" method for finding S_B and the other parameters is to calculate curves of I_N vs. x_1 for many different values of each parameter, then to select the curve that most closely approximates the measured I_N vs. x_1. A faster, less accurate approach might be to assume values for all the parameters except S_B, then to select the value of S_B for which the theoretical curve best matches the curvature of the measurement curve.

This work was done by Oldwig vonRoos and Keung L. Luke of Caltech for **NASA's Jet Propulsion Laboratory.** *For further information, Circle 54 on the TSP Request Card.*
NPO-16243

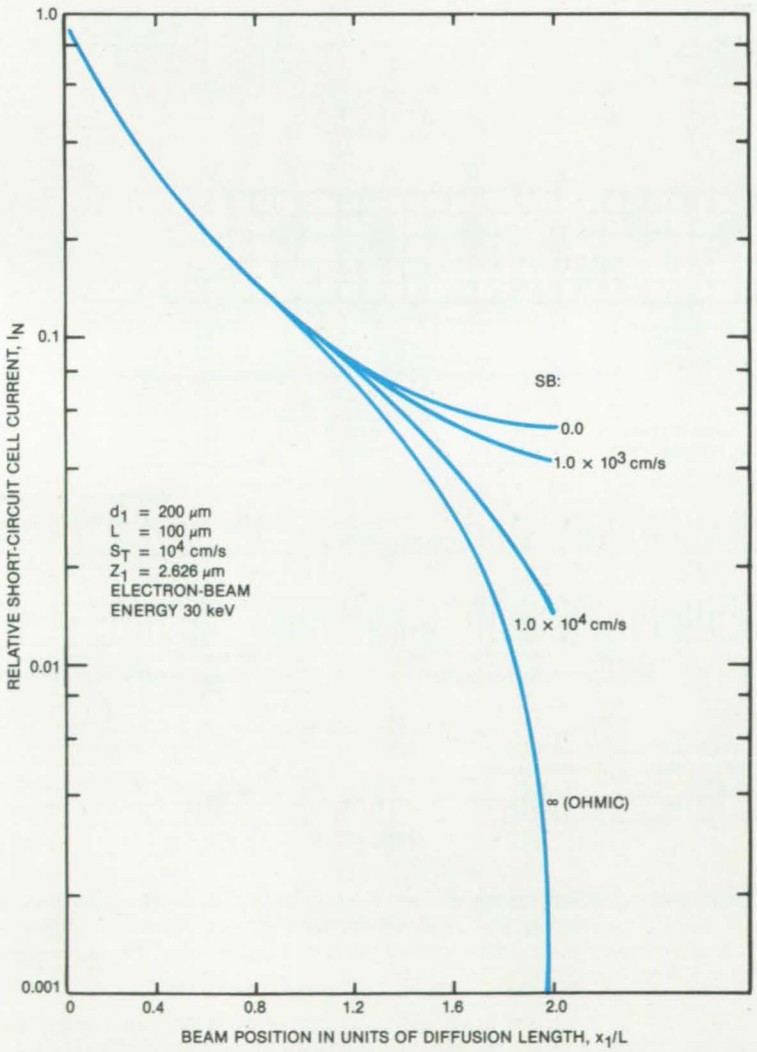

Figure 2. The **Theoretical Relative Short-Circuit Cell Current** generated by the electron beam is shown as a function of the beam position, x_1. The recombination velocity S_B is determined by matching such a curve to a set of measurements.

fisher SPACE PEN

...DEVELOPED FOR N.A.S.A.
...USED BY ASTRONAUTS ON SPACE FLIGHTS

Probably the world's most dependable pen. The patented pressurized cartridge developed for NASA permit these pens to write at any angle (even upside down) in severe temperatures −50° to +400°F, over glossy or greasy surfaces, under water and up to 3 times longer than ordinary pens.

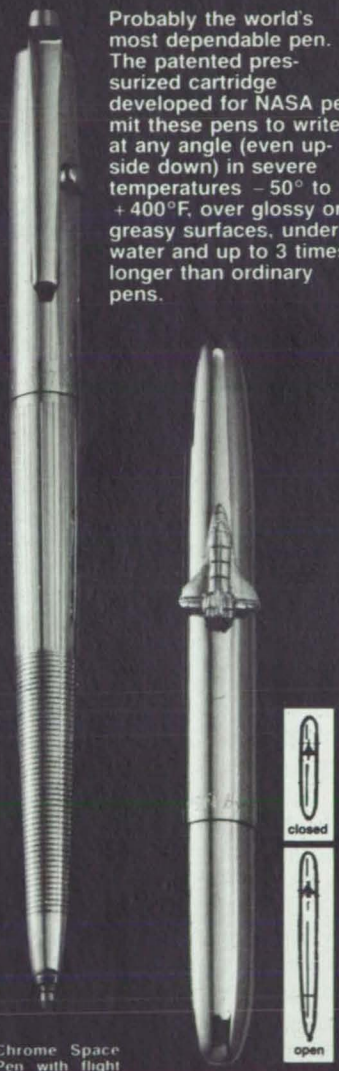

Chrome Space Pen with flight button point retraction. Refills readily available
$10.00

Chrome pocket/purse pen with distinctive Space Shuttle emblem. Unique compact design
$12.50

Fisher Space Pens are available wherever better pens are sold. Corporate logos and emblems are available. You may order or request further information by contacting:

PAUL C. FISHER
743 Circle Avenue
Forest Park, IL 60130
(312) 366-5030

Circle Reader Action No. 7

Hybrid Fiber-Optic/CCD Chip

Unit features low noise, high linearity, and high speed.

NASA's Jet Propulsion Laboratory, Pasadena, California

The low noise and linearity of charge-coupled devices (CCD's) are combined with optical waveguide components in a hybrid, integrated chip package. The concept is planned to be used to measure the laser flux in a fiber-gyro application using sensing fibers that could range from several to several tens of kilometers in length. The optical chip is near-shot-noise-limited by virtue of extremely small size and operates with a quantum efficiency of about 80 percent. Other potential applications include optical delay measurement and as a linear detector of light flux emanating from fiber-optic waveguides.

The chip layout is shown in Figure 1. The CCD detector is also a shift register that operates in a gated mode, typically at a clock rate of 10 MHz per phase in a three-phase application. The CCD elements are typically 30-μm square. Assuming a single-mode fiber diameter of 6 to 12 μm, a single element could collect all the light from the fiber.

As the outgoing laser pulse begins to travel along the fiber-optic path, reflections from components on the chip and backscatter from the fiber cause a spurious signal to reach the detector. Initially large, this signal drops rapidly. It is necessary to remove the spurious signal before the arrival of the weaker return signal, which is the signal to be measured.

Figure 2 illustrates how the detector is swept clean. During the outgoing laser pulse and for about 10 μs, the gate repeatedly shifts the detector vertically, thereby transferring out the charges generated by the spurious light signals. The rapid vertical charge sweeping is stopped just before arrival of the transmitted signal. The clock is then slowed, and the return signal is integrated and transferred out. Three vertical transfers are required to get the signal down to the output register. The signal is then transferred horizontally in the output register until it arrives at the output circuitry.

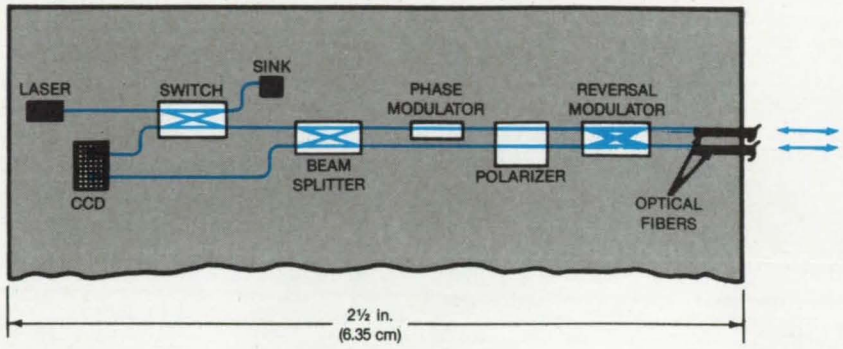

Figure 1. This **Integrated Chip** combines a CCD with a fiber-optic waveguide. The chip comprises all the passive and active optical elements needed to connect with a fiber-optic sensing coil for a fiber gyroscope.

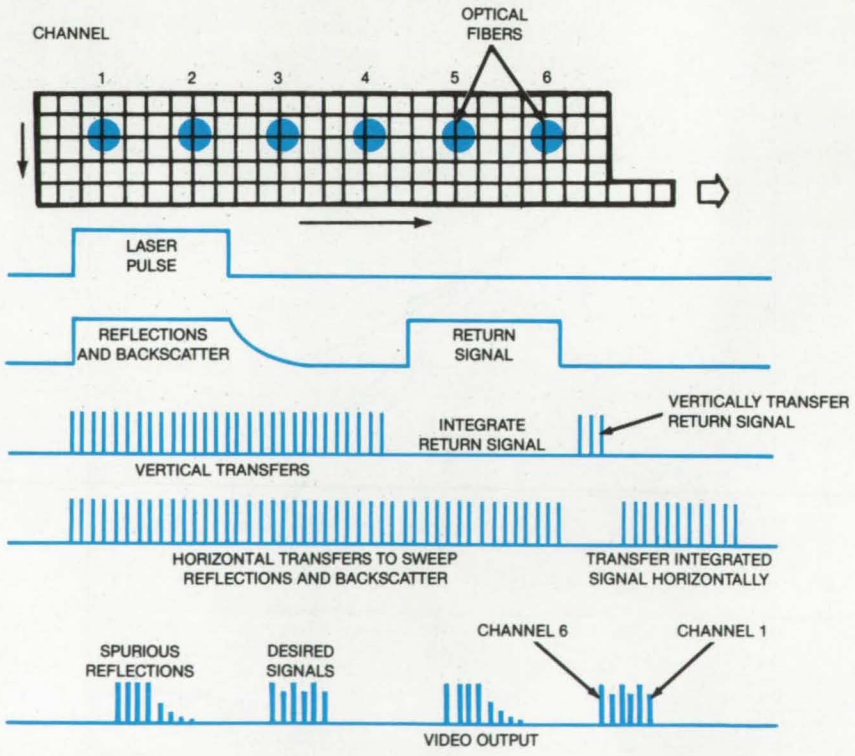

Figure 2. **Backscatter and Reflections** are swept out of the CCD by rapid vertical transfers to eliminate detector swamping. The rapid vertical transfers are stopped just before the arrival of the return signal. Horizontal transfers sweep the signal out of the output register of the CCD to the following stage.

This work was done by Willis C. Goss and James R. Janesick of Caltech for **NASA's Jet Propulsion Laboratory.** *For further information, Circle 56 on the TSP Request Card.*

Inquiries concerning rights for the commercial use of this invention should be addressed to the Patent Counsel, NASA Resident Office-JPL [see page 29]. Refer to NPO-16030.

Digital High-Current Monitor

Technique measures and digitally displays direct current up to several hundred amperes.

Langley Research Center, Hampton, Virginia

A simple technique has been developed for monitoring direct currents up to several hundred amperes and digitally displaying the values directly in current units. This technique can be used to monitor current magnitudes that are beyond the range of standard laboratory ammeters, which typically measure 10 to 20 amperes maximum.

A low-value resistor such as a 50-mV shunt is connected in series with a power supply in the supply remote sensing loop in order to eliminate the voltage drop across the resistor. For most applications, the resistor may be connected outside the loop since the drop is so small. The voltage across the resistor is monitored by a digital multimeter that has an X • Y math capability; i.e., that can multiply the input voltage by a constant and display the resulting current value digitally. For example, a 50-mV, 150-ampere shunt would require a multiplication factor of 150/0.050, or 3,000. If the shunt voltage were 0.025 volts, the meter would display a load current of 0.025 x 3,000, or 75 amperes.

One commercially available meter with an X • Y math capability, used in the prototype device, has four input channels so that four different shunt circuits can be scanned continuously and the current values printed if desired. This technique is applicable to any current-monitoring situation.

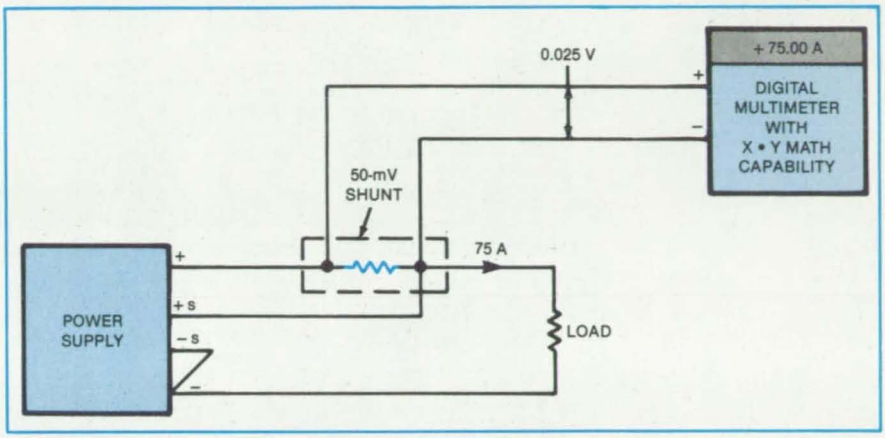

The **Voltage Across a Low-Value Resistor Is Monitored** by a multimeter with X • Y math capability.

This work was done by Bob Cash of Martin Marietta Corp. for **Langley Research Center.** *No further documentation is available.*
LAR-13072

Improved Thick Dichroic Reflector for Microwave Feeds

The geometry of a reflector plate is adjusted to compensate for undesired effects.

NASA's Jet Propulsion Laboratory, Pasadena, California

A small design change reduces depolarization and noise in a thick microwave dichroic reflecting plate that is tilted 30° from an orientation broadside to the incident beam. For all incident polarizations, the change makes the tilted plate exhibit the same electrical thickness that is presented by the unmodified, untilted plate.

As shown in Figure 1, the unmodified dichroic reflector is a thick plate with a hexagonal array of holes. When a circularly polarized beam is normally incident, the plate is nearly transparent at the resonant frequency. However, the plate is ordinarily tilted in use, so that there is a geometric difference between the discontinuities in the free-space-to-circular-waveguide transitions in the E- and H-planes. This difference shifts the E- and H-plane resonances to two different frequencies (one above and one below the normal-incidence resonant frequency) and gives rise to a difference in phase shift between the E- and H-planes.

The resonance shift and phase-shift difference result in partial depolarization of an incident circularly polarized beam, as well as undesired reflection at a fixed operating frequency. In the case of Figure 1, the resonant frequency of 8.415 GHz is split into 8.481 GHz and 8.363 GHz, the differential phase shift is 11.3°, the ellipticity is 1.84 dB, and the undesired power-average reflected-energy level is −18.6 dB at the 8.415-GHz design frequency.

The deficiencies are corrected by making the holes slightly noncircular in cross section to introduce a compensatory phase-shift difference between the E- and H-planes (in this case, −11.3°). The original hole-to-hole spacing and plate thickness are retained, but each hole is made with a pair of flats on opposite sides (see Figure 2), and the diameter of the remaining circular part is slightly changed. The electrical thicknesses of the modified plate in the E- and H-planes at the original resonant frequency then correspond to those of the unmodified plate at the split resonant frequencies.

In the case of the figures, the correction is achieved by enlarging the hole diameters only 0.013 cm and introducing flats of 0.043-cm depth. To test the redesigned holes, a sample section of plate measuring 35 by 53 cm was fabricated. The holes were made with a broach. The best performance was measured at the design frequency of

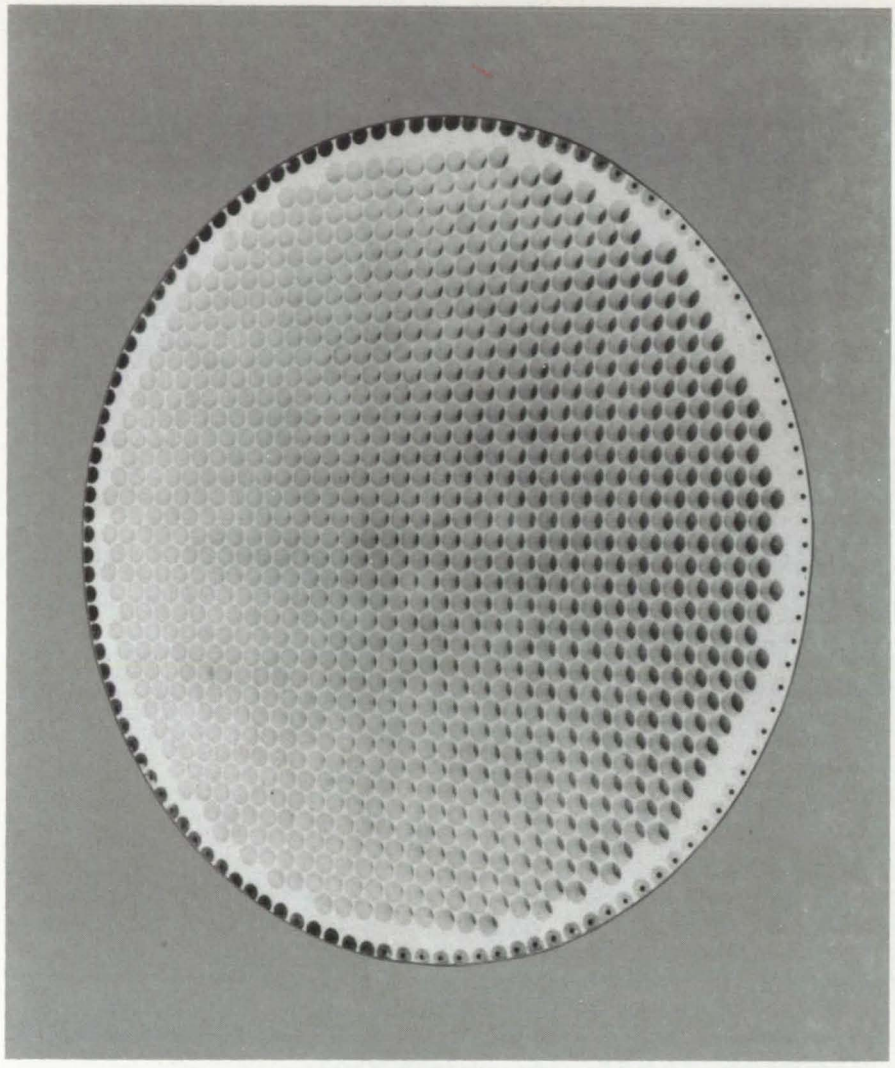

Figure 1. This **Dichroic Reflector** is designed for a resonant frequency of 8.415 GHz. The plate is 3.576 cm thick, with 2.273-cm-diameter holes spaced 2.388 cm center-to-center.

8.415 GHz. No pattern distortion, grating-lobe response, or other unexpected effects were observed. The ellipticity produced by the plate was reduced from 1.8 to 0.4 dB. The power-average reflection-lobe level was reduced to −24.5 dB.

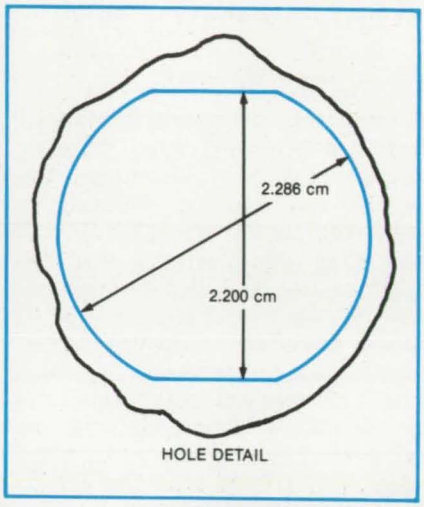

Figure 2. The **Modified Dichroic Reflector** resembles the dichroic reflector of Figure 1, except that the holes include flat side portions and round portions of slightly larger diameter.

This work was done by Philip D. Potter of Caltech for **NASA's Jet Propulsion Laboratory.** *For further information, Circle 60 on the TSP Request Card.*

Inquires concerning rights for the commercial use of this invention should be addressed to the Patent Counsel, NASA Resident Office—JPL [see page 29]. Refer to NPO-13506.

Tiltmeter Indicates Sense of Slope

The output of a dc bridge circuit depends on the tilt angle.

NASA's Jet Propulsion Laboratory, Pasadena, California

A tiltmeter that indicates the sense as well as the magnitude of a slope can be used in locations where the incline is not visible to the operator. Use of direct rather than alternating current greatly simplifies the design of an instrument capable of indicating the sense of the slope. Limiting the applied voltage to a maximum of about 0.5 volts avoids sensor damage that could otherwise result from the use of direct current. The dc excitation is applied across two outer electrodes and a center electrode in a three-electrode sensor connected in a bridge circuit (see figure).

Since the electrodes are immersed in an electrolyte that remains level while the sensor follows the tilt of the body on which it is placed, more of one outer electrode and less of the other are immersed and their resistances fall or rise, respectively. The resistance change causes a change in the output voltage of the bridge circuit.

Power for the instrument is furnished by a battery of two "AA" electrochemical cells. An operational amplifier provides an adjustable, regulated, low voltage to a measuring bridge. The sensor forms the two lower legs of the bridge, and two 1,000-ohm metal film resistors and a 200-ohm cermet balance potentiometer form the two upper legs.

The sensor is mounted with adhesive in a V groove in an aluminum base. A slot in the base accommodates the sensor terminals and lead wires. A cover protects the sensor from damage. Other components are mounted on a printed-wiring board. The board is equipped with banana plugs so that the bridge output can be connected directly to the digital multimeter that reads out the measurements.

In preparation for use, the bridge is balanced by adjusting the balance potentiometer so that the bridge output voltage

INTRODUCING THE LATEST IN DATA GENERAL'S ALL-STAR FEDERAL LINEUP:

THE DATA GENERAL/One™ PORTABLE.

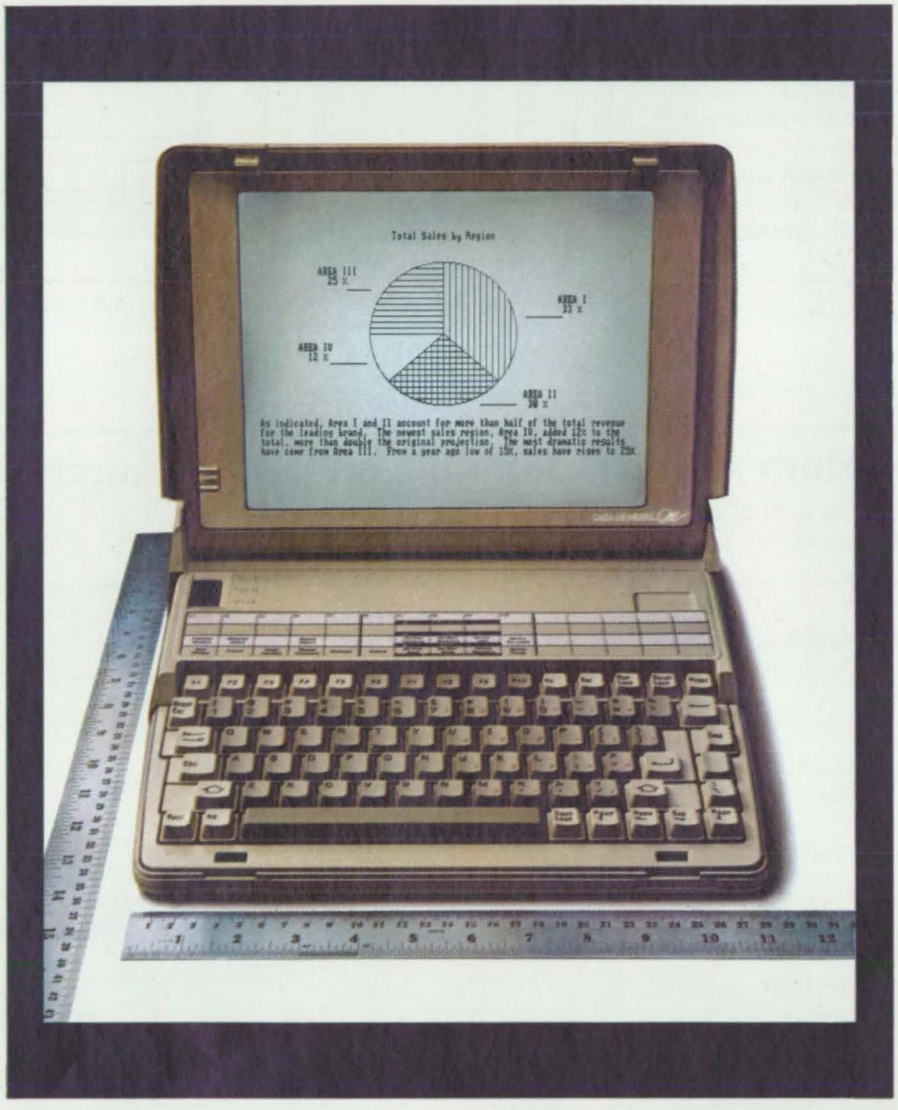

Free yourself from the confinement of your desk-bound computer, with the first full-function system for the Federal manager that lets you work anywhere.

The DATA GENERAL/One portable offers the capability of the leading PC in a size small enough to fit inside the average briefcase: 11.7 x 13.7 x 2.8 inches, and less than 11 pounds.

It's the only portable with a full-size 80-column by 25-line screen.

It's compatible with IBM®-PC software, so you can run the programs available to PC users. Software like 1-2-3™ and Symphony™ from Lotus,™ Wordstar,® dBase II,® Multiplan,® pfs® file and Flight Simulator II.

It's the only portable with two built-in 720 KB diskette drives, giving you twice the storage capacity of the leading PC. And memory is expandable up to 512 KB.

Options include a built-in modem, a portable printer, an 8-hour built-in battery pack, an external 1200-baud modem and an external 5.25-inch diskette drive.

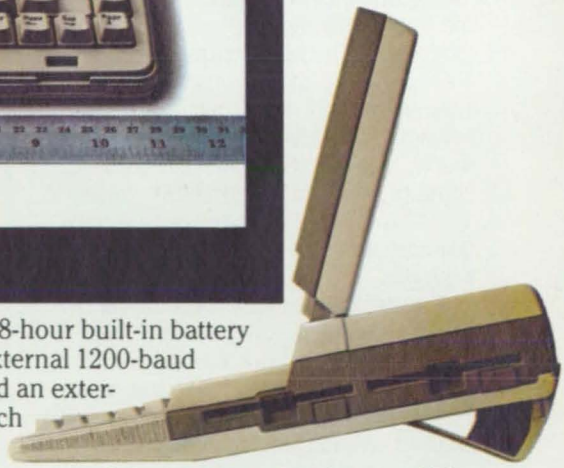

It has two built-in diskette drives and runs thousands of IBM-PC programs.

To find out more about the portable that gives you what the leading PC gives you—as well as your freedom—call 1-800-DATAGEN.

Data General
a Generation ahead.

IBM is a registered trademark of International Business Machines Corporation. 1-2-3, Lotus and Symphony are trademarks of Lotus Development Corp. © 1983. dBase II is a registered trademark of Ashton-Tate. Wordstar is a U.S. registered trademark of Micro Pro Int'l. Multiplan is a U.S. registered trademark of Microsoft Corp. pfs is a registered trademark of Software Publishing.
DATA GENERAL/One is a trademark of Data General Corp. © 1984 Data General Corp., Westboro, MA.

is zero when the sensor is level. Next, the bridge input voltage (dc excitation) is adjusted to provide about 10 millivolts output per degree of slope, the polarity indicating the sense of the slope. This scaling factor allows the multimeter to read directly in degrees if the user makes a mental shift of the meter decimal point. The scaling-factor calibration is done at several angles to determine the curve of output voltage versus angle. (In general, this curve is nonlinear but satisfactorily approximates linearity for angles up to about 5 degrees. A supply voltage of 0.410 volts was found to give the desired scale.

This work was done by James O. Lonborg of Caltech for **NASA's Jet Propulsion Laboratory.** *For further information, Circle 73 on the TSP Request Card.*
NPO-16153

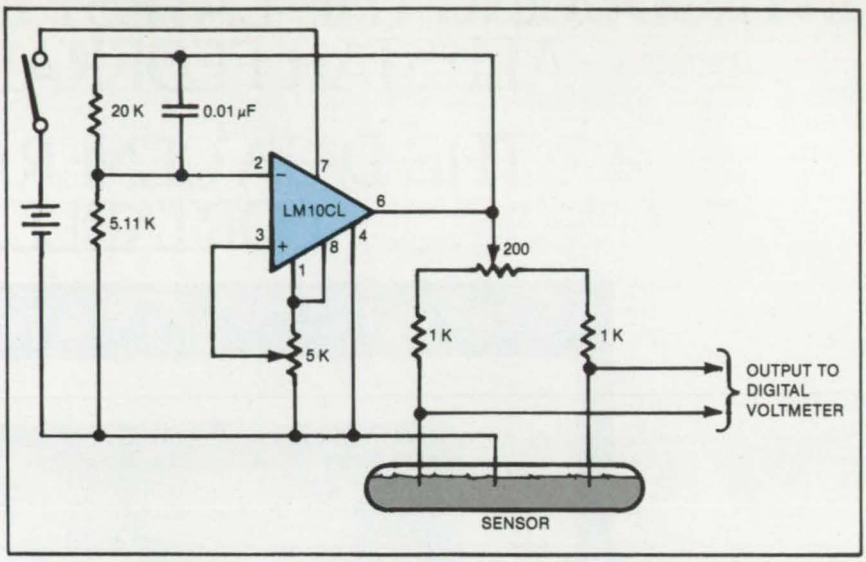

The **Tilt Sensor Forms Two Lower Legs** of a resistance bridge. Because the currents in the bridge are dc rather than ac, the polarity of the output to the digital voltmeter indicates the sense of the slope on which the sensor rests.

Dual-Mode Horn Antenna for Millimeter Wavelengths

Beam has nearly equal shapes in the E- and H-planes.

NASA's Jet Propulsion Laboratory, Pasadena, California

A millimeter-wave feed horn exhibits nearly equal beam-intensity patterns in the E- and H-planes as well as low side-lobe levels. The horn includes a circular waveguide, a step transition, and a conical section (see figure). The feed waveguide receives energy in the TE_{11} mode, and the step transition converts some of this energy to the TM_{11} mode. The TE_{11} and TM_{11} modes radiate from the horn aperture with their main lobes in phase.

The design is a simplified version of the Potter feed-horn design, which includes a matching iris in the circular waveguide and a step transition to an intermediate larger circular-waveguide phasing section adjacent to the cone. The new feed horn is easier to construct, in part because of the simpler shape. In addition, a reduction in the phase change between the step transition and the aperture increases the bandwidth, thereby reducing the precision required to manufacture the phase-sensitive dimensions of the horn.

Models for wavelengths of 0.5 and 1.4 mm were made by electroforming copper on an aluminum mandrel. Models for wavelengths of 3.1 and 34.2 mm were turned directly on a lathe.

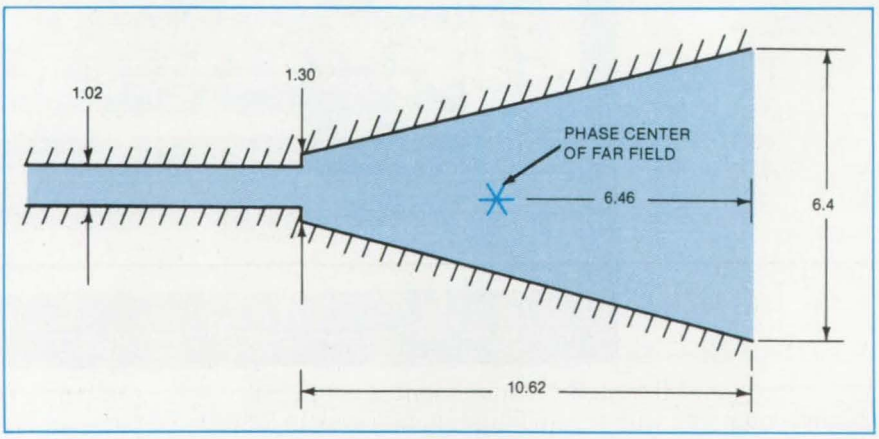

This **Feed Horn** is relatively easy to make, radiates similarly shaped beams in the E- and H-planes, has a well-defined phase center, and has a usable bandwidth of 10 to 20 percent of the design frequency. The dimensions shown here are in wavelengths at the design frequency.

The far-field patterns of the models were measured in the E- and H-planes. In each case, the patterns were equal within 1 dB, down to the −10 dB level. The average half-power beam width was 6° half angle. Far-field measurements for the 34.2-mm horn showed a well-defined phase center 6.46 wavelengths inside the aperture. The waveguide reflection loss was measured over a 30-percent bandwidth centered at 34 mm. The reflected power was less than −23 dB over the whole band, corresponding to a voltage standing-wave ratio of 1.15.

This work was done by Herbert M. Pickett of Caltech for **NASA's Jet Propulsion Laboratory.** *For further information, Circle 17 on the TSP Request Card.*
NPO-16297

Flux Coupling for Wheelchair Battery Chargers

Mobile units plug in magnetically instead of electrically.

NASA's Jet Propulsion Laboratory, Pasadena, California

A battery-charger concept for wheelchairs includes magnetic-flux coupling instead of electrical connections between power sources and wheelchairs. The concept is meant to facilitate operation by patients whose disabilities make it difficult or impossible to maneuver common electrical plugs into or out of ac wall outlets.

In the new charger concept, the transformer core is split (see figure). The primary winding and half the core are mounted at the charging station at a standard distance above the floor. The secondary winding and the remaining half of the core are mounted on the wheelchair at the standard height. The rest of the charging system, including the power-conditioning electronics and the battery, is also mounted on the wheelchair.

The patient maneuvers the wheelchair into a position in which the two core halves are approximately alined with each other. Two tapered shafts on the wheelchair half mate with two tapered holes on the charging-station half to complete the alinement as the wheelchair is moved toward the charging station. The core halves are mounted on springs that absorb small vertical and horizontal misalinements.

This work was done by Colonel W. T. McLyman of Caltech for **NASA's Jet Propulsion Laboratory.** *For further information, Circle 52 on the TSP Request Card.*
NPO-16269

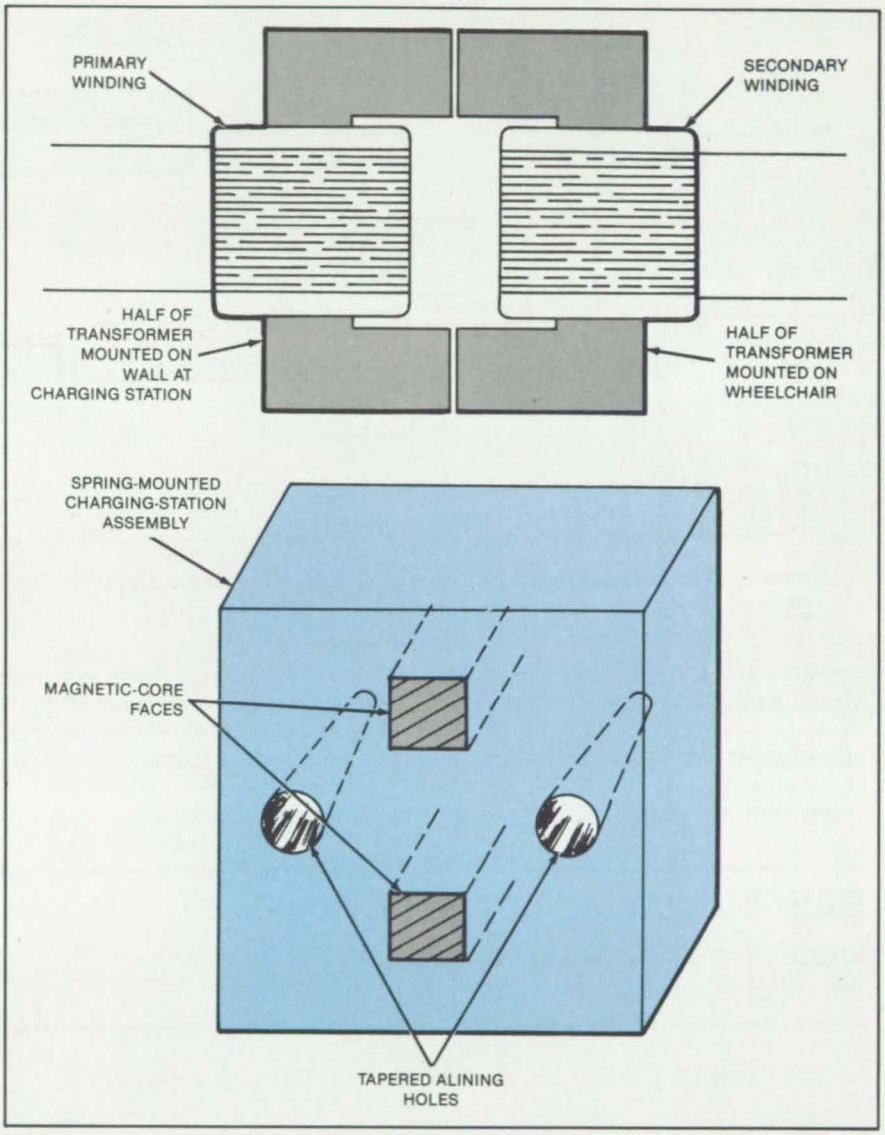

Power is Coupled from the stationary (charging-station) unit to the mobile (wheelchair) unit by bringing the two transformer-core halves together to complete the magnetic-flux path. Tapered holes and shafts help to aline the magnetic-core halves.

Signal Processor for Multirate PSK Signals

A hard-limiting Costas loop improves performance for NRZ and Manchester data.

Lyndon B. Johnson Space Center, Houston, Texas

Any of six different data formats at any of five different data rates from a phase-shift-key (PSK) modulated input signal is extracted by a digital radio receiver originally developed for the Space Shuttle. The ability to handle 30 different input combinations with a minimal number of filters is a result of the use of a hard-limiting Costas loop in the receiver (see figure). The loop makes it possible for the receiver to accept data in Manchester code as well as in

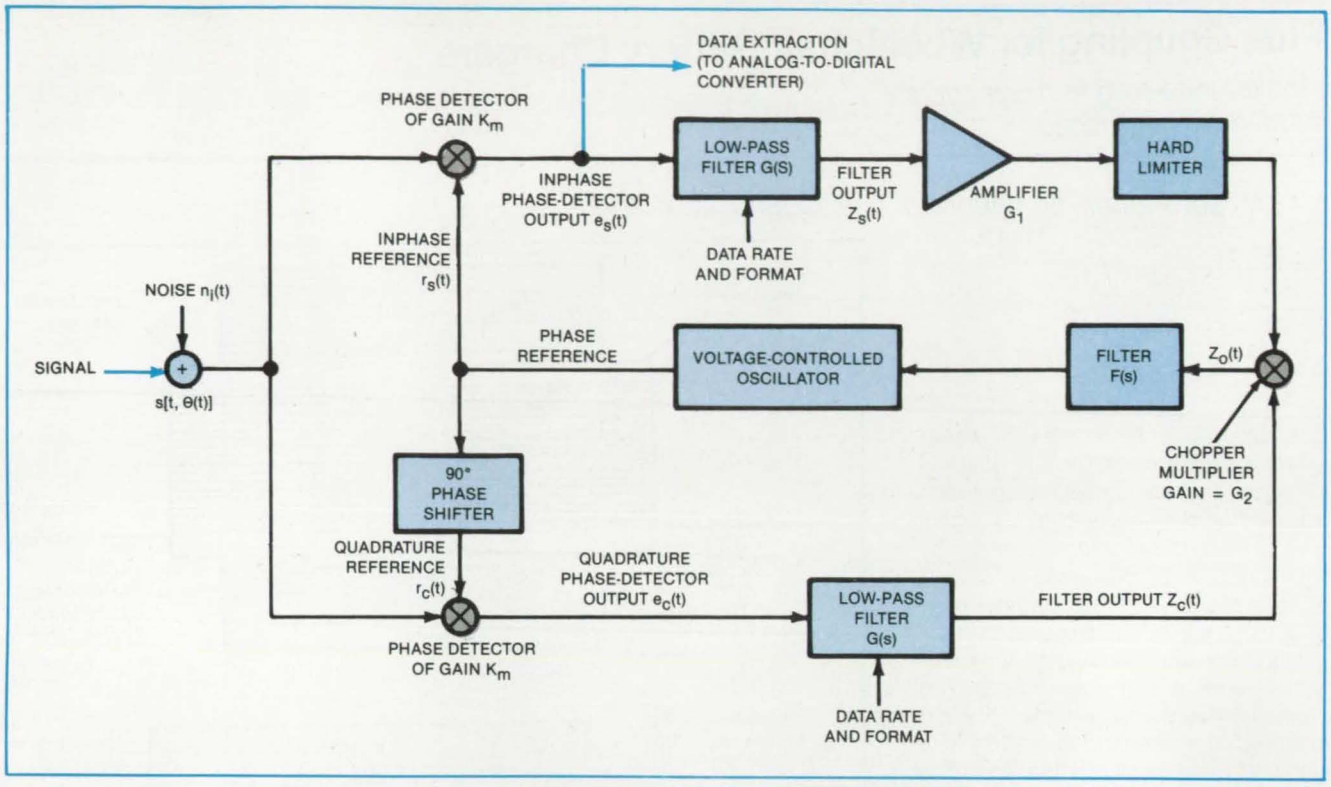

The **Subcarrier Demodulator** is a Costas loop with a hard limiter in the inphase arm. There are six low-pass filters, each selectable for the rate and format of data to be processed.

nonreturn-to-zero (NRZ) code. The hard-limiting loop outperforms the conventional Costas loop for signal-to-noise ratios greater than 2 dB in both NRZ and Manchester formats.

The receiver extracts data from a 1.024-MHz subcarrier that is PSK-modulated in either Manchester or NRZ format at 1, 2, 4, 8, or 16 kilobits per second. It has performed successfully in breadboard and engineering-model tests.

This work was done by Richard J. Helgesen of TRW, Inc., for **Johnson Space Center.** *For further information, Circle 53 on the TSP Request Card.*
MSC-20195

SAW-Modulated Image Device

Image resolution is varied by adjusting the modulation frequency.

Langley Research Center, Hampton, Virginia

A proposed imaging device uses surface-acoustic-wave (SAW) charge transfer for image readout. The spatial resolution of the image can be changed electronically by changing the frequency of an applied signal.

In the proposed device (see figure), surface acoustic waves create traveling longitudinal electric fields. These fields, in turn, create potential wells that carry along stored charges. The charges are injected into the wells by photoelectric conversion when light strikes the device.

Several SAW charge transfer devices are constructed side by side on a monolithic substrate, such that the traveling longitudinal electric fields created in the substrate are in evenly spaced parallel straight lines. Each charge transfer device is fed by two frequency sources. The first frequency source (f_1) creates traveling electric fields along the straight lines in one direction. The second frequency (f_2), a harmonic of the first, results in a traveling longitudinal electric field in the opposite direction. The second frequency signal has the same amplitude as the first frequency signal and is phase stable with respect to it.

The traveling longitudinal electric fields superimpose to create a standing wave at a frequency equal to the difference between the frequencies of the input signals. Consequently, when light strikes the device, charges are stored in the wells of the standing waves.

After the charge is stored, the second frequency signal is removed, causing the standing wave to break up. When this happens, the traveling longitudinal electric field caused by the first frequency signal pushes the charges through the device. An electrode for each standing wave is located so that the charges can be removed from the device and applied to an external circuit. The magnitude and time of arrival of each charge are indicative of the intensity of the light and the spatial location of that intensity. The second frequency can be changed to vary the spatial resolution of the device.

This work was done by Harry F. Benz of **Langley Research Center.** *Further information may be found in the U.S. Patent referenced below, which may be purchased for $0.50 a copy from the U.S. Patent and Trademark Office, Washington, D.C. 20231.*

This invention has been patented by NASA [U.S. Patent No. 4,279,001]. Inquires concerning nonexclusive or exclusive license for its commercial development should be addressed to Howard J. Osborn, Langley Research Center, Mail Code 279, Hampton, VA 23665, Telephone: (804) 865-3725. Refer to LAR-12633.

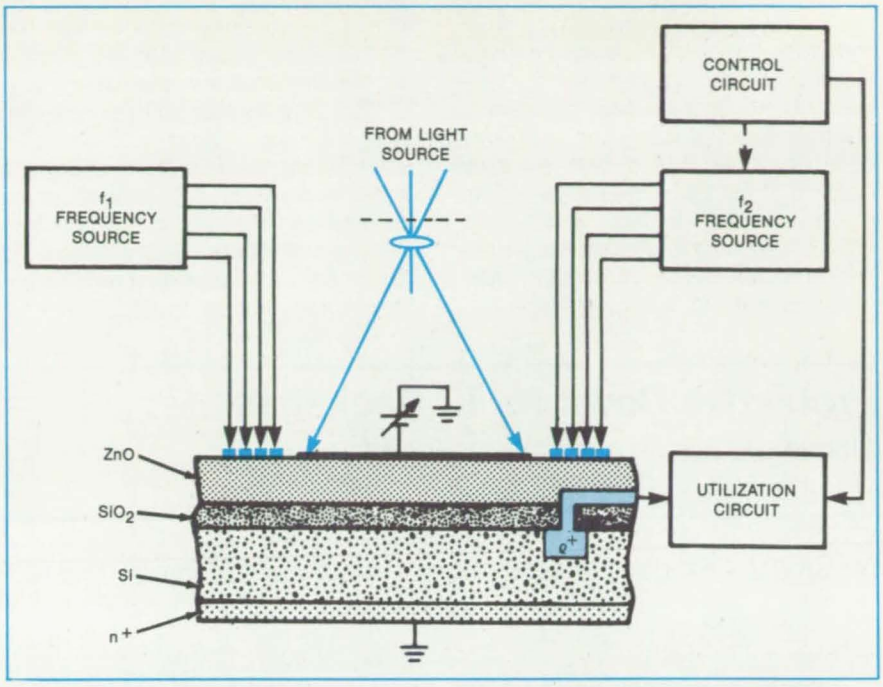

The **Imaging Device** includes an n-type silicon substrate, a thermally grown silicon dioxide layer, and a sputtered film of piezoelectric ZnO. A ground electrode is deposited on the substrate. A transparent metallic biasing plate deposited on the piezoelectric layer is connected to ground through a variable voltage. The biasing plate enhances the acoustoelectric potential at the silicon dioxide interface, resulting in higher efficiency. A charge detecting diode is located in the silicon layer.

Damping Relaxation Oscillations in Laser Diodes

Modulation frequency could be varied from dc to near resonance in proposed device.

NASA's Jet Propulsion Laboratory, Pasadena, California

A proposed semiconductor laser could be modulated at frequencies up to near its resonant frequency more efficiently than could older devices. Until now, two of the ways to prevent relaxation oscillations at resonance have been to connect an untuned impedance in parallel with the laser diode or to diffuse carriers out of the active region. Both methods consume a significant fraction of the laser current even at frequencies far from resonance, where damping of relaxation oscillations is not needed. A tuned parallel impedance gives some improvement, but is ineffective when the resonant frequency changes because of aging or a shift in the laser bias.

The new laser would use two different effective carrier lifetimes: one for dc and low-frequency operation and another for operation near the resonant frequency. The laser would be part of a bipolar transistor with a capacitor that serves as an ac short circuit (see figure). The laser active region would be part of the transistor emitter.

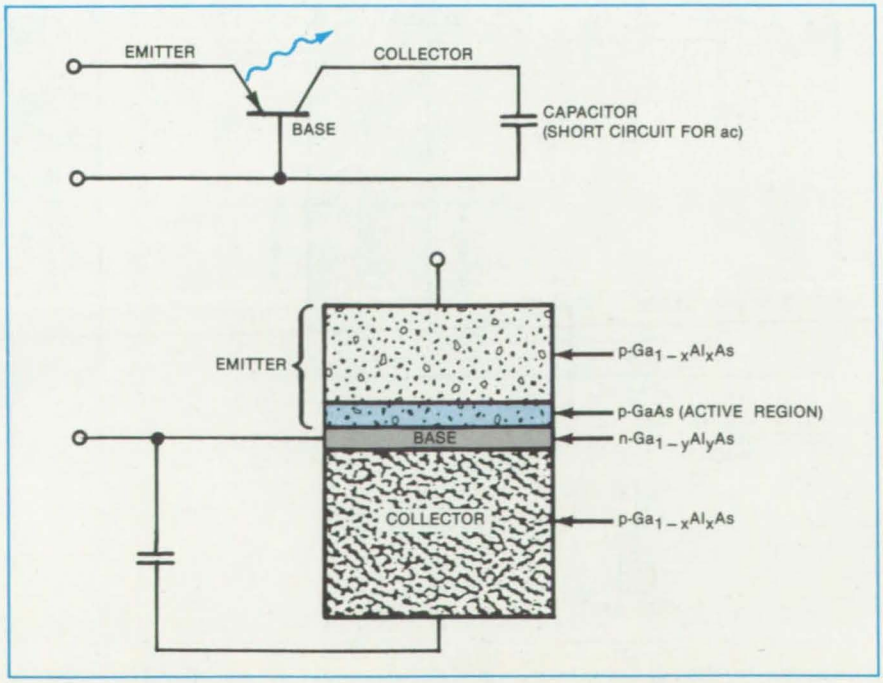

This **Dual-Carrier-Lifetime** laser is part of a transistor in which the emitter is the light source.

At dc and low-frequency modulation, there is only a small reduction in carrier lifetime by the recombination of carriers leaking from the active region into the base. At frequencies near resonance, however, the photon and carrier populations decouple, and a carrier-density gradient is set up in the active region. Since the collector/base junction is short circuited for ac, the excess carrier concentration there is zero. In the base, on the other hand, a large diffusion current created by the carrier-density gradient causes a large leakage current out of the active region, and the effective carrier lifetime is reduced there.

This damping mechanism comes into play only near resonance. The efficient operation of the laser is not affected at other frequencies. An additional advantage arises from the fact that both transistor junctions are forward biased: The laser can be operated as a two-terminal device with dc bias applied at one terminal and modulation applied at the other terminal.

This work was done by Joseph Katz, Amnon Yariv, and Shlomo Margalit of Caltech for **NASA's Jet Propulsion Laboratory.** *For further information, Circle 29 on the TSP Request Card.*

Inquires concerning rights for the commercial use of this invention should be addressed to the Patent Counsel, NASA Resident Office-JPL [see page 29]. Refer to NPO-15980.

Protective Cover for IC Packages

Aluminized plastic protects integrated circuits from static discharge.

NASA's Jet Propulsion Laboratory, Pasadena, California

A snap-on cover shorts the leads of an integrated-circuit flatpack to prevent damage from electrostatic discharges during transport, installation, or other handling before final testing. The cover is removed only during lead bending and testing. Although originally developed by NASA for use with flatpacks for spacecraft electronics, the design can be adapted to other package shapes.

The protective cover shown in the figure is fabricated in plastic, such as molded PVC, and is aluminum-coated on all sides by vacuum deposition. Aluminum-coated Mylar (or equivalent) strips, 0.001 to 0.002 in. (25 to 50 μm) thick, are bonded to the inner surfaces using a conductive adhesive. The conductive strips short the flatpack leads.

This work was done by Thomas J. Borden of Caltech for **NASA's Jet Propulsion Laboratory.** *For further information, Circle 57 on the TSP Request Card.* *NPO-15537*

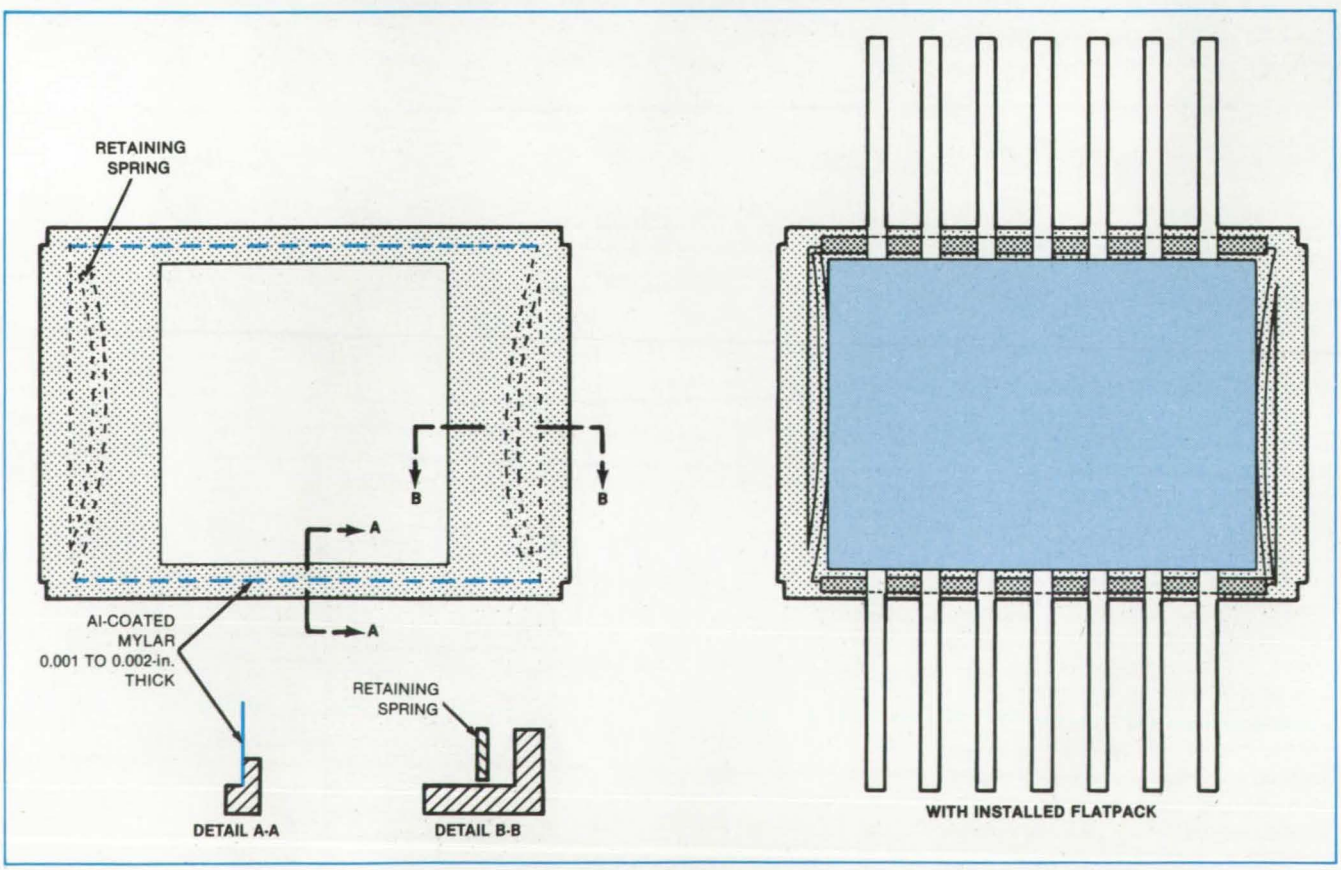

The **Protective Plastic Cover** is aluminum-coated on all surfaces. Aluminum-coated strips are bonded to the inner surfaces. Springs molded into each end of the cover secure it on the integrated circuit.

Recovering Energy From Relays

Circuit returns inductively stored energy to the powerline.

NASA's Jet Propulsion Laboratory, Pasadena, California

The magnetic energy stored in a relay is recovered with the aid of a simple circuit. The circuit recovers more than 20 percent of the energy stored in the relay winding and returns it to the powerline.

Ordinarily, a standard commercial single-coil relay is equipped with a suppression circuit consisting of a diode and a resistor (see figure). When the relay coil current is turned off, the suppression circuit disposes of the energy stored in the coil and thereby prevents arcing and transient voltages. When the relay transistor Q_1 is on, there is current in the coil L_1. When Q_1 is turned off, the energy stored in the coil is dissipated in the resistor R_1.

It would be possible to recover the energy by adding a winding that is inductively coupled to the original winding. However, the extra winding would add considerably to the cost of the relay. As before, when transistor Q_1 is on, there is current in coil L_1. When Q_1 is turned off, the energy in L_1 is transferred to the added coil L_2, commutated through D_1, and returned to the source.

The new three-transistor driver circuit, however, requires no additional winding. When transistor Q_3 is on, transistors Q_1 and Q_2 are on, and there is current in coil L_1. When Q_3 is turned off, Q_1 and Q_2 are also turned off. The energy stored in L_1, which acts as an isolated voltage source, is commutated through diodes D_1 and D_2 and returned to the source.

This work was done by Colonel W. T. McLyman of Caltech for **NASA's Jet Propulsion Laboratory.** *For further information, Circle 111 on the TSP Request Card.*
NPO-16268

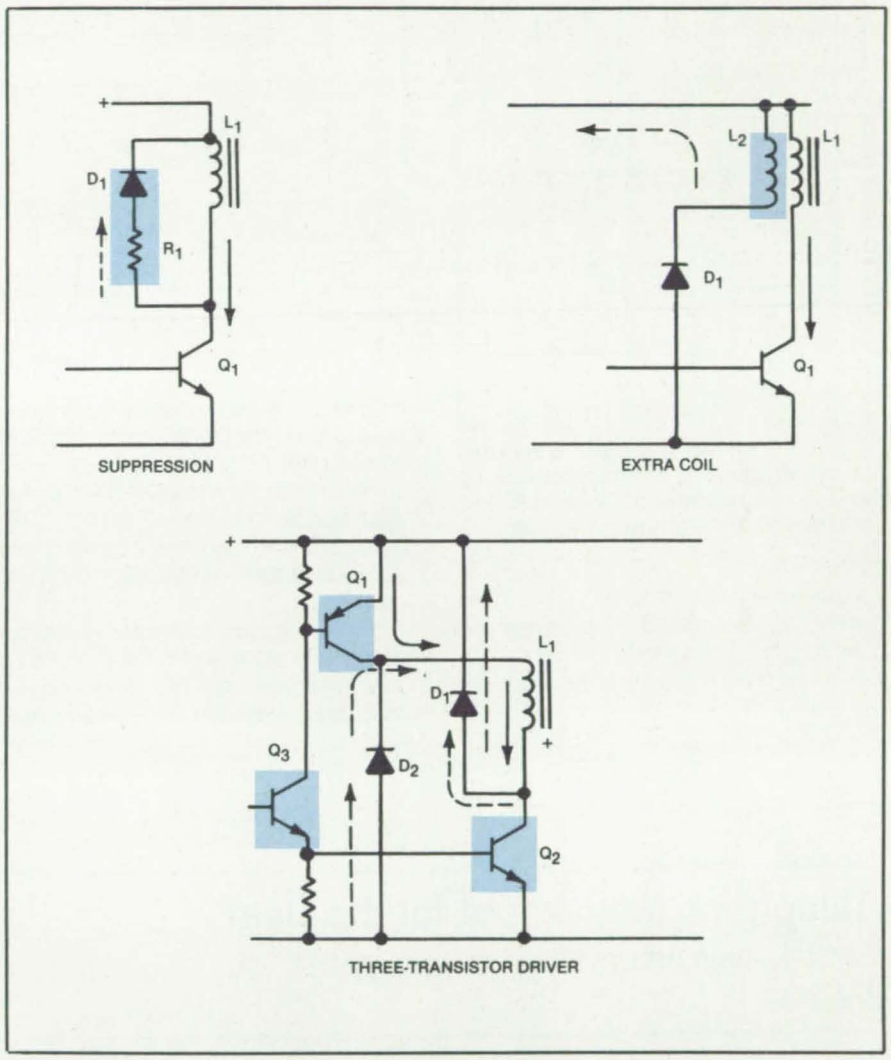

Three Ways of Handling Energy released by a turned-off relay are to dissipate it in a suppression circuit, to return it to the line with the aid of an extra relay coil, and to return it to the line with the aid of a three-transistor, two-diode circuit. The last method not only saves energy but also uses only inexpensive components. Solid arrows indicate current when relay is on. Dashed arrows show current immediately after turnoff.

Resistive Fine Tuning of Resonant Circuit

Frequency is continuously adjustable over a narrow range.

NASA's Jet Propulsion Laboratory, Pasadena, California

A simple fixed-inductance/fixed-capacitance tank circuit is modified for fine adjustment of the resonant frequency by the addition of a small inductance with a potentiometer across it. The additional winding could be built into the full winding as an integral part or could be added externally, as in the circuit of Figure 1. A typical value of the additional inductance would be about 10 percent of the main inductance.

With the tuning capacitor connected to the potentiometer cursor instead of to the end of L_1, the resonant frequency is continuously variable via the potentio-

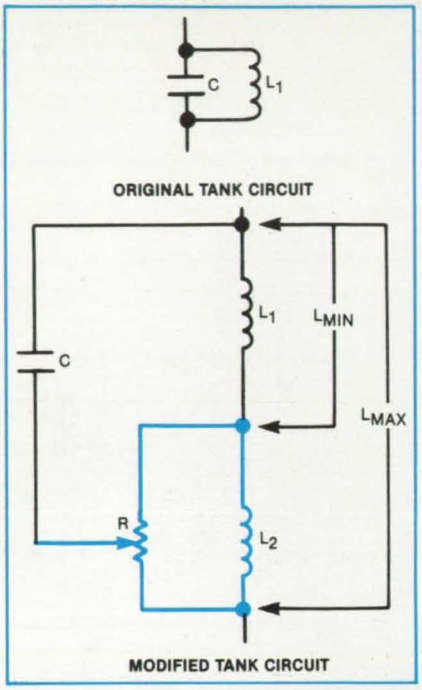

Figure 1. A **Simple Tank Circuit Is Modified** by the addition of a small inductance, L_2, and a potentiometer, R, to enable fine adjustment of the resonant frequency.

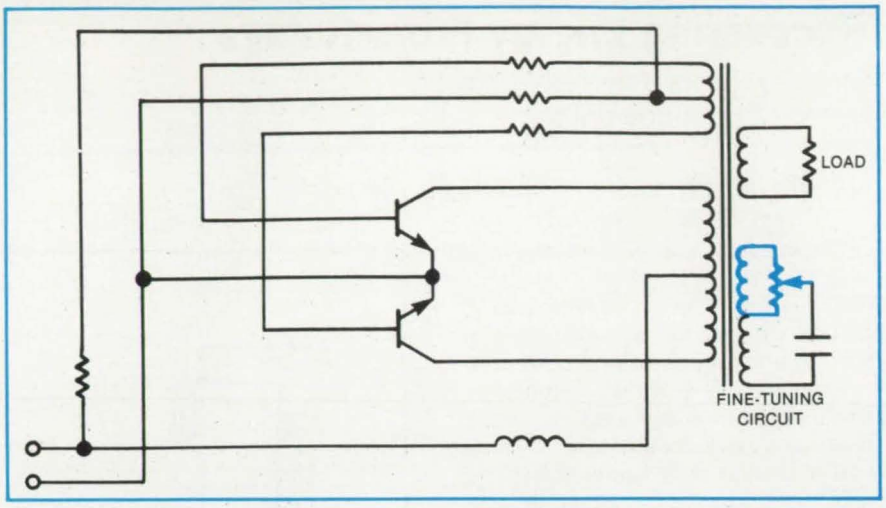

Figure 2. The **Fine-Tuning Circuit** is used here to adjust the frequency of a sine-wave oscillator.

meter adjustment. When the tap is at the end of L_1, the inductance is lowest and the frequency is highest. The opposite is the case when the tap is at the outer end of L_2.

This technique provides a quick way of tuning the reactance out of a power-transformer circuit to maximize power transfer or to adjust the frequency of an oscillator like the one in Figure 2. Likely applications include rotary transformers, servo amplifiers, and analog computer modules.

Some care must be taken in the use of this technique and in the selection of the potentiometer. The potentiometer resistance may critically damp or overdamp the circuit, thereby destroying the resonance. In such a case, one may have to resort to such conventional tuning means as variable capacitors or inductors, switchable chains of fixed capacitors, transformer taps, or trial-and-error selection of components.

This work was done by Colonel W. T. McLyman of Caltech for **NASA's Jet Propulsion Laboratory.** *For further information, Circle 79 on the TSP Request Card.*
NPO-16276

Telephone Instrument for the Deaf

Letters and numbers would be transmitted by tones to a decoder.

John F. Kennedy Space Center, Florida

A proposed telephone-communication scheme for the deaf would use existing tone-encoded telephone equipment to transmit messages. The only special equipment required is a decoder at the receiving telephone. A deaf person, if able to speak, could verbally instruct a hearing person at the other end how to transmit messages.

In the proposed system, numbers would be transmitted by pressing the number buttons, thereby generating the number tones normally used for dialing. To transmit one of the three letters on a number button, one would first press the "#", "0" (zero), or "*" button to signify the left, center, or right letter, then press the number button bearing the desired letter.

At the receiving end, a standard tone decoder would convert the stream of signals to a digital code. The digital code would be processed to drive an alphanumeric display, computer, or teletype. A numerical "reset" sequence of tones would be sent at the start of a message to reset the decoder.

In an alternative scheme, the first of three letters on a number button would be sent by pressing that button. The second and third letters would be sent by pressing that button and simultaneously pressing the "*" or "#" button. The disadvantages of this scheme are that it would not work on all tone-encoded telephones and that combinations of letters and numbers cannot be sent.

This work was done by William Henry Brown of **Kennedy Space Center.** *For further information, Circle 107 on the TSP Request Card.*

Inquiries concerning rights for the commercial use of this invention should be addressed to the Patent Counsel, Kennedy Space Center [see page 29]. Refer to KSC-11303.

Double Light-Emitting Diode

Two diodes are packaged together for greater reliability.

Goddard Space Flight Center, Greenbelt, Maryland

Two GaAs light-emitting diodes packaged as a single unit offer greater reliability than the conventional single-diode package. One diode is the primary light source. If it fails, the backup diode is switched in. Each diode has a separate power lead, so that either or both can be switched on or off at the same time.

So that readjustment of the associated optics is not necessary when switching from one diode to the other, the light sources lie within 0.006 in. (0.15 mm) of each other. At the same time, the package minimizes the mechanical stress on the fragile GaAs and serves as a heat sink.

The two-diode package is shown in the figure. The two diode chips are stacked with a copper-mesh ribbon between them serving as the common positive power lead: The mesh imposes less stress on the chips than would a solid ribbon. The active area of both chips is grown as close as possible to the ribbon to obtain the required light-source spacing. For additional mechanical support, one end of the ribbon is mounted on a non-light-emitting, reverse-biased GaAs chip. The assembly is mounted on the modified header of a standard TO-18 package.

This work was done by Robert L. Johnson and Thomas C. Hall of Hughes Aircraft Co. for **Goddard Space Flight Center.** *For further information, Circle 24 on the TSP Request Card.*
GSC-12832

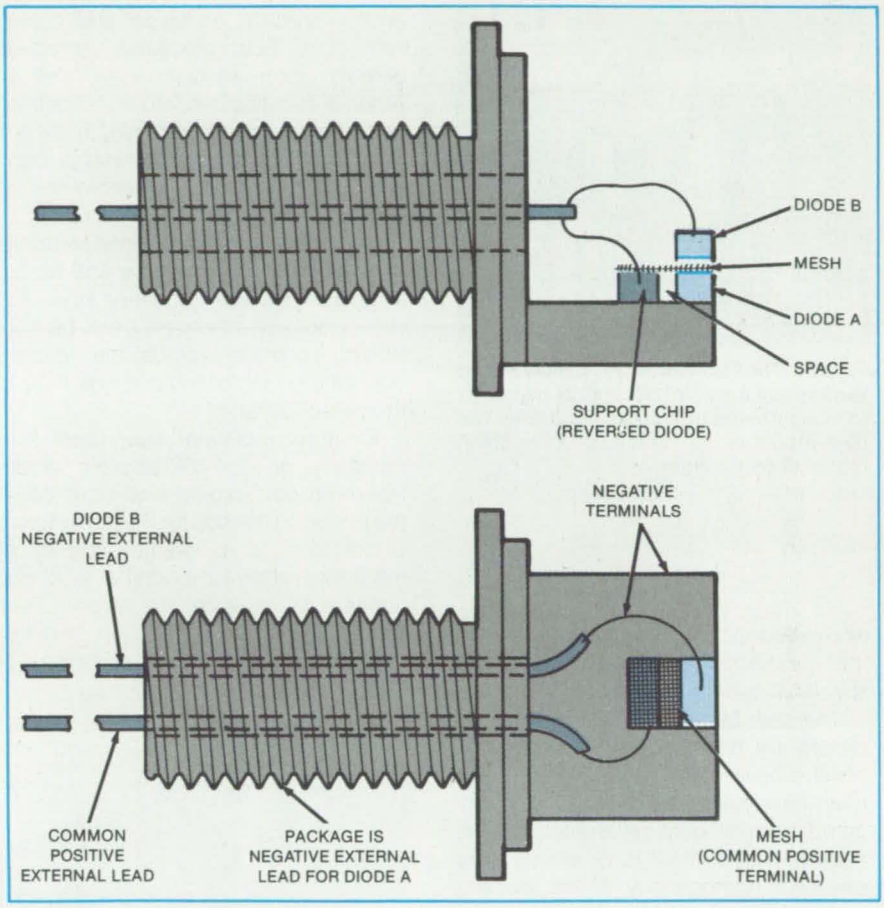

Two Light-Emitting Diodes are stacked together to provide redundant line sources of light. This arrangement gives the required mechanical support to the delicate GaAs diode chips while permitting them to be closely spaced and adequately cooled by thermal conduction through the package.

Fast-Recovery, High-Voltage Power Diode

The diodes are rated at a peak reverse voltage of 1,200 V and average forward currents of 50 and 150 A.

Lewis Research Center, Cleveland, Ohio

A new family of fast-recovery high-voltage power diodes compatible with the D60T and D7ST transistors [*NASA Tech Briefs* "High-Speed, High-Power, Switching Transistor," Vol. 3, No. 3, p. 320 (LEW-13021), and "High-Power Switching Transistor," Vol. 7, No. 4, p. 371 (LEW-13728)] has been developed. They have a wide range of applications in spacecraft and aircraft electrical distribution equipment, in dc/dc inverters, and in ac motor controllers for high-horsepower electric motors operating from 480-volt ac lines.

The new diodes are rated on the basis of peak reverse voltage at 1,200 volts and average forward current ratings of 50 and 150 amperes. Both diodes are shown in Figure 1. The 50-ampere model has a peak surge-current capability of 1,000 amperes and is being packaged in a modified DO-5 package. The 150-ampere model will pass a peak surge current of 3,000 amperes in a standard DO-8 package. Both diodes have a forward voltage drop of less than 1.5 volts at rated current and recover their blocking capability in 200 to 400 nanoseconds when commutated from rated current at 25 to 50 amperes per

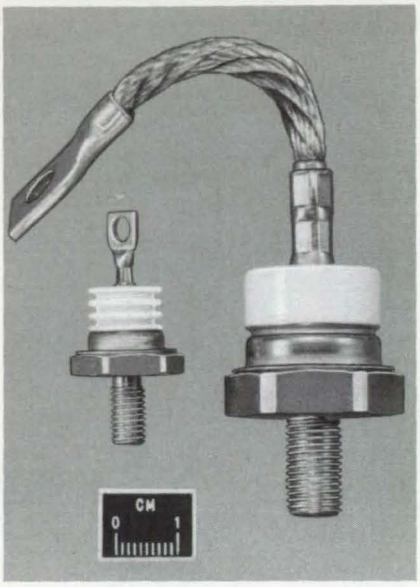

Figure 1. The **Fast-Recovery, 1,200-V Power Diodes** use a chip of hexagonal geometry to maximize the effective silicon area. The 50-A model is on the left, and the 150-A model is on the right.

microsecond. The ceramic tops enable the packages to meet all NEMA specifications for 480-volt ac systems.

The new fast-recovery silicon power diodes are designed and built using a positive-bevel, PIN mesa structure with glass passivation. The devices are fabricated from 35-ohm-centimeter, n-type, neutron-doped, float-zone silicon. The excellent homogeneity of the starting material results in better manufacturing yields and device performance.

A hexagonal geometry for the diode chip is used to maximize the effective silicon area within the circular walls of the packages. Figure 2 shows the hexagonal silicon chip mounted and contacted within a DO-5 header for the 50-ampere diode. Maximizing the effective silicon area keeps the forward voltage drop low by reducing current density.

A positive-bevel mesa structure is used to reduce surface electric fields on the silicon chip. A circular or hexagonal (either is effective) mesa moat is etched through the n^+/n cathode and some distance into the p^+ anode region resulting in a positive-beveled junction. The moat is then filled with high-temperature glass to passivate the junction, providing an effective hermetic seal for the silicon chip.

A unique trimetal, metalization process compatible with glass-passivated junctions and with solder-reflow assembly was developed for the diode. The trimetal — aluminum, titanium, and nickel — metalizing on the anode and cathode results both in extremely high reliability in the solder bonds and in low-cost manufacturing procedures.

To obtain the fast recovery times of 200 to 400 nanoseconds, the lifetime of minority carriers within the diode was modified. Two methods were used: high-energy electron radiation and doping with gold. Both processes introduce defects such as vacancies and interstitial substitutions into the silicon lattice. These defects provide traps and energy levels within the energy band gap of silicon that act as recombination centers for the current carriers.

Increasing the defect density reduces the average carrier lifetime and results in shorter reverse recovery time. The defect density, however, must be controlled accurately since the forward voltage drop increases proportionally to the defect density.

Electron radiation was used successfully on the 50-ampere diode. However, gold doping was selected as the preferred method for the 150-ampere diodes due to its greater stability at the solder-reflow temperature. Gold also appears to enhance the surge-current rating of the devices. Therefore, gold doping will be used in the manufacture of both diode models.

Reverse recovery times were tested in a JEDEC circuit. The tests were performed at 100° C with recovery from the rated currents of 50 and 150 amperes at dI/dt values of 25 and 50 amperes per microsecond, respectively. Reverse recovery times run typically from 200 to 500 nanoseconds.

Reverse leakage at 1,000 volts and 150° C is 0.2 to 5.0 milliamperes for the diodes. Forward voltage is typically in the range of 1.35 to 1.50 volts at rated current.

This work was done by G. R. Sundberg of **Lewis Research Center** *and A. H. Berman, V. Balodis, C. Gaugh, J. J. Duffin, H. Karatnicki, and E. Larson of Power Transistor Co. Further information may be found in:*

NASA CR-165411 [N81-32382/NSP], "Development & Fabrication of a Fast Recovery, High Voltage Power Diode" [$11.50], and

NASA CR-168196 [N84-13443/NSP], "Development & Fabrication of a Fast Recovery, High Voltage Power Diode" [$10].

Copies of these reports may be purchased [prepayment required] from the National Technical Information Service, Springfield, Virginia 22161.

LEW-14036

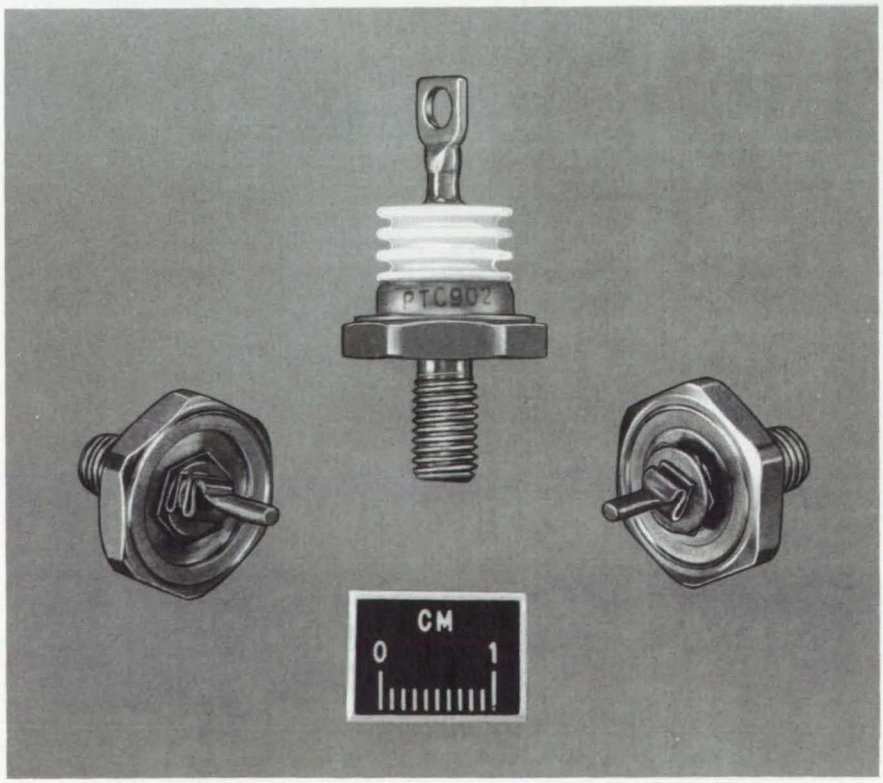

Figure 2. **View of the 50-A Diode With Two Uncapped Bases:** On the left is a reverse-polarity diode in which the glass-filled circular moat area and hexagonal geometry are visible. The standard diode on the right requires a higher pedestal to prevent arc-over to the base at high voltage.

Complementary-Logic Fault Detector

Error-correcting complementary-logic signals are the output.

NASA's Jet Propulsion Laboratory, Pasadena, California

A circuit for checking two-line complementary-logic bits for single faults is used as a building block for a self-checking memory interface for Hamming-coded data. It is intended for such applications as fault-tolerant computing, data handling, and data transmission. The circuit performs an exclusive-OR function.

Two-line complementary logic uses redundancy to provide an error check. Suppose that two signals are denoted A and B, with the four conductors and their logic states denoted a_0, a_1, b_0, and b_1, respectively. Line A is said to be in the logic "1" state when the voltage on its conductors correspond to $a_0 = 0, a_1 = 1$. The logic "0" state of line A is $a_0 = 1$, $a_1 = 0$. Similarly, the logic "1" and "0" states of line B are $b_0 = 0, b_1 = 1$ and $b_0 = 1, b_1 = 0$, respectively. All other states indicate a fault condition.

When the circuits are operating correctly, a_0 and a_1 or b_0 and b_1 are in opposite logic states at all times. Erroneous conditions include both lines in the "0" state, both lines in the "1" state, or both conductors in the same line at the "0" or "1" voltage level. The only correct states are the two shown at the top of the table. Any other combination of logic levels on the four conductors represents a fault.

The circuit shown in the figure accepts inputs from lines A and B and gives an output on line C depending on the condition of the inputs. If lines A and B are in either of the two correct states, the output is A exclusive-OR B. An erroneous input combination gives rise to one of the output error indications shown in the table.

The circuit can also be used to complement (invert) a bit signal. This feature can be used to correct an error if the error can be attributed to the proper bit line. With the proper Hamming code, a single error can be corrected by converting the data to the configuration that requires the least change from the erroneous configuration. Many such circuits can be combined to produce a complete memory interface with both detection and correction abilities.

This work was done by John C. Wawrzynek of Caltech for **NASA's Jet Propulsion Laboratory.** *For further information, Circle 51 on the TSP Request Card.*
NPO-15410

Only Two Logic States Are Correct for the four conductors in lines A and B. These are shown at the top of the table. Any other combination of logic levels signifies an error in data processing or transmission. The circuit of the figure produces an output indicative of the correctness or of the type of error in the logic levels on the four conductors.

INPUTS				OUTPUT	
A		B		C	
a_0	a_1	b_0	b_1	c_0	c_1
0	1	1	0	0	1
1	0	0	1	0	1
0	1	0	1	1	0
1	0	1	0	1	0
0	0	x	x	0	0
1	1	x	x	1	1
x	x	0	0	a_0	a_0
x	x	1	1	a_1	a_1

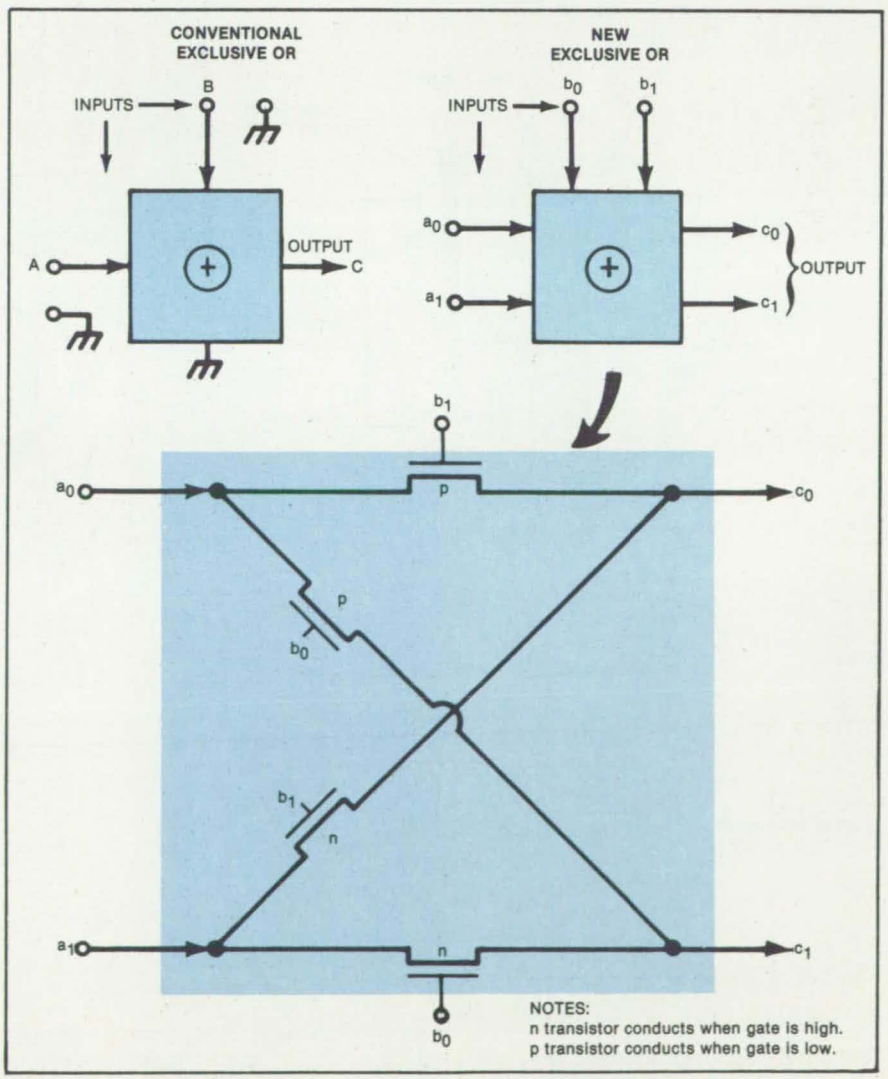

Signals A (a_0, a_1) and B (b_0, b_1) are fed to the new circuit. An error indication is obtained for any input combination other than (a_0, a_1; b_0, b_1) = (0, 1; 1, 0) or (1, 0; 0, 1).

High-Voltage Isolation Transformer

Construction avoids airgaps in which arcs can form.

Goddard Space Flight Center, Greenbelt, Maryland

Arcing and field-induced surface erosion are reduced by electrostatic shields around the windings and ferromagnetic core of an 80-kilovolt isolation transformer. Fabricated from a high-resistivity polyurethane-based material that is brushed on the critical surfaces, the shields are maintained at approximately half the potential difference of the windings.

The primary and secondary windings of the transformer are each held on spools mounted on a ferromagnetic core (see figure). The bores and channels of the spools are coated with the resistive layers. These layers completely encase and electrostatically separate the coils from the other components of the transformer.

In construction of the transformer, a layer of epoxy is first applied to the bores and channels. This layer, about 0.001 to 0.002 inch (0.03 to 0.05 mm) thick when hardened, is brushed on as a thin solution. It dries to become an insulating layer having high breakdown voltage.

Next, the adhesive layers are coated with the resistive layers. Also brushed on as a thin solution, these layers consist of carbon black as the conductive constituent in a polyurethane medium. Again, the resistive layers are 0.001 to 0.002 inch thick.

The primary and secondary coils, consisting of insulated copper wire, are wound in the channels. Then, the electrostatic shielding can be completed. The solution of polyurethane and carbon black is brushed on the coils. The solution is drawn into the spaces between turns of the wire by capillary action.

The channel conductive layers are connected electrically to their respective coil return leads to prevent arcing between shields and leads. Similarly, the conductive

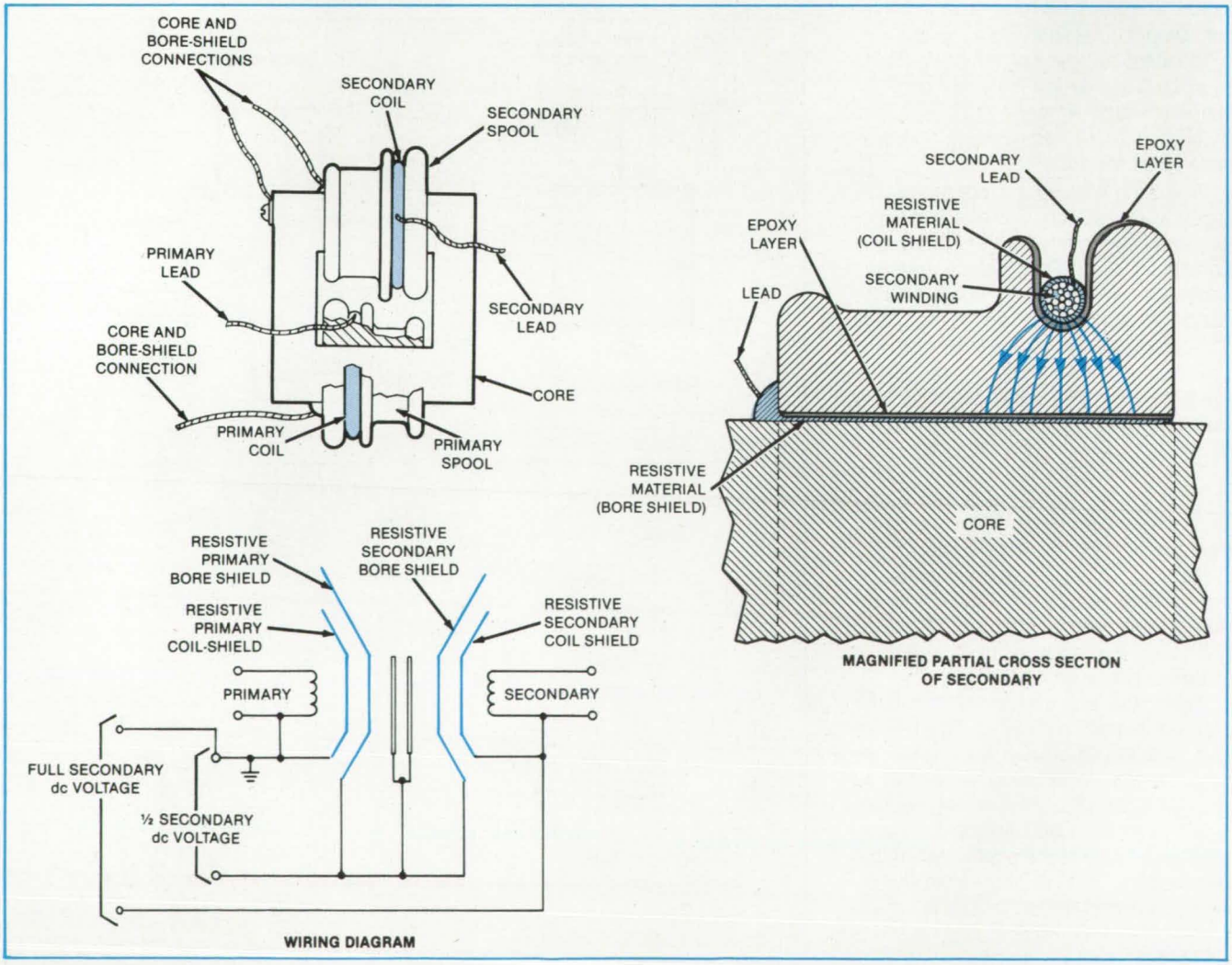

Conformal Electrostatic Shielding decreases electric fields by spreading out local charge concentrations, as indicated by spreading of the field lines that would otherwise concentrate at the individual wires in the windings. As a result, less stress is placed on the insulating materials in the windings and spools. Moreover, the proximity of the outer turns of the coils and the conductive coatings and the intimate adhesive contact between the conductive coatings and the channels prevent local concentrations of field across air pockets.

layers in the bores are connected electrically to the core to prevent sparking.

In one application of the transformer, a constant voltage of −80 kV was applied to the conductive coating and return lead of the secondary coil while a constant voltage of −40 kV was applied to the core and conductive coatings in the bores of both the primary and secondary spools. An alternating voltage of 9 to 18 volts was applied across the primary coil. Under these conditions, the transformer performed without sparking or corona and completely isolated the constant voltage on the secondary coil from the primary coil.

This work was done by Carroll H. Clatterbuck and Arthur P. Ruitberg of **Goddard Space Flight Center.** *For further information, Circle 58 on the TSP Request Card.*

This invention is owned by NASA, and a patent application has been filed. Inquiries concerning nonexclusive or exclusive license for its commercial development should be addressed to the Patent Counsel, Goddard Space Flight Center *[see page 29].* *Refer to GSC-12817.*

Fast Clock Recovery for Digital Communications

Circuit synchronizes with unprecedented speed.

NASA's Jet Propulsion Laboratory, Pasadena, California

A circuit extracts the clock signal from a random non-return-to-zero data stream, locking onto the clock within one bit period at a 1-gigabit-per-second data rate. The circuit is used for synchronization in optical-fiber communications. It derives its speed from the very short response time of gallium arsenide metal/semiconductor field-effect transistors (MESFET's).

The circuit employs only two dual-gate MESFET's, two single-gate MESFET's, two microwave delay lines, and a few associated operational amplifiers, capacitors, and resistors (see Figure 1). The circuit essentially consists of two NAND gates and two delay transmission lines (see Figure 2). This combination works as two oscillators, each of which runs freely when its input line is in a high state. The unsynchronized (freely running) oscillator frequency, f, depends on the transmission line delay, τ_d, and the gate delay, τ_g, according to

$$f = \frac{1}{2(\tau_g + \tau_d)}.$$

The transmission line is designed so that τ_d gives an oscillator frequency nominally equal to the clock frequency.

When the state of the input is low, the first oscillator does not run freely, and its output remains in the high state, causing the second oscillator to run freely. If the input to the first NAND gate is made high by the receipt of a 1 bit, the first oscillator goes through one cycle of oscillation, creating an inverted return-to-zero (RZ) 1 bit at its output. During this time, a 0 is initially present at the input of the second NAND gate, causing its output to be high regardless of the state of the other input.

The trailing edge of the inverted RZ 1 bit starts the second NAND-gate oscillator in phase with the single incoming 1. The circuit thereafter provides a clock signal that remains in phase with the clock of the incoming data as long as such data are received. When data cease to be received, the oscillators return to free running and slowly drift out of synchronization at a rate that depends on the actual oscillator frequency.

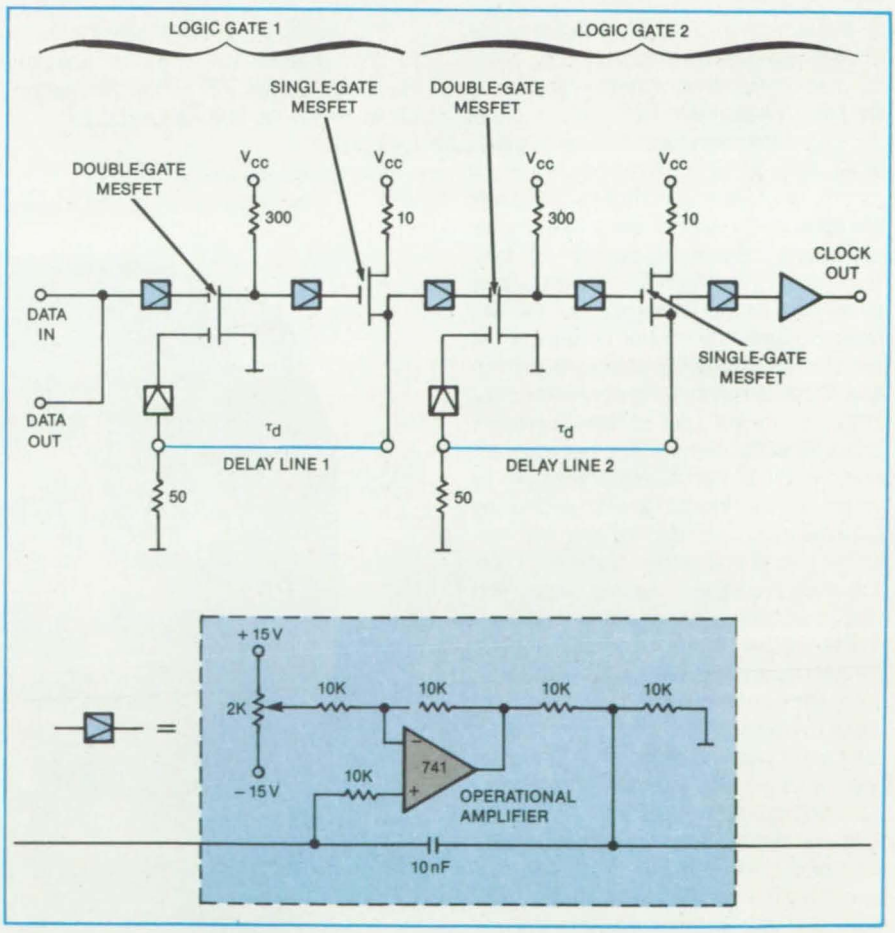

Figure 1. The **Circuit Includes Operational Amplifiers** to change the level of the incoming signal to a value appropriate for the gates of the MESFET's. The slew rate of the operational amplifiers must be high enough to charge the 10-nF capacitors before the input signal itself does. Single-gate MESFET's are used as source followers. The microwave delay lines must be terminated with 50-ohm resistances to avoid reflections back to the outputs of the source followers.

The performance of the circuit was measured with equipment capable of measuring bit-error rates in a 1-gigabit-per-second data stream. A 4,095-bit-long pseudorandom output from a transmitter was fed into the circuit, then into the error detector. The error rate was less than 1 in 10^{12} — that is, no errors were detected. This error rate is the same as that which would be measured in the clock taken directly from the transmitter.

This work was done by Robert G. Tell of Caltech for **NASA's Jet Propulsion Laboratory.** *For further information, Circle 114 on the TSP Request Card.*
NPO-16083

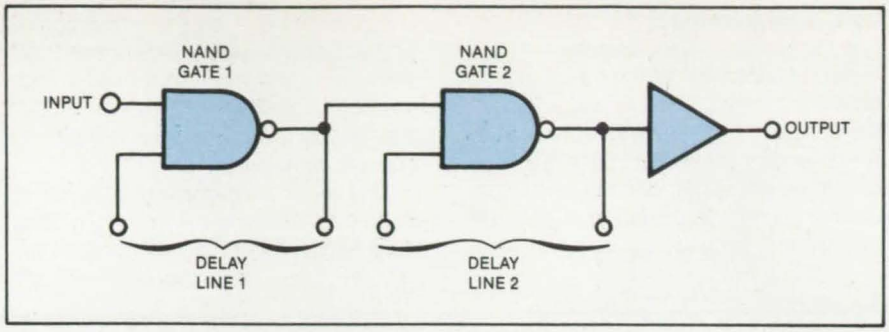

Figure 2. The **Frequency of Oscillation** of this NAND-gate-and-delay-line combination is determined by the delays in the gates and the propagation delays in the transmission lines. The gate delay, which is highly temperature-sensitive, should be small in comparison to the propagation delay.

Aircraft Control-Position Indicator

Easily readable, zero-lag display is maintenance-free.

Langley Research Center, Hampton, Virginia

The aircraft control-position indicator is a cockpit-mounted instrument that displays the positions of the elevator and the ailerons to the pilot. The display is mounted in a standard flight instrument case 3 inches (7.6 centimeters) in diameter. The display is a cruciform array of lights: A horizontal row of amber lights and a vertical row of green lights representing aileron and elevator positions, respectively (see figure). A single, larger green light at the intersection of the two rows indicates the neutral position of the elevator. Two exposed amber lights at each side of the center green light provide a clear indication to the pilot of less-than-exact centering of the ailerons. All other lights are covered by a translucent shield. All indicators are electronically driven by instantly-acting transducers and an integrated circuit that senses the analog voltage level, providing a zero-lag display and easy readability under all light conditions.

The display has been used extensively in spin testing and has been trouble-free, with no maintenance required after about 30 hours of operation. No preflight checks or setups are required of the pilot. The main features of the display are easy readability and zero lag in showing control-surface positions. The display allows rapid, precise, control repositioning with very little overshoot tendency. The aircraft control-position indicator is reliable, maintenance-free, and extremely easy to read with immediate perception of its message. These features should make it valuable for other flight-test and flight applications where similar requirements apply.

This work was done by Dale V. Dennis of Kentron International, Inc., for **Langley Research Center.** *For further information, Circle 110 on the TSP Request Card.*
LAR-12984

This invention is owned by NASA, and a patent application has been filed. Inquiries concerning nonexclusive or exclusive license for its commercial development should be addressed to the Patent Counsel, Langley Research Center *[see page 29].* *Refer to LAR-12984,*

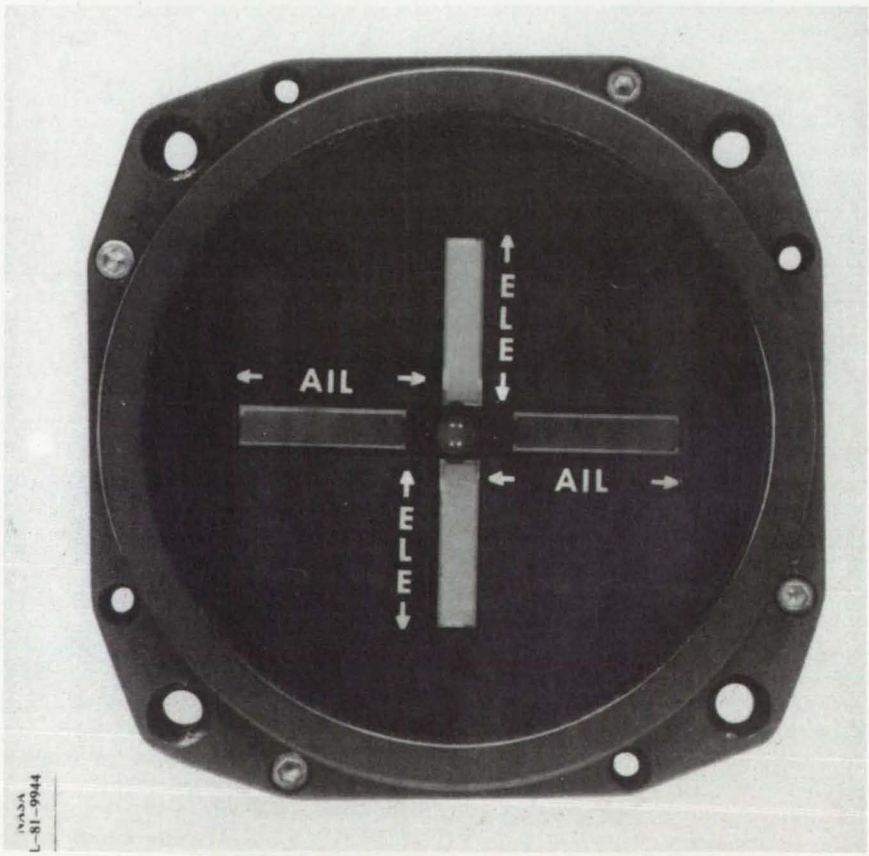

Vertical and Horizontal Light Arrays indicate the elevator and aileron positions.

Solar Cells With Multiple Small Junctions

As junction area is reduced in relation to total cell area, efficiency should go up.

NASA's Jet Propulsion Laboratory, Pasadena, California

A concept for improving the efficiency of photovoltaic solar cells, based on decreasing the p/n junction area in relation to the total surface area of a cell is proposed. Instead of a single continuous junction underlying the entire surface of the cell, multiple round junctions would be formed (see figure). The junctions would be 10 micrometers in diameter. Their centers would be spaced 50 micrometers apart. Their total surface area would be about 3 percent of the surface area of the cell.

The open-circuit voltage of a silicon p/n junction cell is given by

$$V_{oc} = \frac{kT}{q} \ln\left(\frac{I_{sc}}{I_o} + 1\right)$$

where k = the Boltzmann constant, T = the absolute temperature, q = the electronic charge, I_{sc} = the short-circuit current, and I_o = the saturation current. According to this equation, the open-circuit voltage would be increased by increasing the ratio I_{sc}/I_o.

The short-circuit current depends on the total illuminated area of the cell while the saturation current depends on the junction area. According to the proposal, the junction area would be reduced while the total illuminated area would be kept constant, so that I_o would be reduced and the ratio I_{sc}/I_o would be increased. If a single junction is replaced by many small round junctions of the size and shape described above, the open-circuit voltage should rise by more than 60 mV, thereby increasing the cell efficiency and output power. Cells should be made by the following procedure.

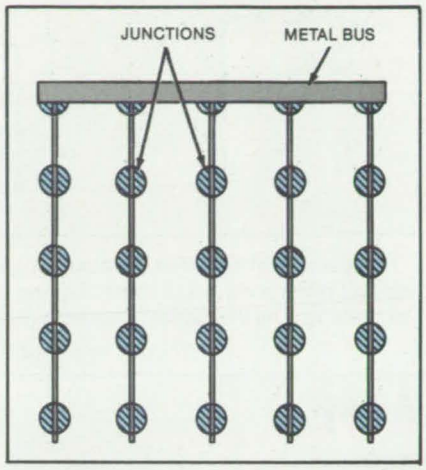

Many Small Junctions cover a small portion of the solar-cell collection area. A metal grid and bus collect current from the junctions.

- Polish and clean silicon wafers,
- By chemical vapor deposition or thermal growth, deposit a 1,000- to 5,000-angstrom-thick oxide,
- Etch round windows in the oxide on the front of the wafers to define the junction areas,
- Thermally diffuse phosphorus through the windows to form the multiple small junctions,
- Remove the front oxide, and passivate the front surface with thermally grown oxide or nitride,
- Etch out windows in the oxide or nitride,
- Deposit metal-conductor patterns on the front and back, and
- Deposit an antireflection coating.

Because of the reduced junction area, the surface leakage should drop, and the saturation current density should decrease. The surface passivation should help to ensure that short-circuit current remains at a high value and that the response of the cells to blue light increases.

This work was done by Taher Daud and Krishna M. Koliwad of Caltech for **NASA's Jet Propulsion Laboratory**. *For further information, Circle 80 on the TSP Request Card.*

Inquires concerning rights for the commercial use of this invention should be addressed to the Patent Counsel, NASA Resident Office-JPL [see page 29]. Refer to NPO-16126.

Lowering Ammeter Input Impedance

An operational-amplifier feedback circuit reduces the input voltage.

NASA's Jet Propulsion Laboratory, Pasadena, California

A feedback circuit operates in conjunction with a sensitive microammeter or other current-measuring instrument to reduce the input impedance of the composite circuit.

As shown in the figure, the current I to be measured enters the composite circuit at terminal a and leaves at terminal b. If the operational amplifier has a voltage gain of A, then $V_1 = I_1R_1$, $V_2 = AV = A(V_1 + V_2)$, and these equations can be solved to obtain

$$\frac{V}{I_1} = \frac{V}{I - I_3} = \frac{R_1}{1 + A}$$

Since I_3 is very small and A is very large in operational amplifiers, the ratio V/I_1 closely approximates the input impedance V/I, and the equation shows that this impedance is much less than the instrument resistance R_1.

Most of the input current, I, flows through the instrument even though the feedback circuit reduces the input voltage greatly. Even if the operational amplifier should fail, the current-measuring instrument would continue to work, though it would then exhibit the high input impedance of $R_1 + R_2$. In contrast with older current-amplifier circuits, this current is much less subject to drift and noise, calibration is not necessary, and the values of the components are not critical. The value of R_2 and the characteristics of the

operational amplifier can vary between wide limits without adversely affecting the performance.

As part of an experiment requiring current measurements with low impedance, currents ranging from 0 to 100 microamperes were fed to a current recorder having a resistance of 1,000 ohms. Without the operational-amplifier circuit, this current range would cause a voltage variation from 0 to 300 millivolts across the recorder. However, with resistor R_2 equal to 1,000 ohms and the type 741 operational amplifier, the voltage difference between terminals a and b varied by less than 1 millivolt.

This work was done by Clifford Myron Siegel of the University of Virginia for **NASA's Jet Propulsion Laboratory.** *For further information, Circle 84 on the TSP Request Card.*
NPO-16067

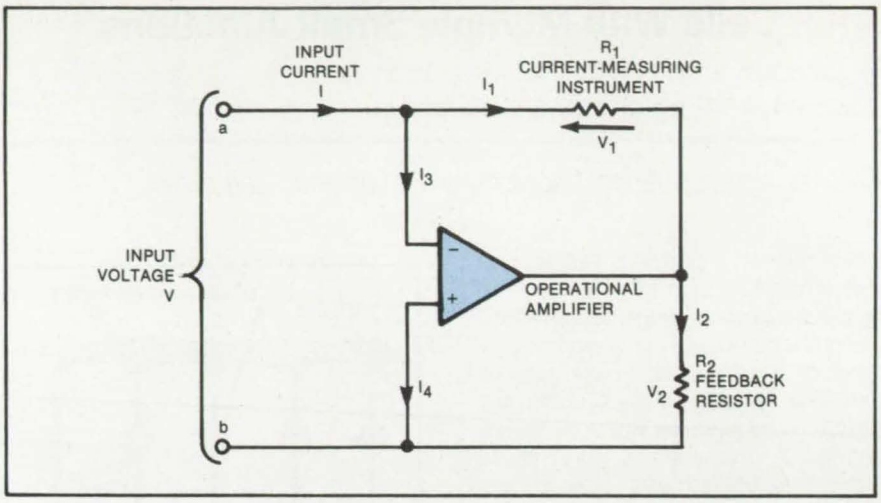

The **Operational Amplifier** maintains the voltage across R_1 and R_2 at essentially zero. The current-measuring instrument R_1, therefore, minimally influences the quantity it is measuring. The instrument may be a recorder, ammeter, or other device.

Infrared Linear Imaging Array

Photodiodes, multiplexer, and preamp reside in a hybrid ceramic package.

NASA's Jet Propulsion Laboratory, Pasadena, California

A hybrid microcircuit produces 128-element line images of infrared scenes. Each picture element is 0.008-in. (0.2-mm) square. Even without image data processing, the microcircuit can resolve temperature differences as small as 0.05° C in infrared images.

Packaged on a ceramic substrate, the microcircuit includes a line of 128 photodiodes, a multiplexer, and a preamplifier (Figure 1). Resistors and interconnections are applied to the substrate by thick-film techniques. Fanlike, fine-line interconnections bridging the gap between the coarse pitch of the photodiode array and the finer pitch of the multiplexer input terminals are applied by thin-film techniques.

The substrate contains an internal shield to reduce the coupling of switching transients to the video output. The microcircuit consumes little power — less than 5 milliwatts. It requires only 14 connections to the outside world, and it is compact, measuring only 1¾ by 1 by ⅛ inch (4.44 by 2.54 by 0.32 centimeters).

The photodiodes are indium antimonide mesa devices sensitive to radiation at wavelengths between 1 and 5 micrometers. Because the photodiodes have a relatively high reverse breakdown voltage

Figure 2. This **Image of an Infrared Scene** was generated by the photodiode array with the aid of a scanning mirror. Dark-current subtraction and computer processing would further improve image quality.

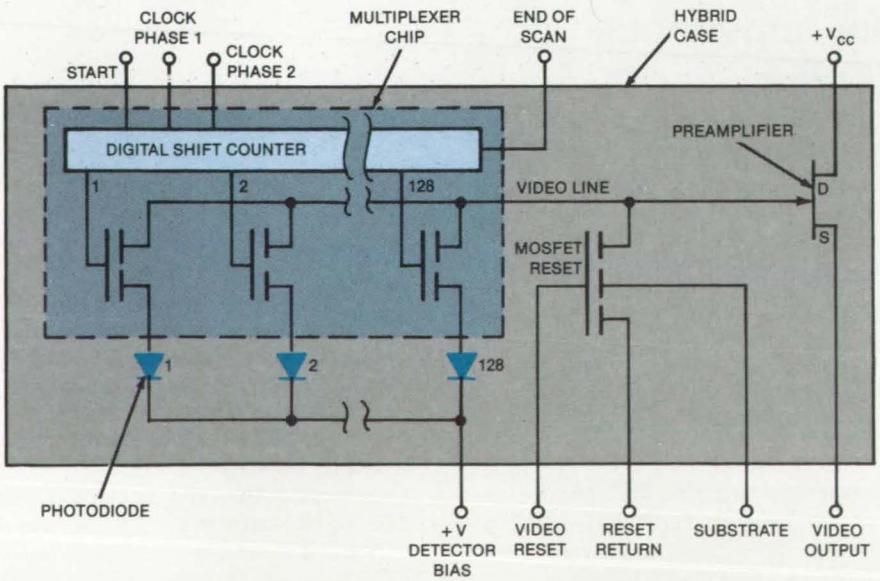

Figure 1. The **Infrared Imager** reads out accumulated charge on each of 128 indium antimonide photodiodes. Only one preamplifier is needed at the output of the video line.

of 2 to 3 volts and no measurable voltage-dependent current leakage at the surface, the photocurrents can be integrated directly at the diode junctions. This eliminates the inevitable loss that would otherwise occur when charge is transferred to another location for integration. About 2×10^7 electrons can be stored on each picture element.

The multiplexer is a commercial integrated circuit containing a series of metal-oxide-semiconductor field-effect transistors (MOSFET's) that sequentially connect each photodiode to a common output. It operates at the temperature (78 K) of the array and does not require individual preamplifiers for each picture element. The microcircuit has been used in a simple camera in which a mirror reflects successive linear segments of a scene onto the photodiode array (Figure 2).

This work was done by Gary C. Bailey of Caltech for **NASA's Jet Propulsion Laboratory.** *For further information, Circle 71 on the TSP Request Card.*

This invention has been patented by NASA (U.S. Patent No. 4,443,701). Inquiries concerning nonexclusive or exclusive license for its commercial development should be addressed to the Patent Counsel, NASA Resident Office-JPL [see page 29]. Refer to NPO-15805.

Books and Reports

These reports, studies, and handbooks are available from NASA as Technical Support Packages (TSP's) when a Request Card number is cited; otherwise they are available from the National Technical Information Service.

Power-Factor Controllers: How Safe?

When misused, they fail to save energy and may cause damage.

Potential safety problems with power-factor controllers (PFC's) are evaluated in a report. Based on a study of PFC's in use with appliances, the report recommends measures to prevent consumers from misapplying these energy-saving devices.

In the study, a consumer sounding board was surveyed to determine consumer understanding of manufacturers' literature, the types of appliances consumers could be expected to use with the PFC, and the ability of a consumer to properly adjust the PFC. Experiments were performed to evaluate the effect of the PFC on various appliance motors and on ancillary electrical devices commonly used in motor-operated appliances.

The PFC was designed for use with induction motors. It monitors the phase angle between the applied voltage and the current. It compares the angle with a reference signal representative of the desired power factor. The PFC responds to a difference by chopping a portion of the motor-voltage sine wave. The device can be used on such appliances as refrigerators, sewing machines, pumps, hair dryers, and food processors.

The mass marketing of the PFC and the ease with which it can be connected to an appliance place the device in the hands of consumers, who may not fully understand its intended uses and limitations. Specifically, a consumer may use it with an appliance that does not contain an induction motor, may use it with an appliance in which nonmotor components may be adversely affected by its action, or may adjust it incorrectly. The study was aimed at identifying and determining the magnitude of the potential hazards associated with such misapplications. The study also developed criteria for reducing the hazards and determined whether the potential problems are solvable without seriously impairing the efficacy of the PFC.

The report presents a set of recommendations including:

- The PFC should be clearly and permanently marked to caution the user. The marking should include the word "caution," should indicate that the PFC should be used with induction motors only, and should note that use with nonmotor loads not only does not save energy but may create a fire hazard.
- To prevent burnout of ancillary devices in a motor-operated appliance, a lower limit should be established on the voltage output of a PFC; 102 volts rms is suggested.
- If adjustments are to be made by the user, the proper settings should be made clear.

This work was done by K. W. Long, W. J. Christian, J. A. Kovacik, and T. Graczyk of Underwriters Laboratories, Inc., for **Marshall Space Flight Center.** *To obtain a copy of the report, "Study of Potential Safety Problems of Power Factor Controllers Used With Consumer Products," Circle 2 on the TSP Request Card.*
MFS-27016

Photovoltaics in Japan

The status of work in industry and universities is reviewed.

A report surveys the status of research and development on photovoltaics in Japan. The report is based on literature searches, private communications, and visits by the author to Japanese facilities. Included in the survey are the Sunshine Project, a national program to develop energy sources; industrial development at private firms; and work at academic institutions.

The Sunshine Project is the main driving force for Japanese photovoltaic research and development. (Although solar photovoltaic energy receives most of the funding, the project also includes geothermal energy, coal conversion, and hydrogen energy.) The major solar photovoltaic activities are:

- Low-cost refining of silicon;
- Solar-panel production in a pilot plant;
- Solar-cell test standards and procedures;
- Demonstrations of small systems, including 3-kW residential systems, a 20-kW multiresidence system, a 200-kW school system, and a 100-kW factory system;
- Demonstrations of powerplants, including a 200-kW distributed system and a 1-MW central system;
- Completion of a hybrid photovoltaic/thermal system of 5 kW electrical output and 25 kW thermal output; and
- Research on amorphous-silicon solar cells leading to 8 to 10 percent efficiency.

The report concludes that conventional silicon solar-cell technology is still a few years behind that of the United States, especially in mass-production processes. Japanese technology for amorphous-silicon solar cells, however, leads the world.

This work was done by Katsunori Shimada of Caltech for **NASA's Jet Propulsion Laboratory.** *To obtain a copy of the report, "Photovoltaic Research and Development in Japan," Circle 115 on the TSP Request Card.*
NPO-16330

Electronic Systems

Hardware, Techniques, and Processes

58 **High-Visibility Data Display**
59 **Storing Data and Video on One Tape**
60 **High-Speed Computer-Controlled Switch-Matrix System**
61 **Low-Cost Teleconference System**
62 **Dynamic-RAM Data Storage Unit**
63 **Redundant Asynchronous Microprocessor System**
64 **Designing Test Chips for Custom Integrated Circuits**
65 **Self-Identifying Reflecting Targets**
65 **Finding Bright-Spot Coordinates in Television Images**
66 **Synchronizing Data-Bus Messages**
67 **FIFO Buffer for Asynchronous Data Streams**
68 **Synchronization for Optical PPM Signals**
69 **High-Temperature Hall-Effect Apparatus**
70 **Single-Frequency Multitransmitter Telemetry**

Books and Reports

71 **Doubly-Differenced Measurements for Orbit Determinations**

High-Visibility Data Display

Sixteen parameters are monitored and displayed under microcomputer control.

Marshall Space Flight Center, Alabama

A data-monitoring system continuously senses the output voltages from transducers and provides large, easy-to-read displays of the quantities represented by the voltages. Measurements of power-supply voltages and currents, pressures, temperatures, strains, and masses, for example, can be displayed. The system is intended to operate 24 hours a day, producing uninterrupted readouts of critical parameters.

The data are presented on 16 large 7-segment displays. Four rack-mounting panels, 3½ inches (8.9 centimeters) high, hold four displays each. The panels can be placed anywhere within about 100 feet (30 meters) of the system microprocessor. On command from the user, the microprocessor changes the quantity shown on a given display or shows the same quantity on several displays.

The system is built from off-the-shelf microcomputer boards and assemblies. It is divided into five major sections (see figure): An analog-to-digital converter, an electrically erasable and programable read-only memory (EEPROM), the microcomputer, the display panels, and a cathode-ray tube terminal. The EEPROM stores measurement-system and calibration data, retaining these data even during power outages. The microcomputer converts the digitally coded voltages from the transducers into the corresponding engineering units and displays them on the terminal and the panels in four-digit, floating-decimal-point format.

The analog voltage inputs may be calibrated either manually or automatically. For automatic calibration, values representing 0 and 80 percent of full-scale transducer output are applied to the inputs and stored for scaling to engineering units.

This work was done by K. J. Slusser of Rockwell International Corp. for **Marshall Space Flight Center.** *For further information, Circle 55 on the TSP Request Card.*
MFS-19925

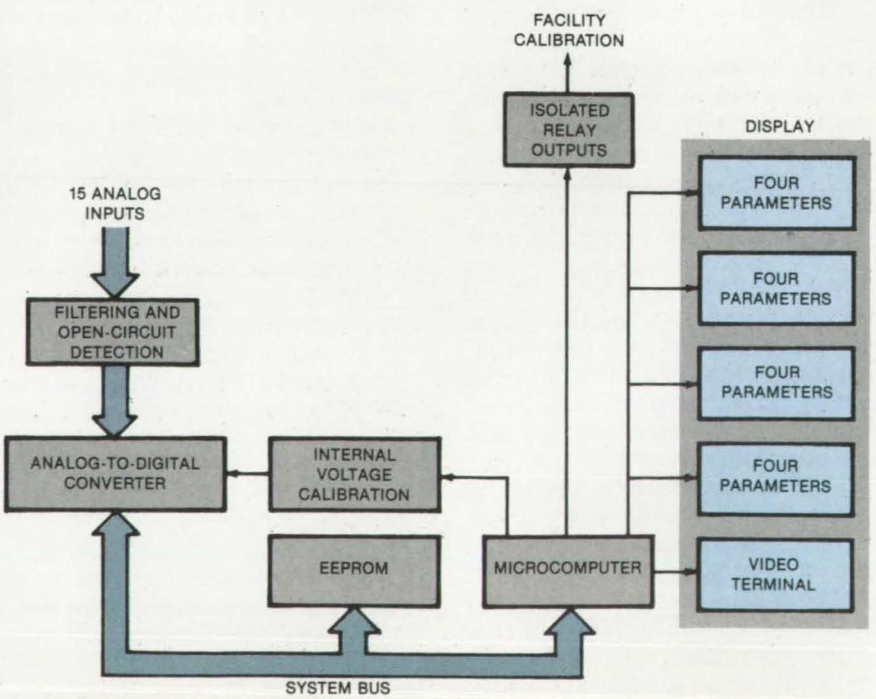

Fifteen Analog Inputs are converted to up to 16 numerical displays with 1-percent accuracy. Before analog-to-digital conversion, the inputs are filtered. If any input is an open circuit, its channel automatically displays a full-scale value to alert the user.

Storing Data and Video on One Tape

Two signal forms are made compatible and merged.

Lyndon B. Johnson Space Center, Houston, Texas

A microprocessor-based system originally developed for anthropometric research merges digital data with video images for storage on a video cassette recorder. The combined signals can later be retrieved and displayed simultaneously on a television monitor. The system can also extract the digital portion of the stored information and transfer it to solid-state memory.

As shown in the figure, the unit consists of a microprocessor, a programable communications interface, a video interface, and two memory banks. The microprocessor controls the communications interface, synchronizes the digital data with the video, and controls the video-interface hardware. The programable communications interface accepts the digital data and converts them into a serial stream. The video-interface hardware transforms the serial stream into the proper video signal levels.

The dual-bank computer memory transfers data to and from the communications interface. Two banks are used to increase the data flow rate and to ease timing constraints.

A data-error indicator lights up when a data error is detected. A frame-overrun lamp lights up when a video frame containing digital data has been missed during playback. The data-error indicator quickly shows whether the system is operating properly or whether there is a problem with either the storage medium or with the system itself. The frame-overrun lamp is similarly useful since, if the host computer falls behind while the system is retrieving data from tape, it is possible that at least one video frame of data will be lost.

Varying amounts of data may be stored from one consecutive frame to the next. A number is stored for each frame indicating the amount of data on that frame; the numbers are checked continuously as a further check on synchronism.

This work was done by James H. Nixon and John P. Cater of Southwest Research Institute for **Johnson Space Center.** *For further information, Circle 33 on the TSP Request Card.*

Inquires concerning rights for the commercial use of this invention should be addressed to the Patent Counsel, Johnson Space Center *[see page 29].* *Refer to MSC-20705.*

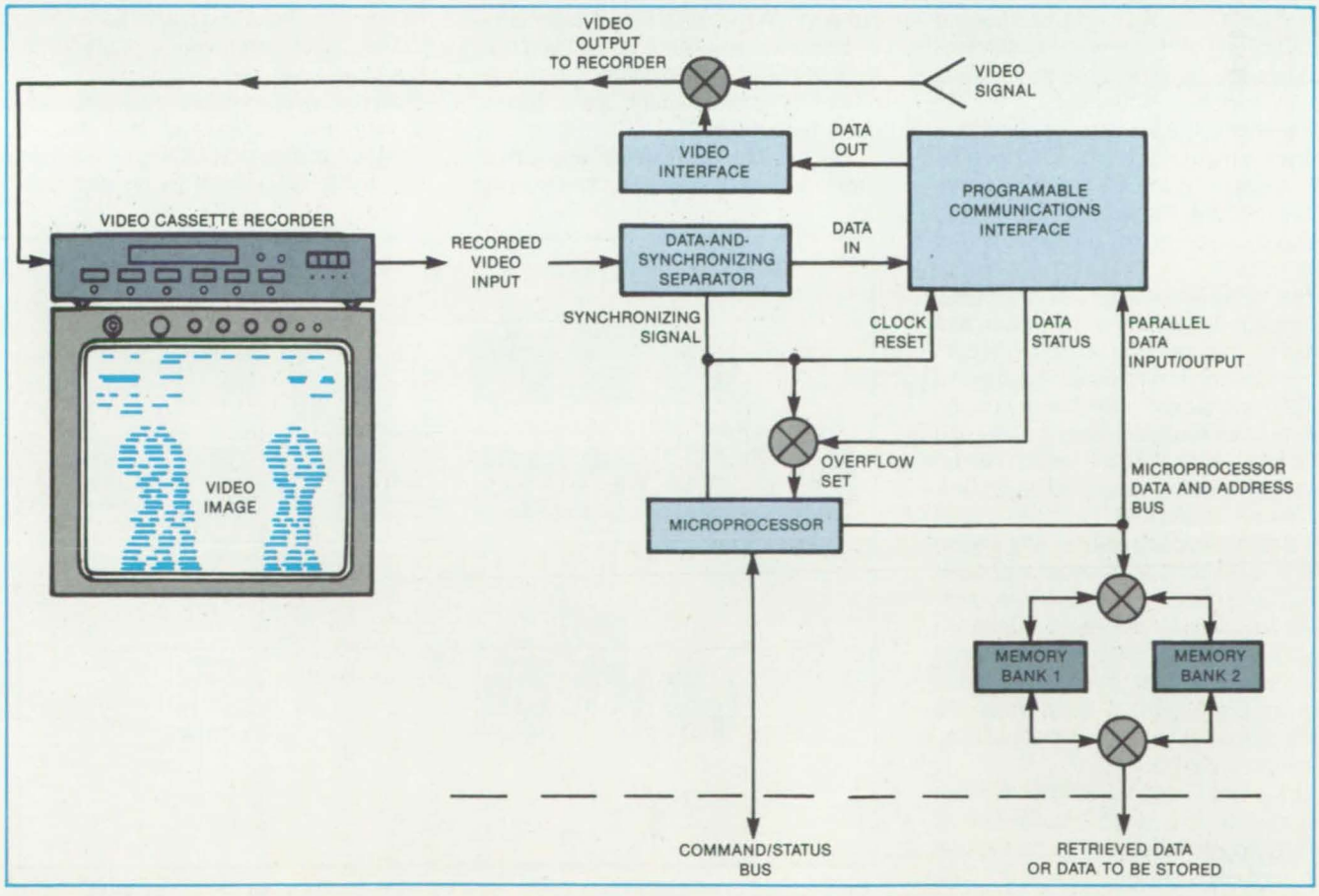

This **Video/Data System** merges digital data and video images. Approximately 345 megabytes of digital data can be stored on a two-hour video cassette.

High-Speed Computer-Controlled Switch-Matrix System

A message requires only a 2-microsecond interconnect period, repeated every millisecond.

Lewis Research Center, Cleveland, Ohio

A high-speed computer-controlled switch-matrix system has been developed for communication satellites. The next generation of communication satellites will use multibeam antenna systems operating in a Time-Division-Multiple-Access (TDMA) mode in order to achieve high data rates and high levels of frequency reuse. The satellite system will be controlled by an onboard computer and all message-routing functions between uplink and downlink beams will be handled by this newly developed switch-matrix system.

The function of the switch-matrix unit can best be described by considering the routing of a message from a starting location (e.g., New York) to a destination city (e.g., Los Angeles). A ground-based master-control terminal recognizes the destination request of the NY message, assigns it a time slot, and informs the satellite computer to prepare accordingly. When the assigned time slot occurs, the NY message is beamed via the RF uplink channel to the satellite, the satellite switch matrix is commanded to route the message to the LA downlink transmitter, and the message is beamed to the LA ground terminal and eventually to the end user.

The entire message-routing process operates in an extremely high-speed and dynamic manner. The actual interconnection between NY and LA requires only a 2-microsecond interconnect period that must be repeated every millisecond for the message duration, which can be seconds, minutes, hours, or days. During the remaining 998 microseconds of the one millisecond period, the switch matrix is available to consider 499 other possible connections from NY to other cities serviced by the satellite-antenna system. Servicing the NY to LA message for 2 microseconds every millisecond can, by operating in a burst mode, be made to appear to the LA users as an uninterrupted connection.

The design concept which has been devised for the switch-matrix unit is called coupled-crossbar architecture. The concept is shown in the figure. The architecture consists of orthogonal input (uplink) and output (downlink) transmission lines that are indirectly connected by input and output directional couplers through a switching element. For each of the input transmission lines, the input signal always travels the entire length of the line and is terminated at the end. At each input/output intersection (called a crosspoint), a portion of the signal propagating along the transmission line is always coupled to the switching element by the input directional coupler. If the switching element is open (off), the coupled signal is terminated. If the switching element is closed (on), the coupled signal passes through the switch and is coupled by the output coupler to the output transmission line.

The size, or number of input and output ports, governs the complexity of the switch-matrix unit. The unit under development consists of 20 input and 20 output ports. A matrix of these dimensions is referred to as a 20 by 20 unit and consists of the 400 crosspoints that are required to connect each input port to every output port.

For the intended satellite application, the frequency of the transmitted signal is approximately 5 GHz and the bandwidth is greater than 1 GHz. For this frequency range, the circuit network can be realized in microstrip. The high-technology microstrip design used for the 400-switch crosspoints consists of 800 dual-gate gallium arsenide field-effect transistors (GaAs FET's), 800 directional couplers, and 400 input, output, and interstage matching networks, and is packaged in a 20 in. by 20 in. by 5 in. (51 mm × 51 mm × 13 mm) enclosure that weighs less than 35 pounds (15.9 kg) and requires less than 25 watts of power.

The switch element consists of two sequential dual-gate GaAs FET's, which are operated in an amplifier mode that provides approximately 20 dB of signal gain. The two-stage switch/amplifier approach is required in order to minimize the coupling losses introduced by the couplers between the input and output ports.

The major performance characteristics that have been demonstrated by proof-of-concept models are the dynamic-switching capabilities that permit changes in message routing at rates as high as 500,000 times a second with turn-

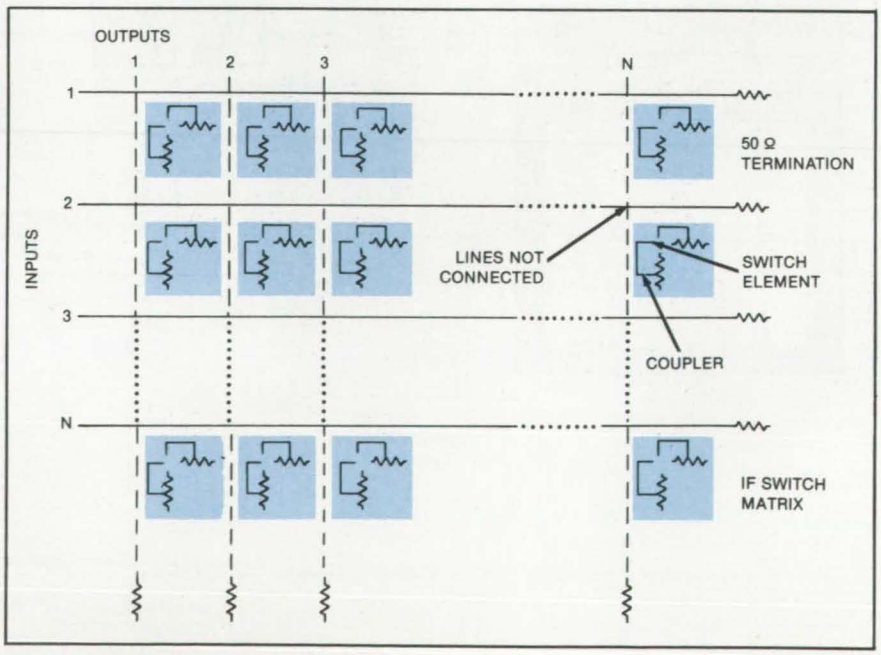

The **Coupled-Crossbar-Switch Matrix** includes orthogonal input (up link) and output (down link) transmission lines that are indirectly connected by input and output directional couplers through a switching element.

on and turn-off switching times of less than 20 nanoseconds. The high switching speeds permit the effective utilization of 1.96 microseconds of the total 2 microseconds available for useful message transmission and, for a 20 by 20 unit, allow each input port to address each output port every 40 microseconds if necessary.

This work was done by E. Spisz of **Lewis Research Center** *and B. Cory of General Electric Co., P. Ho of Ford Motor Co., and M. Hoffman of Mitre Corp. Further information may be found in:*

NASA CR-159682 [N80-12260/NSP], "Applications of Advanced On-Board Processing Concepts to Future Satellite Communications Systems" [$31], NASA CR-168089 [N83-34998/NSP], "Spacecraft IF Switch Matrix for Wideband Service Applications in 30/20 GHz Communication Satellite Systems" [$19], and NASA CR-168175 [N83-29492/NSP], "Spacecraft IF Switch Matrix for Wideband Service Applications in 30/20 GHz Communication Satellite Systems" [$26.50].

Copies of these reports may be purchased [prepayment required] from the National Technical Information Service, Springfield, Virginia 22161.

LEW-14050

Low-Cost Teleconference System

Widely scattered participants would communicate by voice, graphics, and images over telephone lines.

NASA's Jet Propulsion Laboratory, Pasadena, California

A proposed video teleconferencing system would display drawings, photographs, and text for conferees. Although the new system, called TELEDEMO, would not present live scenes from the conference locations, it would cost far less than conventional teleconference services. A block diagram of the system is shown in the figure.

With a parallel voice and data communications, TELEDEMO would allow two-way conferences between separated groups of people at data rates as low as 1,000 bits per second. Ordinary voice-grade telephone lines can easily handle this data rate. In contrast, full-video teleconferencing requires at least 1.5 megabits per second.

Each TELEDEMO conference site would include a display device (a television monitor or projection television) and one or more interactive devices (a joystick or graphics tablet), two telephone lines, a modem, and data-compression equipment. Optionally, a hard-copy device for film or paper, a video digitizer, and a video recorder (see figure) could be included.

Interactive graphics software would allow a user to construct electronic viewgraph art rapidly by copying existing hard-copy artwork, by using a rough sketch, or by on-the-spot improvisation. The user could also include (and modify) existing viewgraphs, either from a local collection or from materials obtained from remote sites. Two or more remote users could work on the same viewgraph together. Photographs could be incorporated as well.

Once in electronic form, the viewgraphs could be segmented into overlays and could include animation, such as blinking or moving objects, indications of flow, and rapidly changing colors. The electronic viewgraphs could then be arranged by editing software into a presentation sequence. During presentation, the viewgraphs could be shown out of sequence if necessary, and backup viewgraphs could be retrieved and displayed to aid in answering questions from conferees.

It would take about 10 seconds to transmit a typical viewgraph in full color at a transmission rate of 1,000 bits per second. If the viewgraph contained a photograph as well as text and art, the transmission time would be longer. The transmission time would not cause awkward pauses, however; viewgraphs would be transmitted and recorded while preceding viewgraphs were still on display and under discussion.

TELEDEMO, without its teleconferencing links, could serve as an unusual word processor. The addition of TELEDEMO capability to a microprocessor-driven office information-management system results in a combination called TELEDIMS, which would allow an operator to incorporate illustrations in textual material, including elaborate full-color figures and images. The operator could originate the illustrations or withdraw them from a data bank. The combined text and illustrations would be stored for future retrieval in the same way that pure text is stored in ordinary word processors.

This work was done by Robert F. Rice and Alan P. Schlutsmeyer of Caltech for **NASA's Jet Propulsion Laboratory.** *For further information, Circle 59 on the TSP Request Card.*

NPO-16057

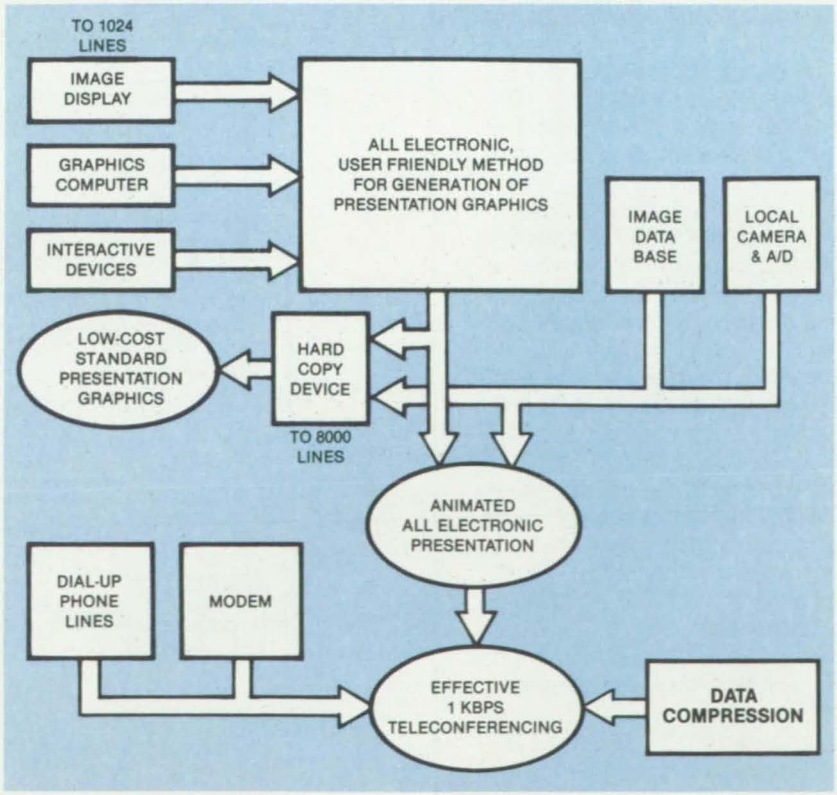

This **Functional Block Diagram** of TELEDEMO is an artist's version of an image originally drawn using interactive graphics software. The original diagram took about 20 minutes to prepare and can be transmitted to teleconference sites in 10 seconds over ordinary telephone lines.

Dynamic-RAM Data Storage Unit

It stores 256K of serial data, with independent read and write capability.

Lewis Research Center, Cleveland, Ohio

A dynamic random-access-memory (RAM) data delay and storage unit was developed to insure that data received from a satellite would be stored and not lost when the satellite was not within range of a ground station. Originally, a flight-qualified tape recorder weighing 8 pounds (3.6 kg), measuring 20.3 by 12.7 by 15.2 cm (8 by 5 by 6 inches), and requiring 8 watts of power was going to be used. Its weight and bulk were unacceptable, it reversed the data flow on readout, and it did not have the capability for multiple readouts of the recorded data.

By comparison, the newly developed data-store unit, shown in the block diagram (see figure), fits on one 13.8- by 19.7-cm printed-circuit card and draws only 125 mW at 5 V. It has complete flexibility in readout and recording: They are independent. When the storage is full, the oldest data are overwritten automatically. Overwriting can be prevented by stopping the write clock. Should selective recording be desired, it can be controlled by gating the write clock to record only the desired data. In normal operation, data are written into storage (as generated) at a 64-bps rate. Readout is continuous at 512 bps and is fed directly to telemetry.

The data-store system uses state-of-the-art dynamic random-access memories, DRAMS, to provide 262,144 bits of serial data storage with independent read and write capability. All of the supporting logic is CMOS, which minimizes the power required. The DRAMS operate at a refresh cycle rate in excess of 70 kHz, which allows input and output rates approaching 10 kHz. Internal anticoincidence circuitry on the read and write inputs prevents improper operation should both commands occur simultaneously. These functions are therefore completely independent and can be commanded at any rate below the maximum. They need not have any frequency or phase relationships; in fact, both could be completely random.

The circuit operation is as follows: The memory is composed of four 64-kbit DRAMS that have their internal operation sequenced by a counter operated from a 700-kHz clock. The counter provides sequential outputs used to control the memory cycle as well as the read/write functions. Each of the three functions, read/write/refresh, is sequenced by its own counter. The refresh counter requires only eight bits, as only the rows need be addressed to accomplish a refresh operation. The read and write counters are both 18 bits long as required to address any one bit in memory.

When no read or write inputs are present, the refresh counter continuously counts. Its outputs are gated to the memories by a tristate gate via a common 8-bit-wide address bus, and the memories are refreshed at about a 70-kHz rate. Whenever a read or write command is received, the next refresh cycle is delayed, the read or write counter is gated to the bus, and that function is executed. When the read or write cycle is completed, the system returns to the refresh mode and continues cycling until the next command.

Read and write commands function like a priority interrupt to insert the appropriate cycle into the operating sequence. When a read cycle is executed, the DRAM output is stored in a flip-flop that provides a latched output until the next read command updates it.

The unit can be interfaced with data-taking systems and computers. It provides for slow collection of data with fast playback or simple data delay with no change of data rate. Because of low power consumption it can be powered by a battery.

This work was done by John C. Sturman of **Lewis Research Center.** *For further information, Circle 64 on the TSP Request Card.*
LEW-14017

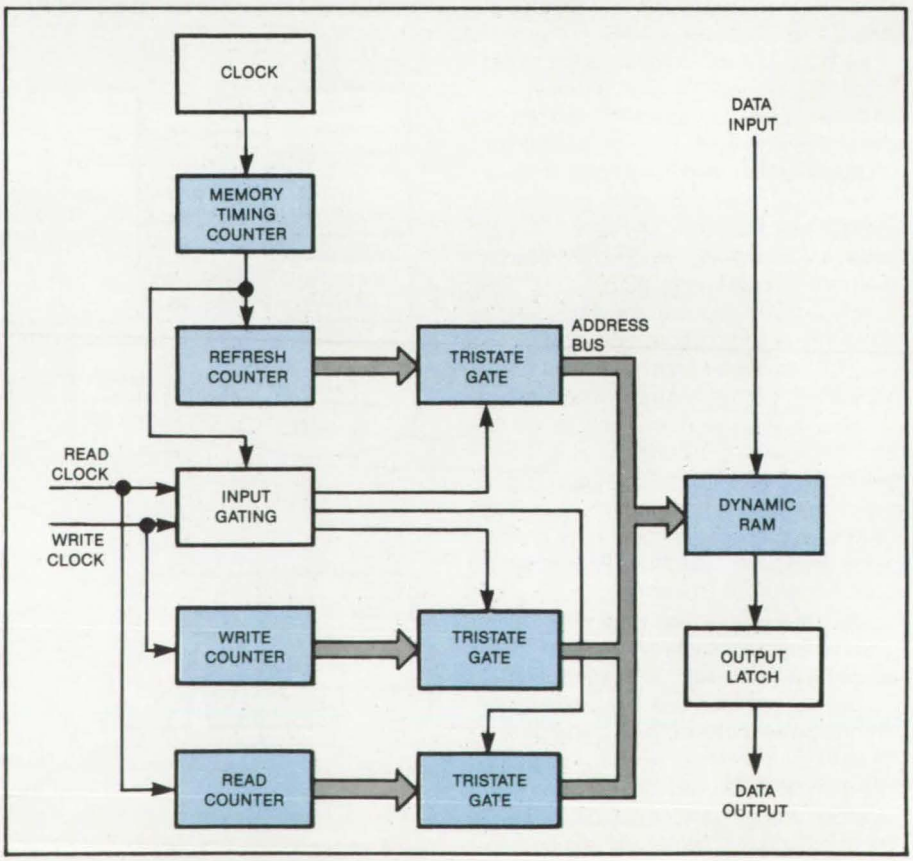

The **Data Storage Unit** includes four 64-kbit dynamic RAM's with internal operations sequenced by a timing counter. The counter controls both the memory cycle and the read/write functions.

Redundant Asynchronous Microprocessor System

Configuration guards against permanent failures and intermittent faults

Ames Research Center, Moffett Field, California

A fault-tolerant computer structure called RAMPS (for redundant asynchronous microprocessor system) has the simplicity of static redundancy but offers the intermittent-fault handling ability of complex, dynamically redundant systems. The new structure is useful wherever several microprocessors are employed for control — in aircraft, industrial processes, robotics, and automatic machining, for example.

In such applications, the multiple-microprocessor system can experience either permanent failure or — in more than 90 percent of the cases — intermittent failure. These failures can have serious consequences — in automatic control of aircraft during landing, for instance. The RAMPS protects against both types of failure.

In the past, such systems have employed either of two types of redundancy. In statically redundant systems, multiple identical processors are used so that if one unit fails, the survivors continue to operate and maintain control. These systems are simple and relatively inexpensive, but they provide no capacity to recover from intermittent faults. This predominant type of fault, however, is accommodated in dynamically redundant systems. In the event of a failure, good processors identify a bad unit, reload it with correct data, and attempt to restart it.

In the RAMPS (see figure), redundant processors sample redundant sensors and commands. Each of these processors transmits its output to a second set of redundant processors. The latter processors select correct input data and use them to execute the control algorithm, then transmit the resulting data to fault-tolerant actuators. The processors operate independently, each having its own clock. Therefore the system as a whole operates asynchronously.

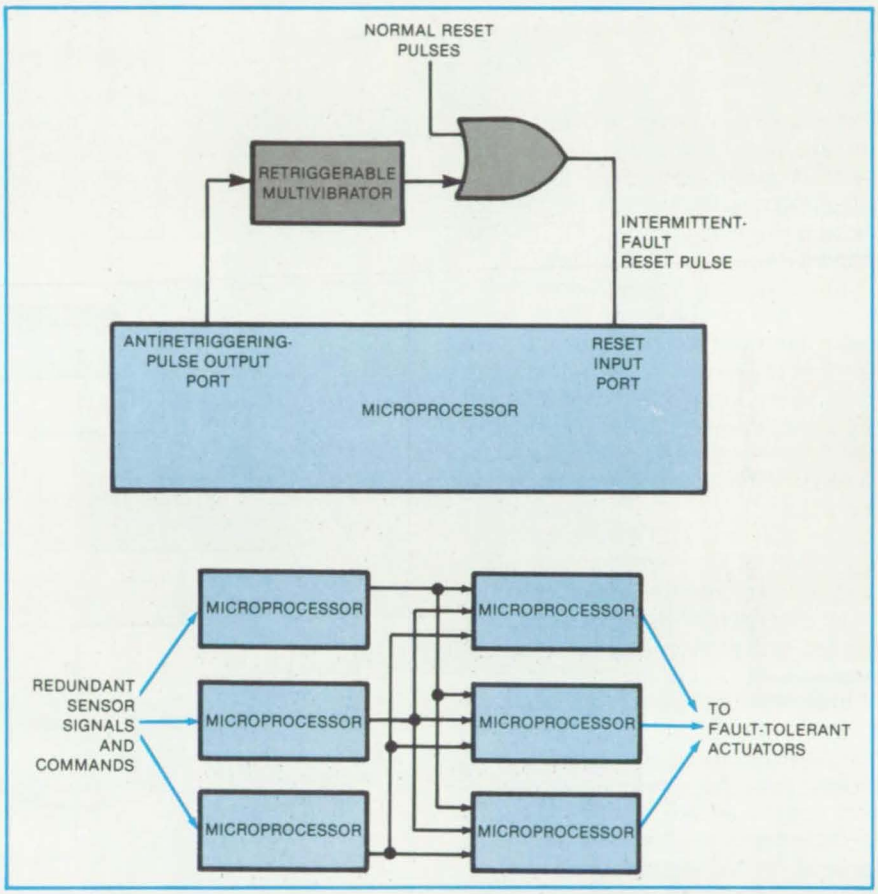

Each Microprocessor in the RAMPS is equipped with a multivibrator to accommodate intermittent faults. The structure can be expanded readily to a more generalized architecture. Additional distributed functions can be performed by expanding horizontally. Reliability can be improved through increased redundancy by expanding vertically. Finally, computational capacity can be increased by adding parallel processors out of the plane of the page.

The statically redundant configuration of the RAMPS is intrinsically tolerant of permanent faults. It is made tolerant of intermittent faults through the addition of a simple retriggerable multivibrator, shown in the figure. Since intermittent faults stop normal computer-program flow, control software is supplemented by a short subprogram that generates periodic antiretriggering pulses to the multivibrator. As long as this pulse train is present, the multivibrator is inactive. When an intermittent fault stops program flow, the pulse train ceases, and the multivibrator automatically restarts the processor program. The antiretriggering pulses resume, inactivating the multivibrator.

Because the resident control algorithms are asymptotically stable — a prerequisite for asynchronous operation, they force the failed processor to generate data that match those in the good processors. The RAMPS and the restart multivibrator have been successfully tested in the laboratory.

This work was done by George Meyer and Jay O. Johnston of **Ames Research Center** *and William R. Dunn of the University of Southern Colorado. No further documentation is available.*
ARC-11348

Designing Test Chips for Custom Integrated Circuits

Test structures and procedures are generated automatically.

NASA's Jet Propulsion Laboratory, Pasadena, California

A collection of design and testing procedures partly automates the development of built-in test chips for CMOS integrated circuits. The test-chip methodology is intended especially for users of custom integrated-circuit wafers.

Test chips are needed because the number and complexity of circuits on a wafer make it uneconomical to test every function of every circuit in a production lot of wafers. Instead, lot acceptance and the assurance of reliability of the fabrication process are based on results obtained from the representative circuits of the test chips.

On a typical wafer, the test chips cover from 10 to 50 percent of the wafer area. Test chips are interspersed with product chips. The microelectronic structures of the test and product chips are laid out and fabricated in the same process.

Each test structure is contacted by an array of electrical probes. (A representative set might be a square array of 2 by 10 probes, each of 80-μm-square cross section, spaced 80 μm apart.) The probe measurements are analyzed for one or more of the following purposes:

- Checking conformity with layout rules,
- Determining device and process parameters,
- Determining circuit-performance parameters, and
- Locating faults that occur during fabrication.

The plan for assembling test chips and generating testing procedures is illustrated schematically in the figure. To automate and systematize much of the testing effort, a computer program called Test Chip Assembler (TCA) has been prepared. This program consists of parametrized procedures that generate the test structures such as: conductors, capacitors, diodes, transistors, resistors, and mechanical structures. Each test module in the TCA includes the module name (e.g., "resistor," "capacitor,"), a description of the information to be obtained from the test (for example, leakage current or oxide thickness), the geometric parameters of the structure, the density of the probe pads, and procedures for testing.

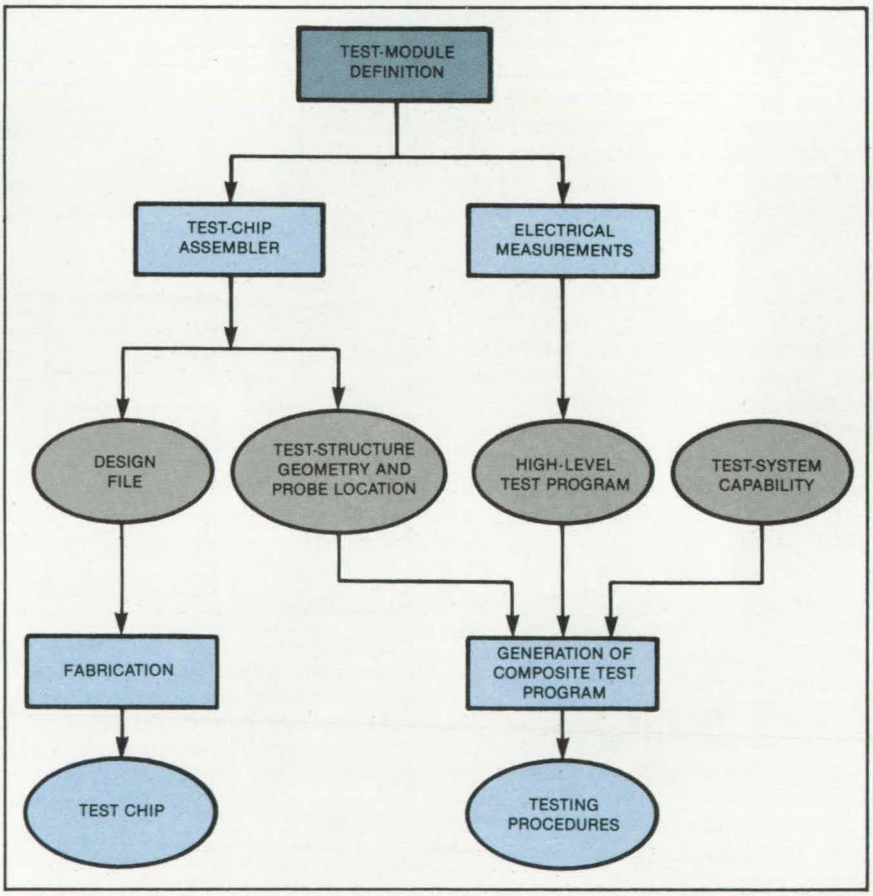

Test-Chip Designs and Testing Procedures (including data-reduction procedures) are generated automatically by a computer from programed design and testing rules and from information supplied by the user.

Some of the geometric parameters of a test structure are fixed or determined by rules, while others are supplied by the user before the calculation. The complete set of physical dimensions that specifies a test structure is calculated by the computer according to design rules in the test module. For example, a test module may describe a transistor for which the user specifies the channel width and length but for which all other dimensions are determined according to the module algorithm.

This work was done by Martin G. Buehler, Thomas W. Griswold, Cesar A. Pina, and Constantin C. Timoc of Caltech for **NASA's Jet Propulsion Laboratory.** *For further information, Circle 9 on the TSP Request Card.*
NPO-15988

Self-Identifying Reflecting Targets

A modulated reflector impresses its signature on reflected light.

NASA's Jet Propulsion Laboratory, Pasadena, California

A proposed scheme for target identification would require no radiation of energy by the target itself. Instead, the target would alter a light beam reflected from itself back to an interrogating station in a unique way. The interrogator would then identify the target from its signature impressed on the returned beam. The self-identifying target would be useful in surveying, navigation, and remote monitoring (for example, of mountain-climbing parties).

The target would use a cube-corner mirror to reflect the collimated light beam back to the interrogator, which might be on a passing airplane, for example. (A cube-corner reflector returns light along a path parallel to the path of incidence and its reflection is therefore seen only by the interrogator.) The cube reflection would be modulated to introduce a unique signature into the beam.

Mechanisms are proposed for impressing a signature on the reflected beam. For example, if the cube corner is a solid transparent body and light is reflected by total internal reflection from each face, a material of similar refractive index could be brought within half a wavelength or less of one face and its distance from that face varied to alter the degree of internal reflection. The material, in the form of a plate or diaphragm, might be oscillated by a magnetic or piezoelectric actuator driven by a sinusoid of known frequency, a coded voltage, or current pulses (see figure). If a hollow cube corner with reflecting surface is used, the reflection could be modulated by mechanically distorting one of the faces.

The reflected beam would be received by a photodetector at the interrogating station, and logic or other circuitry would identify the modulating pulse code or frequency. For navigation or other purposes, it might be desirable to have a target that returns different signals when observed from different directions. In the example of the figure, corner cubes grouped into a target are aimed so each is centered on a different 90° portion of the azimuth. Each is modulated with a different frequency or code. Thus, for example, an interrogating aircraft could determine its azimuth from the target to within a quadrant. Ambiguity could be reduced by using narrow wavelength bands in the interrogating beam and wavelength selection at the cube corner.

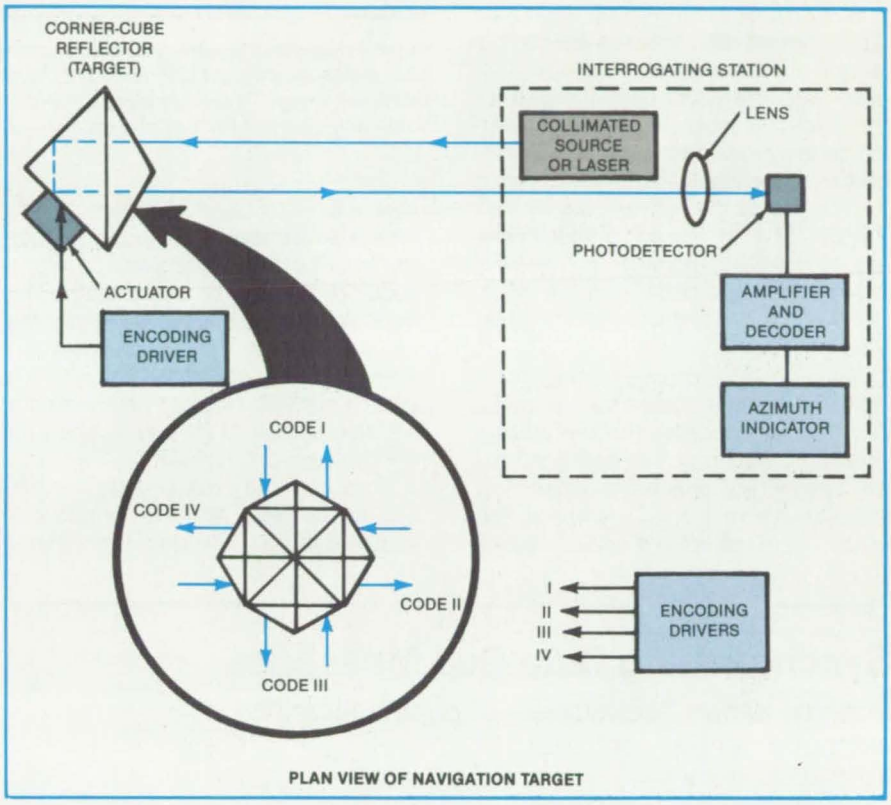

A **Cube-Corner Reflector** returns a parallel, slightly displaced beam of light to an interrogating station. Pulses from the encoder/driver modulate the reflection, thereby providing a coded optical signal that can be used for target identification or navigation.

This work was done by Robert E. Frazer of Caltech for **NASA's Jet Propulsion Laboratory.** *For further information, Circle 45 on the TSP Request Card.*
NPO-16106

Finding Bright-Spot Coordinates in Television Images

Video-processing circuit aids in calculation of spot centers.

Marshall Space Flight Center, Alabama

A circuit provides data for a computer to calculate the coordinates of a bright spot of light in a video image. The calculation is performed while the image is being scanned, and the results are available immediately at the end of the video frame. The center of the spot can be determined regardless of its size, whether it fills only one picture element (pixel) or fills the entire frame. Developed to aid in automatic docking and rendezvous of spacecraft, the video-processing circuit has a variety

of potential uses in commerce and industry. For example, it can locate tagged-parts on a factory assembly line or track airplane landing lights.

The inputs to the video-processing circuit are video signals from a television camera and control signals from a computer. The outputs of the circuit are three quantities from which the computer can determine the location of the bright spot in the television image.

A microprocessor in the circuit (see figure) passes data between the computer and a video terminal. The microprocessor also intercepts data intended for the video-processing circuit by recognizing certain characters in the data. A synchronizer coordinates requests for action intercepted by the microprocessor with the start of a video image from the camera. A comparator converts the video signal from analog to digital form. The digital signal is ON for a bright pixel and OFF for a dark pixel.

There are three counters in the circuit. The pixel counter counts the ON pixels detected by the computer. The column counter counts up by 1 for each pixel in a line, whether the pixel is ON or OFF. The line counter counts lines in the image. The outputs from the column and line counters are fed through adders to two accumulators, which are synchronized with the camera. The total in the column counter is added to the column accumulator, and the total in the line counter is added to the line accumulator. The accumulators tally the number of bright pixels, the sum of the column numbers for rows with bright pixels, and the sum of the row numbers for columns with bright pixels.

Data from the pixel counter, the column accumulator, and the line accumulator are fed to a multiplexer. The output of the multiplexer goes to differential drivers, which send the data to the computer. The computer determines the coordinates of the centroid of the bright spot by taking the ratio of the line-number total to the pixel total and the ratio of the column-number total to the pixel total.

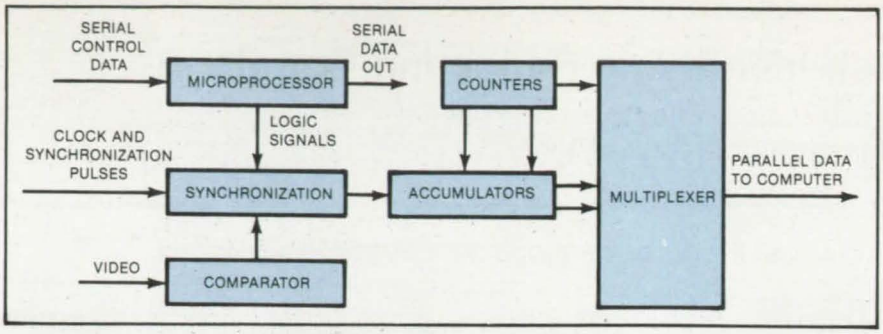

Video-Processing Electronics examine a television signal to arrive at three quantities from which a computer can calculate the coordinates of the center of a bright spot in the television image. The processing circuitry uses digital techniques to reduce component costs and produce immediate results.

This work was done by Thomas E. Richardson and John C. Tietz of Martin Marietta Corp. for **Marshall Space Flight Center.** *For further information, Circle 61 on the TSP Request Card.*
MFS-25999

Synchronizing Data-Bus Messages

Scheme allows "collision-free" communications without a central controller.

Lyndon B. Johnson Space Center, Houston, Texas

An adapter allows communications among as many as 30 data processors without a central bus controller. The adapter thus improves the reliability of a multiprocessor system by eliminating a point of failure that could cause the entire system to fail.

A transceiver transfers data from a host processor to the data bus (see figure). The adapter includes a "state machine" that requires four input signals and provides two output signals. The input signals are as follows:

1. Dead Bus — this is a flag that indicates that the data bus has been inactive for a period exceeding 20 microseconds.
2. Address Compare — the 5-bit terminal address of the host processor is compared to the address in the 5-bit terminal-address counter. If the two addresses are identical, the address-compare signal is said to be true.
3. Bus Request — this is a signal from

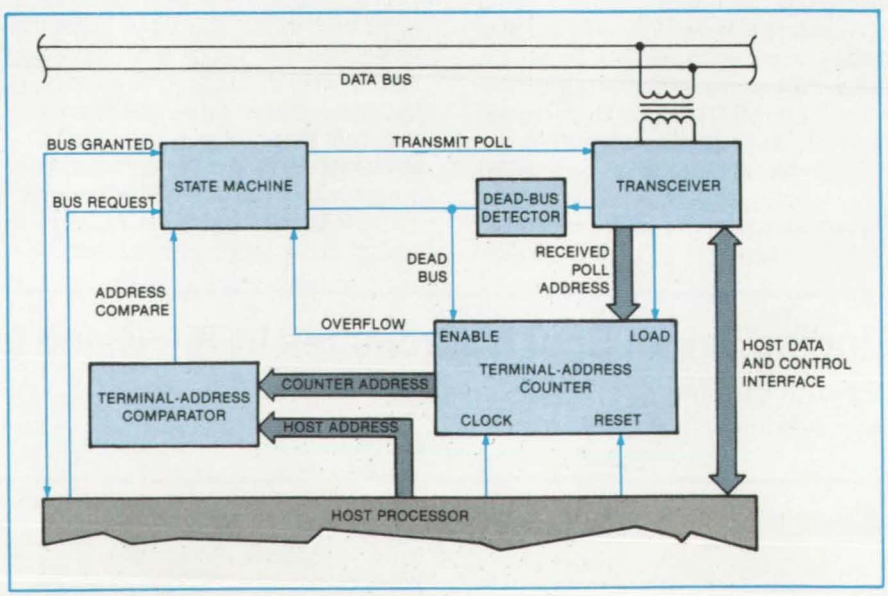

Access to a Data Bus is granted to a host processor on the basis of four signals to and two signals from the state machine. The scheme assigns data-bus timeslots and prevents data collisions.

the host processor requesting access to the data bus.

4. Overflow — the overflow of the terminal-address counter is stored in a latch.

The output signals are the following:

1. Transmit Poll — a request to the host processor to transmit its terminal poll address, and
2. Bus Granted — a signal to the host processor that access to the bus has been granted.

When a poll command is issued, it is received by every terminal in the network of processors. At the same time, the address of the host terminal is loaded into the terminal-address counter, and the counter overflow latch is reset. These events synchronize all terminals in the network to the same terminal address.

If the bus is inactive long enough for the terminal-address counter to overflow its setting and if the bus remains inactive until the counter arrives at the host-terminal address, a poll command is transmitted. The poll command is a query to other processors as to whether they have a message for the host processor.

The terminal with the lowest numerical terminal address transmits its address in a poll command during each cycle of the terminal-address counter as long as the bus remains inactive. The cycle time is 620 μs; 20 μs for polling, 20 μs for dead-bus detection, and 620 μs for the counter to overflow.

If the polled terminal has a message for the host, it can transmit it to the host when the data bus becomes available. This scheme prevents data collisions and eliminates nonessential polling, thereby reducing power consumption.

This work was done by Lewis H. Harris of Lockheed Engineering and Management Services Co., Inc., for **Johnson Space Center.** *For further information, Circle 90 on the TSP Request Card.*
MSC-20640

FIFO Buffer for Asynchronous Data Streams

Data are melded into a single constant-rate stream.

Lyndon B. Johnson Space Center, Houston, Texas

Variable-rate, asynchronous data signals from up to four measuring instruments or other sources are combined in a first-in/first-out (FIFO) buffer for transmission on a single channel. Constructed in complementary metal-oxide-semiconductor (CMOS) logic, the buffer consumes low power (only 125 mW at 5 V) and conforms to aerospace standards of reliability and maintainability.

The buffer accommodates data streams that issue from sources at rates from 10 bits to 64 kilobits per second in frames, with subframes of 8 to 1,024 bytes. To prepare the data for the FIFO buffer memory, the signal from each source is fed through one of four prebuffers called data-interleaver decommunicators (see figure). The data from each decommunicator are assigned in subframes to various sections in the FIFO buffer memory. The memory address assignments are done by control logic that keeps account of the data that have come in and gone out and of the loaded and unloaded memory locations.

Data are taken out of the buffer memory for interleaving onto the output bus upon receipt of a "fetch" command from the master unit of the pulse-code modulator. Memory sections are listed in the fetch-pointer memory (FPM) in the order in which they are to be unloaded. The FPM contains a sufficient number of entries to insure that data are retrieved at least as fast as they are written into the buffer. "Fetch" commands are formulated by a data-interleaver compiler at a preset rate according to telemetry specifications. Each such command specifies the memory section to be unloaded and the number of data words expected. A new "fetch" command is issued when all the data specified in the preceding command have been transmitted.

To insure flexibility, to reduce mass-storage memory requirements, and to reduce the number of FPM loads, an

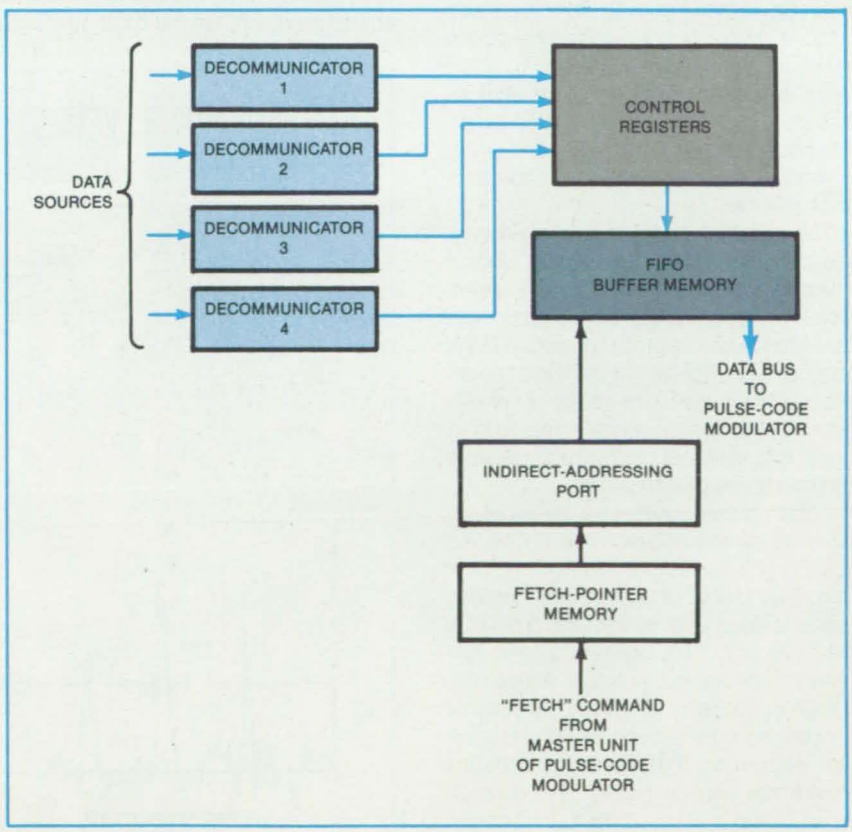

The **FIFO Data Buffer** interleaves up to four variable-rate, asynchronous data streams into a single constant-rate output data stream. Input data rates range from 10 bits to 64 kilobits per second.

indirect-addressing port allows each data source to operate through any of the four decommunicators. A "fetch" command causes the FPM to increment to the number of the next section to be unloaded. This section number is compared with entries in a memory that tracks the decommunicator data-source assignments and their corresponding memory addresses. When a match is found, the indicated section of memory is unloaded onto the data bus. If a match is not found, fill data are sent.

This work was done by Kent P. Bascle of Harris Corp. for **Johnson Space Center.** *For further information, Circle 34 on the TSP Request Card.*
MSC-20403

Synchronization for Optical PPM Signals

A clock signal is recovered from the received optical signal and noise.

NASA's Jet Propulsion Laboratory, Pasadena, California

A method based on the statistical properties of a weak pulse-position-modulated (PPM) signal enables the synchronization of a receiver clock with the received-signal time base. The method applies to weak optical M-ary PPM signals, for which there is only one pulse of length T_p transmitted during one of the timeslots of length T in each successive interval of M timeslots. The method requires a small dead time, T_d, at the beginning and end of each timeslot, during which the pulse amplitude is zero (see Figure 1).

At the receiver, the signal and noise are fed through a threshold detector to remove low-amplitude thermal noise, amplified, then clipped (see Figure 2). The clipper output is a series of equal-amplitude pulses much shorter in duration than T_p, each pulse representing one or more photons that may be part of a transmitted pulse. The photon pulses are assumed to occur at random points within each transmitted-pulse interval.

The clipper output is fed to a decoder and to a tracking loop. The receiver clock is a voltage-controlled square-wave generator in the tracking loop and must be synchronized to assure proper operation of the decoder. The first step in the synchronization process is the multiplication of the clipper output by a square wave. The product signal is a series of positive and negative versions of the photon pulses.

If the receiver clock and the received-signal clock are in synchronism (but 90° apart in phase) then, on the average over time, the number of positive and negative pulses is equal and the average product is therefore zero. If the signals are not in synchronism or not in the proper phase relationship, there is a slowly-varying or nonzero dc error component in the product. Assuming that Poisson statistics govern the photon pulses, the average error voltage is proportional to the time error between the received-signal and receiver clocks when that error is less than the dead time.

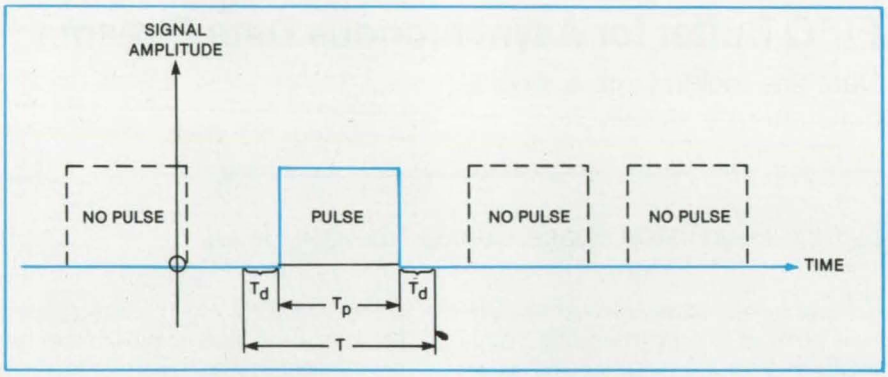

Figure 1. The **Transmitted Signal** consists of sequences of M timeslots, with only one pulse in one timeslot during each set of M. The information is conveyed by the pulse position; that is, by the number of the slot in which a pulse appears. Each timeslot includes a short "dead" time at the beginning and end of the pulse time T_p.

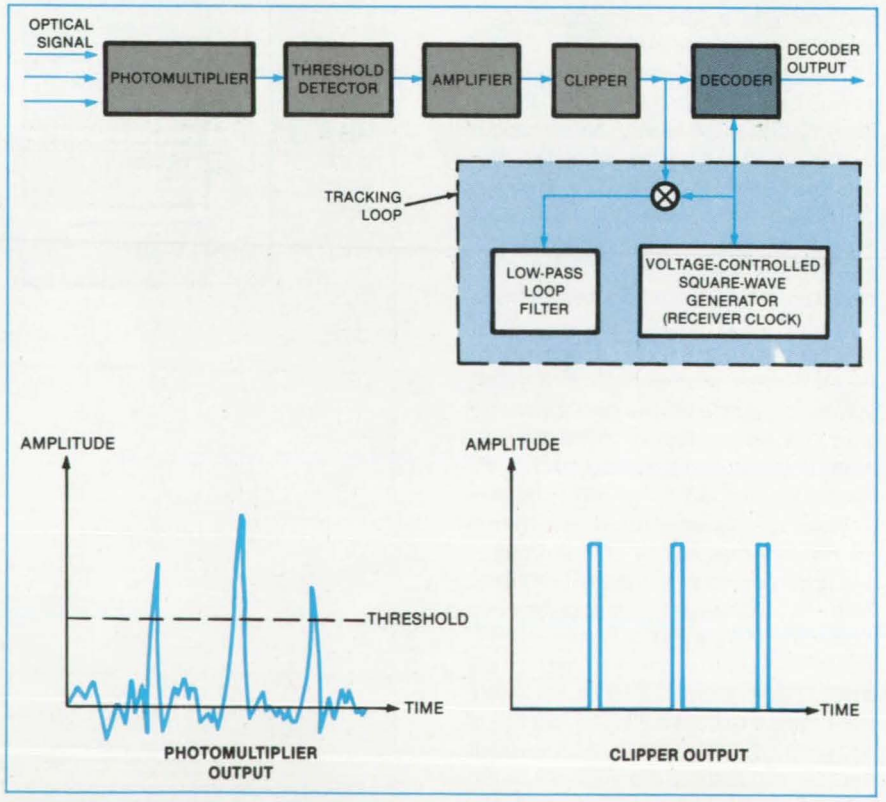

Figure 2. In this **Receiver**, the tracking loop synchronizes the local clock with that of the received PPM signal.

To remove the rapidly varying components, the product signal is fed through a low-pass filter, the bandwidth of which is much less than the inverse of the PPM word duration, MT. The filter output is the slowly-varying error voltage that adjusts the square-wave generator frequency to maintain synchronism.

The statistical analysis shows that tracking improves with decreasing tracking-loop bandwidth, increasing M, and increasing received-signal photon rate. Practical values of T_d/T_p are in the neighborhood of a few percent.

This work was done by Victor A. Vilnrotter of Caltech for **NASA's Jet Propulsion Laboratory**. *For further information, Circle 76 on the TSP Request Card.*

Inquires concerning rights for the commercial use of this invention should be addressed to the Patent Counsel, NASA Resident Office-JPL [see page 29]. Refer to NPO-16256.

High-Temperature Hall-Effect Apparatus

A compact furnace minimizes thermal gradients and electrical noise.

NASA's Jet Propulsion Laboratory, Pasadena, California

A semiautomatic Hall-effect apparatus takes measurements on refractory semiconductors at temperatures as high as 1,100° C. Intended especially for use with samples of high conductivity [10^2 to 10^3 $(\Omega\text{-cm})^{-1}$] and low charge-carrier mobility [10^{-2} to 10^2 $cm^2/V\text{-s}$] that exhibit low signal-to-noise ratios, the apparatus is carefully constructed to avoid spurious electromagnetic and thermoelectric effects that could further degrade the measurements.

The sample holder (see top of figure) is made of alumina or boron nitride. Boron nitride is used because this material is easily machined and also performs well as an electrical insulator at high temperatures. Electrical contact with the sample is made by four tungsten probes having chisel-shaped ends to assure high contact pressure. Each probe is spring-loaded against the sample by a sapphire cantilever spring. Sapphire is used because of its high strength, Young's modulus, availability, and retention of elasticity at the operating temperature.

The sample holder is housed in a molybdenum case that helps to even out local temperature variations and acts as an electrical shield. The probe leads are insulated in alumina tubing. A molybdenum tube welded to the case serves as an electrical shield for the dc powered leads.

The furnace that encloses the sample case is made from a molybdenum box of 0.25-in. (6.4-mm) wall thickness, with grooves to accept the heating rods (see bottom of figure). The heating rods are made of double-bore alumina tubing with molybdenum resistance-heating wire in the bores. To minimize the stray magnetic field of the heating current, the wire is fed through one bore of each rod, winding all the way around the furnace, and then back through the opposite bore of each rod. Sheets of molybdenum foil wound around the furnace box act as heat-radiation baffles.

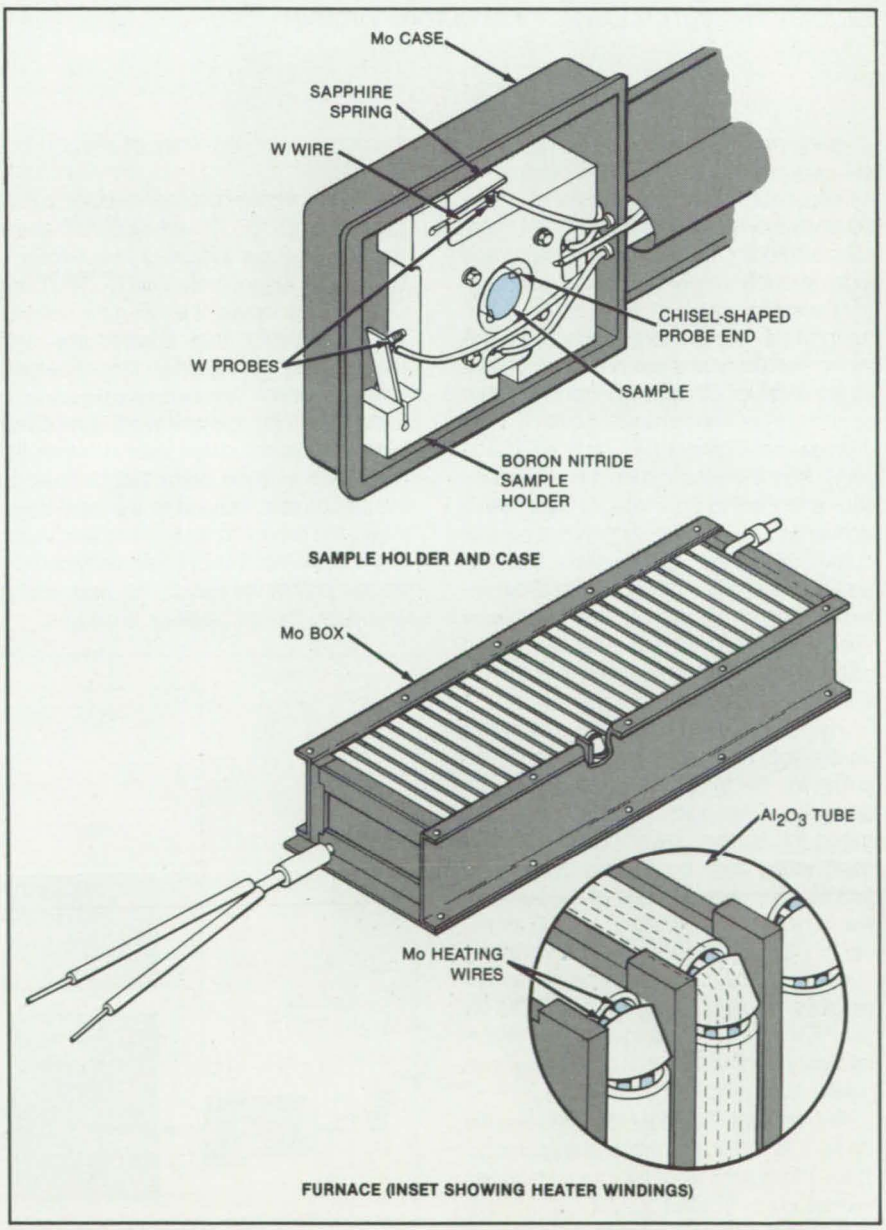

The **Sample Case** (above) is mounted in the furnace box (below). The furnace box is mounted inside a water-cooled vacuum jacket that fits in a 2-in. (5.1-cm) gap between electromagnet pole pieces.

The furnace box is placed inside a water-cooled stainless-steel vacuum enclosure with coaxial electrical connectors in the end caps. This outer enclosure fits in the 2-in. (5.1-cm) gap between the pole pieces of the electromagnet used to generate the Hall magnetic field.

All external wiring is shielded with low-noise coaxial cable, and connections are made with low-thermal-voltage solder. Probe voltages and currents are read with sensitive digital nanovoltmeters and ammeters.

The external electronic instruments are controlled by a computer that automates the measurements and performs all the Hall-effect calculations. A measurement is taken every 0.25 seconds. After a sequence of measurements, the computer prints intermediate results and asks the operator for approval. If the operator questions some data, the computer orders the repetition of the affected portion of the measurements.

This work was done by Charles Wood, R. Addis Lockwood, Artur B. Chemielewski, James B. Parker, and Andrew Zoltan of Caltech for **NASA's Jet Propulsion Laboratory.** *For further information, Circle 101 on the TSP Request Card.*
NPO-16279

Single-Frequency Multitransmitter Telemetry

Nonsynchronous time-division multiplexing eliminates overlap errors.

Langley Research Center, Hampton, Virginia

A telemetry technique for data collection on general aviation aircraft involved in aeronautical research consists of many sensor/transmitter units at different locations on the aircraft. Individual signaling and logic at each sensor/transmitter send signals to a single receiver in the airplane. The transmitters operate independently on the same frequency and are not synchronized to the receiver, eliminating erroneous data resulting from two-transmitter overlap.

In each transmitter (Figure 1), an analog signal from the sensor is input to a low-pass filter and then to an analog-to-digital (A/D) converter. The A/D converter has a parallel output; additional identification bits are added at the converter output to allow determination of the data source. A biphase encoder is used, where the data are mixed with the clock and transmitted over the RF link to the receiver.

The control portions of the transmitter enable and disable the logic and analog circuitry for the proper sequencing of the operation. The control circuit also minimizes the battery power consumption by deactivating the circuitry not being used and sets the sampling rate of the transmitter. When the transmitter is not in the transmission mode, the only circuit drawing current is the control circuit. The transmitter employs frequency-shift keying (FSK) for the RF link. The modulation signal is in digital binary format with only two frequencies generated, f_o and $f_o + \Delta f$.

The receiver detects only one frequency at a time for a nominal transmission. Thus, the detection of two frequencies simultaneously implies that there is more than one active transmitter. In almost all cases, the overlap of the two signals is partial; therefore, a memory is used to record the occurrence of overlap of any part of a data word.

In the overlap-detector/receiver circuit (Figure 2), OUTPUT and OUTPUT correspond to the demodulated frequencies f_o and $f_o + \Delta f$, respectively. With $\overline{\text{OUTPUT}}$ and $\overline{\text{OUTPUT}}$ as inputs, the OR gate disables the data buffer and enables the shift register and memory when acknowledging a data reception. The data word is stored in the register until the total word is received; then the system determines whether the data word is to be discarded because of overlap or sent forward to the next stage. When the reception is over and an overlap is not detected, the OR gate and memory flip-flop enable the data buffer, and, after a time delay, the shift register is cleared.

If, during the reception, OUTPUT and $\overline{\text{OUTPUT}}$ are simultaneously high, implying that two or more transmitters are active and overlapping, gate 1 triggers the memory flip-flop. When reception is over, the memory flip-flop makes the OR gate clear the shift register before the data buffer is enabled, and the data received during the overlap period are discarded. Since the identification bits are cleared together with the data bits, the demultiplexing process does not send the stream of logical zeros to any valid channel, and each channel holds the preceding data until new information is received.

For the general-aviation data system (9 transmitters, 2-Hz signal bandwidth, and 40-μs sample length), a minimum aliasing

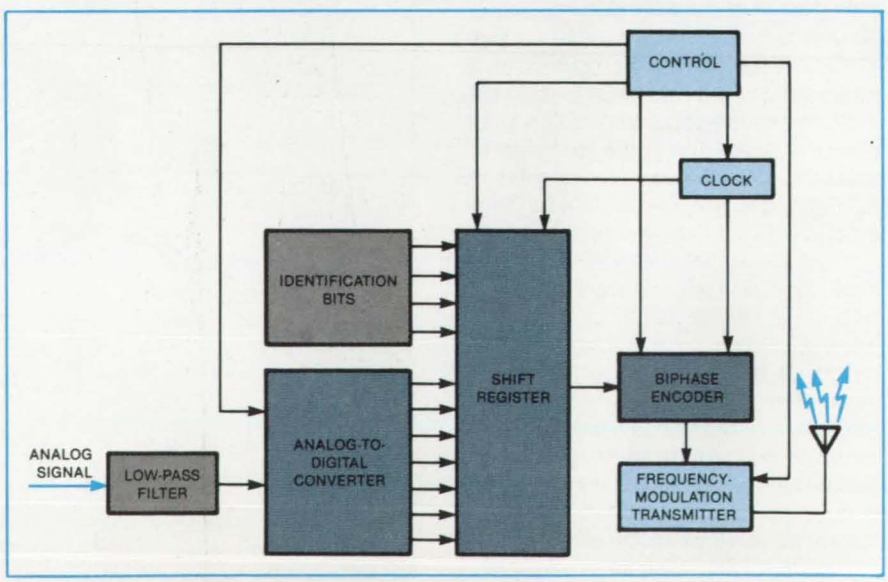

Figure 1. The **Control Portions of a Transmitter** enable and disable logic and analog circuits for proper sequencing. To keep power consumption low, only the control circuit is on between transmissions.

error of less than 0.01 percent is obtained with a sample rate of 800 samples per second. For other applications, a compromise should be made between link accuracy, number of channels (transmitters), RF bandwidth (sample length), and signal bandwidth (sample rate).

This work was done by Victor A. Carreno of **Langley Research Center.** *For further information, Circle 103 on the TSP Request Card.*

This invention is owned by NASA, and a patent application has been filed. Inquiries concerning nonexclusive or exclusive license for its commercial development should be addressed to the Patent Counsel, Langley Research Center [see page 29]. Refer to LAR-13006.

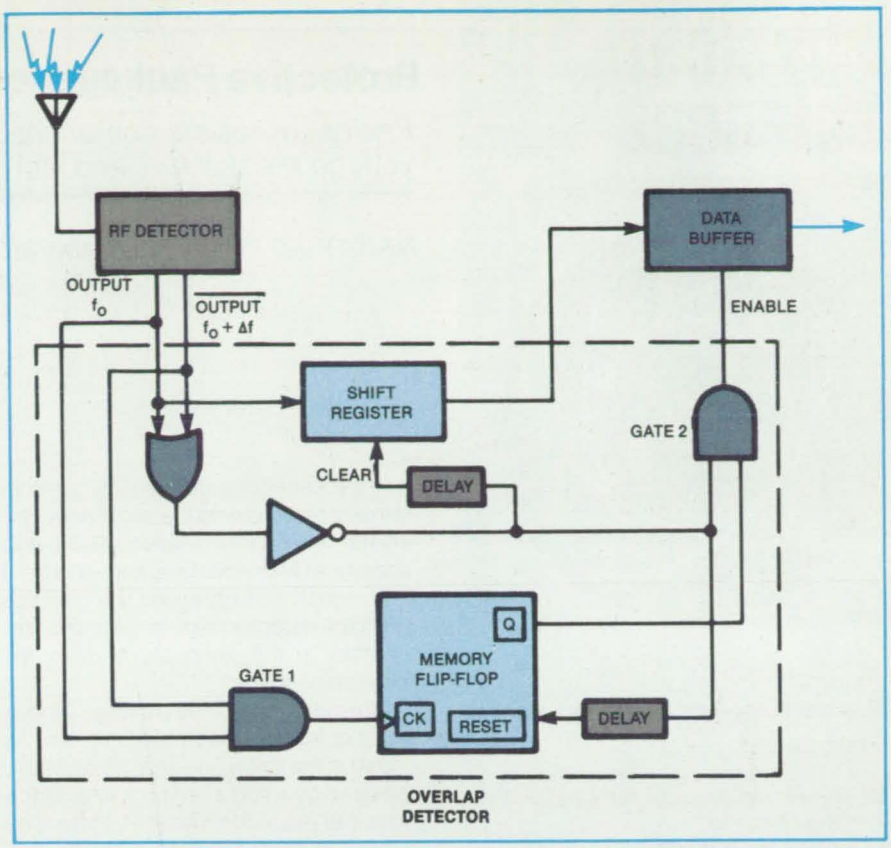

Figure 2. The **Overlap Detector/Receiver Circuit** uses a memory to record overlap of any part of a data word. If overlap occurs, the data are considered erroneous and not sent on to the buffer.

Books and Reports

These reports, studies, and handbooks are available from NASA as Technical Support Packages (TSP's) when a Request Card number is cited; otherwise they are available from the National Technical Information Service.

Doubly-Differenced Measurements for Orbit Determinations

Accurate measurements enhance data from geodetic and oceanographic satellites.

A report describes an accurate method of determining the orbit of a low-altitude Earth satellite. The method is insensitive to clock errors and provides a continuous determination of the orbit. For a constellation of 18 satellites of the Global Positioning System (GPS) and 13 ground stations, the altitude of a satellite at approximately 1,300 km can be determined within 5 cm in 2 hours of tracking. The report examines the effects of employing fewer ground stations, of applying different solution strategies, and of introducing fictitious thrust parameters to minimize geopotential modeling error — one of the major error sources.

The method makes it possible to realize the full potential of low-altitude satellites in geodetic and oceanographic applications. The orbital positions of these satellites must be known accurately so that the performance of their very precise sensors can be exploited.

The satellites of the GPS are in high orbits that provide them with long viewing periods of both low-altitude satellites and Earth stations. Moreover, the worldwide coverage of GPS signals allows continuous tracking of low-altitude satellites without a large number of Earth stations. Doppler measurements are made at a user satellite and at ground stations on signals from GPS satellites, and these measurements are processed along with GPS ephemeris data to yield the orbital position of the user satellite.

In particular, the method uses doubly-differenced GPS Doppler. The difference between the Doppler measurements on signals from the GPS satellite to the user and on signals from that GPS satellite to a ground station is subtracted from the difference of similar measurements on signals from a second GPS satellite to the user and the same ground station. The doubly-differenced GPS Doppler measurements are easy to make, accurate, and are very insensitive to clock errors (biases or instabilities) between the user satellite and the ground station. The only timing requirement is that the low-altitude satellite and the Earth station clocks provide time measurements that are accurate within 1 microsecond. Such clocks are readily available.

This work was done by Sien-Chong Wu and V. John Ondrasik of Caltech for **NASA's Jet Propulsion Laboratory.** *To obtain a copy of the report, "Orbit Determination of Low-Altitude Earth Satellites Using GPS RF Doppler," Circle 11 on the TSP Request Card.*

NPO-16111

Physical Sciences

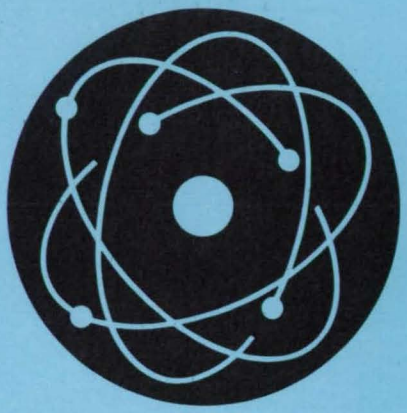

Hardware, Techniques, and Processes

72 **Protective Package for a Gamma-Ray Detector**
73 **Variable-Temperature-Gradient Device for Solidification Research**
74 **Telescope With Reflecting Baffle**
75 **Out-of-Focus Alinement of Solar Concentrators**
75 **Measuring Clouds With Microwaves and Infrared**
76 **Imaging Spectrometer for Geophysical Surveys**
77 **Nearly Anastigmatic X-Ray Telescope**
78 **Thermally-Rechargeable Electrochemical Cell**
78 **Spectrophotovoltaic Power Generation**
79 **Methanol Fuel Cell**
80 **Manipulator for Heating and Cooling in Ultrahigh Vacuum**
81 **Wide-Angle, Wide-Band Camera for Remote Imaging**
82 **Segmented Detector for Cosmic Gamma Rays**
82 **Altering Flashlamp Output for Realistic Solar Simulation**
85 **Estimates of Latent Heat in Clouds**
86 **Laser-Assisted Analysis of Aerosol Particles**
86 **Ultrahigh-Vacuum Sample-Transfer System**
87 **Battery-Charge-State Model**

Books and Reports

88 **Environmental Degradation of Solar Reflectors**

Protective Package for a Gamma-Ray Detector

Enclosure resists contamination, voltage breakdown, and vibration.

NASA's Jet Propulsion Laboratory, Pasadena, California

A package for a germanium gamma-ray detector protects the semiconductor crystal from contamination, allows it to operate at high voltages, and isolates it from shock and vibration. The package seals the detector from its surroundings, whether in the atmosphere or in the vacuum of space.

The main parts of the package, a base and a cover, are made of aluminum. As shown in the figure, the cover is sealed to the base by a soft aluminum ring. Since no solder is used for the seal, there is no danger of contamination of the germanium by flux outgassing inside the package.

A high-voltage power connection and a low-voltage signal connection are soldered to the cover. Nitrogen is introduced into the sealed package through the evacuation port. The nitrogen gas inhibits high-voltage arcs in the package cavity, prevents oxidation of the crystal, and provides back pressure to minimize the release of gases from the package metal. A small amount of helium in the nitrogen charge allows leakage from the package to be measured with a sensitive helium leak detector.

A clamping ring surrounds the jaw fingers and ceramic jaws and clamps them to the germanium crystal. The device is thus supported without damage to sensitive crystal surfaces, even during high acceleration.

This work was done by Marshall Fong, Charles Lucas, Albert Metzger, Donald M. Moore, Robert Oliver, and Walter Petrick of Caltech for **NASA's Jet Propulsion Laboratory.** *For further information, Circle 28 on the TSP Request Card.*
NPO-16019

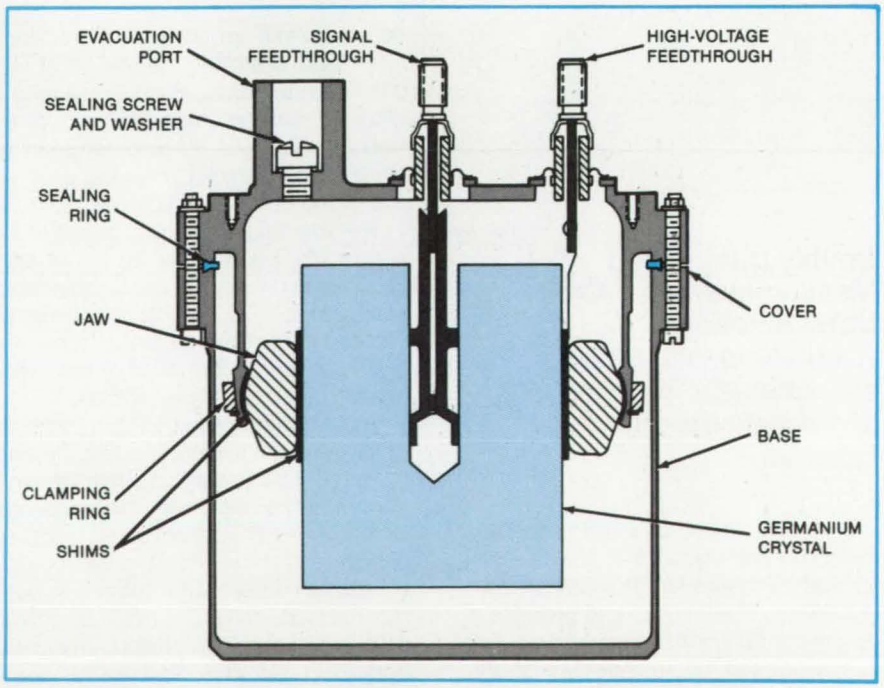

This **Housing for a Germanium Detector**, part of a gamma-ray spectrometer, holds the germanium crystal securely while protecting it from contamination. Although designed to hold nitrogen, the package can also be evacuated if necessary.

Variable-Temperature-Gradient Device for Solidification Research

A moving stage keeps the solidification front stationary while the gradient changes.

Marshall Space Flight Center, Alabama

A device for research in solidification and crystal growth allows crystallization of a melt to be observed as it occurs. The temperature gradient across the melt specimen can be increased or decreased rapidly while the solidification front proceeds at a constant speed across the sample. The device moves the sample at the same speed, thereby holding the position of the liquid/solid interface stationary within the field of an optical microscope. The device, a variable-temperature-gradient microscope stage, can thus be used to study crystal growth at a constant rate while the thermal driving force is varied.

The specimen is held in a cell as a thin transparent film between two glass slides. One end of the film is heated while the other is cooled. A researcher views the film through the glass-slide sandwich by light transmitted through it from the opposite side. The specimen, usually an organic alloy, is selected for its metallike solidification characteristics. The specimen melting temperature should be compatible with the materials in the stage structure; at present, melting points in the range -20 to +100° C are acceptable. The temperatures of the hot and cold ends of the specimen are controlled so that a solid/liquid interface exists in the film and the required thermal gradient extends from one end to the other.

The specimen cell rests on two blocks— one hot and one cold — which provide the controlled heating and cooling for the specimen (see figure). The hot block is heated by one thermoelectric device while the cold block is cooled by another. The same constant-temperature water bath flows through blocks below the thermoelectric devices. Maintained at the melting temperature of the specimen, the bath provides a temperature reference for heating and cooling.

The temperature of each block is monitored by a thermocouple, and a small computer regulates the current to each thermoelectric device on the basis of the thermocouple signals. To adjust the temperature gradient, the computer increases or decreases the currents to the thermoelectric devices at programed rates. At the same time, the specimen is pushed over the blocks toward the cold side, under computer control, so that the line of solidification sweeps across the specimen but stays in the microscope field of view. Diffraction at the liquid/solid interface reveals details of the solidification process.

Thermal stability is essential. It would not be acceptable to increase stability by increasing the masses of the heating and cooling blocks; it would not then be possible to change gradients smoothly and rapidly at the required rate of 2° C per centimeter per minute. Instead, very close temperature control is employed. The water bath is continuously circulated to maintain an even temperature. Meanwhile, the computer calculates the currents for the thermoelectric devices. The computer sends control signals by way of a digital-to-analog converter to a sample-and-hold amplifier, which provides analog control signals to the high-current power supplies for the thermoelectric devices.

This work was done by William F. Kaukler of USRA for **Marshall Space Flight Center.** *For further information, Circle 37 on the TSP Request Card.*

Inquires concerning rights for the commercial use of this invention should be addressed to the Patent Counsel, Marshall Space Flight Center [see page 29]. Refer to MFS-26008.

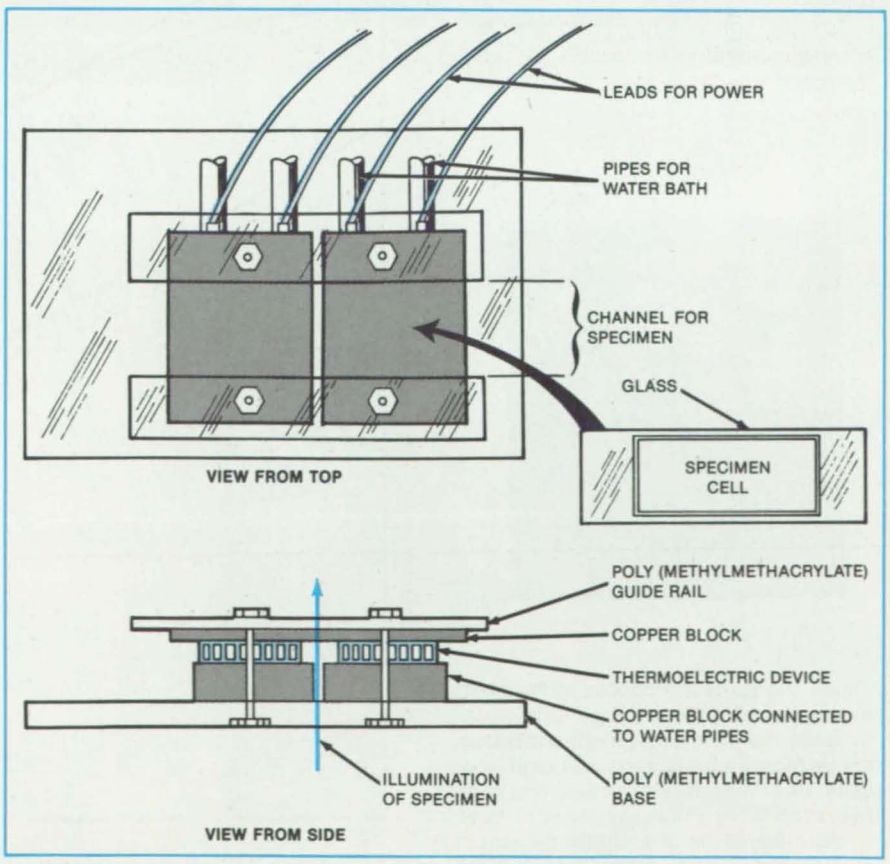

The **Specimen Cell** is pushed through a channel over a pair of copper blocks. Thermoelectric cells and a constant-temperature water bath flowing through cooling blocks maintain a controlled-temperature difference between the blocks.

Telescope With Reflecting Baffle

Undesired light is rejected by reflection.

Ames Research Center, Moffett Field, California

A telescope baffle is made from a combination of reflecting surfaces. In contrast with previous ellipsoidal reflecting baffles, the new baffle reflects skew rays more effectively and is easier to construct. For infrared telescopes, reflecting baffles are better than absorbing baffles because the heat load is reduced, and it is not necessary to contend with the insufficiency of infrared absorption exhibited by black coatings.

The principle of operation for meridional rays is shown in the figures. A ray coming in at an angle with the telescope axis undergoes multiple reflections between the two reflecting surfaces.

A special property of this configuration is that after bouncing back and forth between the reflecting surfaces, the light is reflected back out in a direction nearly opposite to the direction of entry. Thus, the entrance pathway for stray light can also be used as the pathway for rejection.

To reject light entering throughout the complete range of undesired paths, a telescope may have to include a series of such baffles. The design parameters of each baffle would be chosen to minimize the angular difference between the incoming and outgoing light paths for the range of angles served by that baffle.

While meridional rays are relatively easy to calculate and to depict on paper, the analysis of skew rays is more complicated. From sample calculations for one infrared telescope designed with respect to meridional rays, it appears that most undesired skew rays would also be rejected.

This work was done by William I. Linlor of **Ames Research Center.** *Further information may be found in NASA TM-84406 [N84-13985/NSP], "Baffle System Employing Reflective Surfaces" [$8.50]. A copy may be purchased [prepayment required] from the National Technical Information Service, Springfield, VA 22161.*

Inquires concerning rights for the commercial use of this invention should be addressed to the Patent Counsel, Ames Research Center [see page 29]. Refer to ARC-11502.

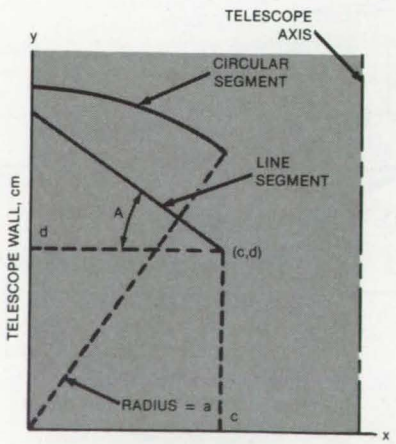

Figure 1. A **Baffle Is Produced by Rotating** this figure about the telescope axis. Upon rotation, the circular segment generates the surface of a torus, and the straight line generates the surface of a cone. This configuration is the simplest case of retroreflectors based on a multiple reflection between adjacent surfaces. For this configuration, the reflection properties depend on the parameters A and d and on the shape of the curved segment.

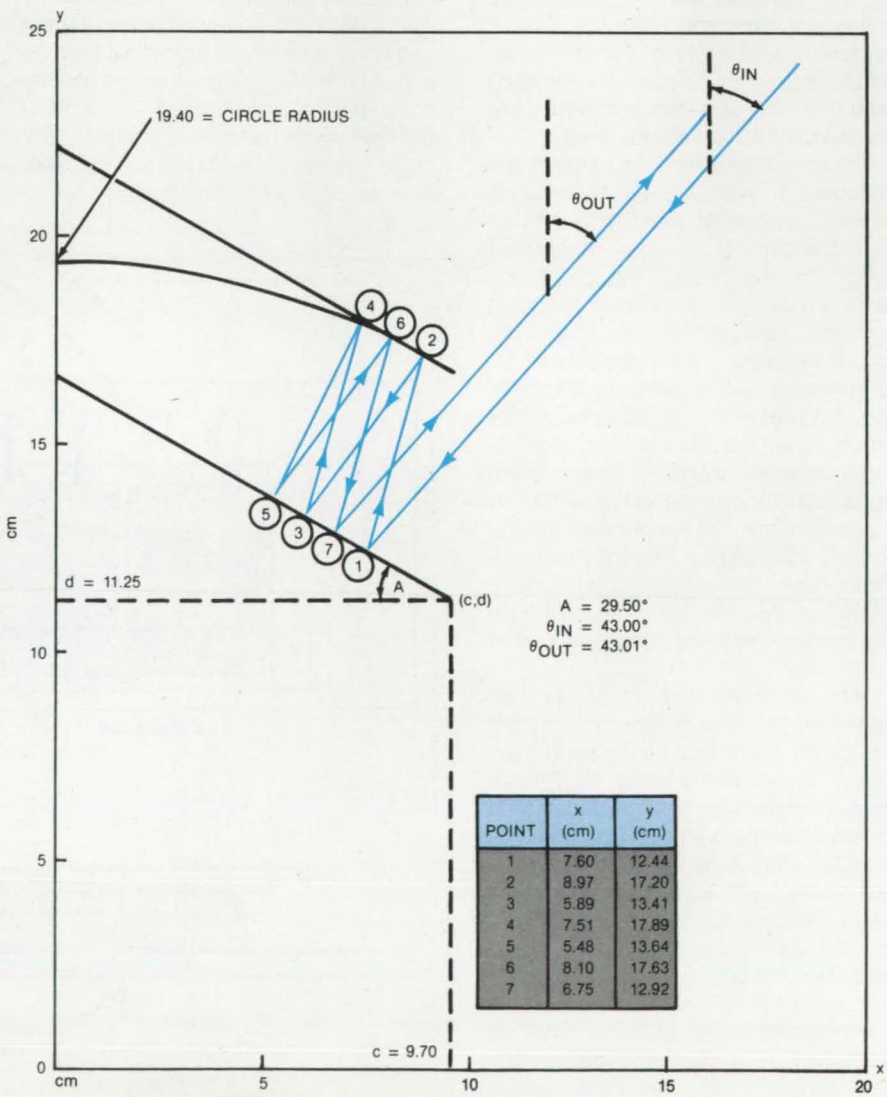

POINT	x (cm)	y (cm)
1	7.60	12.44
2	8.97	17.20
3	5.89	13.41
4	7.51	17.89
5	5.48	13.64
6	8.10	17.63
7	6.75	12.92

Figure 2. **Ray Reflections** for a baffle angle of A = 29.50° are shown. To achieve less deviation in angle between the incident and reflected rays, the circular segment can be replaced with a parabolic, elliptic, or a more complicated segment. The straight line can similarly be replaced by a more suitable curve.

Out-of-Focus Alinement of Solar Concentrators

Mirror facets are adjusted to place their reflections at calculated positions.

NASA's Jet Propulsion Laboratory, Pasadena, California

The alinement of the approximately 250 mirror facets of a paraboloidal solar concentrator is simplified by precalculated images reflected from all the facets.

Previously, the facets had to be alined by uncovering each one in turn, then adjusting them to place the image of a distant [3.6 mile (5.8 km) away] light source at the nominal focal point. In the new alinement technique, no attempt is made to simulate an infinitely distant light source, and all the mirrors are left uncovered throughout the procedure. The light source is placed at a distance of 1,650 feet (503 m); other distances could be used.

Using standard ray-tracing formulas, the nominal boundary is calculated for the patch of light from the source that should be reflected from each properly alined facet onto a target plane placed a convenient axial distance from the nominal focal point (see figure). A screen with the light-patch boundaries drawn on it is placed at the designated target plane.

Each light patch on the screen can be traced to its mirror by its unique shape and orientation. Therefore, it is relatively easy to find and adjust that mirror to move the light patch to its correct position within its outline.

Although developed for large solar concentrators, the technique can be used with other multiple-mirror or multiple-light-source systems for producing specified illuminance patterns. General-purpose ray-tracing computer programs are available and are readily adaptable to in- and out-of-focus alinement problems.

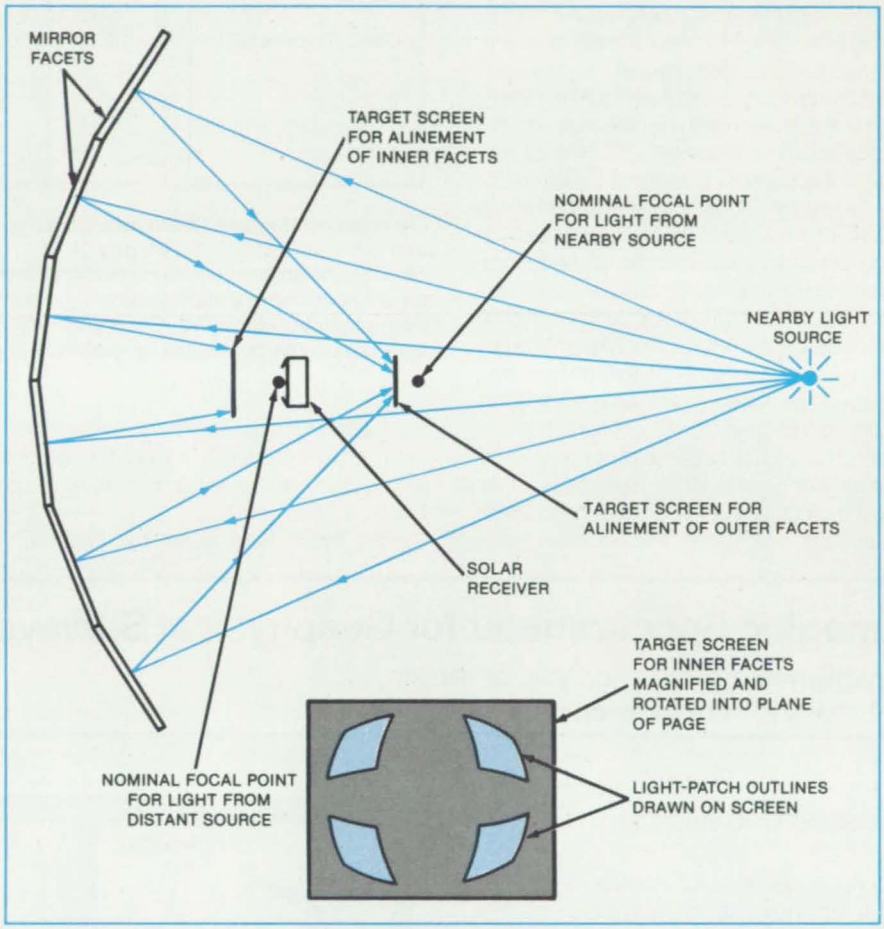

Patches of Light are produced on non-focal-plane targets by reflecting light emitted by a nearby source from the mirror facets. When the facets are properly alined, the light patches in the non-focal plane are in the precalculated positions shown. Also, when the facets are properly alined, light from an infinitely-distant light source would be concentrated in the receiver aperture near the nominal focal point.

This work was done by Maurice J. Argoud and Edwin W. Dennison of Caltech for **NASA's Jet Propulsion Laboratory.** *For further information, Circle 31 on the TSP Request Card.*
NPO-15563

Measuring Clouds With Microwaves and Infrared

Microwave techniques make standard infrared measurements more meaningful.

NASA's Jet Propulsion Laboratory, Pasadena, California

A combination of microwave and infrared measurements from satellites yields data from which the thicknesses and temperatures of clouds can be inferred. Microwave radiation measured by the satellite is used to determine the thickness of a cloud and the difference between the cloud-top temperature and the mean temperature of the interior. The technique extends the capability of a previously established method in which infrared radiation returned to a satellite by a cloud is used to determine the temperature and altitude of the cloud top and the fractional area of Earth covered by the cloud.

The addition of data from microwaves, which can penetrate deeply into clouds,

provides information more complete than that from infrared alone. Infrared radiometry has been applied extensively in the past to cloud research by satellite, but has been limited by the opacity of clouds to these wavelengths. In the combined infrared/microwave method, a scanning multichannel radiometer on board the satellite measures microwave radiation at 18, 21, and 37 GHz with both horizontal and vertical polarizations. These measurements, in combination with infrared radiometer measurements, make it possible to determine the top-to-mean temperature difference within an rms error of 3° C and the cloud thickness within about 0.4 km rms.

Extraction of geophysical parameters from the microwave data is complicated by the dependence of microwave emissions from clouds on the microwave frequency and the water content and temperature of the cloud. A regression technique for processing measurements of the infrared and microwave radiometers takes these and other dependencies into account: For the cloud thicknesses and mean temperatures, regression coefficients (see table) that relate these quantities to conventional cloud-top-height data and to the microwave-channel brightness temperatures are obtained by correlation of predicted values with radiosonde measurements of several hundred clouds.

Parameter To Be Found	Intercept in km	Microwave Channel of Predicting Function $f(T_B)$	Coefficients in km	rms Error in km
Cloud Temperature Differential (°C)	−119.9238	18 V	31.3095	3.1
		18 H	−64.7607	
		Cloud Top	−1.8383	
		21 H	13.8590	
		37 V	−36.2355	
		37 H	31.2996	
Cloud Thickness (km)	−1.3155	18 V	−3.2125	0.43
		18 H	3.9367	
		21 V	2.4566	
		21 H	−2.3741	
		37 V	−0.5631	
		Cloud Top	0.2245	

Cloud Temperature and Thickness are inferred from microwave brightness at three frequencies and two polarizations (18, 21, and 37 GHz; horizontal and vertical) and from conventional cloud-top-height predictions made from infrared measurements. The regression coefficients are obtained from a statistical simulation using data from meteorological measurements and from prediction formulas. For a given microwave channel, the predicting function $f(T_B)$ depends on the brightness temperature in that channel: $f(T_B) = \ln(280\text{-}T_B)$.

This work was done by Prem C. Pandey, Eni G. Njoku, and Joe W. Waters of Caltech for **NASA's Jet Propulsion Laboratory.** *For further information, Circle 48 on the TSP Request Card.*
NPO-16265

Imaging Spectrometer for Geophysical Surveys

Instrument permits analysis of terrain at many infrared wavelengths.

NASA's Jet Propulsion Laboratory, Pasadena, California

An airborne spectrometer combines the technologies of television imaging and spectroscopy to produce data for geophysical surveys, agricultural assessments, forest and land management, and exploration for oil and minerals. For compactness, the instrument employs an f/3 Schwarzschild folded-telescope objective of 70.7-mm focal length and folded monochromator optics with an aperture of f/1.6 and a magnification of one half. Light from the terrain enters through a hole in mirror 1 and is focused by mirrors 1 and 2 onto the spectrometer slit (see figure). The slit is oriented so that it passes a narrow strip image corresponding to a strip of terrain across the aircraft ground track.

The combination of the grating and mirrors 3 and 4 acts as the monochromator. Light from the image strip enters and leaves the monochromator through the hole in the grating, coming to final focus on an HgCdTe charge-coupled-device (CCD) detector array of 32 by 32 elements, each 68 μm square. Each picture element along the slit axis corresponds to a position on the crosstrack

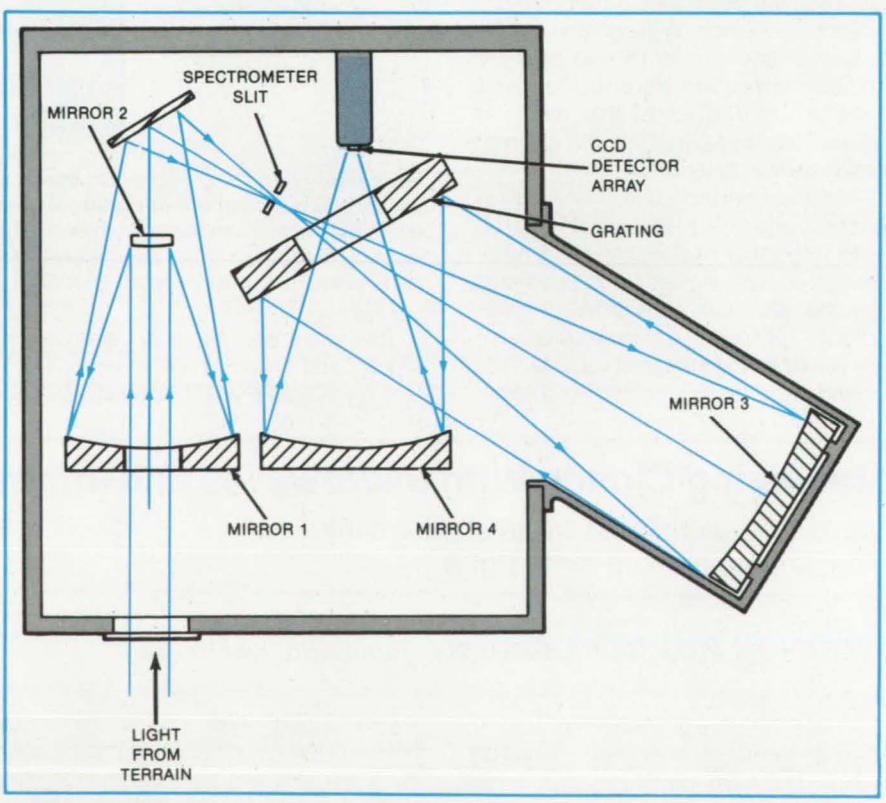

Designed for Small Size, this infrared imaging spectrometer uses a folded telescope and passes the input and output of its monochromator through a hole in the monochromator grating.

strip on the ground, while each picture element across the slit axis corresponds to a portion of the spectrum.

The instrument images the wavelength range of 1.2 to 2.4 μm in four bands. For each band, the grating is tilted in increments of 0.42°. The linear spectral dispersion of the grating gives a spectral (cross-slit) resolution of 10 nm per picture element (128 wavelengths total). At a typical height of 3,000 m, the crosstrack spatial (along-slit) resolution is about 6 m per picture element. The total ground swath width is 183 m.

An electronic-equipment rack provides power and synchronization signals to the CCD array and the monochromator solenoids. An airborne magnetic tape recorder stores data acquired during a flight. A computer controls the instrument, the tape recorder, and the CCD readout. The computer also controls a status display, organizes the data into the proper format for recording, and performs preliminary data processing (dark current subtraction, offset suppression, and gain correction). Data taken at each grating position are placed on separate tape recorder tracks for easier retrieval and processing.

The spectrometer is timed to give a 10-percent overlap between successive images along the track and to allow for the integration-and-readout time of the CCD detectors. To aid in correlating instrument data with the terrain, a 35-mm film camera, on the same boresight as that of the spectrometer, takes photos in synchronism with the instrument.

This work was done by Clayton C. LaBaw of Caltech for **NASA's Jet Propulsion Laboratory.** *For further information, Circle 27 on the TSP Request Card. NPO-16072*

Nearly Anastigmatic X-Ray Telescope

Many short reflecting elements result in diminished aberration.

Marshall Space Flight Center, Alabama

A proposed X-ray telescope would be made of many concentric reflecting rings, each of which consists of two portions of a cone. The proposed design is a variation on a conventional grazing incidence X-ray telescope, which has just one two-segment reflecting element but which suffers from excessive astigmatism and field curvature. By using many short elements instead of a single long element, the new design would give a nearly anastigmatic image.

The new telescope (see figure) operates on the same principle as that of a conventional grazing-incidence X-ray telescope. The mirror elements are shortened in the axial dimension, however, because the main lateral aberration in the image is proportional to the axial length of the reflecting elements. In principle, this aberration could be reduced to zero with elements of infinitesimal length, ignoring the problem of diffraction. The engineering compromise is to use elements of a convenient short axial dimension and to use many concentric elements to achieve sufficient image intensity.

The new telescope configuration offers the following advantages over the conventional design:

- the quality of the image away from the axis is improved due to the reduction of astigmatism and field curvature;
- the telescope is more compact, the short mirror elements forming a structure resembling a Fresnel lens; and
- the mirror elements may be simpler to make.

This work was done by Dietrich Korsch of Korsch Optics, Inc., for **Marshall Space Flight Center.** *For further information, Circle 25 on the TSP Request Card.*

Inquires concerning rights for the commercial use of this invention should be addressed to the Patent Counsel, Marshall Space Flight Center [see page 29]. *Refer to MFS-25984.*

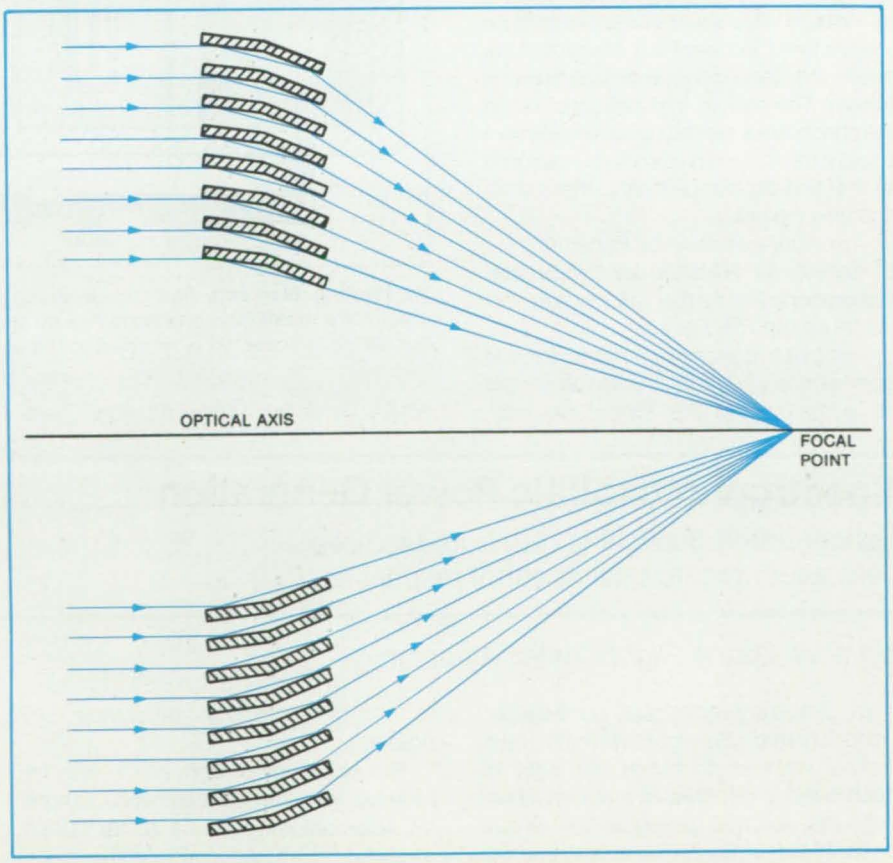

The **Improved Grazing-Incidence Telescope**, consisting of many concentric reflecting rings, is analogous to the multiple refracting rings of a Fresnel lens.

Thermally-Rechargeable Electrochemical Cell

Sodium ions would be driven across a membrane with the aid of a temperature differential.

NASA's Jet Propulsion Laboratory, Pasadena, California

A proposed liquid-sodium/sulfur electrochemical cell would be recharged by heat, rather than by an electric generator. The concept is suitable for energy storage for utilities, mobile electronic equipment, and solar thermoelectric power systems.

According to the concept, a second solid-electrolyte membrane would be added to a sodium/sulfur cell. The second membrane would separate the compartment containing sulfur and sodium/sulfur products from the compartment containing the cooled condenser surface (see figure).

When the cell is to be recharged, heating element 1 is energized, and opposite surfaces of the second membrane are connected electrically via an ammeter or a short circuit. This connection allows sodium ions to flow across the membrane toward the condenser under the influence of a concentration differential. The differential is established by heating the sodium and sodium/sulfur compounds and cooling the sodium that has crossed the membrane on the condenser surface.

After the sulfur and sulfur/sodium liquids have been largely depleted of their sodium, as indicated by a lower current reading on the ammeter, the electrical connection between the second-membrane surfaces is broken. The sodium that has solidified on the condenser is heated by heating element 2 until it melts. The liquid sodium is pumped to the sodium compartment, thereby recharging the cell.

This work was done by Robert Richter of Caltech for **NASA's Jet Propulsion Laboratory.** *For further information, Circle 89 on the TSP Request Card.*

Inquiries concerning rights for the commercial use of this invention should be addressed to the Patent Counsel, NASA Resident Office-JPL [see page 29]. Refer to NPO-16273.

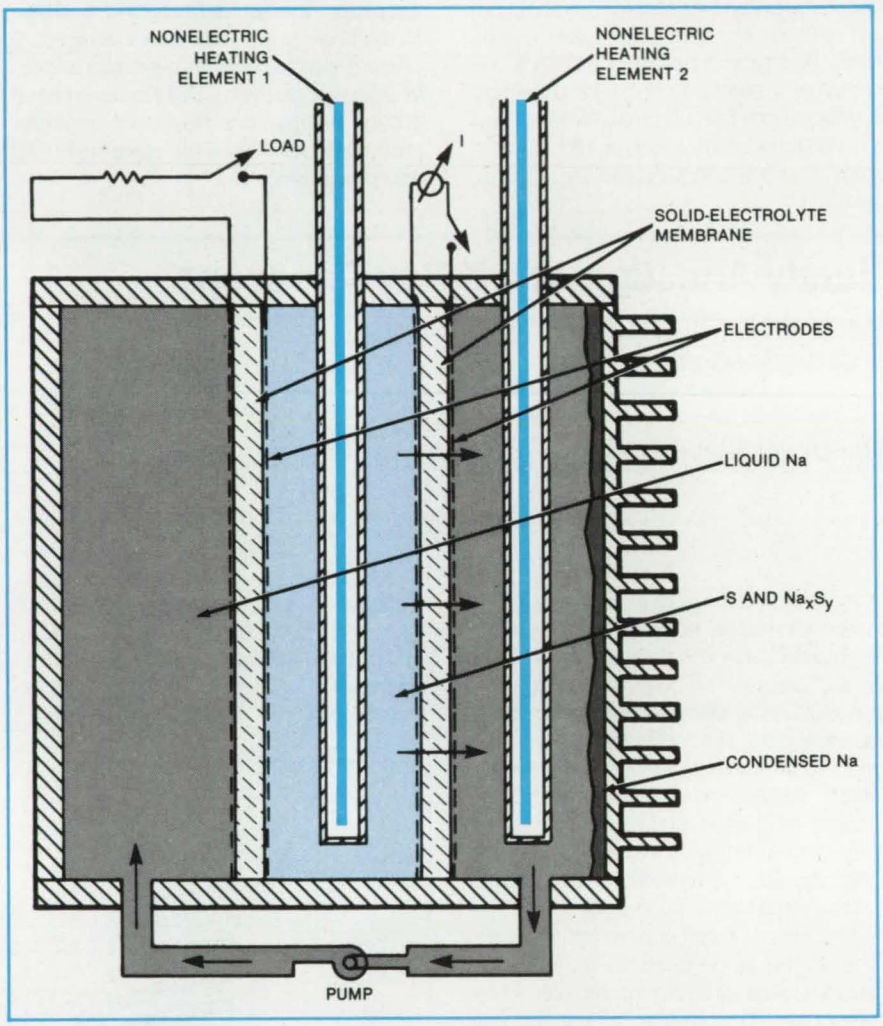

As Heating Elements heat the S/Na_xS_y mixture, sodium migrates through a solid-electrolyte membrane and solidifies on the condenser. After it has been liquefied, the sodium thus collected is recycled to the liquid-sodium compartment.

Spectrophotovoltaic Power Generation

Concentrated Sunlight is distributed to solar cells according to their spectral responses.

Marshall Space Flight Center, Alabama

In spectrophotovoltaic conversion, concentrated Sunlight is split into distinct wavelength bands; the light in each band is directed to a photovoltaic cell, the spectral response of which peaks in that band. The available energy in Sunlight is thus exploited more fully and, according to a study, improvements in energy-conversion efficiency are possible.

The efficiency of conversion also increases with the concentration ratio if the solar-cell temperature is maintained at about 300 K. Accordingly, the study examined a system with a 1,000:1 concentration ratio using a Cassegrain telescope as the first-stage concentrator (geometric concentration factor about 270, less obscuration loss) and compound parabolic concentrators for the second-stage concentration (4.7).

Systems employing up to four cells were considered; but when the costs of the optics, beam splitter, radiator,

and new cell technology were considered, the most-cost-effective system was found to be a two-cell gallium arsenide/silicon system (see figure). The gallium arsenide cell produces its greatest power at wavelengths from about 0.4 to 0.9 micrometer, while the silicon cell produces significant power at wavelengths up to about 1.05 micrometers.

An operating scale model of such a system was built and tested. With a 10-inch (25.4-centimeter) aperture, efficiency was 15.5 percent. The gallium arsenide cell produced 86 percent of the total energy output, and the silicon cell produced 14 percent. The efficiency for the same cells with perfect optics was estimated at about 20 percent.

Dramatic gains in efficiency cannot be expected with gallium arsenide and silicon cells because the Si cell "sees" only 10 percent of the energy that the GaAs cell does not use. However, aluminum gallium arsenide cells with good response to blue light may become available in the future, and such a cell would form a more efficient combination with a silicon cell.

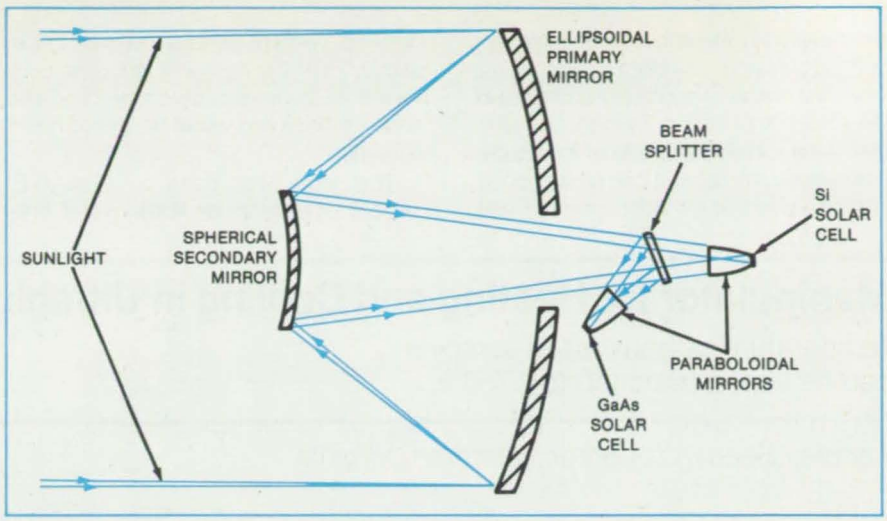

The **Optical Components** of a spectrophotovoltaic system concentrate light from the Sun and redirect the short-wavelength portion of the spectrum to a solar cell having a large gap in the energy band (a gallium arsenide cell). The longer-wavelength portion of the spectrum passes through a beam splitter to a cell with a smaller gap in the energy band (a silicon band).

This work was done by Gary Knowles and Joe Carroll of Honeywell Inc., for **Marshall Space Flight Center.** *For further information, Circle 46 on the TSP Request Card.*
MFS-27027

Methanol Fuel Cell

The cell would aid a fuel processor in converting methanol to hydrogen.

NASA's Jet Propulsion Laboratory, Pasadena, California

In a proposed fuel-cell system, methanol is converted to hydrogen in two places. An external fuel processor converts only part of the methanol. The remaining methanol is converted in the fuel cell itself, in a reaction at the anode. As a result, the size of the fuel processor is reduced, system efficiency is increased, and cost is lowered.

Methanol and steam are fed to the fuel processor, which is a catalytic steam reformer (see figure). The size of the processor is adequate to convert only 50 to 70 percent of the methanol to hydrogen at the maximum fuel flow rate. The steam and methanol react to form hydrogen, carbon monoxide, and carbon dioxide. These gases, along with unreacted steam and methanol, pass to the anode of the fuel cell.

In the fuel cell, the steam and most of the remaining methanol react to produce more hydrogen. In a fuel cell with a phosphoric acid electrolyte, the reaction takes place at about 200° C. Whatever hydrogen, carbon monoxide, methanol, and other combustible gases are not consumed in the fuel cell are fed to a combustor where they are burned to heat the fuel processor.

The processor contains a catalyst of copper or palladium supported on a metallic sponge or honeycomb structure that transfers heat efficiently from the burning gases in the combustor through the catalyst bed. The processor operates at a steam-to-carbon ratio between 1.3 and 1.5. The temperature of the gases leaving the processor is less than 280° C.

A catalyst is also provided at the fuel-cell anode. Strips of an insulator such as silica

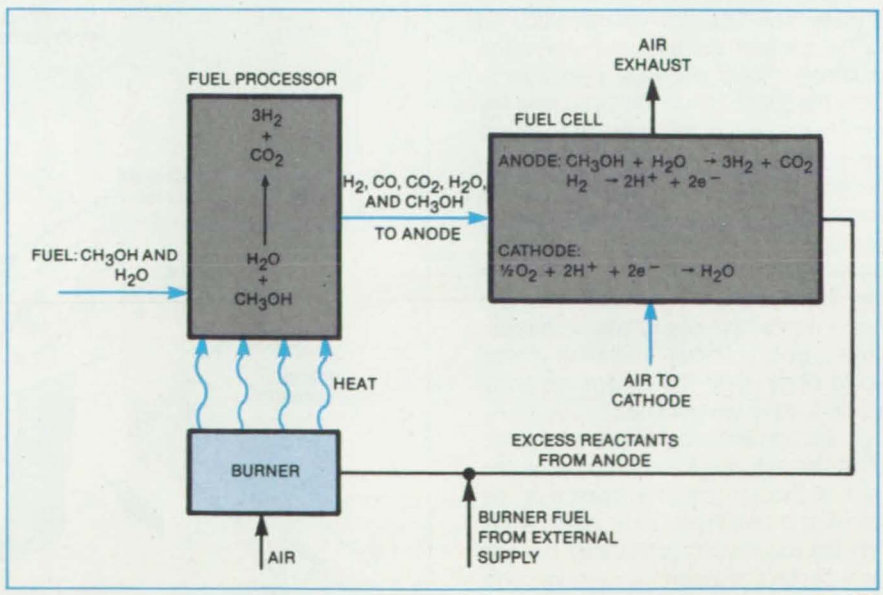

Steps 1 and 2 of the Methanol Conversion take place in the fuel processor and in the fuel cell, respectively. When the fuel flow is reduced or less power is demanded from the fuel cell, a higher proportion of the methanol is converted in the processor. At higher flow or higher demand, more methanol (up to 50 percent) is converted in the cell.

are installed in the anode; the strips support the copper or palladium catalyst. Thus, when the methanol contacts the catalyst in the presence of steam, it produces hydrogen in the immediate vicinity of the anode. Alternatively, the catalyst can be supported in such a way that it is independent of, and does not interfere with, the platinum in the anode. Then the methanol would be converted to hydrogen uniformly over the anode surface and would be utilized more efficiently.

This work was done by Gerald E. Voecks of Caltech for **NASA's Jet Propulsion Laboratory.** *For further information, Circle 62 on the TSP Request Card.*

Inquires concerning rights for the commercial use of this invention should be addressed to the Patent Counsel, NASA Resident Office-JPL [see page 29]. *Refer to NPO-15823.*

Manipulator for Heating and Cooling in Ultrahigh Vacuum

Temperature of transferred samples can be varied from 150 to 1,750 K.

Langley Research Center, Hampton, Virginia

In a sample-transfer system for use in ultrahigh vacuum, the samples are mounted on a threaded circular holder that is transferred to the flip mechanism of the manipulator by simple translation and rotation. The flip mechanism contains an electrode assembly and a thermocouple that make direct contact with the sample. A copper plate and flexible strap are attached to the receiving block to cool the sample. These simple modifications allow a broad range of sample temperatures (150 to 1,750 K) and direct temperature measurements, while retaining the advantage of the additional degree of freedom provided by the flip mechanism of a precise manipulator.

When the sample and sample holder are attached to the manipulator, the current used to heat the sample enters through the sample-holder heater wires and exits through the rear electrode assembly that contacts the back of the sample (see figure). A carbon-coated Ta/Re contact on the rear electrode assembly allows electrical continuity to carry the 0 to 20 A necessary to heat the sample and still permit separation of the sample after the experiment. A spring-loaded thermocouple assembly (axially positioned) also makes contact with the back of the sample to measure its temperature directly. This direct measurement is very important since the emissivity and size of the sample cannot always be controlled, and unknown radiation losses would complicate the determination of actual sample temperature.

In addition to the axial spring force exerted through the thermocouple on the back of the sample, the rotation of the sample and the sample holder into the modified flip mechanism enhances the intimate contact between the thermocouple and the sample. Samples that cannot be tacked directly to the sample holder or are not conductors are encased in a 0.05-mm Ta sheet envelope with holes in front and back for the surface analysis and temperature measurement.

The flexible copper strap used for sample cooling is attached to the flip mechanism and to a heavy copper feedthrough on the chamber wall. On the outside of the chamber, an extension to the copper feedthrough is immersed in liquid nitrogen. The lowest equilibrium sample temperature achieved by this technique is approximately 150 K. Intermediate temperatures are obtained by a combination of heating and cooling.

This work was done by R. A. Outlaw and Bill T. Baugh of **Langley Research Center.** *For further information, Circle 104 on the TSP Request Card.*

This invention is owned by NASA, and a patent application has been filed. Inquiries concerning nonexclusive or exclusive license for its commercial development should be addressed to the Patent Counsel, Langley Research Center [see page 29]. *Refer to LAR-13040.*

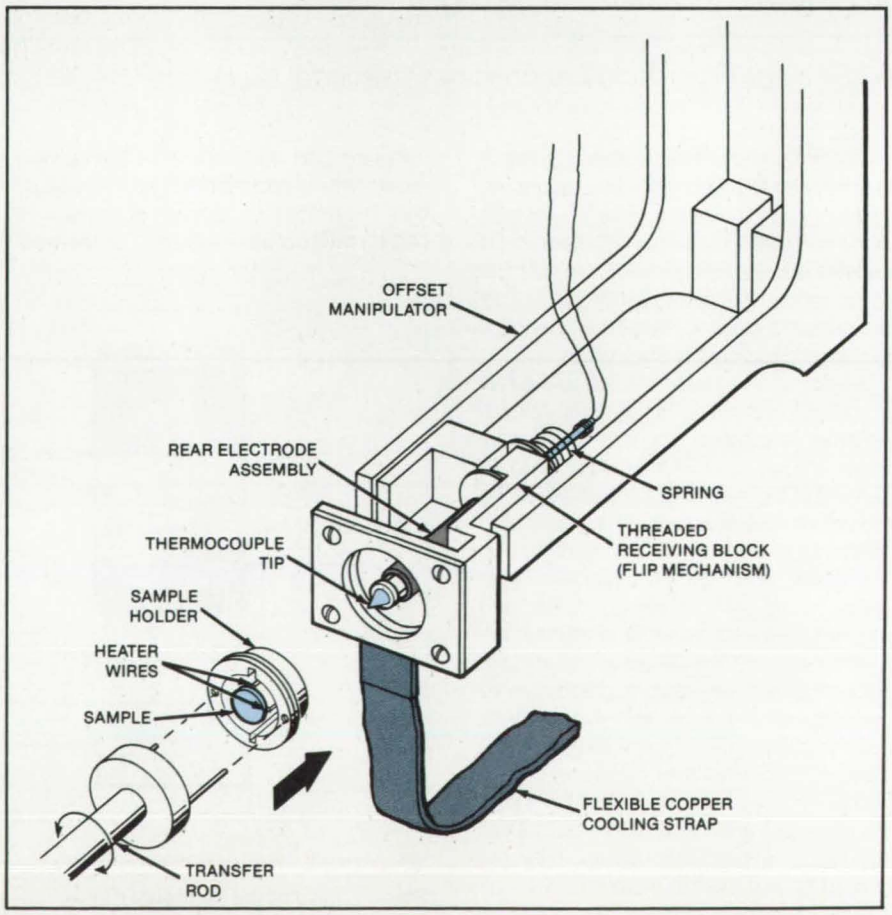

The Sample Holder Is Rotated into the Receiving Block until the sample back contacts the thermocouple and the rear electrode.

Wide-Angle, Wide-Band Camera for Remote Imaging

Resolution and field of view are enhanced.

NASA's Jet Propulsion Laboratory, Pasadena, California

An improved ultraviolet-to-infrared camera design combines high resolution and a relatively wide field of view in a remote-imaging system. Although the design is intended for a satellite-borne system to give information on such Earth features as vegetation, pollution, and land formation mineral deposits, the optical principle may also be useful in ground-based or airborne high-resolution television for imaging objects at great distances.

The camera employs a Schmidt imager, which consists of a fused-silica/sapphire refracting corrector plate, a spherical primary mirror of 200-mm radius, and a spherical coupling mirror of 133-mm radius (see figure). The curved surfaces of the components share a common axis of symmetry, but the components consist of only small off-axis portions of these surfaces, and an off-axis entrance aperture is used. The corrector plate lies off axis near the center of curvature of the primary mirror. The spherical coupling mirror is placed at the primary-mirror focal position.

The off-axis arrangement is necessary to allow access to the image plane for field flattening and to prevent changes in vignetting between different image points. The spherical coupling mirror helps to flatten the field and reflects the light onto the first paraboloidal relay mirror. From there, the light goes to the second paraboloidal relay mirror, then to the final image plane.

The center of curvature of each paraboloid (vertex radius of curvature 750 mm) lies at the vertex of the other paraboloid, and both are equidistant from the final image plane. Consequently, the relay system has unit magnification. The relay system makes available a region near the image plane for the insertion of filters and shutters comparable in size to the system focal length of 100 mm.

A 12-mm-square charge-coupled device

This **Off-Axis Schmidt Imager and Relay System** has a 7°-by-7° field of view. The charge-coupled device at the image plane contains an array of 800 by 800 picture elements, each 15 μm square.

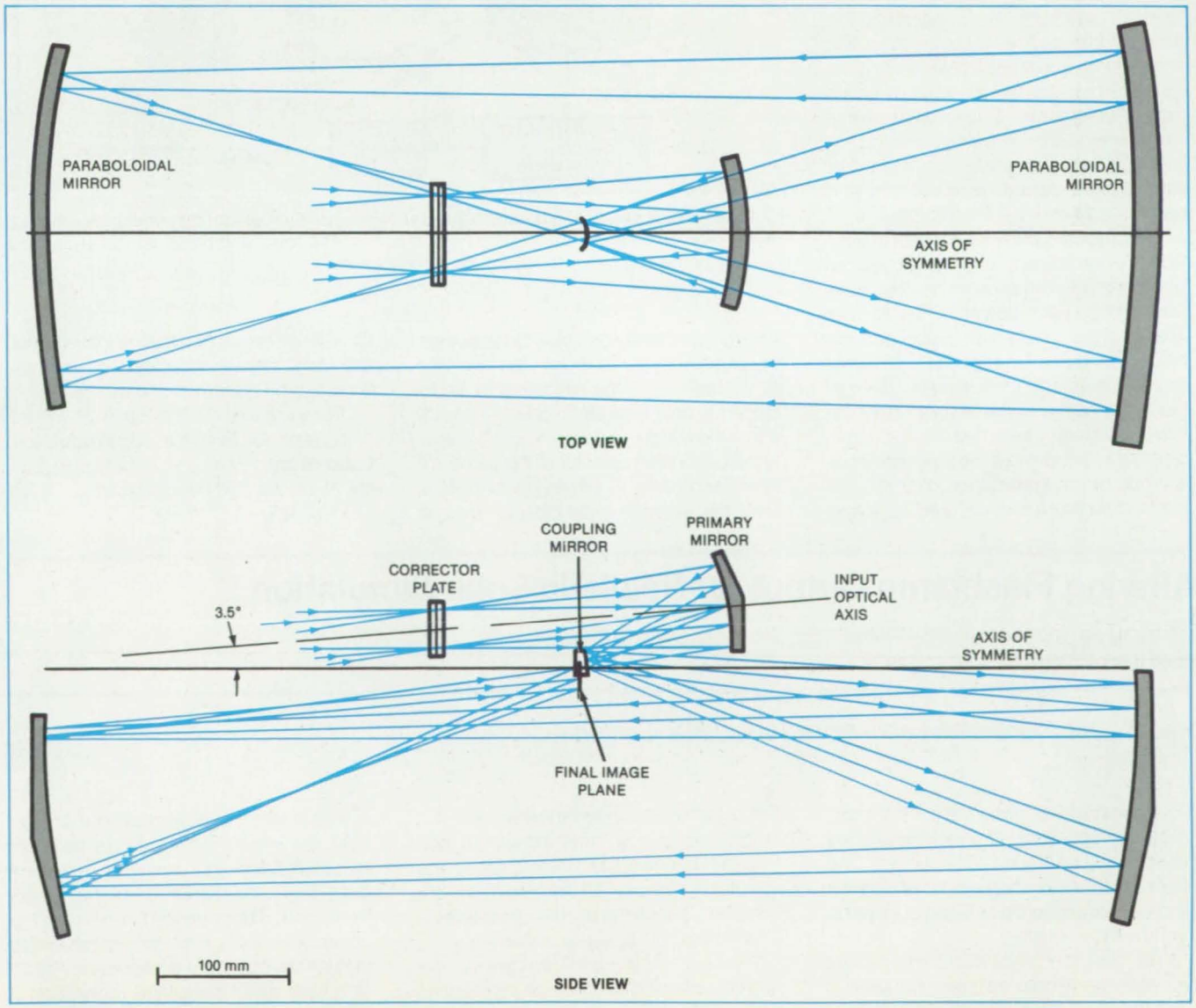

of 800 by 800 picture elements is placed at the final image plane. (The current system has 400 by 400 elements.) The device is sensitized to ultraviolet and detects light over the spectral range of 0.215 to 1.10 μm (ultraviolet through visible to infrared). The field of view is square, measuring 7° by 7°.

This work was done by Paul D. Atcheson of the University of Arizona for **NASA's Jet Propulsion Laboratory.** *For further information, Circle 50 on the TSP Request Card.*
NPO-15799

Segmented Detector for Cosmic Gamma Rays

A segmented structure allows gamma rays of cosmic origin to be distinguished from internal radioactivity.

NASA's Jet Propulsion Laboratory, Pasadena, California

A proposed germanium gamma-ray detector is divided into electrically independent regions so that cosmic gamma rays can be distinguished from background events due to the decay of internal radioactivity produced from particle bombardment of the detector in the environment of space. Internal radioactive beta decay events deposit energy predominately at a single detector location. Cosmic gamma rays usually interact at several locations. By separating the detector into segments and connecting each segment to a separate counting circuit, the number of interaction regions can be determined. Background events can be rejected by requiring interaction in two or more segments. On the other hand, cosmic gamma rays interacting in several segments will be accepted.

The proposed detector consists of a cylinder 6 centimeters in diameter, divided electrically into five sections, each 1 centimeter thick. Each segment has its own analog signal chain with pulse discriminators to monitor the deposition of energy in that segment (see figure). A high-resolution energy signal is taken from the inner electrode, then fed to a charge-sensitive preamplifier. If the outer electrode is made by ion implantation of boron, the topmost segment can be used as a low-energy gamma-ray detector. External logic circuitry enables additional combinations of interactions in the segments to be included in data analysis to obtain a greatly improved sensitivity compared with that of an unsegmented detector of the same volume. According to Monte Carlo calculations, the sensitivity of the detector is two to three times better than that of conventional detectors because background interactions can be discerned and eliminated.

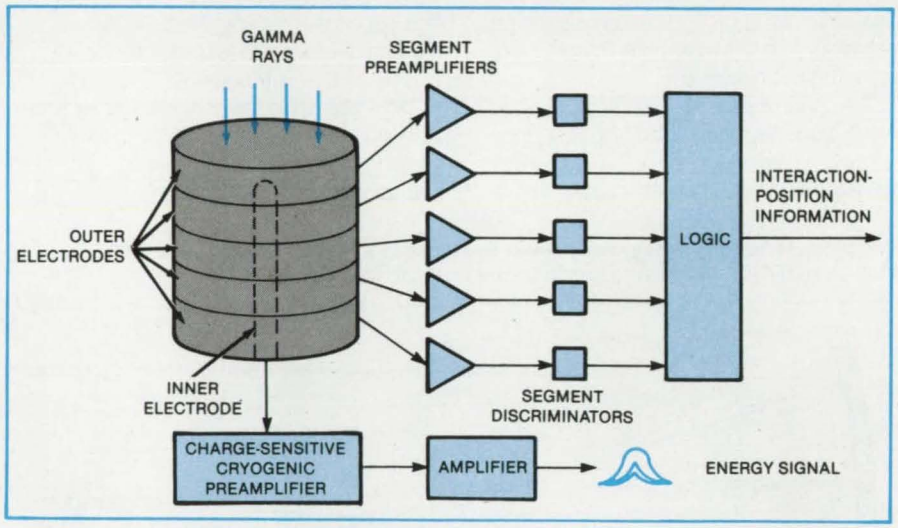

A Preamplifier and Discriminator Channel connects each electrically independent segment of a gamma-ray detector to logic circuitry. The logic compares and analyzes the events in the segments to determine their sources.

This work was done by Larry S. Varnell of Caltech for **NASA's Jet Propulsion Laboratory.** *For further information, Circle 75 on the TSP Request Card.*
NPO-16245

Altering Flashlamp Output for Realistic Solar Simulation

Filter in large-area simulator ensures long-term accuracy.

NASA's Jet Propulsion Laboratory, Pasadena, California

A commercial glass optical filter corrects the spectrum of xenon flashtubes used to test photovoltaic solar cells. The filter withstands thousands of flashes without perceptible alteration of its passband characteristics.

The filter is a 2-mm-thick Schott GG-4 (or equivalent) colored glass. It is used in conjunction with a modified version of the originally-designed intensity slit in a large-area pulsed solar simulator (see Figure 1). While the filter reduces the spectral irradiance of the simulator, the modified slit restores the available illumination and ensures uniformity of illumination within ± 1 percent at the target plane where the solar cells under test are located.

The desired spectrum is that of Sunlight shining through 1.5 standard air masses. Such light contains less blue than does the xenon-flashlamp spectrum, and, if uncorrected, the flashlamp spectrum could cause calibration errors as high as 8 percent in some solar cells. The filter attenuates blue more than it does red, the exact filter spectral

"Page missing from available version"

"Page missing from available version"

dependence being such as to make the output spectrum closely resemble the desired spectrum (see Figure 2). With the filter, calibration errors are reduced to less than 1 percent.

This work was done by Robert L. Mueller and Clay H. Seaman of Caltech for **NASA's Jet Propulsion Laboratory.** *For further information, Circle 74 on the TSP Request Card.*

Inquires concerning rights for the commercial use of this invention should be addressed to the Patent Counsel, Marshall Space Flight Center [see page 29]. Refer to NPO-16167.

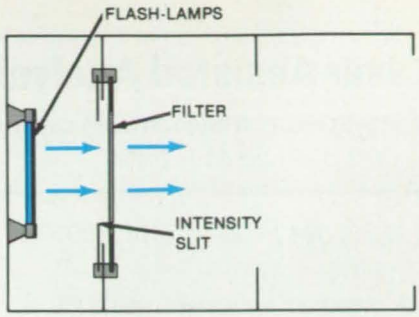

Figure 1. A **Solar Simulator** provides uniform flashes of light for measuring the output and efficiency of solar cells. The filter corrects the spectrum of the flashlamps.

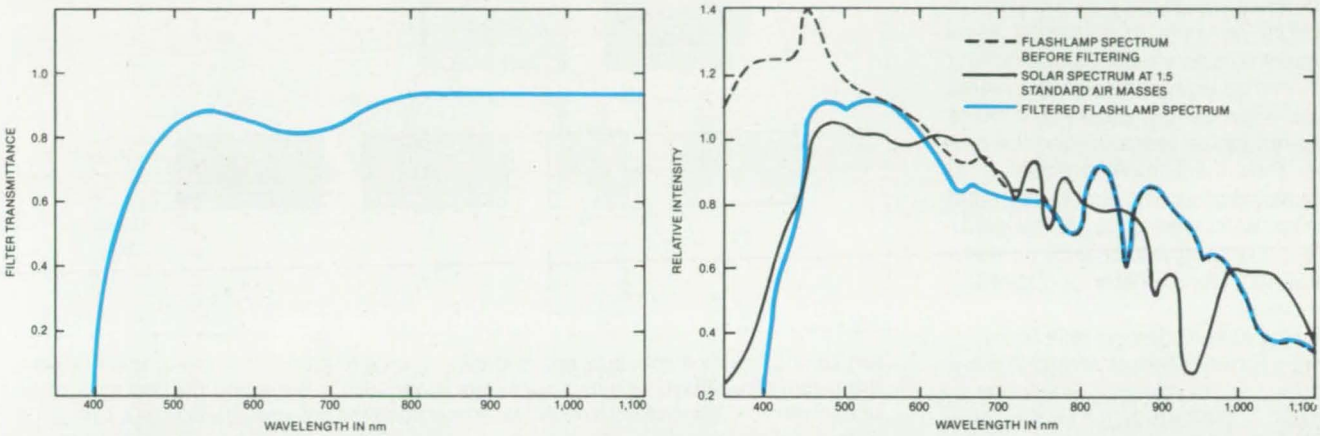

Figure 2. The **Output Spectrum (The Flashlamp Spectrum After Filtering)** approximates the desired spectrum of Sunlight shining through 1.5 standard air masses.

Estimates of Latent Heat in Clouds

Satellite cloud imagery is combined with rawinsonde data.

Marshall Space Flight Center, Alabama

The release of latent heat in the formation of clouds and precipitation is estimated more accurately with a simple technique that merges satellite cloud imagery with rawinsonde (tracked-radiosonde) data on air pressure, temperature, humidity, windspeed, and wind direction. The technique was created to improve the diagnosis of energy states and transformations in extratropical cyclones.

The input data in the new estimating technique are the latent heat, Q_O, calculated at a specified grid point in the conventional way from rawinsonde data, and the local cloud fraction, α, obtained from satellite photographs. The improved estimate, Q_O^*, of latent heat at the grid point is calculated according to the following algorithm:

- If $Q_O \neq 0$, then $Q_O^* = \alpha Q_O$.
- If Q_O and α are both zero, then $Q_O^* = 0$.
- If $Q_O = 0$ but $\alpha \neq 0$, then a weighted interpolation is made from the surrounding grid points according to

$$Q_O^* = \frac{\sum \frac{\Omega_i}{d_i}}{\sum \frac{1}{d_i}}$$

where d_i = the distance to the ith grid point.

The technique was tested over a 2-day period with standard rawinsonde data from 99 North American stations on a grid of 1.25° in latitude by 1.603° in longitude. The cloud images for the test were obtained from a Sun-synchronous polar-orbiting satellite. The technique yielded an average 15-percent improvement in latent-heat-release estimates in regions with abundant conventional data. A 30-percent improvement was noted in regions with sparse conventional data simulated by ignoring one-third of the rawinsonde stations.

The primary sources of error are the inaccuracies in the rawinsonde measurements and any inability to deduce the local cloud fraction from the available satellite photographs. Another obstacle to the further refinement of the technique is that the cloud altitude cannot be determined from the satellite photographs.

This work was done by Phillip J. Smith of Purdue Research Foundation for **Marshall Space Flight Center.** *No further documentation is available.*
MFS-25977

Laser-Assisted Analysis of Aerosol Particles

Mass spectrometer would determine the composition of one particle at a time.

NASA's Jet Propulsion Laboratory, Pasadena, California

A proposed instrument would make rapid mass-spectrometric analyses of individual particles in aerosols. Each particle would be vaporized and ionized by an intense laser pulse, which creates ions of minimum complexity. The pulse would not ionize gases around the particles. Only the sample species of interest would be ionized, and background noise would thus be reduced. The instrument should be able to analyze particles of around 1-μm diameter and perhaps even smaller.

The instrument concept (see figure) includes a particle-beam generator like that described in "Continuous Monitoring of Aerosols," (NPO-15292), *NASA Tech Briefs*, Vol. 7, No. 1 (Fall 1982), page 54. Ambient air is drawn into the particle-beam generator, which focuses the aerosol particles in the air into a beam while removing most of the air. The beam enters the ion-source region where the arrival of each particle is sensed by a photomultiplier tube from the light pulse of a helium/neon laser, scattered by the particle. The photomultiplier output triggers a pulsed neodymium:yttrium aluminum garnet (Nd:YAG) laser, the focused light of which vaporizes the particle and ionizes the vapor.

The ions are then mass separated in a double focusing focal plane mass spectrograph [Maltanch-Herzog (or equivalent) type]. Ions having molecular weights of 25 to 500 atomic mass units can be monitored simultaneously along the focal plane.

An electro-optical ion detector at the spectrograph focal plane converts the ion currents into electron currents in a microchannel electron-multiplier array, then converts the electron currents into photons where they impinge on a phosphor-coated window of optical fibers. The overall ion-to-photon gain of the detector is about 1 million. Linear self-scanning photodiode arrays measure the spatial distribution and the photon intensity, thus yielding a spectrum of number of ions as a function of mass-to-charge ratio. This spectrum represents the composition of a given single particle.

After each burst of ions from the ion source, the detector output is read, and the detector is prepared for the ion burst from the next particle. About 20 particles per second can be analyzed in this fashion. A scanning mass spectrometer cannot be used to obtain the complete mass spectrum from a single particle due to the brevity of the ion-pulse width.

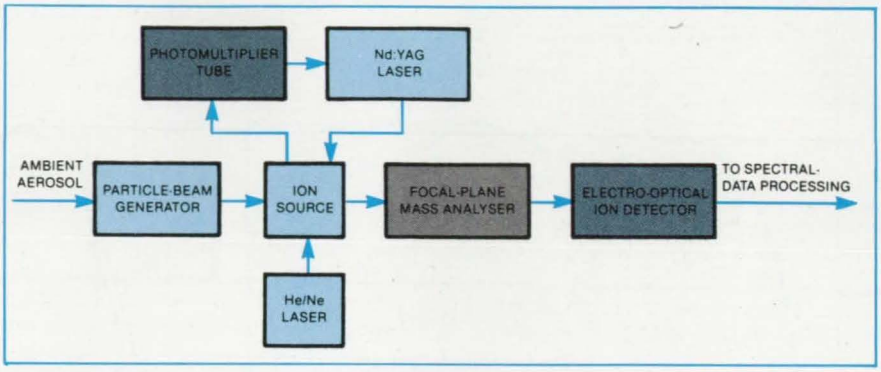

Two Lasers function cooperatively in the ion-source portion of the mass spectrometer. The helium/neon laser, with its continuous beam, aids in detecting the presence of an aerosol particle. The pulsed Nd:YAG laser vaporizes the detected particle and ionizes its constituent molecules.

The ability to analyze single aerosol particles continuously makes the technique suitable for the detection of toxic aerosol particles on a real-time basis and for the identification of their sources. This ability will also yield more detailed data on the chemical nature of particle emissions from coal-burning powerplants.

This work was done by Mahadeva P. Sinha, Charles E. Giffin, David D. Norris, and Sheldon K. Friedlander of Caltech for **NASA's Jet Propulsion Laboratory.** *For further information, Circle 32 on the TSP Request Card.*

Inquires concerning rights for the commercial use of this invention should be addressed to the Patent Counsel, NASA Resident Office-JPL [see page 29]. Refer to NPO-15308.

Ultrahigh-Vacuum Sample-Transfer System

Low-cost system features short-term sample transfer.

Langley Research Center, Hampton, Virginia

An ultrahigh-vacuum (UHV) sample-transfer system developed and in use at Langley Research Center features short-term (less than 30 minutes) transfer of samples from atmospheric pressure into a sample manipulator within the UHV analysis system without significantly degrading the system pressure. The system allows the samples to be transferred to a 5-degree-of-freedom manipulator at UHV levels of 10^{-9} torr.

The conventional procedure for installing

samples into a UHV analysis system without sample-transfer capability involves exposing the system to atmospheric pressure during installation with a subsequent high-temperature bakeout (250° to 450° C) for 4 to 5 days to achieve or recover pressures of 10^{-10} torr or less. In addition to the long delay, the repeated bakeouts required for each new sample cause degradation of seals, electrical leakage in instrumentation, and other cumulative, deleterious effects. Further, high bakeout temperatures limit the types of experiments that can be conducted and can alter the sample material. Commercial UHV transfer systems are available but are very expensive.

This new system is an austere approach to sample transfer, involving no automation. The sample is loaded onto a transfer rod located within a small ion-pumped chamber separated from the main UHV chamber by an isolation valve. After evacuation, the isolation valve is opened, the sample is transferred to the manipulator in the UHV chamber, and the transfer rod is retracted. The isolation valve is then closed. The sample may be heated or cooled while simultaneously being analyzed by any diagnostic instrument in any position within the UHV analysis chamber, since the sample is completely transferred to the manipulator. Thus, the analysis takes place at the lowest system pressure. The sample-transfer chamber can also be baked out at temperatures up to 450° C, permitting pretreatment of the sample under UHV conditions before insertion into the analysis chamber. The total cost of the system in use is a factor of 10 less than that of commercially available instruments.

This work was done by R. A. Outlaw and Bill T. Baugh of **Langley Research Center.** *For further information, Circle 108 on the TSP Request Card.*
LAR-12993

Battery-Charge-State Model

Equations approximate the effects of electrochemical processes.

NASA's Jet Propulsion Laboratory, Pasadena, California

A charge-state model for lead/acid batteries has been proposed as part of an effort to make the equivalent of a fuel gage for battery-powered vehicles. The model is based on equations that approximate the observable characteristics of battery electrochemistry. In contrast with earlier, nonlinear models, this one uses linear equations, is easier to simulate on a computer, and gives smooth transitions between charge, discharge, and recuperation.

The diffusion phenomena near an electrode are visualized in the model with the help of a fluidic analogy (see Figure 1). The large tank at the left represents the bulk or reserve storage capacity of the cell, and the fluid height ϱ_B corresponds to the electrolyte ion density relative to its value at full charge. The width of the tank, V_B, represents the volume of the electrolyte in bulk storage.

The right tank represents the conditions in the immediate vicinity of an electrode, with the height representing the relative electrolyte ion density immediately available for reaction and V_P representing the volume of electrolyte immediately available in the region of the active surface. The analog fluid current i_D corresponds to the ion-diffusion current, which is proportional to the difference in ion densities between the bulk and storage zones; namely,

$$i_D = \frac{Q_o}{\tau_D}(\varrho_B - \varrho_P)$$

where Q_o = the total charge capacity of the battery, and τ_D = a characteristic diffusion time constant.

The drain at the right represents the flow of current, i_o, to the load. The restrictor Q_o/τ_I limits the current to a value proportional to the ion density near the electrode; that is

$$i_o \leq \frac{Q_o}{\tau_I}\varrho_P$$

where τ_I = another characteristic time constant related to the maximum possible discharge rate.

Suppose that Q_o represents the total charge-storage capacity of the battery, $Q_{Po} = K_c Q_o$ represents the electrode-region storage capacity, and $Q_{Bo} = (1 - K_c)Q_o$ represents the capacity of the bulk storage zone. Then starting from full charge, the electrolyte concentration in bulk storage after a discharge time T is given by

$$\varrho_B = 1 - \frac{1}{(1 - K_c)Q_o}\int_o^T i_D dt$$

Similarly, the electrolyte concentration in the electrode zone is determined by tak-

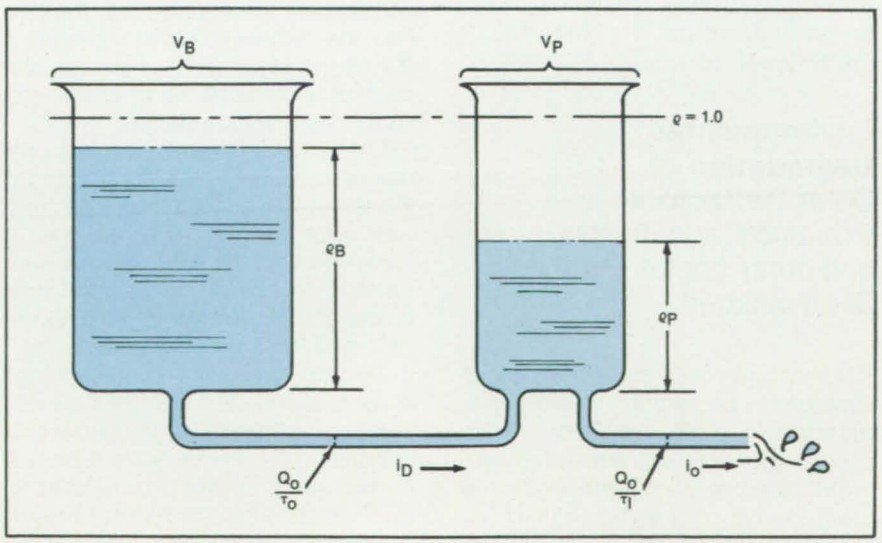

Figure 1. This **Fluidic Visualization Model** is used as an aid in deriving the diffusion equations that characterize the electrochemical activity near an electrode.

ing into account the charge added by diffusion minus the charge delivered to the load:

$$\varrho_P = 1 - \frac{1}{K_c Q_o}\int_o^T (i_D - i_o)dt$$

Together, the four equations constitute the model. Figure 2 illustrates the functional blocks of a microprocessor that would implement the model in a charge-state gage. The model coefficients Q_o, τ_D, τ_I, and K_c are derived battery test data. Although simple iterative methods are required to do this, the coefficient values are bounded, and good matches to standard test data of capacity versus discharge current and recuperation characteristics can be obtained with only two or three iterations of trial coefficients. It is expected that if these two criteria are satisfied, the model charge and discharge characteristics at constant and variable rates will correlate well with those of any real battery of the same type and capacity. Compensation for individual manufacturing variations, temperature characteristics, and aging effects of production batteries can also be accommodated by adjusting the coefficients as functions of history and service conditions.

To complete the characterization of a battery, a terminal-voltage model has been proposed. This model incorporates resistances obtained from voltage-versus-current testing along with the relative electrode charge, ϱ_P, determined from the charge-state model.

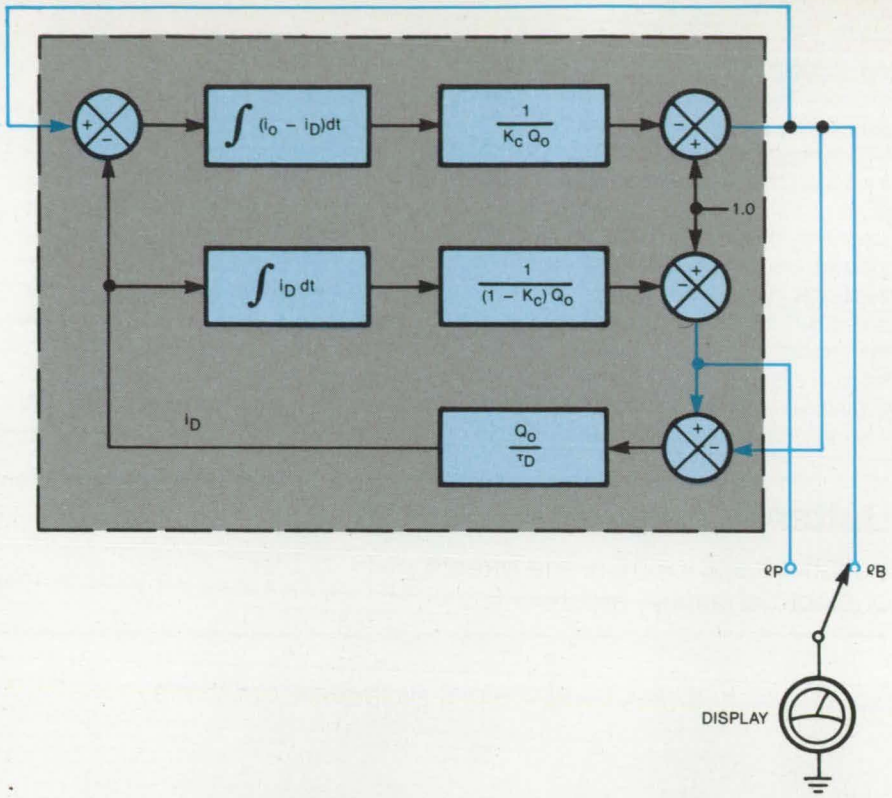

Figure 2. A **Microprocessor Continuously Monitors the Battery Discharge Current.** The current value serves as the input to circuits that perform the four-equation charge-state algorithm. The available outputs are signals that are proportional to the electrode charge ϱ_P and to the reserve charge ϱ_B.

This work was done by Howard C. Vivian of Caltech for **NASA's Jet Propulsion Laboratory.** *For further information, Circle 96 on the TSP Request Card.*
NPO-16158

Books and Reports

These reports, studies, and handbooks are available from NASA as Technical Support Packages (TSP's) when a Request Card number is cited; otherwise they are available from the National Technical Information Service.

Environmental Degradation of Solar Reflectors

Corrosion, dust buildup, and other contamination are evaluated.

A report presents results of a study of atmospheric degradation of large solar reflectors for power generators. Three general types of reflective surfaces were investigated: second-surface-silvered glass mirrors, first-surface-aluminized reflectors, and second-surface-metallized polymeric surfaces. The report also describes a computer model of natural buildup and removal (by rain and dew) of contamination from reflectors. The data from the study can be used to determine the effects of soil buildup and the best method and frequency of washing at various geographic locations.

Over a dozen glass, metal, and polymer reflective surfaces were exposed to the environment in southern California. Data were taken at three sites: two at Pasadena and one at Goldstone, near Barstow. In additon, a model of dust buildup and removal was based on worst-case data for six nationwide sites.

The report presents plots of the change in specular reflectance at the California sites. Interestingly, a dip in the plot corresponds to an oil-refinery fire in the Los Angeles area: Contamination reduced reflectance by 59 percent. Standard mirror-backing paint eliminated visible corrosion, at least during the 1-year period of the study. Unpainted samples, in contrast, showed corrosion within a week after they were set up.

The equation used to model the degradation in specular reflectance is discussed. Representative values of coefficients for fitting the equation to experimental data are given for various reflector materials and various locations.

An example illustrates an application of the model in estimating the effects of the mirror-replacement interval and slope error on energy costs. The costs per kilowatt-hour of second-surface-silvered glass-mirror reflectors are plotted for different replacement intervals with a 30-day cleaning interval.

This work was done by Frank L. Bouquet of Caltech for **NASA's Jet Propulsion Laboratory.** *To obtain a copy of the report, "Environmental Responses of Solar Reflective Surfaces," Circle 72 on the TSP Request Card.*
NPO-16053

BEI's LED-equipped Optical Encoders. Proven thru Time and Space.

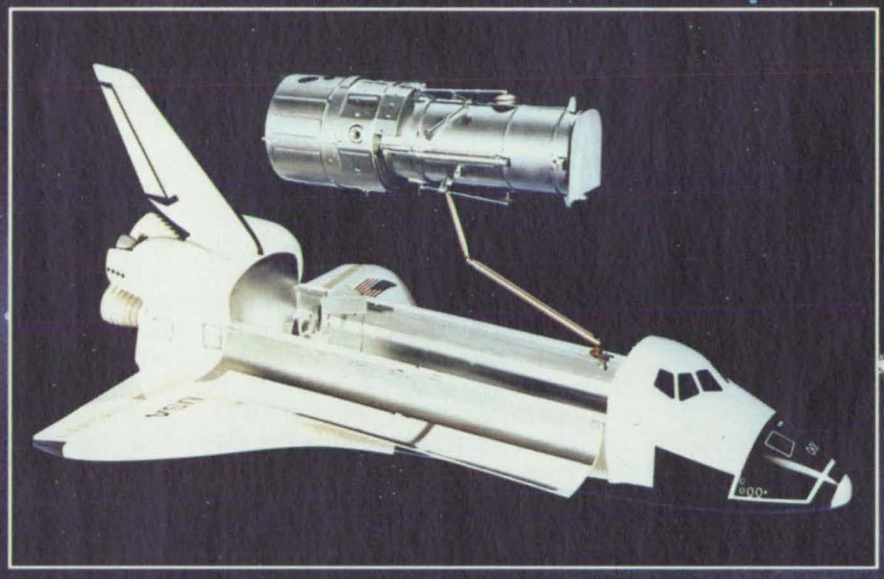

BEI's LED-equipped optical encoders help position the space shuttle arm and provides guide star position data on NASA's Hubble Space Telescope.

This totally integrated motor-encoder system for the Hubble space telescope provides resolution and accuracy to 21 bits.

The space shuttle's remote manipulator arm uses high-reliability BEI encoders.

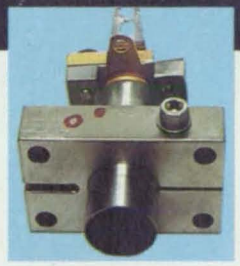

LED read station with optics.

Our remarkable code disk, unequaled for accuracy in the world ... and beyond.

BEI introduced the first 19-bit LED light source encoder design to NASA almost twenty years ago. We've both traveled a long way since then.

Our LED-equipped "pancake" encoders designed for the space shuttle in 1974 have reliably helped position the remote manipulator arm on many successful missions. Only 1.6" thick including electronics, they offer a direct read of 16-bits resolution and accuracy.

In 1979, BEI's Ultra-Loc® precision drive with LED-equipped motor-encoders were selected for the space telescope's fine guidance system. This lightweight beryllium motor-encoder is totally integrated including motor commutation. It provides resolution and accuracy to 21-bits — with rotational drive speeds varying from 0.5 arcseconds/second (one revolution every 30 days), to 16384 arcseconds/second. The design life is ten years.

Our long established systems and procedures are in compliance with quality criteria NHB-5300.4 (1B) and MIL-Q-9858A, and high reliability criterion MIL-STD-785. Contact BEI for more details.

BEI Motion Systems Co.

BEI

Digital Products Division

BEI Motion Systems Co. • Digital Products Division • P. O. Box 3838 • Little Rock, Arkansas 72203 • (501) 851-4000

Circle Reader Action No. 2

Materials

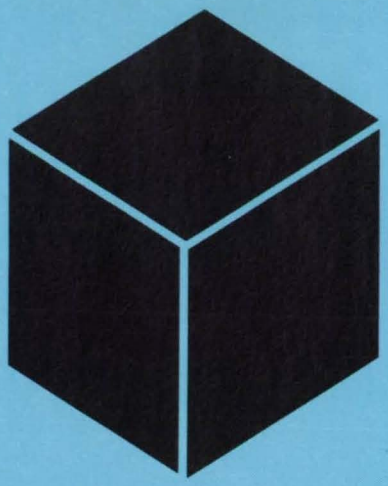

Hardware, Techniques, and Processes

90 **High-Purity Silicon Seeds for Silane Pyrolysis**
91 **Thermosetting Phthalocyanine Polymers**
94 **Increasing Fire Safety of Epoxies**
94 **Ceramic Coatings for Engine Parts**
95 **High-Performance Filleting and Channel Sealants**
96 **Purifying Aluminum by Vacuum Distillation**
96 **Foam Insulation for Cryogenic Flowlines**
97 **Shielding Against Intense Laser Beams**
98 **Silicone Coating on Polyimide Sheet**
98 **Melt Stirring by Horizontal Crucible Vibration**
99 **Nonyellowing Polycarbonate for Outdoor Use**
100 **Reversing Glass Wettability**
103 **Resin Characterization in Cured Composite Materials**
104 **Efficient Process for Making Polycrystalline Silicon**
105 **Synthesizing Metal Phthalocyanine Imide Polymers**
106 **Solar-Assisted Oxidation of Toxic Cyanide**
107 **Ethynyl-Terminated Ester Oligomers and Polymers**
107 **Static-Suppressing Optical Paint**
108 **Improving Emittance of High-Temperature Insulating Tile**
109 **Rubberized, Brominated Epoxies**
109 **Waterproofing Agents for Silica Tiles**

Books and Reports

110 **Preparation and Characterization of $Hg_xCd_{1-x}Te$**
110 **Strength of Graphite/Metal Composite Lap Joints**
111 **Predicting Effects of Impacts on Confined Explosives**
111 **Further Tests of 38 Ball-Bearing Greases**

High-Purity Silicon Seeds for Silane Pyrolysis

Seeds are ground from coarse particles without introducing impurities.

NASA's Jet Propulsion Laboratory, Pasadena, California

Seed particles for fluidized-bed production of silicon can be made by a new contamination-free, economical method. Until now, fluidized-bed seeds have been made by grinding semiconductor-grade silicon in a ball or hammer mill and leaching the product with acid, hydrogen peroxide, and water. This process is time-consuming and costly and tends to introduce impurities through the metal grinders.

In the new method, large particles of semiconductor-grade silicon are fired at each other by high-speed streams of gas and thereby break up into particles of suitable size for a fluidized bed. No foreign materials are introduced, and leaching is unnecessary. The method can be used to feed a fluidized-bed reactor for continuous production of high-purity silicon.

Large particles are fed into a jet mill by opposing streams of nitrogen (see figure). The streams impinge on each other, and the particles break up into small ones, which are fed to a fluidized bed. Silane flowing through the bed decomposes, depositing silicon on the seed particles in the bed. As silicon deposits on the seeds, they grow in size and can be easily removed from the bottom of the fluidized bed. This product is collected for conversion to single-crystal ingots for solar cells. A portion of the product, however, is directed into the jet mill. A continuous supply of silicon seeds is thus provided.

In a demonstration of the method, particles ranging in size up to 2,000 μm were fed into a subsonic-jet mill. In a single pass, 15 to 30 percent of the particles were broken into fragments about 400 μm or less in size. The efficiency of fragmentation can be increased by raising the impact velocities and adjusting the impact area, feed rate, and initial particle size.

This work was done by George C. Hsu, Naresh K. Rohatgi, and Andrew Morrison of Caltech for **NASA's Jet Propulsion Laboratory.** *For further information, Circle 85 on the TSP Request Card.*
NPO-16287

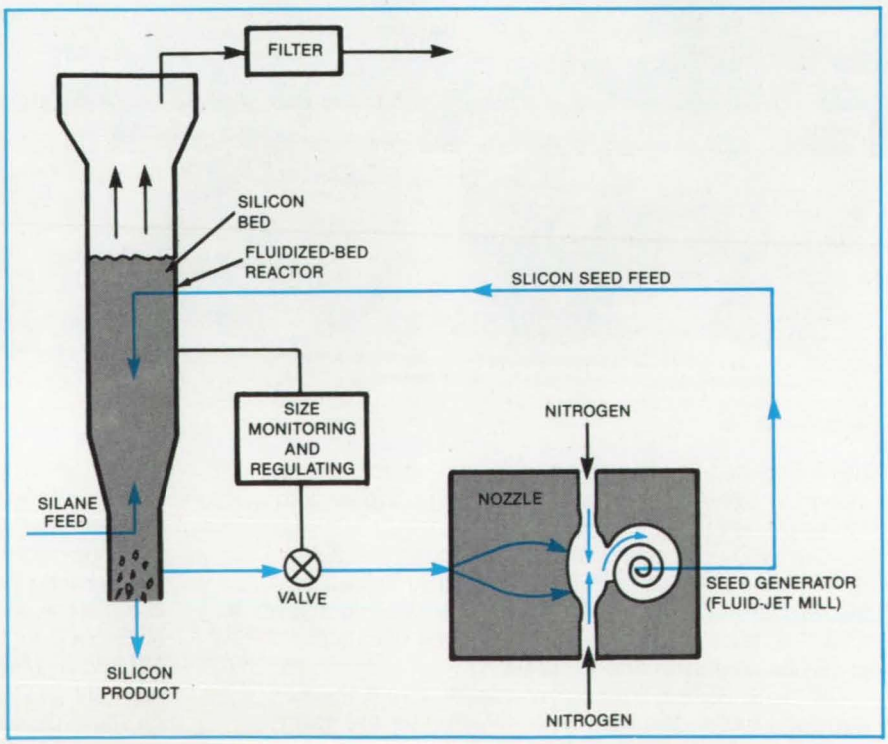

In this **Continuous Process** for the production of high-purity silicon, the supply of silicon seeds in the fluidized bed is constantly replenished. A small portion of the product is withdrawn and reground for seeds by a jet mill.

Thermosetting Phthalocyanine Polymers

Some formulations resist thermal degradation up to 500° C.

Ames Research Center, Moffett Field, California

A group of phthalocyanine polymers resist thermal degradation. Based on earlier work with similar materials, the polymers are expected to be semiconducting, with conductivities of the order of 10^{-2} $(ohm\text{-}cm)^{-1}$. Their principal applications will probably be in molded or laminated parts that have to withstand high temperatures.

The polymers are made from either of two classes of monomer (see figure). One class consists of bisphthalonitriles with imide linkages. The synthesis of such a monomer occurs in two steps, beginning with the reaction of a 4-aminophthalonitrile derivative with dianhydride to form a bisphthalonitrile derivative with amic acid linkage. In the second step, the amic acid linkage is thermally dehydrocyclized to the imide form.

The other monomer class consists of bisphthalonitriles with ester-imide linkages. The starting ingredients in this case are trimellitic anhydride acid chloride and an aromatic or aliphatic diol. These are reacted in the presence of pyridine (which removes HCl) to form a bisphthalic anhydride with an ester linkage. The anhydride is reacted with 4-aminophthalonitrile to obtain a bisphthalonitrile with ester and amic acid linkages. Upon dehydrocyclization of the amic acid linkages to imides, the desired monomer is obtained.

The monomer (which is a solid) is prepared for polymerization by grinding it to a powder and mixing it with a powdered metal or metal salt — preferably cuprous chloride. The mixture is heated in flowing nitrogen to a temperature ranging approximately from 245° to 420° C during a time ranging from about 15 minutes to 1½ hours, the exact values depending on the monomeric constituents. The color of the resulting polymer varies from deep blue to bluish black to blue with pinkish reflection, while the decomposition temperature lies in the range of 350° to 500° C (again, depending on the constituents).

This work was done by G. M. Fohlen and J. A. Parker of **Ames Research Center** *and B. N. Achar of the National Research Council. For further information, Circle 100 on the TSP Request Card.*

Inquiries concerning rights for the commercial use of this invention should be addressed to the Patent Counsel, Ames Research *[see page 29]**. Refer to ARC-11511.*

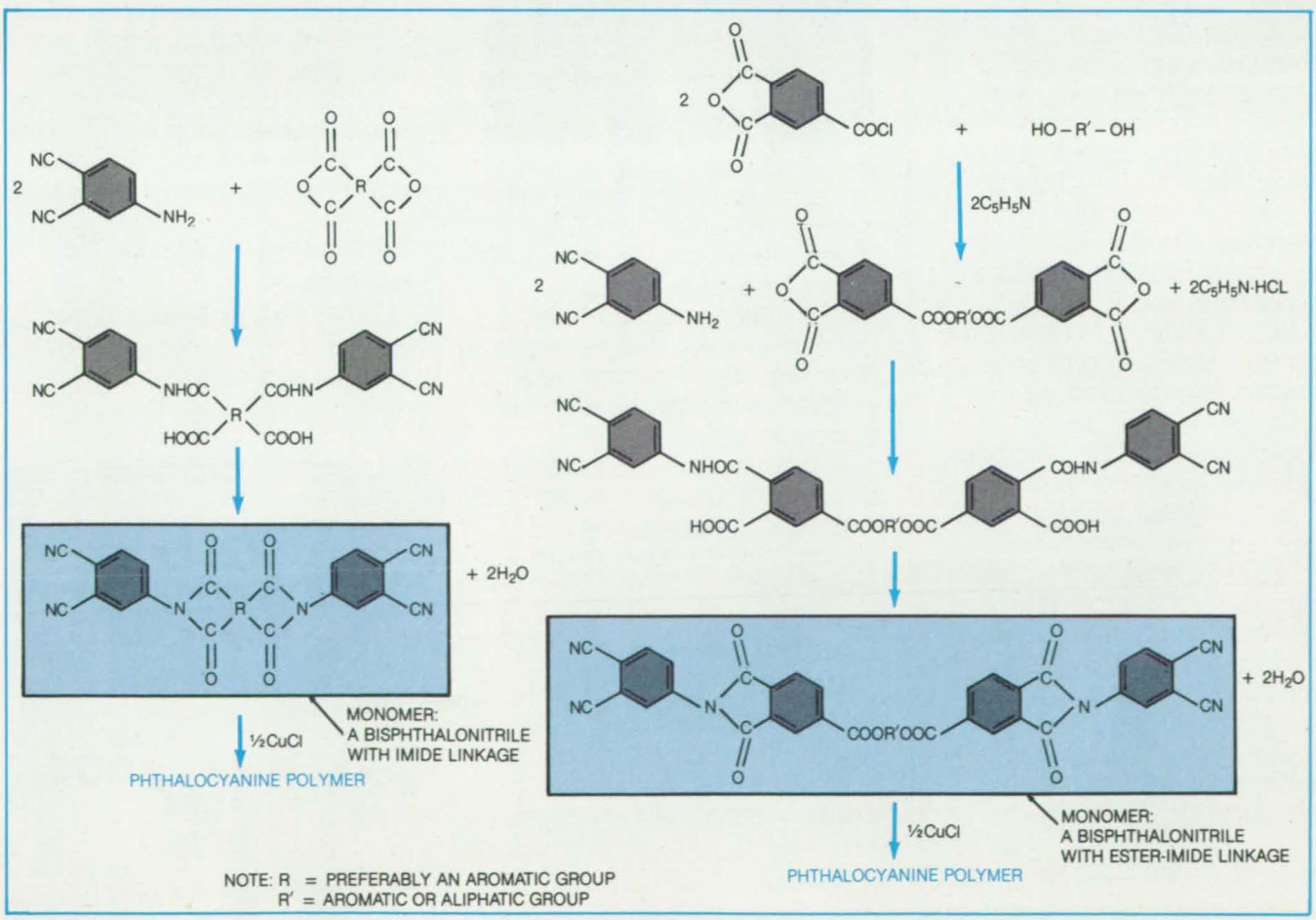

Two Kinds of Monomer are synthesized to produce the new phthalocyanine polymers. A monomer is polymerized by heating in the presence of cuprous chloride and an inert atmosphere.

MULTI-TEC

How to multiply your technology and shorten R&D time.

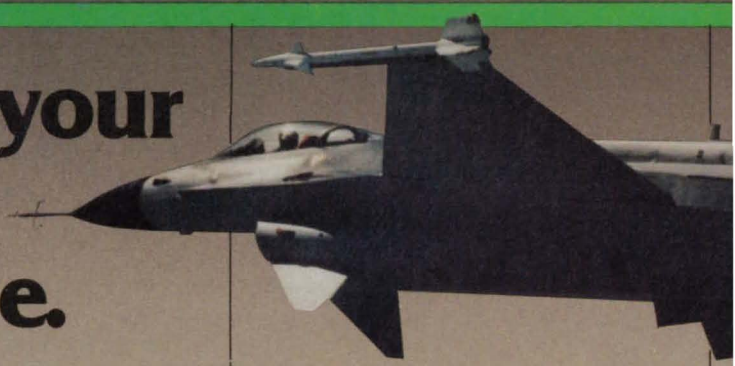

Your ability to put ideas into practice—take technology to the marketplace—is the single most critical factor in your success.

Emerson & Cuming's Multi-Tech System capabilities are based on five technologies, each individually unique but capable of working together for cost-effective solutions to your materials problems.

We manufacture a *comprehensive range of standard and custom polymer* systems, such as resin/syntactics for aerospace applications, and hybrid silicones for high frequency electronics. Our conductives technology includes cost-effective *"quick-fix" products* for EMI/RFI shielding in production and field repair. We also maintain a *Value in Use Program*—matching product performance with cost factors.

Our *RAM-Scan (Radar Absorbing Materials Scan)* provides microwave application analysis that can eliminate prototyping or further experimentation. Our *finite element analysis* program measures materials/properties for finished parts applications. We also maintain materials applications software for polymers and conductives problem solving.

Our client assistance services include our MDT team (*Multi-Discipline Task Force*) of chemical, electrical and mechanical engineers. Assigned specifically to you, the MDT team works with your engineers to provide tactical and strategic design research, and systems development.

Production-quality prototyping is possible with composite systems, which include ERM® (Elastic Reservoir Molding). ERM allows for a wide variety of materials and structural components to meet design criteria—all in one step. Finished parts production is possible with ERM prototype tooling.

Testing capabilities extend through the design process, and include our Applications Laboratories for each discrete technology.

Compounded polymers and resins.

Our Polymer Systems incorporate materials with properties critical to contemporary design. These include epoxies, silicones, urethanes, and polyesters with technical features that provide you with more than 1,600 standard solutions and infinite applications.

Electromagnetic wave absorbers.

Our Microwave Systems represent the leading edge in this growing industry. We manufacture materials in many forms, for reducing radar cross section (RCS), improving antenna performance, and developing communications systems. We also have the experience to design and manufacture the world's most sophisticated anechoic chambers.

Lightweight syntactic materials.

Our Lightweight Systems are comprised of hollow, synthetic bubbles that combine with

H SYSTEMS

specially-formulated resins to create lightweight, syntactic foam. These materials offer superior strength; they withstand high compressive pressures; and they're usable in applications from hydrospace to aerospace. New developements in syntactic technology provide ready-to-use materials for avionics, telecommunications, and aerospace.

Conductive shielding applications.

We manufacture a range of shielding materials for EMI/RFI, ESD, EGP and EMP. Our product line includes adhesives, coatings, sealants, gaskets, tapes and materials such as conformable foams and heatless solders. We also provide you with a comprehensive line of "quick fix" products for production and field repair.

Molded parts capability.

Our Composite Systems offer prototyping and finished parts production in a simple, cost-effective process. ERM provides you with finished parts that exhibit superior materials strength, greater versatility, and cost-efficient tooling and production. ERM allows for many design-engineered features—such as ballistic resistance, microwave absorption, low smoke and toxic gas emission—all in one step.

Your possibilities with Emerson & Cuming are virtually limitless. From conceptual research and development, to finished parts production, you have the resources to succeed.

For complete details about our Multi-Tech Systems, write for our free product literature c/o: Marketing Services Department, Emerson & Cuming, Canton, MA 02021. Or call our toll-free number, 1-800-TECHWAY (832-4929).

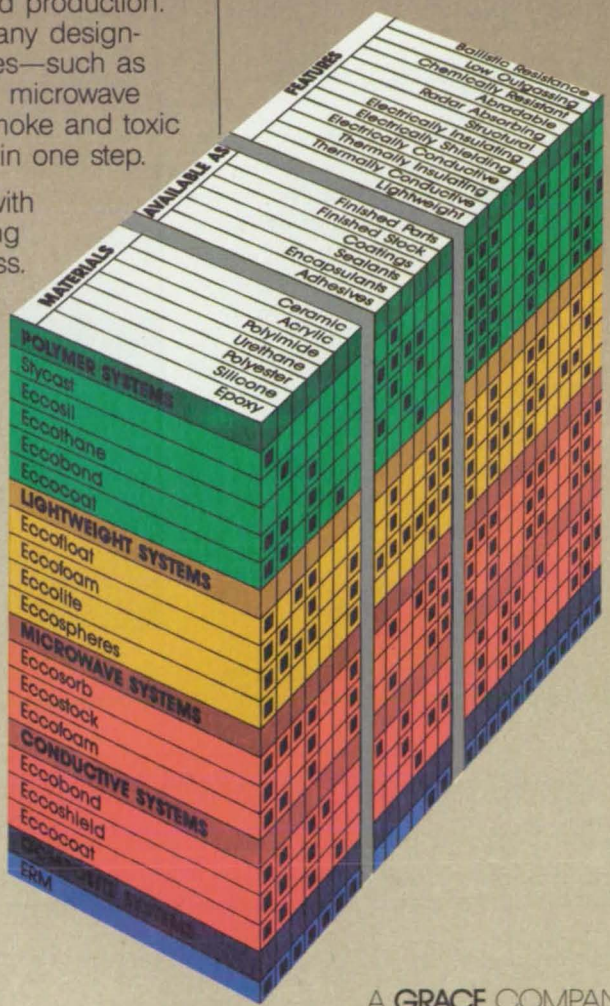

A GRACE COMPANY

EMERSON & CUMING

Where there's a way.

Circle Reader Action No. 26

Increasing Fire Safety of Epoxies

Fire-retardant moieties are incorporated into the molecules.

Ames Research Center, Moffett Field, California

An epoxy with increased resistance to fire is made by reacting any of three commercial epoxide monomers with a curing agent consisting of a mixture of the isomers 1-[di(2-chloroethoxyphosphonyl)methyl]-2,4- and -2,6-diaminobenzene (the mixture is called "DCEPD"). The curing agent incorporates phosphorus and chlorine directly into the cross-linking part of the polymer: Previously, the fire retardance of some epoxies had been improved by introducing various organophosphorous and phosphorous/halogen compounds as chemically separate additives that degraded mechanical properties.

The DCEPD (see figure) is produced by nitrating the precursor phosphonylmethyl benzene, then reducing the resulting isomeric mixture of dinitro compounds. As a consequence of the method of synthesis, the 2,4 isomer predominates. It is not necessary to separate the isomers.

The amino groups of the DCEPD are polymerizable with epoxide or anhydride groups. The DCEPD therefore cures epoxide monomers. Polymer samples were made from each of the commercial epoxide monomers, using 0.25 or 0.50 mole of DCEPD per equivalent weight of epoxide. Samples were also prepared using the conventional curing agents 4,4-diaminodiphenyl sulfone (DDS) and m-phenylenediamine (MPD).

The polymers were compared by differential scanning calorimetry and thermogravimetric analysis. Additional comparisons of heat and fire resistance were provided by the char-yield and limiting-oxygen-index (LOI) tests. Although thermal decomposition generally begins at lower temperatures in the epoxies cured with DCEPD, these epoxies have greater char yields and greater fire resistance as measured by the LOI. Of the three commercial monomers (Epcn 828, XD 7342, and MY 720), the last shows the greatest improvement with 0.25 mole equivalent of curing agent: The LOI is 59.3 for DCEPD versus 30.8 for MPD and 29.0 for DDS.

This work was done by Demetrius A. Kourtides of **Ames Research Center** *and John A. Mikroyannidis of the University of Patras, Greece. For further information, Circle 98 on the TSP Request Card.*

Inquiries concerning rights for the commercial use of this invention should be addressed to the Patent Counsel, Ames Research Center *[see page 29].* *Refer to ARC-11506.*

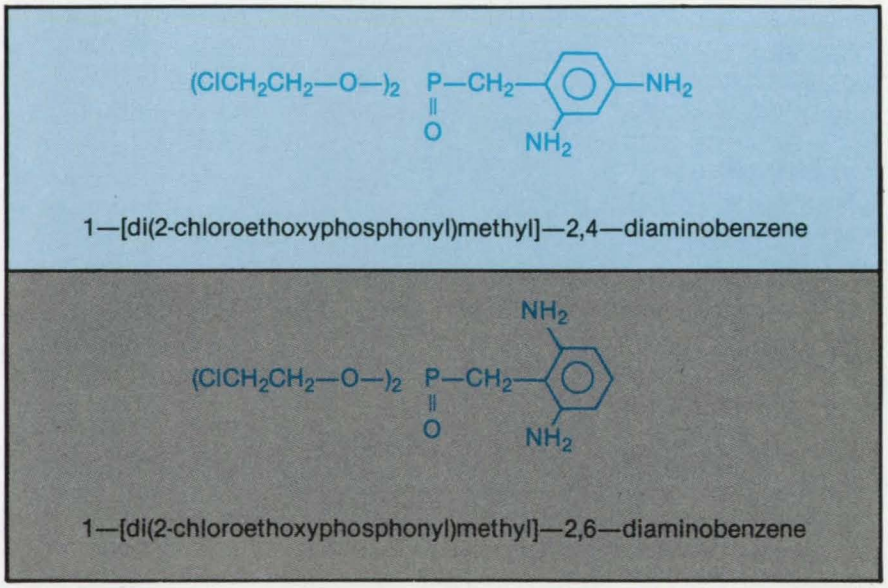

These Isomers are formed together during the synthesis described in the text. The mixture of these isomers is the curing agent that adds phosphorus and chlorine to epoxies to improve fire resistance.

Ceramic Coatings for Engine Parts

Plasma spraying would create hard, heat-resistant surfaces.

NASA's Jet Propulsion Laboratory, Pasadena, California

In a manufacturing concept, dense, nonporous ceramic coatings would be applied to metal parts by plasma spraying. The coatings should improve the resistance of the parts to corrosion and erosion in turbines and other engines. Plasma spraying is faster and cheaper than the previously used method, vapor deposition, and can be used on large parts as well as small ones.

Ceramic precursor particles are fed through an electric-arc plasma gun, where they decompose violently into organic gas and a ceramic powder composed of high-surface-area particles. The precursor is a dehydrated metallo-organic compound, preferably in dehydrated gel form. The precursor decomposes only milliseconds before the molten ceramic particles strike the surface to be coated. The particles impinge with high surface energy, forming an adherent, uniform layer.

Available precursors include aluminum isoproproxide, aluminum hexafluoroisopro-

proxide, zirconium hexafluoroisoproproxide, and zirconium tertiary amyloxide. Upon decomposition during plasma spraying, these materials produce aluminum oxide, or zirconium oxide. Coatings of several ceramics not usually plasma-sprayed (for example, titanium diboride, an extremely hard and chloride-resistant material) may also be applied in this process.

The coating density is determined by the decomposition temperature, plasma atmosphere, precursor particle size, distance from the plasma gun to the substrate, deposition rate, and substrate temperature. Small grain size, which reduces the porosity of the coating, is ensured by including grain-growth inhibitors in the precursor. Inhibitors include magnesium oxide, zinc oxide, zirconium oxide, and calcium oxide.

Precurosrs are produced by conventional chemical methods. Grain-growth inhibitors are mixed with them, and they are dehydrated at a temperature of 100° to 200° C. Dehydrated precursors contain organic materials as well as metallo-organic compounds, but are hard and friable. They can be crushed into virtually any particle-size distribution.

This work was done by James E. Schroeder of Caltech for **NASA's Jet Propulsion Laboratory.** *For further information, Circle 15 on the TSP Request Card.*
NPO-16228

Circle Reader Action No. 5

High-Performance Filleting and Channel Sealants

Compounded fluoroether elastomers are stable to 280° C.

Ames Research Center, Moffett Field, California

Filleting and channel sealants have been developed for sealing cavities in the wings and fuselage of aircraft. The filleting sealants are extruded or applied by spatula over seams, into corners of joints, over fasteners, and around such other tank intrusions as hydraulic lines and electrical conduits. The channel sealants are especially useful for occluding gaps. Both sealants function well at 177° C, as required in current specifications for supersonic aircraft. Lap and tensile strengths of the filleting sealants exceed the military specifications for this application.

The sealants have excellent resistance to fuel and other solvents. They stay flexible, are resistant to vibrational, thermal, and mechanical stresses, and adhere well to aluminum. The filleting sealants also adhere well to titanium. They should prove useful in industrial applications requiring resistance to solvents at high temperatures.

Filleting Sealant		Channel Sealant	
Ingredient	Amount	Ingredient	Amount
Polymer	1.00	Polymer	1.00
Asbestos	0.05	Asbestos	0.15
Carbon Black	0.80	Metal Deactivator	0.05
Epoxy Silane	0.02	Lithium Aluminum Silicate	0.55

Preferred Sealant Formulations are given in parts by weight.

The general type of polymer binder used had already been suggested for use in seals, sealants, and gaskets. However, the new composite sealants perform better than such a polymer alone.

The ingredients of two formulations are shown in the table. The polymer is a triazine ring-cross-linked 1,2,4-oxadiazole elastomer. The asbestos reinforces and thickens to the required consistency. The carbon black provides reinforcement, the epoxy silane promotes adhesion, and the lithium aluminum silicate reduces the thermal-expansion coefficient to extend the range of operating temperatures.

A sealant is prepared by mixing or milling the ingredients together after the polymer has partly or completely cured. Depending on the application, other reinforcing agents, adhesion promoters, metal deactivators, colorants, pigments, thermal-expansion stabilizers, and the like may be added.

Optimum polymer properties for filleting sealants are obtained when the ratio of the number of 1,2,4-oxadiazole linkages to that of triazine linkages is about 0.75:1. For channel sealants, the preferred ratio is 2:1. The placement of these linkages relative to one another on a gross molecular basis is random.

The tensile strength and elongation of

the filleting sealants indicate a lightly-cross-linked system with a glass-transition temperature of −30° C. The compression set of these formulations is similar to that of commercially-available neoprene- and nitrile-based materials, but is not as good as that of other fluoroelastomers.

The adhesive strength of the new sealants did not deteriorate in high-temperature-fuel aging tests. Long-term testing of filleting sealants at 288° C showed no corrosive effect on titanium. Thermogravimetric tests show that the onset of thermal degradation occurs at 280° C for the filleting sealants and at 270° C for the channel sealants. In contrast, older filleting sealants are usable only to 71° C.

Because of the carcinogenic property of asbestos, aramid and processed mineral fibers were also tested as substitutes. Neither performed as well as asbestos, due to failure to mill into the polymer adequately or failure to yield a strong or uniform product.

This work was done by Robert W. Rosser of **Ames Research Center** *and Danute I. Basiulis and Darrell P. Salisbury of Hughes Aircraft Co. For further information, Circle 95 on the TSP Request Card.*

Inquires concerning rights for the commercial use of this invention should be addressed to the Patent Counsel, Ames Research Center *[see page 29].* *Refer to ARC-11408 and 11409.*

Purifying Aluminum by Vacuum Distillation

Low-grade metal may yield high-purity metal in a one-step operation.

NASA's Jet Propulsion Laboratory, Pasadena, California

A proposed method for purifying aluminum would employ one-step vacuum distillation. The raw material for the process is the impure aluminum (typically containing much silicon and titanium) that is produced in the electrolysis of aluminum ore. This impure metal would be melted in a vacuum. Since aluminum has a much higher vapor pressure than the other constituents, it should boil off and condense on nearby cold surfaces in proportions much greater than those of the other constituents.

In one version of the process, the molten metal would be discharged as droplets of precise size into a long evacuated tube and fall under gravity. In the vacuum, aluminum would evaporate from the droplets as they fall and condense on the wall of the tube. For a 100-foot (30.5-meter) tube, the drop time would be 2.5 seconds — enough time for evaporation of a large fraction of the aluminum if the droplet size is carefully controlled.

The droplet size should be chosen to give efficient evaporation so that the metal need not be recirculated excessively. The required droplet size will be determined by such factors as the melt composition, the desired product composition, and the ratio of sensible heat to latent heat of the melt. The size can be controlled by setting the orifice diameter and the pressure on the melt.

According to predictions based on vapor-pressure data, the new method will yield commercially pure aluminum from an Si/Al alloy containing 15 percent aluminum in one pass. It should produce a grade seldom achieved in the laboratory — much purer than conductor-grade aluminum — from structural or casting alloys composed of 95 percent aluminum.

This work was done by Eugene R. du Fresne of Caltech for **NASA's Jet Propulsion Laboratory.** *For further information, Circle 12 on the TSP Request Card.*

NPO-16114

Foam Insulation for Cryogenic Flowlines

Weight is less, and assembly is less critical than with vacuum jacketing.

Lyndon B. Johnson Space Center, Houston, Texas

Welded stainless-steel vacuum jackets on cryogenic ducts can be replaced by plastic foam-insulation jackets that weigh 12 percent less. The foam insulation, which is 1½ inches (3.8 centimeters) thick, has 85 percent of the insulating ability of stainless-steel jacketing enclosing a vacuum of 10 microns of mercury (0.13 N/m^2). The foam insulation is easier to install than the vacuum jacket. Moreover, the foam is less sensitive to damage and requires minimal maintenance. It resists vibration and is expected to have a service life of at least 10 years.

The new jackets are made in segments by pouring a two-part foaming polyurethane compound into cylindrical molds. The cured segments are prefitted on their respective ducts to ensure proper installation. The segments are removed, and a single-ply laminate of Kevlar (or equivalent) fabric and polyurethane elastomer is applied to the interior surface of each to prevent cracking during heating and cooling cycles. A solution applied to the laminate provides flame resistance.

The preformed segments are assembled on the duct and joined by a polyurethane elastomer (see figure). A protective outer cover is then formed directly on the outside surface of the foam segments by applying a laminate of glass-fiber cloth and a mixture of epoxy and polyamide resins. When the laminate hardens, it protects the foam and increases the strength of the joints between segments. The laminate

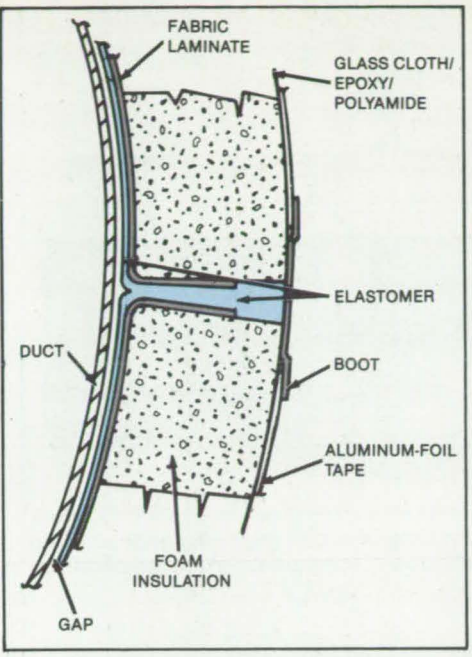

A **Segment of the Duct and Insulation**, shown here in cross section, has layers of material that protect, hold and bond the foam.

may have from one to three plies, depending on the severity of the expected service environment.

Boots made from a laminate of Kevlar (or equivalent) knit material and polyurethane elastomer are bonded to the protective cover with the same polyurethane elastomer. The boots allow venting of the space between the duct and the insulation but prevent liquids from entering.

To provide a measure of insulation for the flexible sections of the duct, they are covered with a flexible thermal barrier, prefabricated from a laminate of silicone and glass fibers. The flexible insulation is bonded to the flexible duct with an adhesive and tied in place with glass-fiber cords.

Finally, all exposed surfaces of the outer protective cover and the boots are covered with a layer of aluminum-foil tape. The tape reduces the emissivity of the surface, thereby enhancing the effectiveness of the insulation. The tape also serves as a flame barrier.

This work was done by Theodore R. Sonju, Robert L. Carbone, and Robert E. Oves of Federal-Mogul Corp. for **Johnson Space Center.** *For further information, Circle 70 on the TSP Request Card.*
MSC-20552

Circle Reader Action No. 22

Shielding Against Intense Laser Beams

Ablative layers of reflecting and absorbing materials are used.

NASA'S Jet Propulsion Laboratory, Pasadena, California

Multiple-layer shielding has been proposed to protect equipment against damage by intense infrared laser beams. The objective is to develop a material able to withstand one or more exposures to radiation of 2 to 10 μm wavelength at an energy density up to 100 kJ/cm^2. In contrast, insulation and shielding now used on spacecraft withstand only 1 kJ/cm^2.

The shielding now used usually consists of a monolithic refractory material with a reflective outer coating. Initially, the surface reflects 90 to 98 percent of the incident radiation. Once the temperature rises to the melting point of the reflective material, however, the reflectance is destroyed, and the subsequent incident radiation is mostly absorbed. The refractory material then melts, vaporizes, sublimes, or possibly even explodes as a result of continued heating.

The new shielding concept reduces the effect of the destructive phase changes upon the reflectance by allowing the exposure of additional reflecting layers after the overlaying layers have been vaporized. In one configuration, the shield might be constructed of small absorbent particles coated with reflective material. In another configuration, the shield would be made of bricks or tiles of absorbent phase-change material encapsulated in thermally conductive shells and coated with reflective surfaces (see figure).

The absorbing material inside a tile

should have a vaporization temperature slightly below the melting point of the reflector. This way, the absorbing layer would vaporize at the same time the reflectance of the outer layer is lost, thereby exposing a new reflecting layer to retard the absorption of energy.

Candidate absorbing materials include alkali-metal halides, flourides, and beryllium metal. High-melting-temperature refactories such as boron carbide, boron nitride and beryllium carbide and high-melting-temperature metals such as boron and graphite could also be used, but these materials would vaporize after the reflective layer was destroyed. Suitable reflecting materials include copper, gold, nickel, silver, and platinum, all of which exhibit high reflectivities in the infrared. Since a very thin reflective coating is adequate, the noble metals can be used in small enough quantities to keep costs within bounds.

The vaporization products of the tiles may form energy-absorbing plasmas. The diatomic alkali-halide vapors could be superior infrared absorbers. The plasma in front of a shield could deflect or diffuse the incident laser energy. An electromagnetic field might be used to control the shape of the plasma.

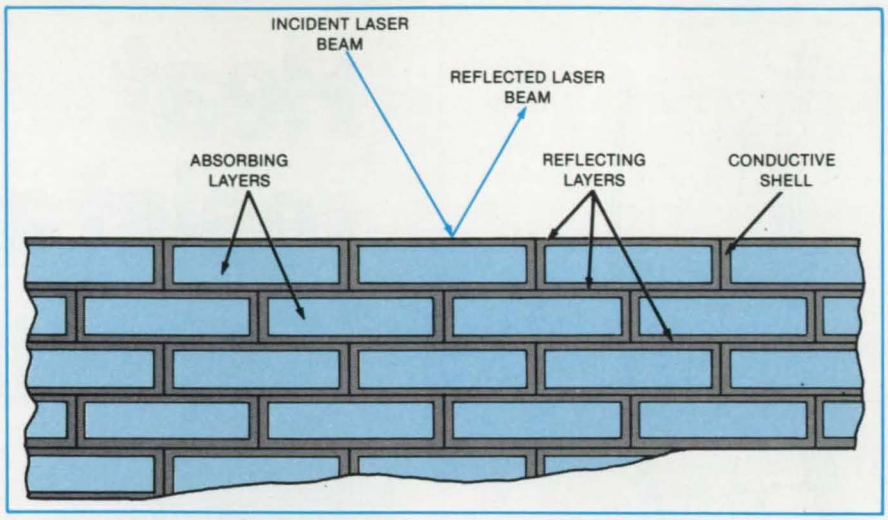

A **Laser-Beam Shield** might consist of alternating layers of absorbing and reflecting material. When an absorbing layer and its reflective coating are vaporized, a new reflecting layer would be exposed.

This work was done by James E. Schroeder of Caltech for **NASA's Jet Propulsion Laboratory.** *For further information, Circle 21 on the TSP Request Card.*
NPO-16166

Silicone Coating on Polyimide Sheet

A protective layer is applied by ordinary methods.

Goddard Space Flight Center, Greenbelt, Maryland

Silicone coatings can be applied to polyimide sheeting for a variety of space-related applications. The coatings are intended to protect the flexible substrates of solar-cell blankets from degradation by oxygen atoms, electrons, plasmas, and ultraviolet light in low Earth orbit and outer space. Since the coatings are flexible, they should be generally useful in forming flexible laminates or protective layers on polyimide-sheet products.

In the solar-blanket application, areas not covered by cells or interconnections can be covered with silicone. The thickness of the coating is not critical; typical values range from 2 to 10 mils (0.05 to 0.25 mm). The silicone can be brushed or sprayed on. To increase spreadability, decrease the coating thickness, or both, organic solvents can be added. A primer might be used to promote adhesion between the silicone and the polyimide.

Suitable commercial silicones include the two-part (resin and curing agent) RTV-615 (or equivalent) or the single-component resin C6-1104 (or equivalent). Both are curable at room temperature, but can be heated to speed the reaction. Both protect the optical emissivity and absorptivity of a polyimide-supported solar array so that these characteristics change by less than 0.01 percent, even when the array is subjected to a high concentration of oxygen atoms in a space atmosphere.

This work was done by John J. Park of **Goddard Space Flight Center.** *For further information, Circle 1 on the TSP Request Card.*

This invention is owned by NASA, and a patent application has been filed. Inquiries concerning nonexclusive or exclusive license for its commercial development should be addressed to the Patent Counsel, Goddard Space Flight Center [see page 29]. Refer to GSC-12913.

Melt Stirring by Horizontal Crucible Vibration

Mixing is more thorough than in rotational oscillation.

Marshall Space Flight Center, Alabama

Horizontal vibration has been suggested as a technique for the more effective stirring of melts in crystal-growth apparatus. The vibrational technique may replace accelerated crucible rotation, the current technique for magnetic garnet and other special crystals.

It is necessary to stir the crucible contents because uniformity of temperature

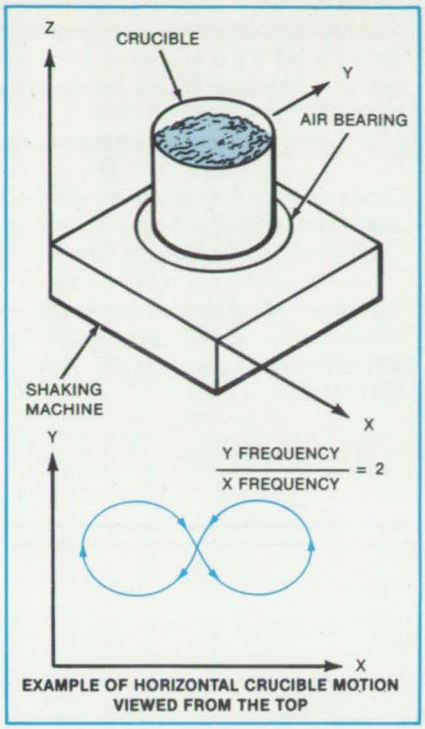

Figure 1. A **Crucible is Shaken Horizontally** in a Lissajous pattern to stir the liquid within.

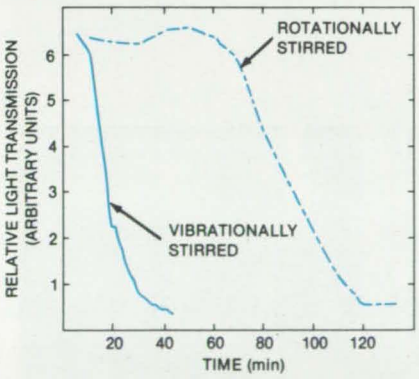

Figure 2. The **Effectiveness of Mixing** India ink into a container of water is measured in terms of the darkening of the water. The vibrationally stirred mixture reaches a given degree of opacity sooner than does the rotationally stirred mixture.

Power tower of Kapton®

Lightweight KAPTON helps make solar array experiment possible

Du Pont KAPTON polyimide film insulated the individual cells of the ten-story solar array deployed by the space shuttle "Discovery."

Why was KAPTON the engineering material of choice? It's lightweight, flexible, bondable, transparent, and it retains its structural strength in temperatures from −269° to 240°C.

Explore the down-to-earth advantages of KAPTON, made only by Du Pont. For free sample and literature, write Du Pont Co., KAPTON, Room X 40804, Wilmington, DE 19898.

DU PONT

Circle Reader Action No. 21

and composition is essential to the growth of a uniform, well-faceted crystal. The accelerated-crystal-rotation technique (in which the crucible is rotationally oscillated about its vertical axis) was developed to enable stirring without a stirring rod, which could react with the melt. In this method, the rotation motor is turned on and off or reversed with an oscillation period ranging from 10 seconds to several minutes.

In the vibrational method, the crucible is oscillated horizontally in two perpendicular directions at once. If the oscillations in both directions are at different but harmonically related frequencies, the crucible motion and the melt vibration are in a Lissajous pattern (see Figure 1).

Typical horizontal-vibration frequencies lie in the vicinity of 10 Hz. Since the period is much shorter than in the rotational method, there is less time between cycles for thermal or compositional inhomogeneities to develop in the melt and cause banding in the growing crystal. The potential superiority of the vibrational technique has been shown by preliminary experiments in which ink was stirred into water (see Figure 2).

This work was done by Martin F. Wolf, Dennis Elwell, and Robert S. Feigelson of Stanford University for **Marshall Space Flight Center.** *For further information, Circle 39 on the TSP Request Card.*

Inquires concerning rights for the commercial use of this invention should be addressed to the Patent Counsel, Marshall Space Flight Center [see page 29]. Refer to MFS-26005.

Nonyellowing Polycarbonate for Outdoor Use

An antiyellowing stabilizer is generated from the polymer and bound to it.

NASA's Jet Propulsion Laboratory, Pasadena, California

A two-step photochemical process prevents the yellowing of polycarbonate plastics. The use of polycarbonate plastics is growing in windows, aircraft glazing, and streetlight globes. However, outdoor exposure of originally-clear polycarbonate panels leads to undesirable yellowing, often within a few days. Although ultraviolet stabilizers can be included in the polycarbonate formulation to retard yellowing, they are leached out of the plastic under conditions of high temperature, humidity, and

solar radiation. As a result, even highly stabilized polycarbonates turn yellow after a few weeks or months of weathering.

The new photochemical process causes the formation of stabilizers that become bound to the polymer chains and therefore cannot be leached out. First, a commercial polycarbonate resin is dissolved in deoxygenated methylene chloride and maintained in a nitrogen atmosphere to exclude oxygen. The solution is placed in a quartz tube and irradiated by a low-pressure mercury-arc lamp with light at a wavelength of 253.7 nanometers. Irradiation is continued until 3 to 5 mole percent of the polycarbonate groups is converted to phenyl salicylate, as monitored by the absorbance by the solution of light at 320 nanometers.

Next, the solution is exposed to light at 313 nanometers from a filtered, medium-pressure mercury-arc lamp. The phenyl salicylate groups, but not the carbonate, absorb this radiation and are thereby converted to 2,2′ dihydroxybenzophenone groups that are bound to the polymer chains. These groups act as ultraviolet stabilizers. The reaction is monitored by measuring the absorbance at 355 nanometers until it is evident that all the phenyl salicylate has reacted.

The polymer is then recovered by evaporation of the solvent or by precipitation. The solid polymer is dried and processed in the usual manner for glazing or other outdoor materials. In a series of outdoor tests, many treated and untreated samples were examined for yellowing. Only the ultraviolet-treated samples remained clear.

This work was done by Amitava Gupta, Ranty H. Liang, Andre Yavrouian, and Ann Clayton of Caltech for **NASA's Jet Propulsion Laboratory.** *For further information, Circle 7 on the TSP Request Card.*

Inquires concerning rights for the commercial use of this invention should be addressed to the Patent Counsel, NASA Resident Office-JPL [see page 29]. Refer to NPO-15836

Reversing Glass Wettability

A silicone treatment makes the surface hydrophobic.

Marshall Space Flight Center, Alabama

A treatment reverses the wettability of glassware: With the treatment, liquids that normally wet glass no longer do, and those that do not wet glass are made to do so. The treatment is useful in research on container effects in the nucleation and growth of a secondary phase from solution.

The treatment consists of spreading a 3 percent (by weight) solution of silicone oil in hexane isomers over the glass, drying it in air, and curing it at 300° C in a vacuum for 1 hour. The silicone oil should have a viscosity of 500 to 1,000 centistokes. The vacuum cure prevents entrapment of hydrocarbons in the silicone film that forms on the surface: Such entrapped material could otherwise form sites for ruptures in the film.

The reversal of the wetting nature of glass thus treated is demonstrated by succinonitrile/water solutions in cylindrical tubes (see figure). A water-rich solution wets the untreated glass, while a succinonitrile-rich solution wets the treated glass.

This work was done by Donald O. Frazier, James E. Smith, Jr., and William F. Kaukler of **Marshall Space Flight Center.** *For further information, Circle 38 on the TSP Request Card.*

Inquires concerning rights for the commercial use of this invention should be addressed to the Patent Counsel, Marshall Space Flight Center [see page 29]. Refer to MFS-26006.

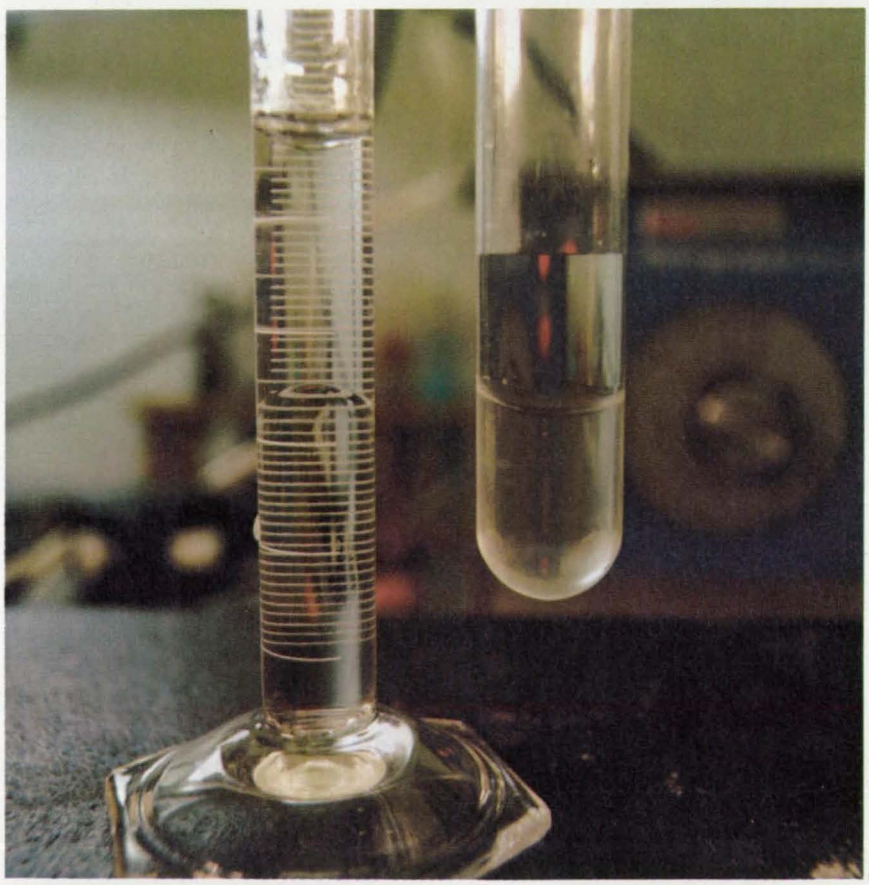

The **Untreated Graduated Cylinder** (left) is wet by the upper layer of a water-rich solution, as the meniscus indicates. The treated test tube (right) is wet by the succinonitrile-rich solution in the lower layer.

"Page missing from available version"

"Page missing from available version"

Resin Characterization in Cured Composite Materials

A spectroscopic method of characterizing polymeric matrix resins determines resin performance on a molecular level.

Langley Research Center, Hampton, Virginia

A molecular-level characterization of the polymeric matrix resin in cured graphite-reinforced composite materials can now be determined through the analysis of diffuse reflectance (DR) with Fourier Transform Infrared (FTIR) spectroscopy. In the past, such characterizations could only be postulated because these materials are both insoluble and opaque and cannot be analyzed by conventional methods that depend either on the ability to dissolve the sample or to detect transmitted radiation.

The improved analytical method is based on diffuse reflectance. This reflectance arises from radiation that penetrates into the opaque sample and reemerges after being scattered numerous times. Because some wavelengths are absorbed during this process, the emerging radiation contains valuable optical information about the sample.

The spectrum is obtained from a small piece of composite pulverized and mixed at 4 percent by weight with powdered potassium bromide and exposed to infrared radiation. The diffusely reflected components are detected. Alternatively, a small portion of the composite may be analyzed directly.

Figure 1 shows the apparatus for collecting the diffuse reflectance information. Infrared radiation from the interferometer is reflected from an ellipsoidal mirror onto the composite sample being analyzed. A second ellipsoidal mirror collects the diffusely reflected components and reflects them to the detector. The sample is positioned at the focal point of the two mirrors. During the analysis, the sample is subjected to multiple scans to improve sensitivity, the FTIR software performs mathematical computations, and the data are optimized to produce an interpretable spectrum providing information as to which molecules are present in the matrix and how they are arranged.

Figure 2 shows DR/FTIR spectra of a new graphite/polymeric matrix resin composite developed for a high-temperature application. Spectra are given for an unaged composite and for one aged in air at 450° F (232° C) for 15,000 hours. Because the graphite fiber makes no contribution to the spectrum, all absorption bands are due to the polymeric matrix resin.

New bands at 1667 and 931 wave numbers (cm^{-1}) for the aged composite indicate that a particular portion of the resin

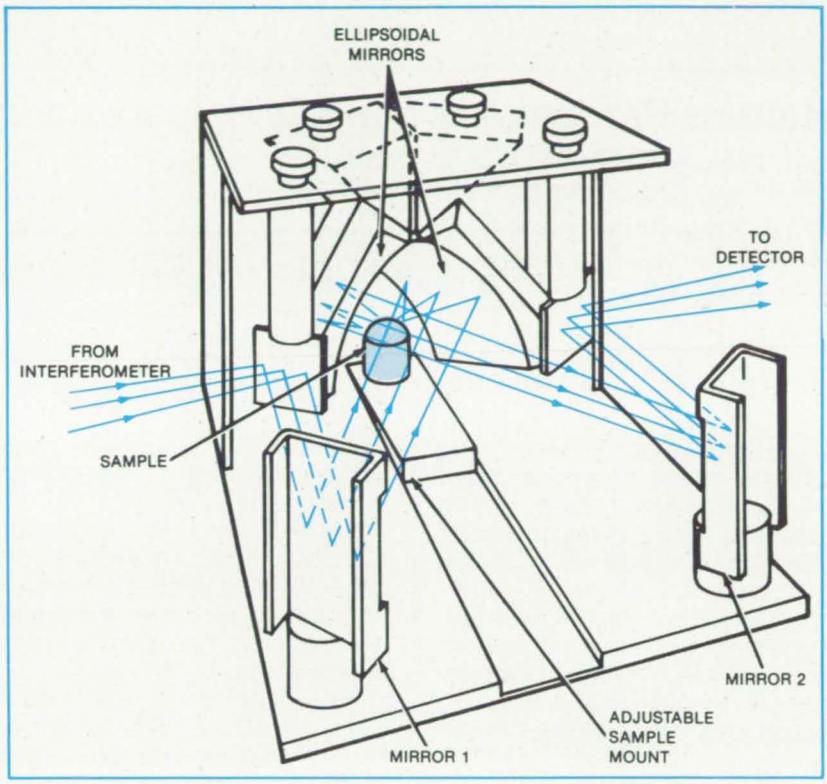

Figure 1. A **Diffuse Reflectance Apparatus** collects scattered infrared beams from the composite sample and transmits this information to a Fourier-Transform spectrum analyzer.

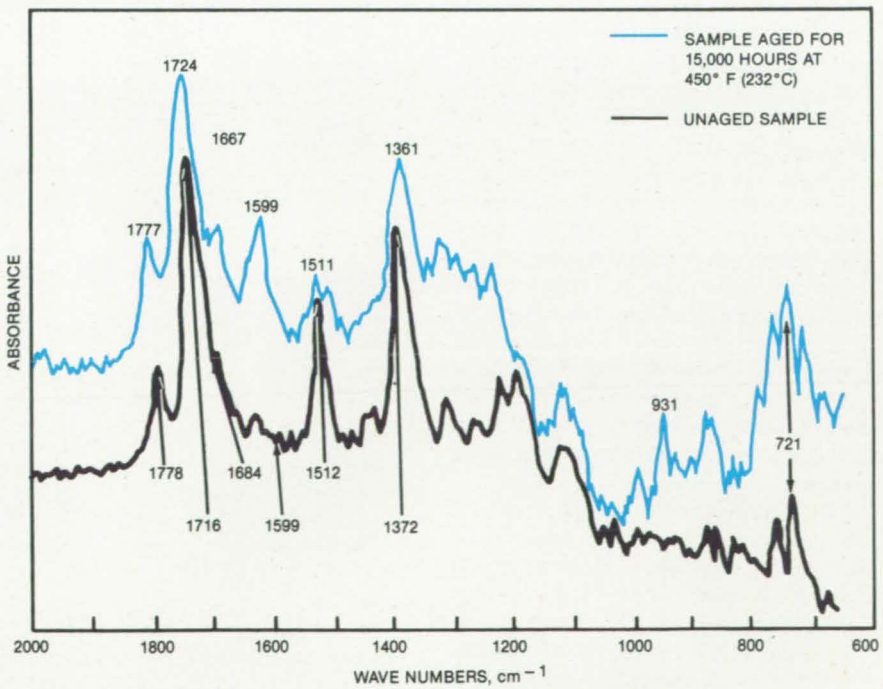

Figure 2. These **Spectra of Graphite/Polyimide Composite** show a marked distinction between aged and unaged samples. This distinction provides fundamental insights on material property changes and is used to suggest ways in which the matrix resin can be improved.

molecular structure oxidized. The change in relative intensity of the 1599 and 1512 cm^{-1} bands confirms this oxidation. Shifts in absorption of the 1716 cm^{-1} band to 1724 cm^{-1} and the 1372 cm^{-1} band to 1361 cm^{-1} due to exposure suggest that the matrix resin has also experienced additional cross-linking. These results provide fundamental insights into observed mechanical property changes in the material and suggest ways in which the matrix resin can be improved. The DR/FTIR technique has been successfully applied to the analysis of several different composites and adhesives that were impossible to analyze by conventional methods.

This work was done by Philip R. Young of **Langley Research Center** *and A. C. Chang of Kentron International, Inc. For further information, Circle 82 on the TSP Request Card.*
LAR-13172

Efficient Process for Making Polycrystalline Silicon

Solar cells may be made with lower capital and operating costs.

NASA's Jet Propulsion Laboratory, Pasadena, California

A process based on the chemical-vapor deposition (CVD) of dichlorosilane produces high-grade polycrystalline silicon for solar cells. The process has potential as a cost-effective replacement for CVD of trichlorosilane.

The conventional way of making silicon for semiconductor devices is by chemical vapor deposition (CVD) from trichlorosilane feedstock. However, this process has shortcomings: It consumes large amounts of energy in the CVD reactor; it generates large quantities of silicon tetrachloride as a byproduct; and it uses both silicon and chlorine inefficiently.

The new process avoids these shortcomings. The dichlorosilane is obtained by catalytic redistribution of high-purity trichlorosilane, which in turn is obtained by hydrogenation of silicon tetrachloride in a fluidized bed of metallurgical-grade silicon followed by purification by standard methods. The high-purity dichlorosilane is decomposed to semiconductor-grade silicon crystals in a rod-type CVD reactor (see figure). Silicon tetrachloride from the catalytic redistribution reaction and hydrogen chloride are both recycled to the fluidized bed. At a feed of 10 mole percent dichlorosilane in hydrogen at 1,050 °C, the conversion efficiency to silicon is 60 percent, as compared to a conversion efficiency of trichlorosilane of only 37 percent.

A key advantage of the new process is the lower thermodynamic and kinetic stability of dichlorosilane in comparison to that of trichlorosilane. This relative instability allows dichlorosilane to be converted to silicon by CVD with greater efficiency — for example, 60 percent for dichlorosilane versus 37 percent for trichlorosilane under a representative set of operating conditions. Moreover, the conversion efficiency of dichlorosilane is less sensitive to variations in reactant concentrations than is the conversion efficiency of trichlorosilane.

The high conversion efficiency of dichlorosilane decomposition results in higher deposition rates and reduced power consumption. Equipment and operating costs per kilogram of silicon produced are thus lower.

Polycrystalline silicon made by the new process was subjected to extensive chemical analysis. Boron, donor ion, and carbon concentrations were comparable to specifications for semiconductor-grade material. Concentrations of other trace impurities by mass-spectrographic analysis was at or below the detection limit of the instrument. No significant difference could be detected between polycrystalline silicon grown from dichlorosilane and that from trichlorosilane. Solar cells made from dichlorosilane by one manufacturer averaged 2.3 percent more efficient than those made from conventional material; another manufacturer realized a 3.5-percent increase in efficiency.

This work was done by James R. McCormick, Frank Plahutnik, Jr., David H. Sawyer, Arvid N. Arvidson, and Stewart M. Goldfarb of Dow Corning Corp. for **NASA's Jet Propulsion Laboratory.** *For further information, Circle 81 on the TSP Request Card.*
NPO-16121

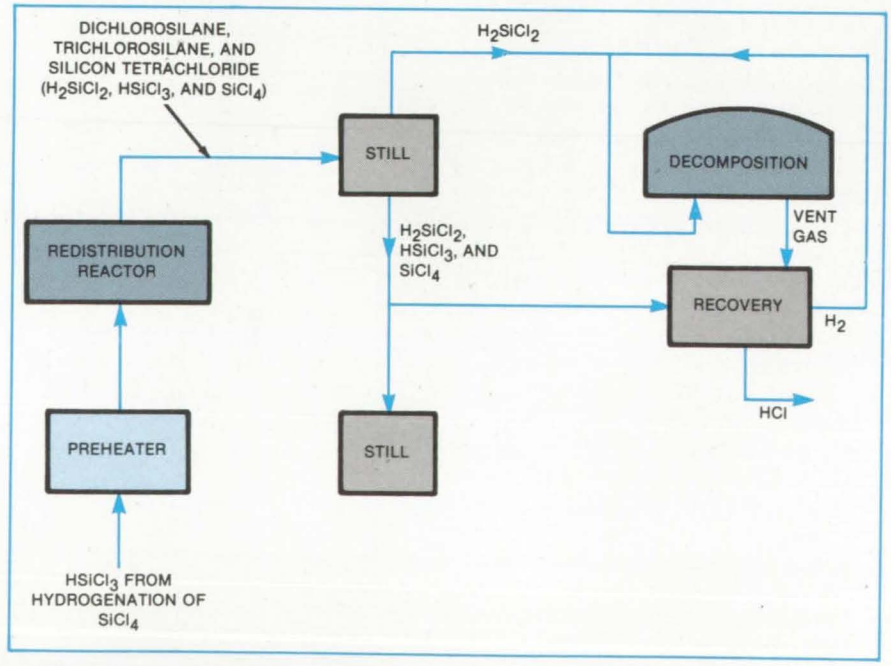

A **Demonstration Unit** for manufacturing semiconductor-grade silicon from dichlorosilane employs hydrogenation of silicon tetrachloride, synthesis of dichlorosilane, and dichlorosilane decomposition. All byproducts of the reactions can be recycled in the process.

Synthesizing Metal Phthalocyanine Imide Polymers

Products should exhibit high thermal stability.

Ames Research Center, Moffett Field, California

An efficient synthesis of analytically-pure metal(II)4,4′,4″,4‴-tetraaminophthalocyanine has been demonstrated in experiments. Metal phthalocyanine imide polymers with decomposition temperatures above 500° C have been made from these amines. The new polymers are expected to be useful in the formulation of thermally stable varnishes, adhesives, and fibers.

The laboratory synthesis is illustrated with an example in which the metal is copper. The method also applies to other metals having atomic radii of about 1.35 Å.

In one of the experiments, the following ingredients were finely ground: 12.0 g of $CuSO_4 \cdot 5H_2O$, 37.0 g of 4-nitrophthalic acid, 4.5 g of NH_4Cl, 0.5 g of $(NH_4)_2MoO_4$, and excess urea (50 to 60 g). These were placed in a 500-ml three-necked flask containing 25 ml of nitrobenzene. The flask was equipped with a thermometer, a condenser, and a mechanical stirrer.

The temperature of the ingredients was slowly increased to 185° C and maintained at 185° ± 5° C for 4½ hours. At the end of this time, a solid reaction product was obtained. The solid was ground, then washed in alcohol until free of nitrobenzene. The material was then boiled for about 5 minutes in 500 ml of 1.0 N HCl saturated with NaCl. After cooling to room temperature, the mixture was filtered to remove the liquid. The remaining solid was treated with 500 ml of 1.0 N NaOH containing 200 g of NaCl and heated at 90° C until the evolution of ammonia ceased.

After filtration of the mixture, the solid was treated with 1.0 N HCl and separated by centrifugation. Alternate treatments with HCl and NaOH were repeated twice. The product was washed with water until free of chloride, then dried in a vacuum at 125° C for 1 hour. The result was a 92-percent yield of the intermediate product copper(II)4,4′,4″,4‴-tetranitrophthalocyanine.

About 10 g of the finely-ground intermediate product was placed in 250 ml of water to form a slurry. Fifty grams of $Na_2S \cdot 9H_2O$ were added and stirred at 50° C for 5 hours. The solid product was separated by centrifugation and treated with 750 ml of 1.0 N HCl. The acid mixture was then centrifuged to separate the bulky blue precipitate of tetraaminophthalocyanine hydrochloride.

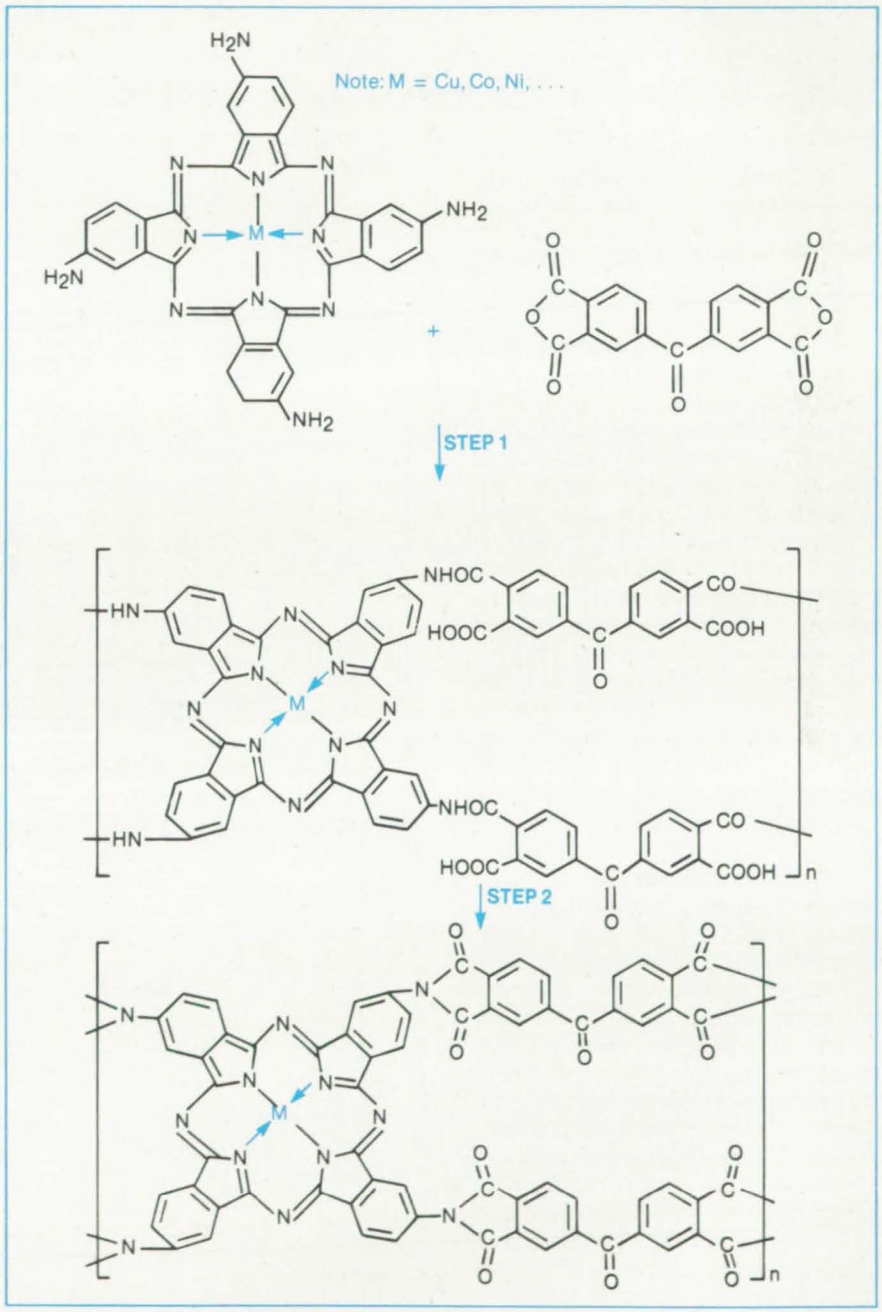

A Typical Polymerization of a Metal(II)4,4′,4″,4‴-Tetraaminophthalocyanine proceeds in two steps: The first is a reaction with 3,3′,4,4″-benzophenone-tetracarboxylic dianhydride. The second step is a cyclodehydration.

The precipitate was treated with 500 ml of 1.0 N NaOH, stirred for 1 hour, and centrifuged to separate the dark green complex of copper(II)4,4′,4″,4‴-tetraaminophthalocyanine. The complex was repeatedly treated with water, stirred, and centrifuged until it was free of NaOH. The purified complex was dried for 2 hours at 150° C.

An amino derivative of metal phthalocyanine made by the above or a similar process can be polymerized by any of a

number of different reaction sequences. One of the preferred sequences is shown in the figure.

The metal(II)4,4′,4″,4‴-tetraaminophthalocyanine and a bisphthalic anhydride are reacted in dimethyl sulfoxide or other aprotic solvent at 22° to 30° C to yield poly(metal phthalocyanine) amic acid. To complete the process, the amic acid is thermally cyclodehydrated by heating at 300° C for 1 hour in a vacuum.

The general process described encompasses many variations. Many different polymers and copolymers can be produced, depending on the selection of metal, amino derivative of the metal phthalocyanine, anhydride, solvent, and cyclodehydration technique.

This work was done by B. N. Achar, G. M. Fohlen, and J. A. Parker of **Ames Research Center.** *For further information, Circle 112 on the TSP Request Card.*

Inquiries concerning rights for the commercial use of this invention should be addressed to the Patent Counsel, Ames Research Center [see page 29]. Refer to ARC-11413.

Solar-Assisted Oxidation of Toxic Cyanide

Illuminated platinized TiO_2 is used to treat industrial wastewaters.

Langley Research Center, Hampton, Virginia

Cyanide is a very hazardous waste product of many industrial processes such as electroplating, case hardening of steel, ore refining, and scrubbing of stack gases from blast and producer-gas furnaces. The currently preferred method of removing this toxic material from industrial wastewater is by alkaline chlorination. This method requires 8 pounds (3.6 kilograms) of chlorine and 7.3 pounds (3.3 kilograms) of sodium hydroxide to completely oxidize 1 pound (0.5 kilogram) of cyanide, resulting in additional volumes of sludge for disposal. Another treatment method is by direct electrolytic oxidation. High current densities (and therefore high energy costs) are required, especially for low cyanide concentrations. These techniques are effective for cyanide concentrations down to about 1,000 ppm.

In the solar-assisted oxidation technique, oxygen-bearing air is bubbled through the cyanide solution in which platinized powdered TiO_2 is suspended (see Figure 1). Light from either an artificial source or natural Sunlight irradiates the solution. Recent research with platinized semiconducting powders and broadband radiation has demonstrated the production of halogens from aqueous solutions of their respective ions. In addition, a significant enhancement of the oxidation of CN^- and SO_3^{2-} has been reported when in the presence of illuminated platinized semiconductor powders. Experiments conducted in both artificial and natural Sunlight with known amounts of cyanide and platinized TiO_2 particles have demonstrated that this technique is effective in reducing the concentration of cyanide to levels well below those achieved by other methods.

Figure 2 shows that the concentration of cyanide is decreased an order of magnitude below that concentration where alkaline chlorination and electrolytic oxidation become relatively ineffective. Experiments have also shown that the platinized TiO_2 powders used in the oxidation of cyanide can be reused. These results suggest an effective and inexpensive method for oxidizing cyanide in industrial wastewaters.

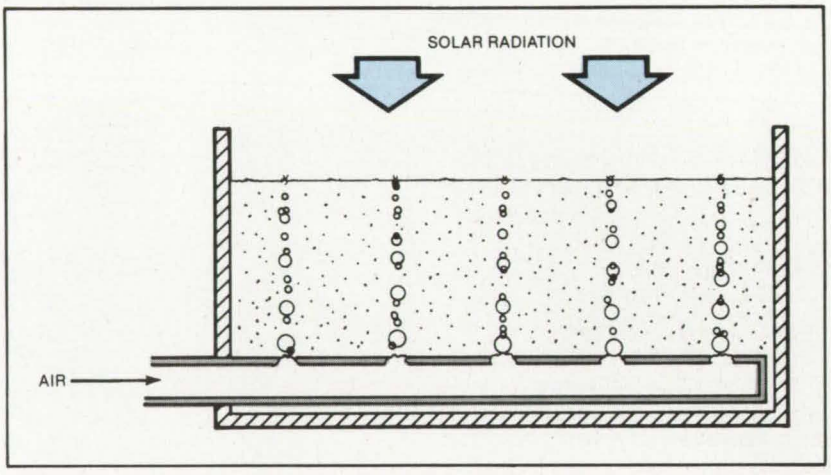

Figure 1. **Oxygen-Bearing Air Is Bubbled Through the Cyanide** solution in which platinized, powdered TiO_2 is suspended and which is irradiated by natural or artificial Sunlight.

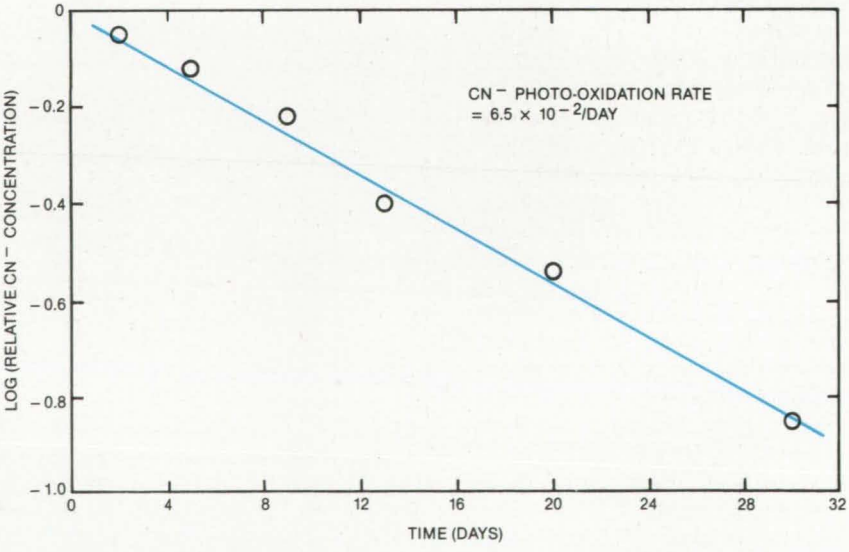

Figure 2. The **Relative Concentration of Cyanide** as a function of time during solar irradiation yields concentrations lower than those achieved by other methods.

This work was done by Charles E. Byvik of **Langley Research Center** *and Allen Miles of Southern University. For further information, Circle 105 on the TSP Request Card.*

LAR-13171

Ethynyl-Terminated Ester Oligomers and Polymers

Use temperature and solvent resistance of polyesters are increased.

Langley Research Center, Hampton, Virginia

Polyesters of various molecular weights were terminated with ethynyl groups. As these ethynyl-terminated polyesters are exposed to elevated temperatures, a thermally induced reaction of the ethynyl groups occurs to provide cross-linking and chain extension. This reaction raises the use temperature of the polymer and greatly improves its resistance to solvents. The new materials produced by this process are potentially useful as adhesives, composite matrices, solvent-resistant coatings, membranes, and films.

There are basically three classes of polyesters: amorphous thermoplastics, crystalline or semicrystalline materials, and unsaturated or cross-linked polymers. Amorphous polyesters generally are sensitive to certain solvents, especially in a stressed condition, and upon exposure undergo solvent-induced stress crazing and cracking. Crystalline polyesters have better solvent resistance but generally are more difficult to process, especially as adhesives and laminating resins. Cross-linked polyesters undergo pronounced shrinkage upon cure, resulting in built-in stresses, and are generally brittle and not thermoformable. The ethynyl-terminated polyesters, however, exhibit improved solvent resistance, good toughness, and thermoformability.

Hydroxy-terminated ester oligomers or polymers are reacted with ethynylbenzoyl chloride to yield ethynyl-terminated ester oligomers or polymers as shown in the figure. Other ethynyl acid chlorides such as 4(4-ethynylphenoxy)benzoyl chloride can also be used. The molecular weight of the ester oligomer or polymer can be controlled readily, thereby controlling the amount of ethynyl groups to provide tailored materials for specific applications. Higher cross-link density in the cured polymer provides better solvent resistance, less thermoformability, and lower toughness. Virtually any polyesters terminated with hydroxy groups can be converted to the corresponding ethynyl-terminated materials.

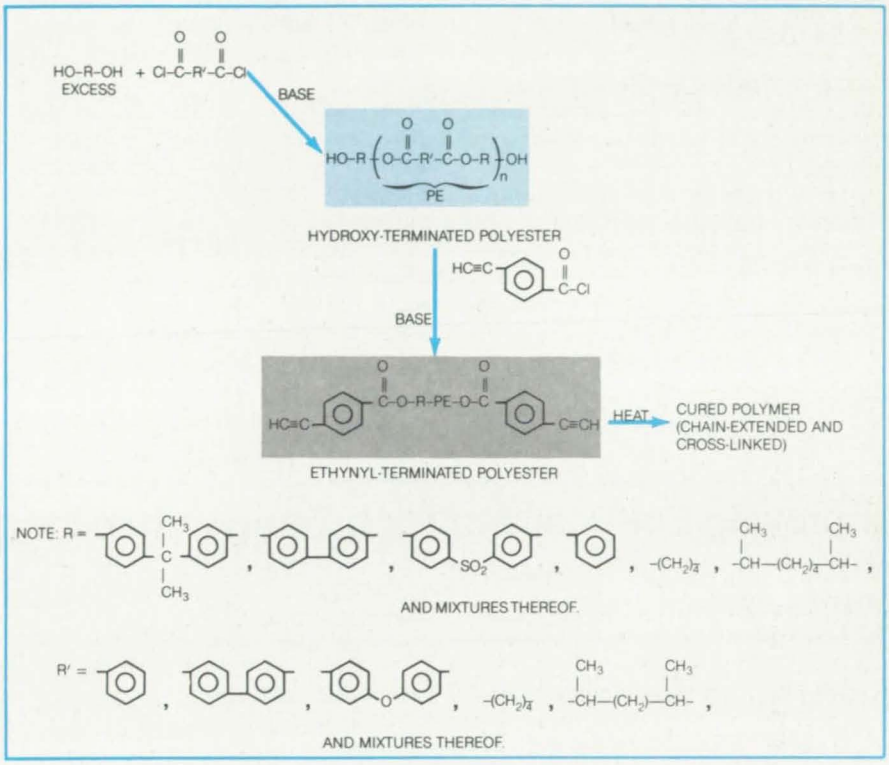

New **Ethynyl-Terminated Polyesters** are produced in the reaction sequence shown here.

This work was done by Paul M. Hergenrother of **Langley Research Center** *and Stephen J. Havens of Kentron International, Inc. For further information, Circle 97 on the TSP Request Card.*

This invention is owned by NASA, and a patent application has been filed. Inquiries concerning nonexclusive license for its commercial development should be addressed to the Patent Counsel, Langley Research Center *[see page 29].* *Refer to LAR-13118.*

Static-Suppressing Optical Paint

Flat black and conductive, a primer and topcoat adhere to a variety of properly prepared surfaces.

NASA's Jet Propulsion Laboratory, Pasadena, California

An electrically conductive flat black paint adheres well to magnesium, aluminum, fiberglass, and other materials. The paint absorbs stray light in optical instruments while preventing the buildup of electrostatic fields and arcing.

The paint consists of a primer and a topcoat, both containing electrically-conductive carbon-black powder. The primer has a two-part epoxy base, and the topcoat has a polyurethane base.

Following proper procedures for surface preparation and cleaning is essential. Polished metals such as aluminum, stainless steel, and titanium should be

finished with a fine abrasive. Machined metals should be polished with No. 400 grit to a 20-microinch (0.5-micrometer) rms finish. Plastics should be rubbed lightly with No. 180 aluminum oxide or garnet cloth.

The conductive paint will not adhere reliably unless the surface is absolutely free of grease, oil, and dirt. Metal parts are cleaned by vapor degreasing, rinsing with distilled water, drying in high-purity nitrogen, and baking at 150° F (66° C) for 1 hour. Plastic parts are washed with isopropyl alcohol, wiped with a clean lint-free cloth before the alcohol evaporates, rinsed with more isopropyl alcohol, rinsed with distilled or deionized water, and dried in a stream of nitrogen gas for 10 minutes.

The primer is formulated from the following ingredients (approximate percentage by weight indicated in parentheses): Epoxy resin (52), epoxy catalyst (9.5), carbon powder (6.5), and thinner (32). The topcoat is made from the following constituents: Polyurethane resin (58), carbon powder (13), and xylene thinner (29).

For the primer, the epoxy base, carbon, and about two-thirds of the thinner are stirred in a beaker, then poured into a ceramic-ball milling jar. The remaining one-third of the solvent is used to rinse out the beaker, then added to the contents of the jar. After 15 minutes of ball milling, the mixture is blended with the epoxy catalyst and milled for another 2½ minutes. Finally, the mixture is poured into the bottle of a spray gun, allowed to stand for 15 to 30 minutes to allow it to gel slightly, and sprayed on the surface to be painted. The primer coat should be allowed to set and dry in air above 70° F (21° C) for at least 20 hours before the topcoat is applied.

To prepare the topcoat, the polyurethane resin, carbon, and xylene solvent are mixed, first in a beaker then in a milling jar, for about 45 minutes. The mixture is sprayed over the primer and allowed to cure for 24 hours in air above a temperature of 70° F (21° C) at a relative humidity of 30 to 80 percent. A final vacuum bakeout for 48 hours at 250° F (121° C) and 10^{-6} torr (10^{-4} N/m^2) completes the procedure.

The resulting paint has a resistivity of 5×10^3 ohms per square, a solar absorptivity of 0.93, and a thermal emissivity of 0.87. It survives standard tape-peeling adhesion tests.

This work was done by Morris M. Birnbaum, Edward C. Metzler, and Edward L. Cleland of Caltech for **NASA's Jet Propulsion Laboratory.** *For further information, Circle 88 on the TSP Request Card.*

Inquires concerning rights for the commercial use of this invention should be addressed to the Patent Counsel, NASA Resident Office-JPL [see page 29]. Refer to NPO-15992.

Improving Emittance of High-Temperature Insulating Tile

An additive protects the tile even when the surface coating fails.

Lyndon B. Johnson Space Center, Houston, Texas

A simple addition to ceramic insulating tiles provides backup properties that minimize the transfer of heat through the tiles when their surfaces become damaged. Previously, such tiles have been coated with reaction-cured glass to provide the surface with the high emittance and other optical properties necessary to prevent the heating of the tile surface to temperatures above 2,300° F (1,260° C). The coating also makes the tiles abrasion-resistant and impervious to water. However, if a tile becomes damaged and loses part of its coating, it no longer protects the underlying structure, because the emittance of the white interior ceramic is less than that of the coating.

The addition of 3 percent by weight of 320- or 600-grit silicon carbide powder to the ceramic during production results in an impregnated tile material that resists overheating. The silicon carbide increases the emittance and decreases the transmittance of the ceramic. As a result, increased radiation outward from the surface reduces the surface temperature, and less radiant energy is transmitted from the tile surface through the ceramic insulation to the aluminum structure.

Tiles with and without the coating were subjected to arc-plasma tests (see figure). The coated tiles withstood a 2,300° F (1,260° C) surface temperature with no degradation. Uncoated tiles eroded and partially melted, and their aluminum substructure melted locally. But uncoated tiles with silicon carbide survived the tests with only minor shrinkage.

This work was done by Edward R. Gzowski of Lockheed Missiles & Space Company, Inc., for **Johnson Space Center.** *No further documentation is available.*

Inquires concerning rights for the commercial use of this invention should be addressed to the Patent Counsel, Johnson Space Center [see page 29]. Refer to MSC-20714.

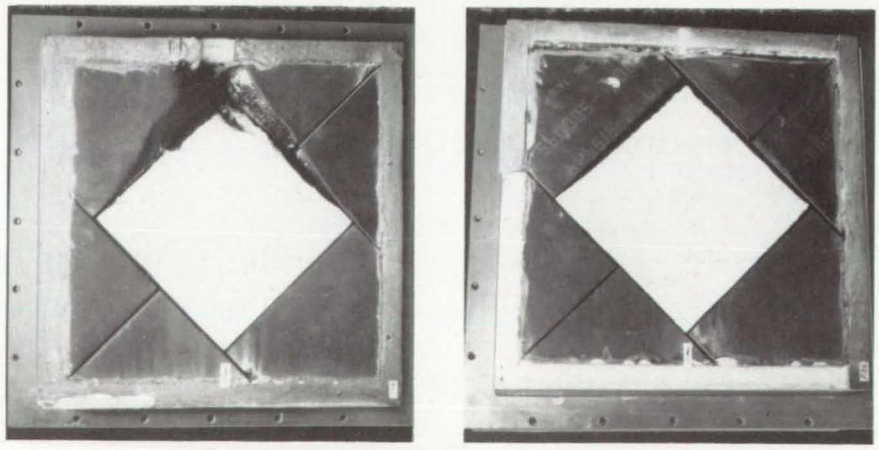

An **Insulating Tile** without reaction-cured glass coating is damaged after arc-plasma testing (left), and the aluminum supporting it is partly melted. A tile with silicon carbide additive (right) is slightly shrunken after the test but is otherwise in good condition, even though it is uncoated. There is also less damage to the aluminum structure.

Rubberized, Brominated Epoxies

New composites are tougher and more resistant to fire.

Ames Research Center, Moffett Field, California

New graphite/epoxy composite materials have been made with resins containing bromine and rubber additives. Previously, the impact resistance of epoxies had been increased by adding reactive liquid rubber to the resins to form phase-separated rubber domains. In the new composites, flame resistance is increased by introducing bromine via commercial brominated flame-retardant polymeric additives.

The ingredients used in the investigation are shown schematically in the figure. Each of the formulations tested was based on one of two epoxy resins: tetraglycidyl 4,4-diamino diphenyl methane (TGDDM), a commercial resin, and tris-(hydroxyphenyl) methane triglycidyl ether (also called "tris epoxy novolac" or "TEN"), an experimental resin. Diamino diphenyl sulfone (DDS) was the curing agent. Two kinds of rubber were used: diglycidyl brominated polymeric additive (BPA) of various molecular weights and a nonbrominated carboxyl-terminated liquid copolymer of butadiene and acrylonitrile (CTBN).

Copolymeric rubber additives were prepared by prereacting each BPA with various proportions of CTBN and 0.15 weight percent of triphenylphosphine at 130° to 150° C under an atmosphere of N_2 for 2 hours. The final epoxy resin mixture was prepared by dissolving the epoxy resin and prereacted rubber additive in methyl ethyl ketone, using a tumbler for 4 hours. DDS was added and the solution shaken for an additional hour.

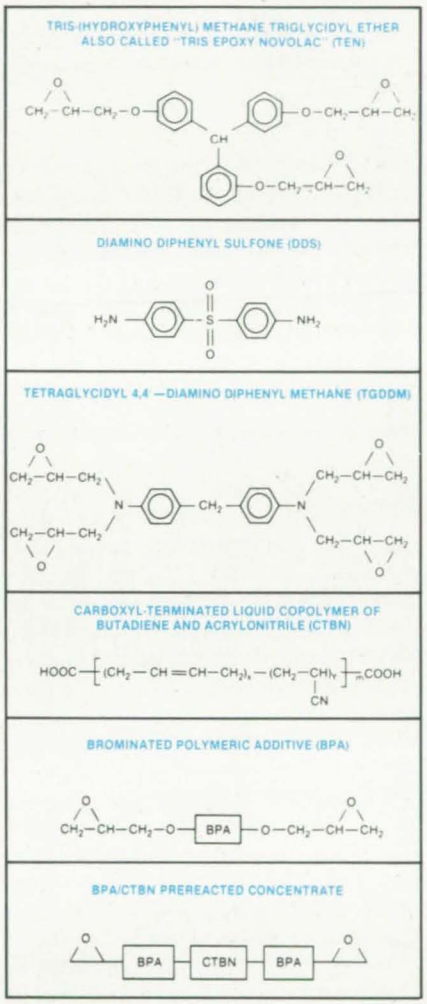

These Compounds Were Used in Various Proportions to form new resins for graphite-fiber/epoxy composites.

Graphite cloths were impregnated with the solution, then dried for 5 minutes at 85° C, followed by 9 minutes at 125° C. Laminates were prepared from stacked impregnated cloths. First, the stacks were heated to 177° C at 4° C per minute. The stacks were pressed at 50 psi (0.34 MPa) while maintaining 177° C for 2 hours, then cooling to ambient temperature over a period of 10 hours. The stacks were postcured at 192° C for 2 hours.

The laminates were tested for mechanical properties, thermochemical characteristics, glass-transition temperature, flammability, and water absorption. Laminates made from new TEN containing brominated rubber additives show somewhat lower flammability and higher impact resistance than were shown by laminates made from other formulations.

This work was done by W. J. Gilwee, D. A. Kourtides, and J. A. Parker of **Ames Research Center** *and Z. Nir of the National Research Council. For further information, Circle 99 on the TSP Request Card.*

Inquiries concerning rights for the commercial use of this invention should be addressed to the Patent Counsel, Ames Research Center *[see page 29].* *Refer to ARC-11427.*

Waterproofing Agents for Silica Tiles

A new silylating agent is easy to apply and withstands high temperatures.

Lyndon B. Johnson Space Center, Houston, Texas

The waterproofing agent methyltrimethoxysilane is applied to silica thermal-insulation tiles in a simple vapor-deposition process. Other waterproofing agents in the same series include methylsiloxane (sprayed with a solvent) and hexamethyldisilazane (deposited from vapor). Of the three materials, methyltrimethoxysilane imparts the best waterproofing and thermal properties. Originally developed for insulating tiles for spacecraft, one or more of these agents may also find uses in roofing tiles, insulation for buildings or solar-energy systems, or solar reflectors.

The vapor deposition can be done under a variety of conditions, including open air at room temperature, bagged or otherwise enclosed at room temperature and pressure, assisted by controlled or directed gas or airflow, the injection of vapor directly into the tile, and other

variations of flow or pressure that facilitate the permeation of the tile. The curing reactions take place at room temperature, but can be speeded by heating. Radiant heating can be used, or the flowing gas can be heated during or after the vapor deposition.

The wettability of the tiles is caused by active hydrogen sites that remain on the silica fibers from the tile-manufacturing process. The methyltrimethoxysilane or other agent reacts with these sites (see figure). The required hydrophobic property is imparted to the silica with only a small increase in weight — typically 0.8 percent.

Tiles treated with methyltrimethoxysilane retain their water repellency after exposure to 427° C in air for 15 hours, whereas tiles treated with the other agents do not. The hydrophobic coatings of all three agents decompose at 649° C, but the decomposition products of the methyltrimethoxysilane and hexamethyldisilazane coatings do not cause darkening or otherwise affect the solar absorption or emissivity of the tiles.

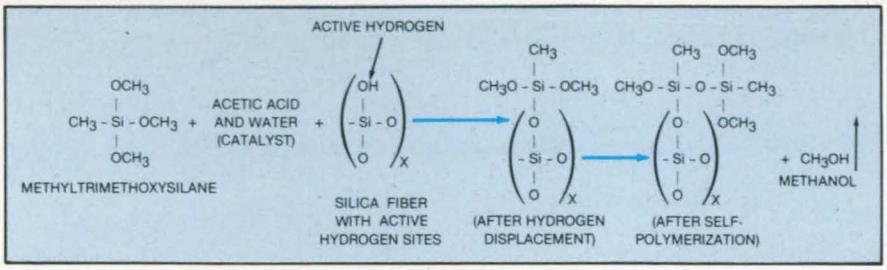

Methyltrimethoxysilane Reacts With Active Hydrogen Sites on silica fibers. The hydrogen is removed and replaced by hydrophobic molecular fragments.

This work was done by Harry N. Nakano, Y. Douglas Izu, and Ernest N. Yoshioka of Lockheed Missiles & Space Co., Inc., for **Johnson Space Center.** *For further information, Circle 83 on the TSP Request Card.*

Inquires concerning rights for the commercial use of this invention should be addressed to the Patent Counsel, Johnson Space Center [see page 29]. Refer to MSC-20364.

Books and Reports

These reports, studies, and handbooks are available from NASA as Technical Support Packages (TSP's) when a Request Card number is cited; otherwise they are available from the National Technical Information Service.

Preparation and Characterization of $Hg_xCd_{1-x}Te$

Crystal growth and properties are studied under variations of composition and processing.

Experimental studies of the growth of $Hg_xCd_{1-x}Te$ crystals are described in a NASA contractor report. $Hg_xCd_{1-x}Te$ is important as an infrared detector material: The studies are part of a greater effort to determine the effects of processing conditions on the chemical, physical, and electrical properties of this material.

The experiments were conducted over the full range of compositions, with x ranging from zero to 1.0. Samples were prepared by melting predetermined amounts of Hg, Cd, and Te together in sealed, evacuated ampoules of fused silica or quartz.

A series of differential-thermal-analysis (DTA) measurements were performed to determine the liquidus temperatures of the alloy compositions, thereby obtaining a ternary Hg/Cd/Te phase diagram, especially in the mercury-rich composition region. In a DTA run, the sample was first equilibrated for 16 hours at 50° C below the anticipated liquidus point, then heated at 2° C per minute until a break in the differential-temperature curve signaled the attainment of the liquidus temperature. A sample of Sb (melting point 630.8° C) was placed next to the alloy sample to provide a temperature reference. Liquidus temperatures on successive runs agreed within 2° C.

In tests of directional solidification, crystals were grown by the Bridgman-Stockbarger method, in which the material is solidified in a vertical ampoule by slowly raising a tubular furnace along the ampoule axis. A longitudinal thermal gradient advances upward along the ampoule as the relatively cool lower end of the furnace rises, causing the solidification front to move up along the sample. The alloy compositions as a function of axial position were determined by mass-density measurements. (It can be shown that mass density depends uniquely on x.)

The samples as grown by the Bridgman-Stockbarger method were p-type. An attempt was made to convert them to infrared-transparent n-type by annealing in Hg vapor at 325° C for 114 hours. The annealing treatment failed to produce infrared-transparent samples that might have been subjected to infrared radial compositional mapping.

Electrical resistivity and Hall-effect measurements were taken on a selected annealed sample in a liquid-helium-cooled Hall-effect apparatus. The temperature dependencies of the Hall electron concentration and mobility indicated that, in the particular sample, either compositional uniformity was low, or the sample did not reach equilibrium during annealing.

This work was done by J. G. Broerman, B. J. Morris, and P. J. Meschter of McDonnell Douglas Corp. for **Marshall Space Flight Center.** *To obtain a copy of the report, "Advanced Methods for Preparation and Characterization of Infrared Detector Materials," Circle 66 on the TSP Request Card.*
MFS-27037

Strength of Graphite/Metal Composite Lap Joints

Test data are given for graphite/aluminum and graphite/magnesium riveted lap joints.

A report presents the results of tests on fastened lap joints between strips of graphite/aluminum and graphite/magnesium composites. The goal of the test program was to establish the practical load range and the effect of such joint parameters as load direction relative to graphite fiber direction, edge distance, fastener diameters, and lateral spacing as a function of net section efficiency.

Two specimen types were tested:

- Graphite fibers infiltrated by aluminum alloy, sandwiched between aluminum-alloy foils of 0.0035-in. (0.09-mm) thickness, and
- Graphite fibers infiltrated by magnesium alloy, sandwiched between magnesium-alloy foils of 0.0025-in. (0.06-mm) thickness.

For both types, the specimens were cut with fiber orientations of 0°, 45°, and 90° relative to the load directions. Aluminum-alloy splicing straps were fastened to the specimens to form the lap joints. Aluminum-alloy cherry rivets were used as the fasteners.

The report concludes that cherry rivets are practical and easy to install in graphite/metal composite lap joints. The test data had relatively low scatter in most cases and can therefore be accepted with confidence. The range of such joint parameters as material type, edge distance, width, and fiber orientation was adequate to establish bounds on joint strength, but additional testing will be needed to develop allowable values for design.

The type of graphite fiber had no effect on the joint since the failure modes were dominated by the strength of the matrix material in shear and tension. Because the failures were matrix dominated, the joint strength was significantly improved when the graphite/metal was solution heat treated and aged.

Shear failures occurred for most specimens when they were loaded parallel to the fiber direction. An edge distance of approximately five rivet-hole diameters was needed before bearing failures appeared in specimens that were not heat treated. In the solution-heat-treated and aged specimens, the minimum edge distance for bearing failure was four diameters. The treated specimens also showed significantly-improved joint strength. The allowable strength of the graphite/metal joints approached the expected strength for wrought aluminum and magnesium alloys, but the joint efficiency was low when based on the ultimate tensile strength of the graphite/metal.

The 45° and 90° specimens failed in transverse tension. Section failures through the fastener occurred as predicted, but there was an unexpectedly high number of failures in tension beyond the fastener. Only as-fabricated 45° and 90° specimens were tested, but solution-heat-treated and aged specimens would have shown improved strength.

This work was done by A. M. Ellison and D. H. Kintis of Lockheed Missiles & Space Co., Inc., for **Marshall Space Flight Center.** *To obtain a copy of the report, "Metal Matrix Composites for Space Exploration," Circle 3 on the TSP Request Card.*
MFS-27030

Predicting Effects of Impacts on Confined Explosives

Scaling relationships may make full-scale experiments unnecessary.

A study aimed at improving the safety of explosive storage has examined the relationship between small-scale experiments and actual explosions. The object of the study was to develop scaling laws that would eliminate the need for full-scale explosion tests and reduce the need for small-scale tests. The results of the study make it possible to predict explosive behavior from small tests and numerical simulation.

The study focused on detonation of stored explosives caused by the impact of fragments or projectiles or by the accidental impact of one explosive container on another, as in a shifting cargo. The dynamic load of an impact causes a shock wave to propagate through the explosive material. If the impact is strong, such as that from a projectile, detonation can occur within microseconds. However, if the impact is relatively mild, such as that between containers, energy is transferred to the explosive material over a longer period of time.

In either case, energy is transferred in the form of shock-wave pressure, elastic work, and plastic work. This energy transfer leads to local temperature rises and hotspots. In fact, in confined explosives, friction with the container can cause hotspots. Hotspots do not necessarily cause detonation: the explosive may dissipate the energy as heat to the environment and remain inert, or it can undergo mild chemical decomposition or constant-pressure deflagration. The last event can easily turn into violent detonation, however.

As a first step toward fully understanding the ignition process, the study examined the stress and deformation propagation in a confined explosive medium. It combined the transient stress and strain pattern with two microscopic ignition mechanisms: void collapse and shear banding. It analyzed hotspot formation in terms of a friction model.

The study found that if the induction time for an explosion is less than the characteristic time of plastic-wave propagation, the size of the test model is not important. However, the thickness of the container is hard to scale without a detailed multidimensional stress/strain analysis. Qualitatively, a thick container tends to diminish pressure and strain rate because of viscosity and dilatation of the wave front. Dimensional analysis itself does not yield a complete solution. As a result of the study, several approximate methods have been proposed for determining the effects of explosive size, viscoplastic wave magnitude, and container thickness.

This work was done by Chung K. Chan of Caltech for **NASA's Jet Propulsion Laboratory.** *To obtain a copy of the study, "Scaling Analysis of Projectiles on Confined Energetic Materials," Circle 77 on the TSP Request Card.*
NPO-16258

Further Tests of 38 Ball-Bearing Greases

Perfluoroalkylpolyether lubricants continue to perform best.

An interim report presents recent results in a program of long-term testing of ball-bearing greases in vacuum, oxidizing, and otherwise hostile environments. An earlier report in the same series was described in "Tests of 38 Ball-Bearing Greases" (MFS-25624), *NASA Tech Briefs*, Vol. 6, No. 3, page 330.

The greases have been tested in ball bearings of electric motors that were subjected to a variety of operating conditions, including humid oxygen, vacuum at 38° C, vacuum at 93.3° C, vacuum at ambient temperature with start/stop operation, and low-temperature start (various temperatures). The lubricants were evaluated qualitatively in terms of the occurrence or nonoccurrence of bearing failure and quantitatively in terms of bearing weight loss.

As in the earlier report, the class of lubricants based on perfluoroalkylpolyether (PFPE) gave the best results in vacuum operation in both 1-year and 5-year tests. In 5-year start/stop tests, one of the PFPE lubricants showed the lowest weight loss. Some silicone, mineral, and synthetic-ester lubricants also showed promise in 1-year vacuum ambient-temperature tests.

This work was done by E. L. McMurtrey of **Marshall Space Flight Center.** *Further information may be found in NASA TM-82533 [N83-31020/NSP], "An Evaluation of Grease-Type Ball Bearing Lubricants Operating in Various Environments (Status Report No. 7)" [$7]. A paper copy may be purchased [prepayment required] from the National Technical Information Service, Springfield, Virginia 22161. The report is also available on microfiche at no charge. To obtain a microfiche copy, Circle 91 on the TSP Request Card.*
MFS-27043

Life Sciences

Hardware, Techniques, and Processes

112 Vision Screening by Color Photography
113 Coculture Production of Butanol by Clostridium Bacteria

Books and Reports

113 Effect of Hydration on Nitrogen Washout in Humans

Vision Screening by Color Photography

A trained observer can screen five children per minute.

Marshall Space Flight Center, Alabama

A screening test has been developed for detecting a range of vision defects in the eye, including those that are common precursors to amblyopia. The test is noninvasive, safe, and can be administered easily in the field by an operator with no medical training. Only minimal momentary cooperation of the subject is required: Thus, the test shows promise for use with very young children.

The test produces color-slide images of the retinas of the eyes under specially-controlled lighting conditions. These are termed "generated retinal reflex" images. A trained observer can evaluate these photographs at the rate of five to seven per minute.

The required equipment (see figure) includes a camera, an electronic flash unit, and a small red light at which the subject looks while the photograph is taken. Prior to taking the photograph, the subject sits in the dark for 2 to 3 minutes to allow the pupils to dilate naturally.

Light from the flash enters the eye, illuminating a portion of the retina. When photographed from the angle shown, the retina of a normal eye appears a uniform red color. Ocular defects are indicated when the retina image is lighter or darker or nonuniform in color or brightness. For example, nearsightedness is indicated by bright crescents at the bottom of the eye, and farsightedness is indicated by bright crescents at the top of the eye. Also, strabismus (crossed eyes) is indicated by the bright corneal reflection from the flash being off center.

In addition to the visual evaluation of the photographs, instrumented quantitative analysis techniques were tried, ranging from color and intensity measurements that averaged over the entire retina to one in which measurements were made at approximately 400 points in each retina image. None of the quantitative techniques gave better or faster results than direct visual evaluation, although further development might yield better results.

In the visual evaluations, photographs from 232 persons were evaluated. Depending on the observer, 80 to 90 percent of the evaluations were correct. The 24 incorrect evaluations by the best observer included 8 persons incorrectly judged to have optically equal eyes and 16 incorrectly judged to have optically unequal eyes. This observer was absolutely correct in identifying persons who were either nearsighted or farsighted, or cross eyed. If the abnormality was caused by other disease processes, the observer could only speculate about the cause of abnormality.

This work was done by R. Jayroe and John R. Richardson of **Marshall Space Flight Center;** *J. H. Kerr and S. H. Hay of Electro-Optics Consultants, Inc.; and*

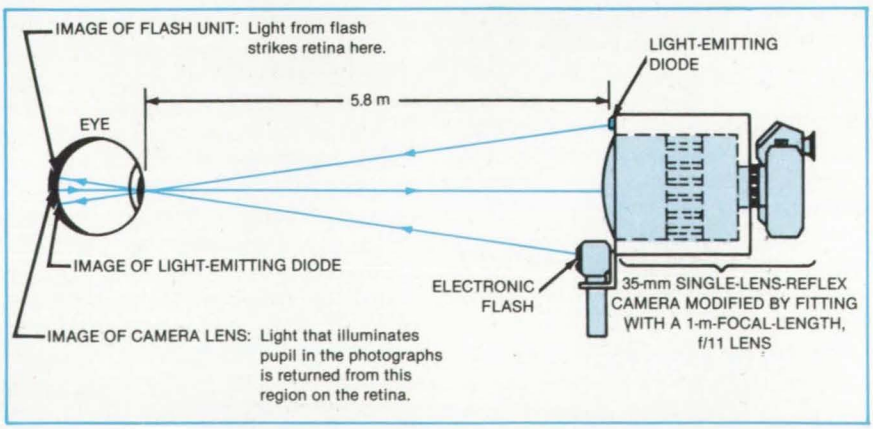

Color Photographs of Retinas are taken with this apparatus, which exploits "red-eye effect" that is usually considered an annoyance in portrait color photography. The proper alinement of the eye is assured by asking the subject to gaze at the light-emitting diode. The "red-eye" patterns of the resulting color photographs are examined by trained observers for signs of ocular defects.

Robert McBride of the Alabama Institute for the Deaf & Blind. For further information, Circle 43 on the TSP Request Card.

Inquiries concerning rights for the commercial use of this invention should be addressed to the Patent Counsel, Marshall Space Flight Center [see page 29]. Refer to MFS-25800.

Coculture Production of Butanol by *Clostridium* Bacteria

Butanol concentration is higher when two species are used.

NASA's Jet Propulsion Laboratory, Pasadena, California

According to preliminary experiments, the production of butanol by the anaerobic fermentation of sugars is enhanced by the use of two *Clostridium* species, one of which feeds on a metabolic product of the other. The renewed interest in a fermentation process for making butanol is stimulated by the potential use of butanol as a surfactant in enhanced oil recovery. Butanol can also be used as a fuel or as a chemical feedstock and is currently produced synthetically from petroleum.

In conventional fermentation with *Clostridium,* the product is a mixture of butanol, acetone, and ethanol, in the approximate ratio of 6:3:1. Mixed-solvent yields of 29 to 33 percent of fermentable carbohydrate have been recorded. The organisms that produce butanol do so by the reduction of butyric acid.

The yield of butanol can be increased with the help of a precursor species that produces butyric acid for consumption by the butanol-producing species. One can use a series coculture, in which the second species feeds on the products of the first species, or a parallel coculture, in which the two species live together.

In the preliminary experiments, the precursor species were *C. butyricum* and *C. pasteurianum,* which produce high concentrations of butyric acid from glucose. The second-stage species were *C. butylicum* and *C. acetobutylicum,* which derive energy from the conversion of butyric acid to butanol. Cocultures with combinations of these species consistently produced butanol concentrations 20 percent higher than that of the corresponding pure culture.

This work was done by Sheryl L. Bergstrom and Gary L. Foutch of Oklahoma State University for **NASA's Jet Propulsion Laboratory.** *For further information, Circle 14 on the TSP Request Card.*

Inquiries concerning rights for the commercial use of this invention should be addressed to the Patent Counsel, NASA Resident Office-JPL [see page 29]. Refer to NPO-16203.

Books and Reports

These reports, studies, and handbooks are available from NASA as Technical Support Packages (TSP's) when a Request Card number is cited; otherwise they are available from the National Technical Information Service.

Effect of Hydration on Nitrogen Washout in Humans

While hydration may reduce decompression effects, nitrogen removal is not the reason.

A series of experiments described in a NASA technical memorandum showed that drinking water before breathing nearly pure oxygen has little or no effect on the rate of removal of nitrogen from the body. The experiments were undertaken because data from some earlier experiments suggested that, under some conditions, hydration might help prevent decompression sickness.

The sickness is caused by bubbles of nitrogen that form when nitrogen comes out of solution in body fluids during decompression. Prior investigators had suggested that hydration would enhance the removal of nitrogen from tissues, fluids, or gas bubbles and would enhance the ability of fluids to retain more nitrogen in solution. To test this hypothesis, the experiments were conducted to measure the amount of nitrogen removal with and without hydration.

Each of five human subjects underwent three experiments. In each experiment, the subjects breathed oxygen while resting for 3 hours, during which time the nitrogen removed in exhaled gas was measured. The subjects did not drink before the first two tests, but each drank 1.5 liters of water before the third test. For each subject, there was no significant difference in nitrogen removal among the three tests.

It has been conjectured that the occasional beneficial effects of hydration are due to phenomena other than nitrogen removal. One possibility is that hydration increases the surface tension of blood, thereby inhibiting bubble formation somewhat. Whether this would influence bubble formation in joints is not known. Hydration may also increase microcirculation, thereby partly counteracting obstructions by gas emboli.

This work was done by James Waligora and David J. Horrigan, Jr., of **Johnson Space Center,** *and Johnny Conkin of Technology, Inc. Further information may be found in NASA TM-58254 [N83-26448/NSP], "Effect of Hydration on Nitrogen Washout in Human Subjects" [$7]. A copy may be purchased [prepayment required] from the National Technical Information Service, Springfield, Virginia 22161.*

Inquires concerning rights for the commercial use of the technology described in this report should be addressed to the Patent Counsel, Johnson Space Center [see page 29]. Refer to MSC-20686.

Mechanics

Hardware, Techniques, and Processes

114 Aircraft Canopy Lock
115 Inspecting Hollow Parts With a CAT Scanner
116 Continuous Laminar-Smoke Generator
116 Inflatable Column Structure
117 Contact Heat Exchanger
118 Microprocessor-Controlled Laser Balancing System
119 Calibrating Droplet Generator for Pressurized Testing Vessel
119 Wingtip Vortex-Augmented Turbopusher Propeller Thrust
120 Superconducting-Cavity Accelerometer
121 Remotely-Controlled Docking System
122 Spring-Loaded Transducer Holder
123 Differential Temperature Control of Electrical Heaters
123 Deployable M-Braced Truss

Books and Reports

124 Multishaker Modal Testing
125 Rocket-Booster Towing Simulation

Aircraft Canopy Lock

Mechanism is easy to open intentionally but resists accidental opening.

Dryden Flight Research Center, Edwards, California

A lock for an aircraft canopy can be operated from both inside and outside the cockpit but is unlikely to be actuated by accidental pilot movements or aerodynamic forces during flight.

To ensure positive engagement of the canopy and the locking mechanism, two simultaneous actions are required to close the canopy: latching the canopy and locking the latch. Similarly, to prevent the canopy from flying open accidentally, two actions are required for opening: unlocking the latch and unlatching the canopy.

To unlock the latch from the inside, the pilot pulls a knob out from the cockpit wall to disengage a pull pin from a recess (Figure 1). Once the pin is disengaged, the arm on which the knob is mounted can be rotated. The motion of the arm is transmitted by a pair of linked rods to a pair of hooks, thus causing the hooks to disengage from a pair of pins on the canopy (Figure 2). The canopy is then free to open upward.

To release the canopy from the outside, an attendant pushes an ejection pin. This action presses the ejection pin against the pull pin in the hole of the conical base, forcing the latter pin out of the hole. The attendant then rotates an exterior handle counterclockwise. This handle is connected to the interior arm with the knob. The motion of the exterior handle therefore causes the arm to rotate and release the hooks.

To fasten the canopy from the inside, the pilot moves the arm forward (counterclockwise in Figure 2), thus driving the rods forward so that the hooks slip over the pins. The tip of the pull pin rides up the cone of the base as the knob is rotated and shoots into the recess under spring compression when it arrives at the peak of the cone.

To close the canopy from the outside,

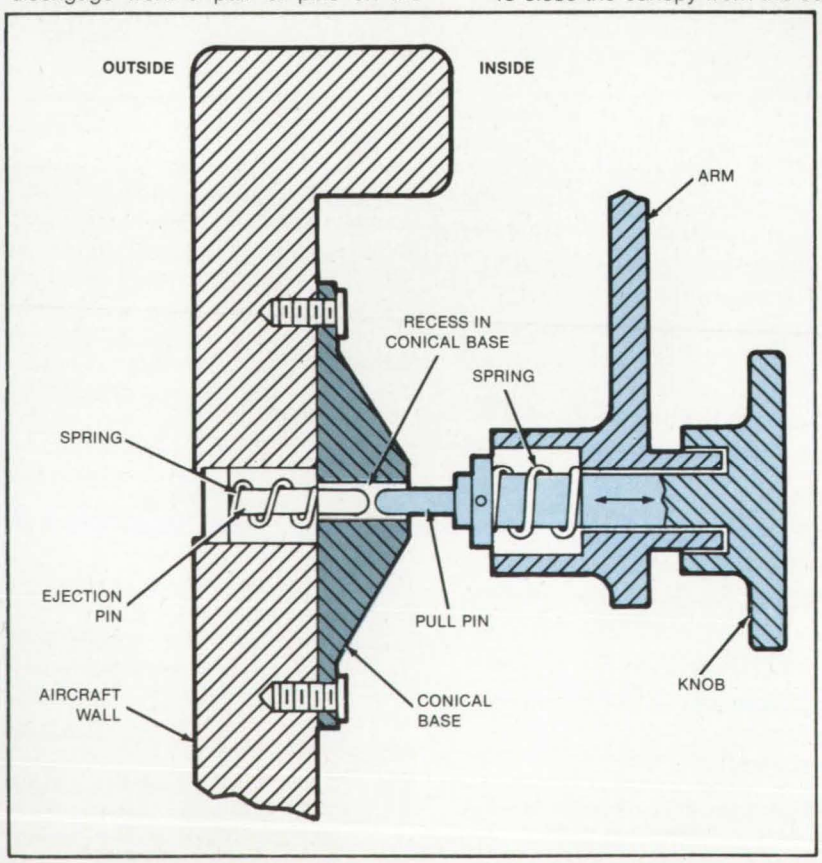

Figure 1. **Locking or Unlocking** occurs when the pull pin enters or leaves the conical base. Pushing the ejection pin or pulling the knob unlocks the mechanism.

the attendant rotates the outside handle clockwise, driving the rods forward and engaging the hooks with the pins. As with interior closing, the pull pin automatically rides up the base cone and shoots into the hole.

Unintentional release is unlikely since accidental pilot motions would push on the knob in most cases. This safety feature, coupled with the simplicity and reliability of the mechanism, may make it useful for emergency exits from land vehicles or even buildings.

This work was done by George H. Nichols of **Dryden Flight Research Center.** *For further information, Circle 44 on the TSP Request Card.*

Inquires concerning rights for the commercial use of this invention should be addressed to the Patent Counsel, Dryden Flight Research Center [see page 29]. Refer to FRC-11065.

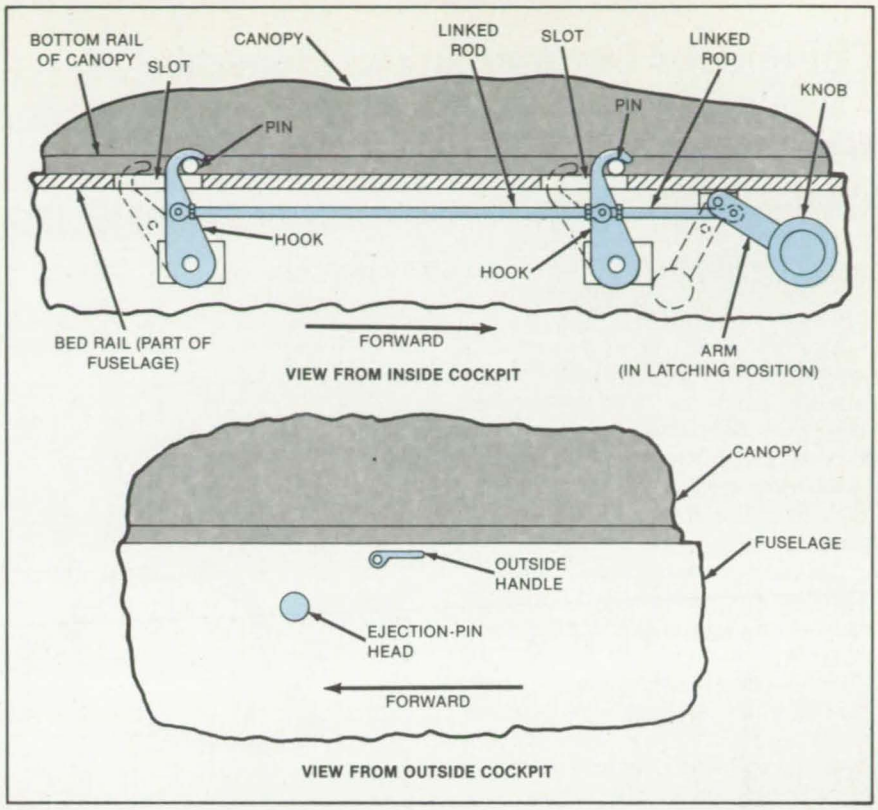

Figure 2. **Latching or Unlatching** occurs when the arm is moved forward or backward. Rotation of the arm with the knob or of an external handle moves the linked rods, causing the hooks to engage or release the pins on the canopy.

Inspecting Hollow Parts With a CAT Scanner

A technique well known in medicine would be used on manufactured objects.

Marshall Space Flight Center, Alabama

Computer-aided tomography (CAT) has been proposed for measuring the wall thicknesses and detecting flaws in hollow turbine blades or other curved parts. The technique is similar to the CAT scans used in medical diagnoses.

The turbine blades for which the technique was proposed are curved and have wall thicknesses of less than 0.1 inch (2.5 millimeters). Their varying radii of curvature and hollowness make conventional thickness measurement difficult. Ultrasonic measurements, for example, require that surfaces on the test specimen be parallel. Special micrometers could be built, but several different types have to be designed if measurements are to be made at more than one point.

The proposed CAT-scanning system would consist of a radiation source, collimators, a rotating table, synchronizing electronics, a detector, and a computer (see figure). A measured quantity of collimated particle or electromagnetic radiation penetrates the part under test. As the radiation travels through the material, part of the beam is scattered; the amount of scattering depends, among other things, upon the total thickness of material that is penetrated. The radiation that emerges from the part passes through a second collimator that removes most of the radiation scattered at small angles from the beam. The remaining beam consists mostly of unscattered and slightly scattered radiation, and this beam reaches the detector.

The detected photon count is a measure of the total thickness of material that has been penetrated. From measurements at various angles, a cross-sectional map of the part can be constructed by the computer and displayed on a television screen. The synchronizing circuitry controls the table that rotates the part through the required angles. Alternatively, in a simpler system, the part could be rotated manually on its table and locked in place during timed exposures.

This work was done by George A. Kuhr of Rockwell International Corp. for **Marshall Space Flight Center.** *No further documentation is available.*
MFS-19916

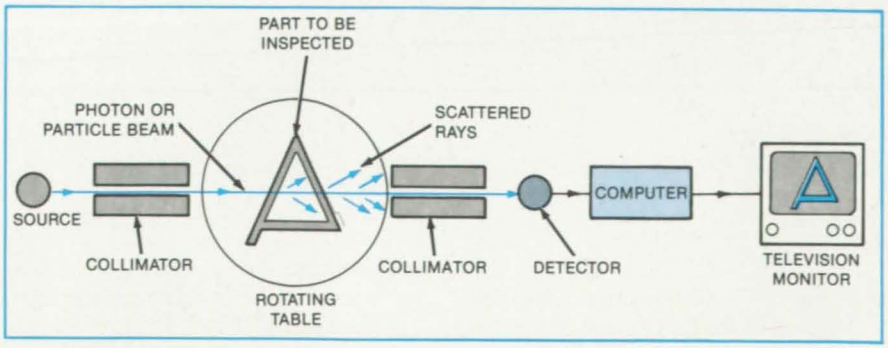

As It Passes Through a Part, a beam of X-rays or other radiation is attenuated and scattered. A computer records the variations in the beam as the part is rotated and constructs a cross section for display on a video monitor.

Continuous Laminar-Smoke Generator

A single smoke filament is used to study flow in low-speed wind tunnels.

Langley Research Center, Hampton, Virginia

A continuous laminar-smoke generator was developed at Langley Research Center to better visualize flow details in low-speed wind-tunnel tests. The use of a small-diameter single laminar smoke stream allows the examination of flow structures at higher resolution, and continuous operation facilitates use.

The generator (see figure) is capable of producing a single filament of smoke and uses a small-diameter feed tube, the wall of which acts as the heater element. The smoke-exit hole is simply a drilled hole in the side of the feed tube. The local flow speed is kept low enough to prevent eddy shedding. By placing the tube in the low-speed part of wind tunnel (just ahead of the contraction), the actual test speed can be made much higher than the local speed around the smoke generator. With a feedline and electrical-wire diameter of 0.50 mm (the feedline used had a 0.25-mm inside diameter), laminar smoke was obtained up to a stream velocity of 11 m/s.

Use of a thin splitter plate just behind the smoke-generator tube could help prevent eddy shedding at somewhat higher speeds. A streamlined, airfoil-shaped smoke generator could also increase the usable speed, especially if it had a blown-base slot to compensate for velocity deficit caused by skin friction. A larger diameter feed and heater tube has "boiling" unsteadiness problems, but a wick or a porous filler in the tube could help eliminate this difficulty. A high oil-feed rate and high heater temperature will produce denser but more turbulent smoke, which would be useful where a thin laminar filament is not required but more smoke volume is needed.

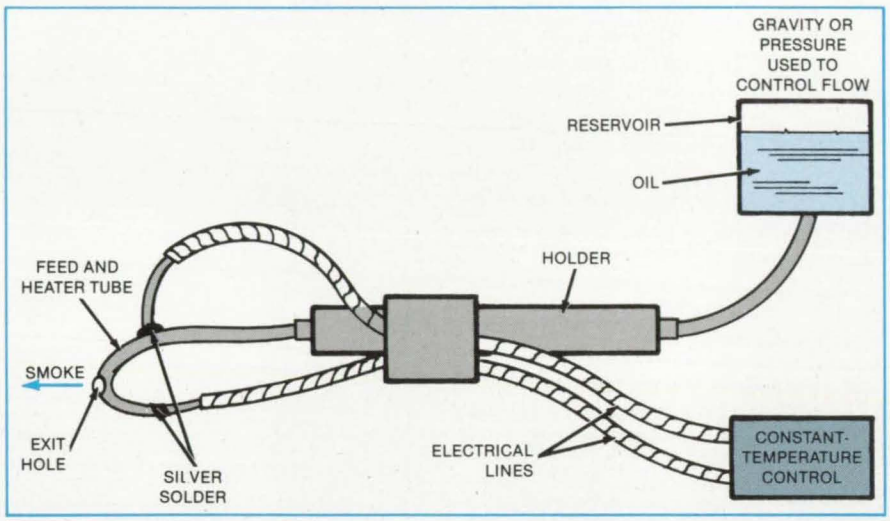

A **Thin, Single Filament of Smoke** is generated for low-speed wind-tunnel use.

The main features of this technique are the combination of continuous operation; a thin, single laminar filament of smoke; ease of use; and minimal adjustment and control. The continuous laminar-smoke generator in its basic form and in modified configurations will be used to study flow over models in a variety of low-speed wind-tunnel tests.

This work was done by Leonard M. Weinstein of **Langley Research Center.** *No further documentation is available.*

This invention is owned by NASA, and a patent application has been filed. Inquiries concerning nonexclusive or exclusive license for its commercial development should be addressed to the Patent Counsel, Langley Research Center [see page 29]. Refer to LAR-13014.

Inflatable Column Structure

Lightweight structural member is easy to store.

NASA's Jet Propulsion Laboratory, Pasadena, California

An inflatable structural column consists of a fiber-reinforced tube segmented at regular intervals by circumferential belts of fiber (see figure). The belts cinch the wall slightly, but the interior of the column is essentially unobstructed.

Uninflated, the column is simply a short stack of fabriclike folds. It is compact and easily stored. The column can be readily inflated to its full length by a tank of gas such as nitrogen or even manually by a foot or hand pump.

In its inflated state, the column takes on a segmented, caterpillarlike form. The length of the column and its thrust, torque, and moment-carrying capacity are determined by the internal pressure, the column dimensions, and the number

and tensile strength of the fibers.

The inflatable column would have applications where a lightweight, easily-stored temporary support is needed. For example, it could serve as a jack for automobiles or for structures during repairs. It can also be used as a support for temporary bleachers or swimming pools.

This work was done by John M. Hedgepeth of Astro Research Corp. for **NASA's Jet Propulsion Laboratory.** *For further information, Circle 49 on the TSP Request Card.*
NPO-16216

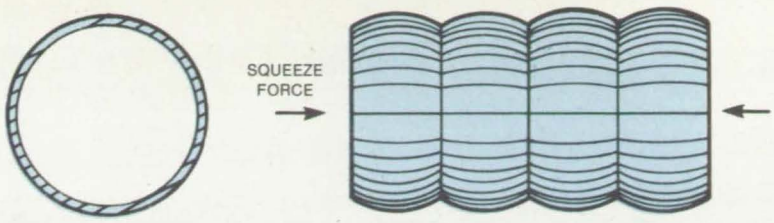

Billowing Between Circumferential Loops of fiber, an inflated column becomes a series of cells. Each fiber is subjected to the same tension along its entire length (though the tension may be different in different fibers). The member is therefore called an "isotensoid" column.

Contact Heat Exchanger

Fluid pressure controls the contact between a heat pipe and a heat exchanger.

Lyndon B. Johnson Space Center, Houston, Texas

A segmented interface moved by fluid pressure controls the amount of heat transferred between a heat pipe and a circulating heat exchanger. Although originally developed for use in space, the new device could find applications on Earth where a fluid system is to be linked with a heat pipe, where rapid assembly/disassembly is required, or where high pressures or corrosive fluids are used.

The device shown in the figure consists of split cylindrical heat-exchanger sections made of soft-aluminum (2024-T0) tubing with small flow tubes brazed on the outside. Gas or hydraulic pressure applied across a flexible metal diaphragm forces these cylindrical heat-exchanger sections into contact with matching sections of the heat pipe evaporator. Contact conductances of 3.4 $kW/m^2 \cdot °C$ were obtained in demonstration tests.

With proper modifications the system could be actuated by a temperature-controlled source of pressurizing gas and could be used to connect any two kinds of heat exchangers. However, possible metallic corrosion of the contact surfaces should be considered when used in atmospheric conditions.

This work was done by Michael L. Fleming, Dennis D. Stalmach, and Roy L. Cox of Vought Corp. for **Johnson Space Center.** *No further documentation is available.*

Inquires concerning rights for the commercial use of this invention should be addressed to the Patent Counsel, Johnson Space Center *[see page 29].* *Refer to MSC-20419.*

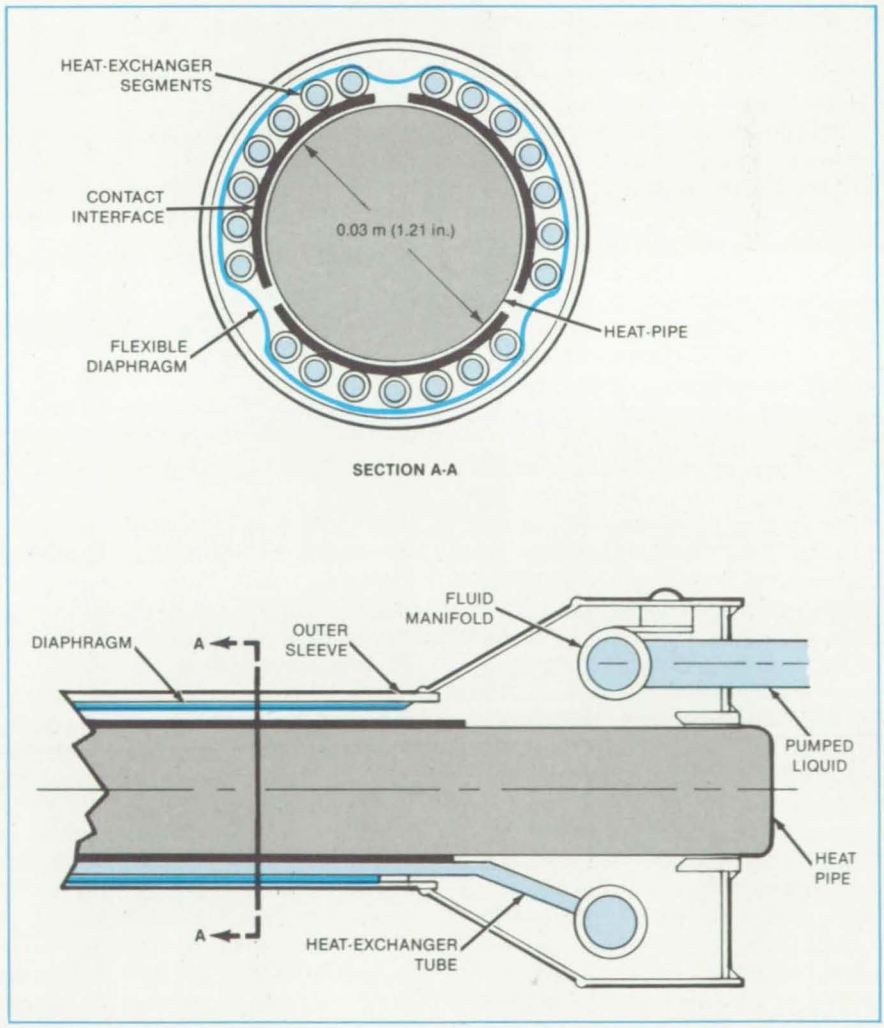

The **Heat-Exchanger System** shown in the cross section provides contact interface between a fluid system and a heat pipe with easy assembly/disassembly of the heat-pipe/pumped-liquid system.

Microprocessor-Controlled Laser Balancing System

Material is removed by laser action as the part is tested for balance.

Lewis Research Center, Cleveland, Ohio

A microprocessor-controlled laser balancing system has been developed for automatic dynamic balancing of rotating components. This system provides complete and accurate balancing in a single load-and-spinup cycle. It computes all balance plane corrections simultaneously and then uses a pulsed laser for precise material removal, even from parts that may be inaccessible for installation of conventional correction weights. Since the unbalance correction is performed by the laser under microprocessor supervision as the part rotates, human error and rejected workpieces are virtually eliminated.

The operator and the microprocessor software interact through a video screen and keypad; no programing skills or unprompted system-control decisions are required. The unit can be retrofitted to existing balancing machines, including low-speed balancing units, vacuum spin pits, and trim balancing systems. It can be used with a number of different lasers, allowing an optimum selection for cost-effective material removal and balancing results.

Directed by the microprocessor, which uses vibration information from the balancing-machine existing sensors in combination with information from memory, the laser fires the appropriate amount of pulses in the correct locations to remove the necessary amount of material. As shown in the figure, the laser machining is basically a high-speed ablation process. The evaporation of a very small portion of liquid metal takes place so rapidly under the high intensities of a focused laser beam that a substantial impulse is transmitted to the liquid. Material leaves the surface not only through evaporation but also in the liquid state at a relatively high velocity.

This technology offers several advantages over the conventional approach of drilling or grinding removal of material. The system does not rely on skilled operators to remove exact amounts of weight from locations that are often difficult to identify and access precisely. In addition, productivity is increased by eliminating the time-consuming steps of removing parts from the balance machine to grind and reinstalling them in the balance machine to check whether the required tolerances are met.

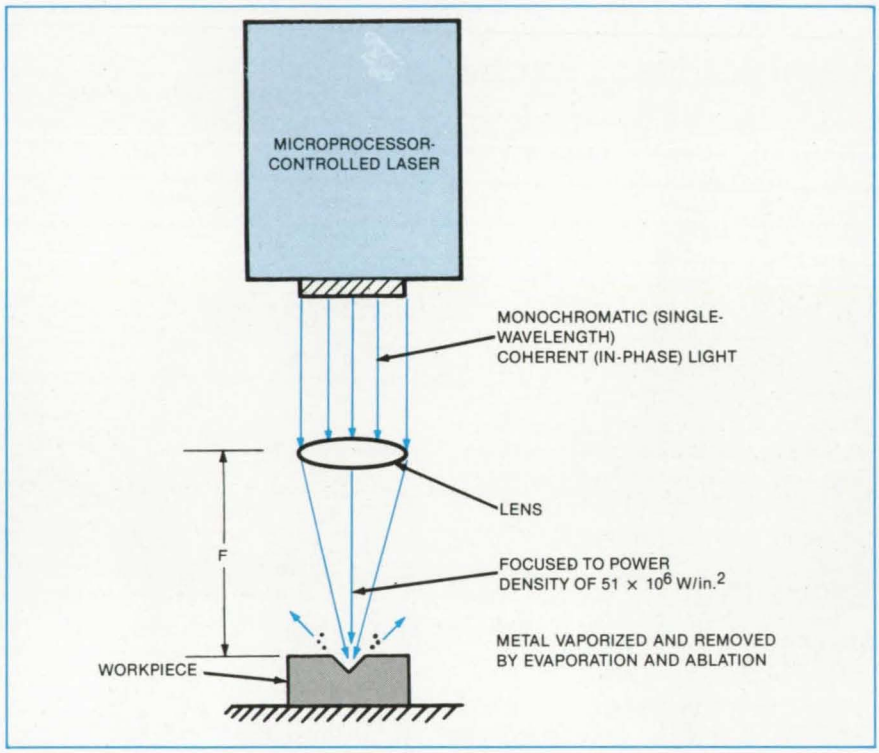

Directed by a Microprocessor the laser fires the appropriate amount of pulses in correct locations to remove the necessary amount of material.

The system operates with closed-loop feedback using the sensors to update the laser commands automatically, assuring that residual unbalance is kept within operator-specified limits. The system may also operate without a laser, using the same software to provide the operator with balance locations and required weight corrections.

Additional software packages have been developed for applications ranging from retrofitting conventional two-plane balance machines to multispeed, multiplane balancing of supercritical rotors. The integrated data-acquisition and rotor-balancing software packages are currently operational on Digital Equipment Corp. PDP 11/34 and 11/03 computers. Potential uses include production environments where large data bases exist and rapid throughputs are required, field services with limited machinery access, and developmental programs with unique or prototype systems where vibration must be minimized.

This work was done by Russell S. DeMuth of Mechanical Technology, Inc., for **Lewis Research Center.** *Further information may be found in NASA CR-3105 [N79-17228/NSP], "Experiments on Multiplane Balancing Using a Laser for Material Removal" [$8]. A copy may be purchased [prepayment required] from the National Technical Information Service, Springfield, Virginia 22161.*

LEW-13294

Calibrating Droplet Generator for Pressurized Testing Vessel

Device helps to aline a laser for a droplet-sizing interferometer.

Marshall Space Flight Center, Alabama

A droplet generator has been adapted to alining and calibrating a laser beam, the focal point of which lies inside a high-pressure tank. The tank is used for injector cold-flow tests by a laser droplet-sizing interferometer. The alinement procedure automatically corrects for the deflection of the laser beam that occurs when the internal tank pressure distorts the tank. This deflection could not be corrected by external alinement and calibration procedures.

The alinement and calibration device is a monodispersing droplet generator (MDG), which provides a stream of uniformly sized droplets through a small orifice in a vibrating piezoelectric crystal ring. The laser beam is adjusted so that it intersects and focuses on the droplet stream (see figure).

The MDG is mounted in a high-pressure flange on the tank. Line extensions pass through the flange to the outside. The flange allows the MDG to operate at the high injector back pressures used for the tests.

This work was done by Guido J. Defever and Tony Exposito of Rockwell International Corp. for **Marshall Space Flight Center.** *No further documentation is available.*
MFS-25992

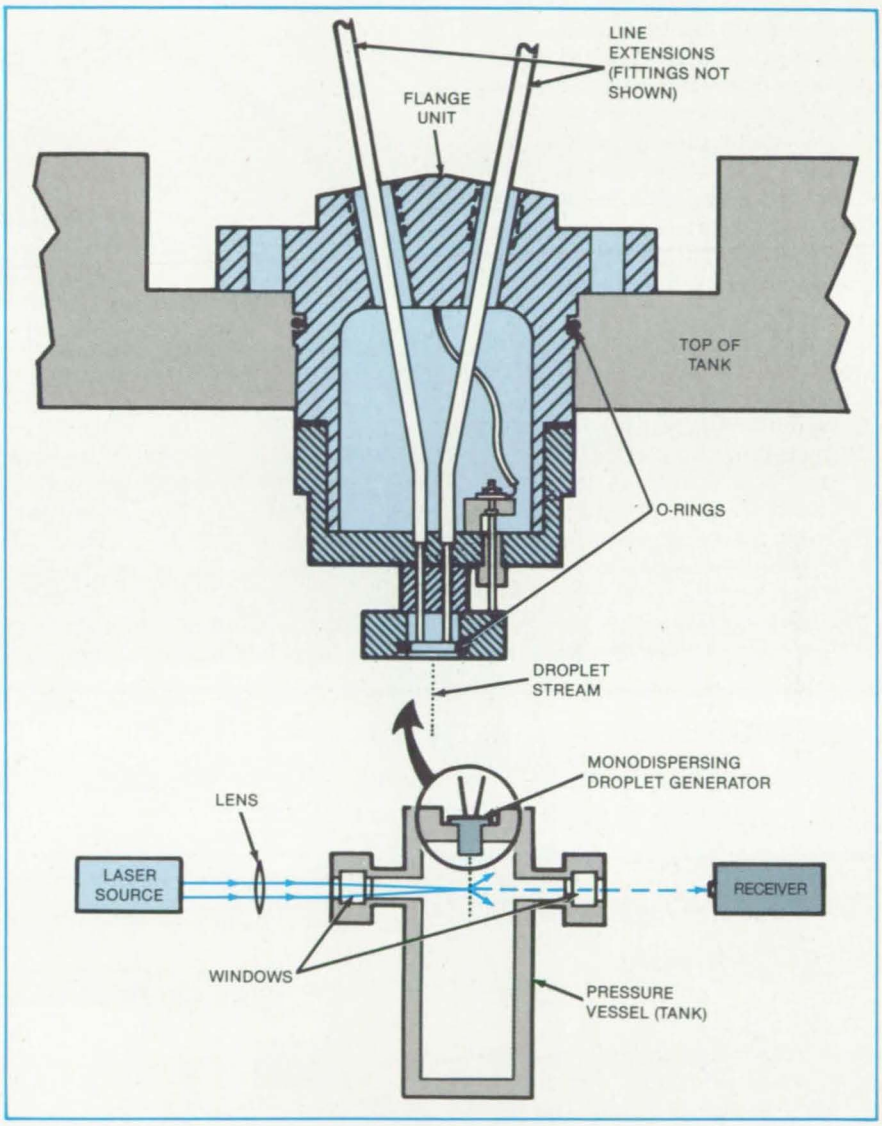

The **Monodispersing Droplet Generator** creates uniformly sized droplets. The laser source and receiver of an interferometer are alined and focused on the droplets.

Wingtip Vortex-Augmented Turbopusher Propeller Thrust

Thrust of propeller is enhanced by the tip vortex.

Langley Research Center, Hampton, Virginia

The thrust produced by a pusher turbopropeller configuration mounted on the wingtip is augmented by the lift-induced wingtip vortex flow. As a result of the weaker vortex, there is a reduction in the induced drag of the wing afforded by propeller-wake mass injection into the core of the vortex, causing it to break down. This location of the pusher turboprop also eliminates the detrimental effect of the propeller swirl, surface-scrubbing drag, and compressibility wave drag.

The direction of lift produced by a propeller blade is approximately perpendicular to the local or resultant velocity, which is a combination of the stream and propeller-rotational velocities. The thrust produced in the flight direction is a component of this propeller lift. Because the turbo-pusher-propeller configuration is mounted in the vortex flow at the wingtip, the vortex and the propeller-rotational velocities will be additive (see figure), increasing the angle of the local velocity relative to the propeller. This change in relative velocity direction would cause the propeller lift vector to be rotated in a streamwise direction, thereby increasing the magnitude of the thrust component. This new relative velocity would allow a reduction in the actual propeller blade angle, thus requiring less energy from the turboengine to maintain the required thrust level. This change in thrust due to the vortex flow is approximately 16 percent based on "simple blade theory."

The total improvement that could be expected by taking advantage of the aerodynamic flows that exist on an airplane in cruise flight may be as high as a 28 percent reduction in the total drag. This includes a 12-percent reduction in the induced drag of a transport-type aircraft due to the vortex dissipation afforded by the prop-wash/vortex core flow interaction.

This work was done by James C. Patterson, Jr., of **Langley Research Center.** *Further information may be found in NASA TN D-5729 [N70-27576/NSP], "An Exploratory Wind Tunnel Investigation of the Wake Effect of a Panel Tip-Mounted Fan-Jet Engine on the Lift-Induced Vortex" [$8.50]. A copy may be purchased [prepayment required] from the National Technical Information Service, Springfield, Virginia 22161.*

This invention is owned by NASA, and a patent application has been filed. Inquiries concerning nonexclusive or exclusive license for its commercial development should be addressed to the Patent Counsel, Langley Research Center [see page 29]. Refer to LAR-13019.

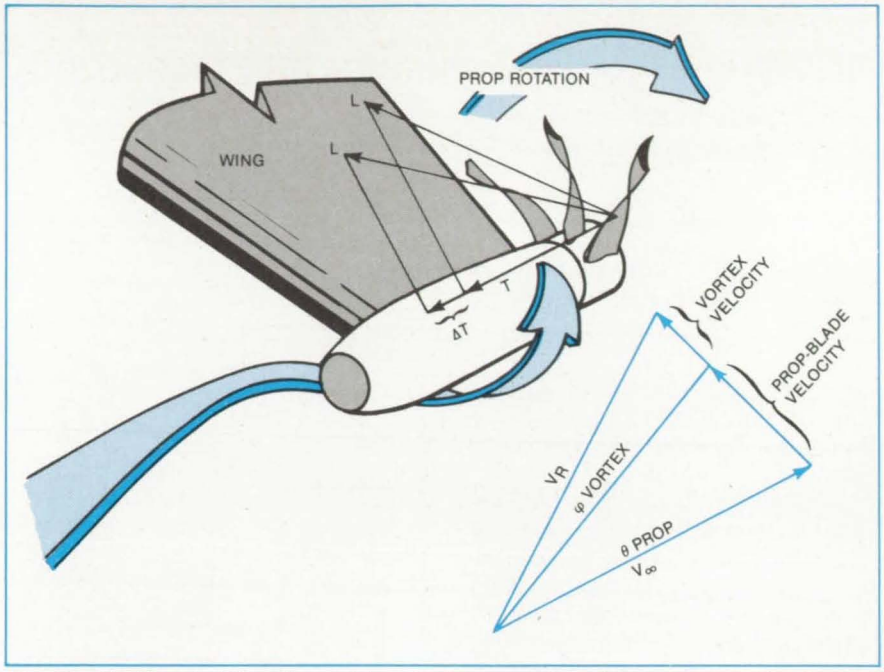

The **Wingtip-Mounted Nacelle** provides a turboprop vortex velocity recovery. The thrust of the turbopusher propeller is increased by the flow of the lift-induced vortex.

Superconducting-Cavity Accelerometer

The resonant frequency of a microwave superconducting cavity is sensitive to gravitation and acceleration.

Goddard Space Flight Center, Greenbelt, Maryland

A sensitive accelerometer would be assembled by combining a superconducting microwave cavity and a conventional microwave semiconductor oscillator. The cavity would serve as the resonant element of the oscillator circuit. It is estimated that the proposed device could measure accelerations as small as 10^{-10} cm/s^2 (10^{-13} g's). It could also be configured to measure small gradients in the gravitational field of the Earth, say in the order of 10^{-2} to 10^{-3} EU (Eötvös units).

Changes in the cavity dimensions caused by an acceleration alter the resonant frequency of the cavity and therefore the oscillator frequency; ie, a relative change in the length of the cavity causes a relative shift in frequency, which can be

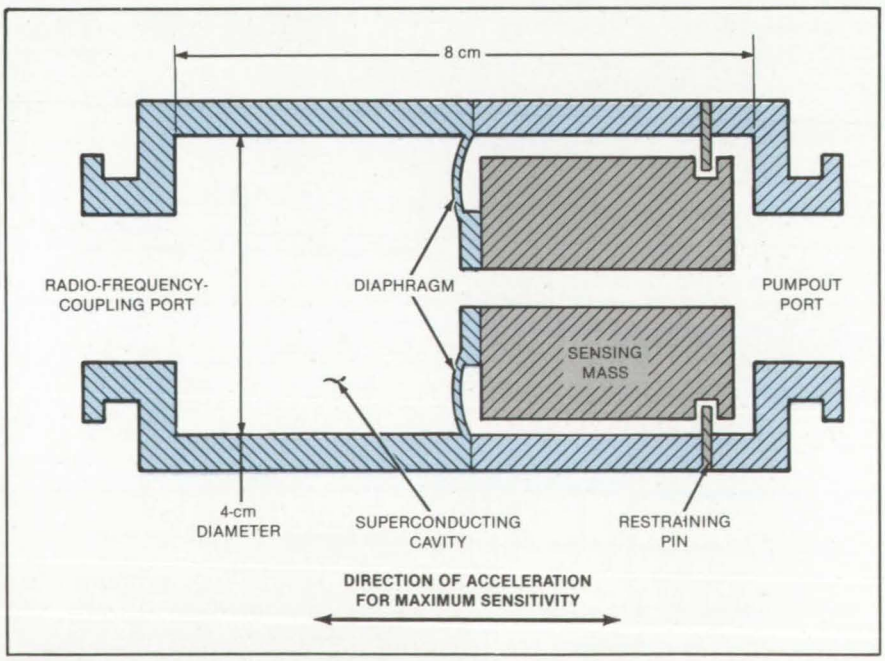

A **Diaphragm Changes the Length** of a superconducting resonant chamber — and hence its resonant frequency — in response to acceleration of a sensing mass.

measured very easily. In the past, this effect was considered a nuisance. However, the sensitivity to the force of gravitation or acceleration can be exploited in a measurement of acceleration.

For this use, one endwall of the microwave cavity is a diaphragm weighted with a sensing mass (see figure). For example, for a cavity 4 centimeters long, 4 centimeters in diameter, oscillating at 9.89 gigahertz, with a 500-gram sensing mass on a diaphragm of spring constant 1.6×10^7 g/s^2, the acceleration or gravitational sensitivity is 10^{-10} cm/s^2.

Two such accelerometers can be placed a fixed distance apart and their output signals mixed to determine the local gravitational gradient. A difference in the gravitational force at the positions of the two oscillators translates into a change in the beat frequency of the two outputs. For a 1-meter separation between, the sensitivity to gravity gradients is 10^{-12} cm/s^2-cm or 10^{-3} EU.

This work was done by Victor S. Reinhardt and Friedrich von Bun of **Goddard Space Flight Center.** *For further information, Circle 63 on the TSP Request Card.*
GSC-12797

Remotely-Controlled Docking System

Spring-loaded drogue cones tolerate and correct misalinement.

Lyndon B. Johnson Space Center, Houston, Texas

A docking mechanism for launching and retrieving payloads includes a passive probe attached to the host vehicle and an active assembly attached to the payload. Originally developed for the Space Shuttle, the mechanism could be adapted for robot manipulator arms, trailer hitches, and docking devices for in-flight refueling of airplanes.

The figure shows the docking mechanism in the "locked" position. The latches are locked by action of the rotary cam on the ball cam followers. This cam has two regions in addition to the one shown. The second region permits free radial motion of the cam followers to allow the spring-loaded latches to be depressed by the probe as it enters the drogue cone. The third region forces the cam followers radially outward to retract the latches for undocking.

In the locked position another cam presses the apex of the cone against the probe, locking it against the latches. The drogue cone is backed by a coil spring and a series of spring-loaded plungers that help to absorb the energy of collision as the probe first touches the cone. The springs reduce the peak forces applied to the probe tip as it enters, smoothing the docking process. The limit switch signals when the probe has entered far enough to have been captured by the latches. The cams are then operated to lock the mechanism.

Exact alinement is not expected as docking begins. To assure maximum stability during docking, the center of gravity of the payload is always within the triangle of attachment points. Thus the vehicle dynamics at impact will tend to aline the docking interface.

As the probes contact the drogue cones, limited damping is provided by the probes sliding along the drogue cones and by the drogue cones sliding on internal spring-loaded plungers. Fully compressed, the springs can store the full kinetic energy of collision. Rebound is prevented by the spring-loaded latches that catch on the shoulders of the probes. The latches are placed so that the probes can be captured with no compression of the drogue-cone springs. Since that is the

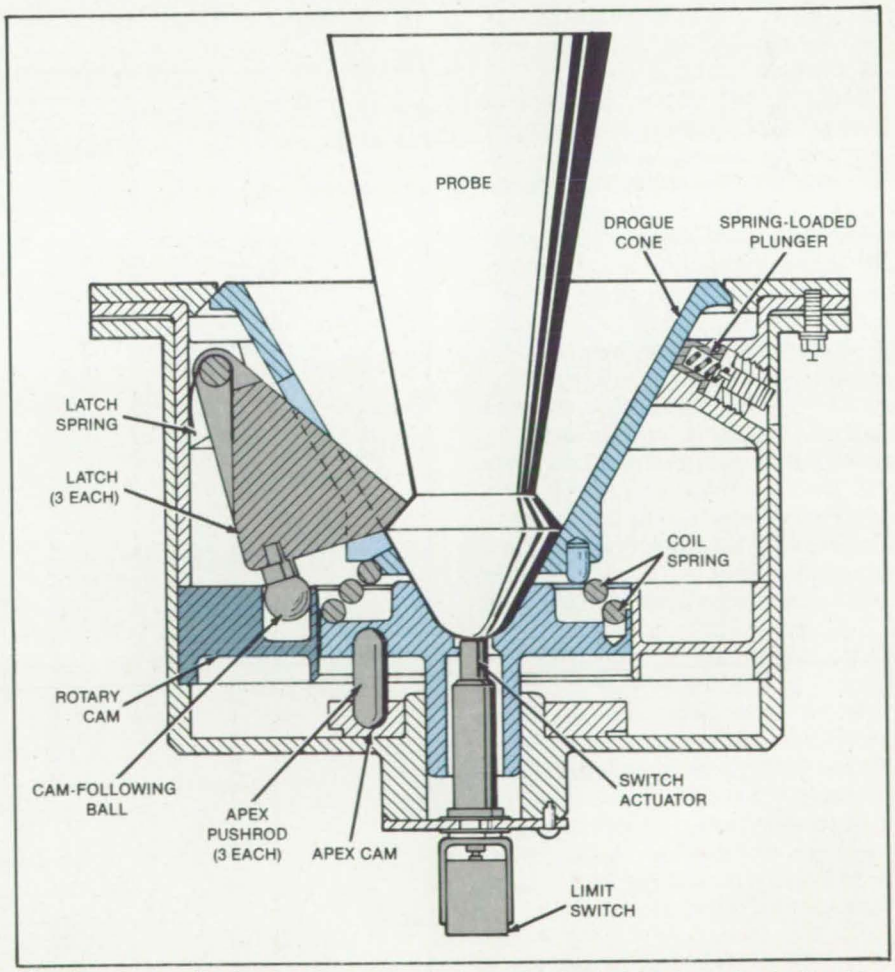

The **Attachment Mechanism** is equipped with spring-loaded latches, shock-absorbing springs, and self-alining conical mating surfaces. The docking system includes three attachment mechanisms like the one shown plus a television camera that views a set of crosshairs for alinement of the vehicle and the payload.

probe position when the mechanism is locked, no momentum is transferred between the load and the vehicle as the mechanism is unlocked.

The payload carries a television camera so that the docking process can be monitored and controlled remotely. Crosshair targets on the probe assembly and in the camera are used to monitor the docking approach.

This work was done by Joseph A. Chandler of **Johnson Space Center.** *For further information, Circle 68 on the TSP Request Card.*

This invention has been patented by NASA (U.S. Patent No. 4,431,333). Inquiries concerning nonexclusive or exclusive license for its commercial development should be addressed to the Patent Counsel, Johnson Space Center [see page 29]. Refer to MSC-18969.

Spring-Loaded Transducer Holder

A portable ultrasonic scanner moves a transducer at constant pressure.

Langley Research Center, Hampton, Virginia

A spring-loaded holder moves an ultrasonic transducer over a test sample at constant pressure. This setup is used to determine the rate of debond taking place in glued materials subjected to fatigue loading. The holder was designed as a portable field unit that could be adapted to a fatigue machine and that could transmit data while the specimen was being tested.

Materials and fatigue specimens at Langley Research Center are subjected to ultrasonic C-scanning, using a tank filled with water and transducers mounted on a tracking arm that is submerged in the water. Water is the energy-coupling medium between the transducer and the specimen. The tracking arm positions the transducers in the tank.

Although this stationary system is very sophisticated, a portable system was required. Portable systems use glycerin as a couplant because its viscosity allows the transducer to be moved along the specimen surface by hand. However, this system proved awkward to use for the application requiring the determination of the precise location of the debond line and its length as referenced back to its origin.

The problem was resolved with a spring-loaded holder for the transducer. The holder was attached to a vernier height gage, the vernier height gage was motorized, and a modified suction cup (borrowed from an electrocardiogram machine) was installed over the transducer.

As shown in the figure, the suction cup is a reservoir for the glycerin and a bumper for maintaining constant contact distance between the fatigue specimen and the transducer. The spring-loaded holder keeps the transducer and the suction cup pushed against the specimen with constant pressure but allows them to move over the specimen. By activating the switch on the motorized vernier, the operator can move the tranducer along the length of the specimen and read the transducer location on the vernier scale. This system produces an electronic signal when the transducer is located over a bonded area, but the signal level drops to zero when the transducer is moved over the debond line.

This work was done by Mickey R. Gardner of **Langley Research Center.** *No further documentation is available.*
LAR-13048

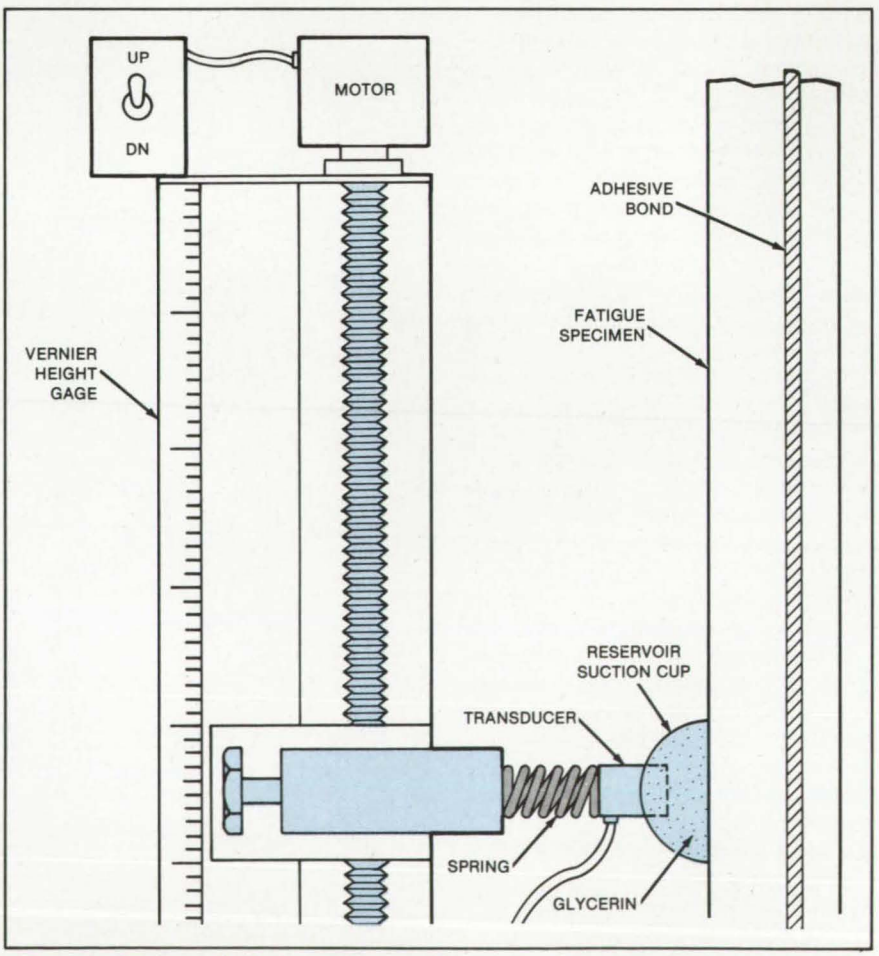

A **Specially Designed Holder** keeps the transducer in good contact with the sample as it is scanned for the exact location of the debond line.

Differential Temperature Control of Electrical Heaters

Energy savings are realized from heaters that maintain low humidity in electrical equipment.

Langley Research Center, Hampton, Virginia

Differential temperature controllers significantly reduce energy use by heaters that prevent moisture condensation in electrical equipment (e.g., wind-tunnel motors). Normally, these heaters are energized at all times except when the electrical equipment is operating; however, they need not be energized as often if differential temperature controllers are included to maintain the equipment at a fixed temperature above the ambient.

A prototype of the differential controller consisted of two thermocouples, a Burr Brown Model 3357 amplifier, a Burr Brown Model 4032 comparator, a Burr Brown Model 553 power supply, a stock relay, and miscellaneous passive circuit elements. A more recent version of the circuit is shown in the figure.

The unit applies power to the electrical-equipment heater only when the equipment temperature drops below a preset differential above ambient. For the initial tests the differential controller was set to maintain the motor 8° F (4° C) above the ambient temperature.

The efficacy of differential temperature controllers was demonstrated on large wind-tunnel motors. A 12-month survey completed on 11 units indicated a total savings of 1,250,000 kWh or a little over $56,000 at a cost of power = $0.045 or 4.5¢/kWh. The cost of installing 11 differential temperature units was $10,000, yielding a first-year net savings of more than $46,000.

The wind-tunnel motors use 22-kW heaters that are constantly on when the motors are not running. With the controller installed and the differential set at 8° F, the heaters may not come on for hours or, in some cases, days after tunnel runs because of heat gained during the run. Actual records indicate that for an average day during a nonrunning period, these particular heaters use 528 kWh without the differential controllers. With the differential controller, however, the power consumed is only 118 kWh for a savings of 410 kWh/day, or a 77-percent energy savings.

This work was done by Kenneth N. Cole of **Langley Research Center.** *No further documentation is available.*
LAR-13047

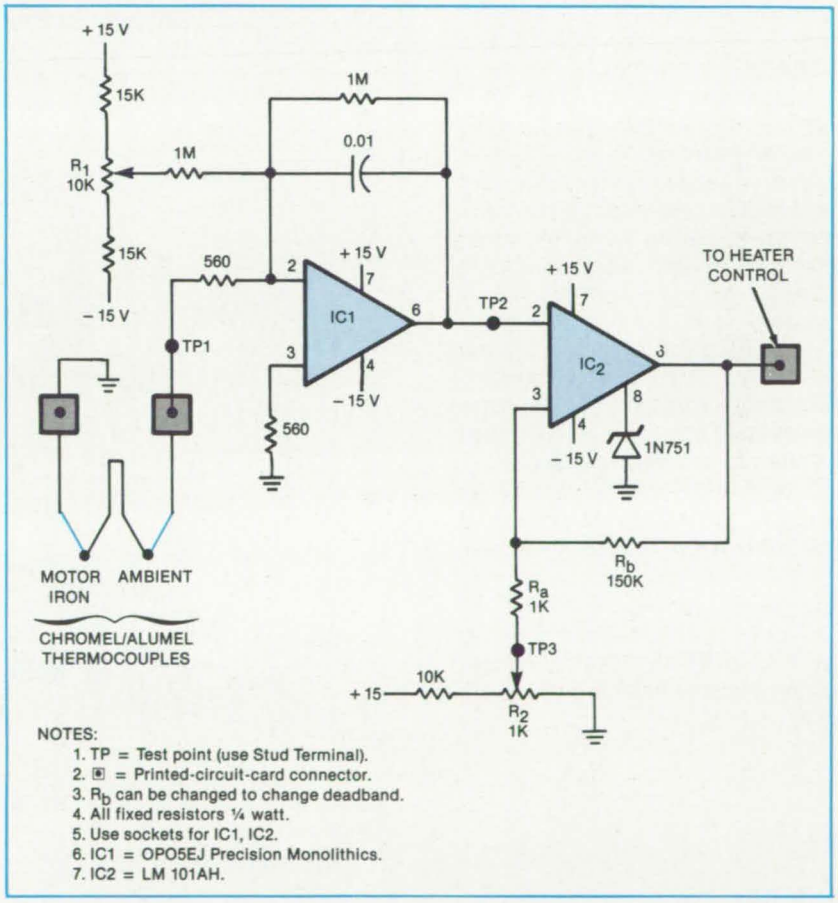

NOTES:
1. TP = Test point (use Stud Terminal).
2. ▣ = Printed-circuit-card connector.
3. R_b can be changed to change deadband.
4. All fixed resistors ¼ watt.
5. Use sockets for IC1, IC2.
6. IC1 = OPO5EJ Precision Monolithics.
7. IC2 = LM 101AH.

A **Typical Controller** turns on a heater relay when the temperature difference between the motor iron and the surrounding air falls below a specified value. For this unit, the preset temperature difference is 8° F (4° C).

Deployable M-Braced Truss

Tension/compression and shear are separated structurally in a deployable beam.

Langley Research Center, Hampton, Virginia

The deployable M-braced truss offers several advantages over the conventional X-braced geometry. In the M-braced configuration, the diagonals intersect at the center of a batten rather than at the batten/longeron intersection.

This construction allows loads introduced in the diagonals to be reacted by batten bending, eliminating movement associated with joint tolerances and ensuring the geometric accuracy of the deployed beam.

The M-braced geometry limits the response of the diagonal to an applied axial load. However, the diagonals can react shear loads because the triangular pattern cannot be distorted without introducing loads in the diagonal members. This design, therefore, effectively separates tension/compression from shear.

Packaging and deployment can be done in several ways. The diagonals and longerons may telescope from the base (as in Figure 1), permitting several sections to be packaged into a single bay section for launch. Or sections may be hinged about two longerons (as shown in Figure 2). Telescoping longerons and diagonals will permit very long structures to be packaged in a compact unit.

The truss can be deployed pneumatically, mechanically by springs or cables, or by a powered reciprocating mechanism. Once deployed, the telescoping members and sections are locked by simple latches to form a stiff structural column or beam.

Components of the M-braced truss may be fabricated from conventional metallic materials or nonmetallic materials such as graphite/epoxy. Typical applications include masts for antenna feed horns and ribs for solar array blankets.

This work was done by Martin M. Mikulas, Jr., and Marvin D. Rhodes of **Langley Research Center.** *No further documentation is available.*

Inquiries concerning rights for the commercial use of this invention should be addressed to the Patent Counsel, Langley Research Center [see page 29]. Refer to LAR-13081.

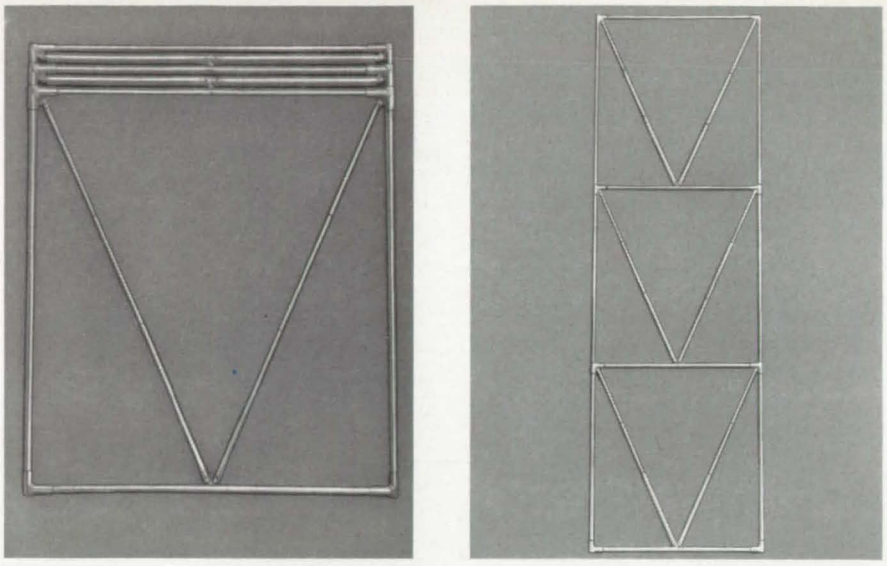

Figure 1. The **Deployable M-Braced Truss** consists of sections that telescope into the base.

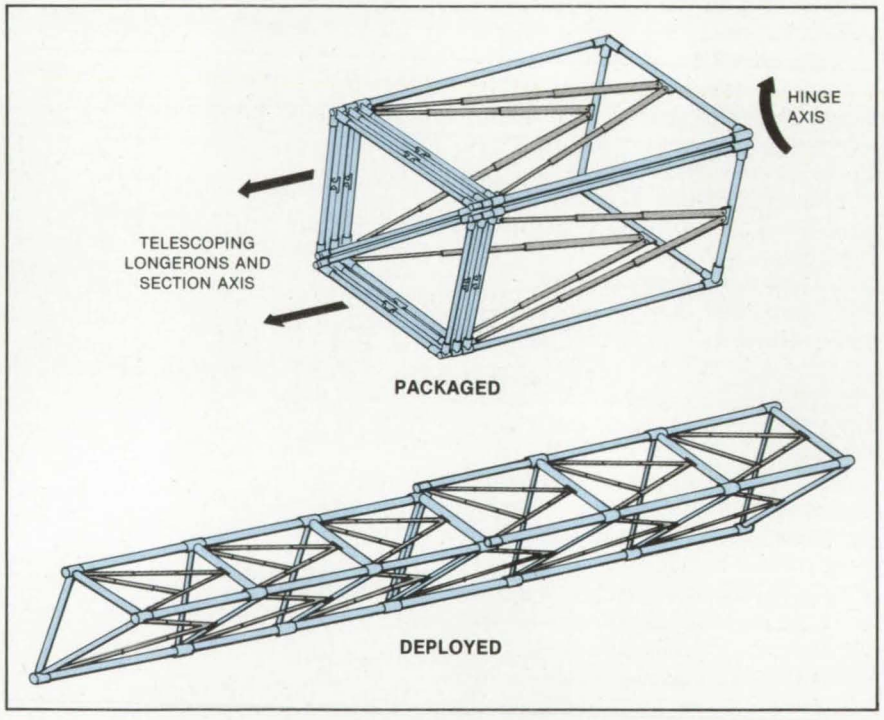

Figure 2. **M-Braced Sections Can Be Packaged** using a combination of hinges and telescoping sections. When the upper sections telescope into the base, the diagonals hinge, telescope, and rotate along the batten.

Books and Reports

These reports, studies, and handbooks are available from NASA as Technical Support Packages (TSP's) when a Request Card number is cited; otherwise they are available from the National Technical Information Service.

Multishaker Modal Testing

Major publications in modal modeling using test data are abstracted.

A report prepared for Marshall Space Flight Center summarizes recent advances in the mathematical analysis of structural vibrations based on experimen-

tal data. The report includes a summary of research by the author as well as abstracts of technical reports and papers presented at meetings or otherwise published.

One of the main research topics is the modeling of vibrational modes using several independently acquired columns of experimental frequency-response data. Another is the modeling of vibrational modes using multipoint excitation. A third main topic is component-mode-synthesis modeling, the goal of which is to refine the modal testing of components to such a degree that the relevant experimental parameters of the components are sufficient for use in synthesizing a mathematical model of the complete structure.

The report contains abstracts of the following papers:

- "Modal Analysis Using a Fourier Analyzer, Curve-Fitting, and Modal Tuning";
- "Modal Vector Estimation for Closely-Spaced Frequency Modes";
- "A Generalized Multiple-Input, Multiple-Output Modal Parameter Estimation Algorithm";
- "Application and Experimental Determination of Substructure Coupling for Damped Structural Systems";
- "A Generalized Substructure Coupling Procedure for Damped Systems"; and
- "A Substructure Coupling Procedure Applicable to General Linear Time-Invariant Dynamic Systems."

The author derives some conclusions from these studies: The modal-tuning procedures of the first two mentioned papers enable the determination of the undamped modes and frequencies of a system from the combination of modal data based on single-shaker frequency-response functions. The generalized multiple-input/multiple-output algorithm employs response data from several transducers, permits excitation at several points and of several types, and is capable of accurately identifying modal parameters from noisy data. The generalized substructural coupling method shows promise, and an effort should be made to determine the experimental procedures that will give the input data required by this method.

This work was done by Roy R. Craig, Jr., of the Bureau of Engineering Research for **Marshall Space Flight Center**. *To obtain a copy of the report, "Multi-shaker Modal Testing," Circle 5 on the TSP Request Card.*
MFS-27052

Are you reading someone else's copy of *NASA Tech Briefs*?

Qualified engineers and other new product development personnel can receive their own personal copy of *NASA Tech Briefs* by checking the subscription box and filling in one of the bound-in cards.

Rocket-Booster Towing Simulation

Techniques may also apply to buoy or ship design.

A report describes a computer simulation of the motion of a solid-rocket booster being towed behind a recovery ship. A listing of the simulation program in FORTRAN and references to the mathematical literature are included. Some of the mathematical techniques could be useful in such other maritime applications as buoy or ship design.

The simulation was undertaken to determine whether there were particular wave conditions under which the booster would fill with water and sink. The booster, approximately a long, hollow cylinder, has an opening to the sea through a large nozzle at the rear end.

In the simulation, the booster is treated as a rigid body, the motion of which is confined to the vertical plane that includes the towing cable. Therefore, the analysis is confined to the three degrees of freedom corresponding to surge (horizontal forward and backward), heave (vertical), and pitch (rocking) motions. The remaining three degrees of freedom, corresponding to roll, yaw, and sway motions, were found in model tests and actual towing not to be significantly excited and are therefore omitted from the calculations.

The basic equations to be solved are treated as a set of rigid-body differential equations. The force terms due to towing, drag, waves, and the sloshing of the water inside are added and the resulting equations solved repeatedly at a series of time increments for the three coordinate velocities using Cramer's rule. The equations are nonlinear in the velocity, but by using small time steps, the effects of nonlinearity are minimized. Time derivatives are treated by linear approximations from step to step. The procedure was found to be computationally stable for time steps up to 0.2 second.

The inertial matrix appearing in the equations accounts for the mass and moment of inertia of the booster, the mass distribution of the water inside, and an added mass of external water dragged along by the towing motion. The force and inertial terms due to the water inside are approximated by considering the sloshing as a one-dimensional, open-channel, frictionless flow along the booster axis. This flow is defined in terms of the axial velocity of the water and the local cross-sectional area that the water fills in a plane perpendicular to the axis. Due to the motion of the booster, this coordinate system is noninertial. The motion is not a "given," like the forcing function of the external waves, but must be calculated, in effect increasing the number of degrees of freedom of the system.

The dominant force acting on the booster is that of the ocean waves. The shapes, velocities, and forces of these waves are represented by trochoidal-wave theory. The alterations of subsurface pressure gradients by wave motions are considered in calculating buoyancy. The booster is pretended not to alter the shape of the waves nor the pressure gradients in the waves. The elasticity of the towing cable is considered in calculating the towing force. The various drag forces are treated separately and summed.

The calculations reveal no combination of conditions in which the booster would sink. It was found, however, that under severe wave and towing conditions, the towing cable could break. In that case, the booster would partially fill with water and rotate from the nearly-horizontal towing orientation to a vertical orientation.

This work was done by Thomas A. Trovillion of Planning Research Corp. for **Kennedy Space Center.** *To obtain a copy of the report, Circle 19 on the TSP Request Card.*
KSC-11289

Machinery

Hardware, Techniques, and Processes

126 Simulating Pressure Effects of High-Flow Volumes
127 Low-Loss Fuel and Oxidizer Injector
128 Continuously Variable Transmission
129 Spill-Detector-and-Shutoff Device
130 Reciprocating Magnetic Refrigerator
131 Flushing Ring for EDM
131 Back-Pressure Regulator for Large Gas Flows
132 Air Bearing for Small Planar Vibrations
133 Quasi-Porous Plug With Vortex Chamber
134 Hinged-Blade, Vertical-Shaft Windmill
137 Fastening Parts Having Mismatched Thermal Coefficients
138 Performance Improvement for Nonaxisymmetric Nozzles
139 Automatic Erection System for Antenna Masts
140 Long-Life Cryogenic Cooler
141 Mechanical Mixer for Rudder/Braking Wedge
141 Wide-Grasp Latching Mechanism
142 Cutthrough Warning Circuit

Books and Reports

143 Remotely Piloted Aircraft for Research
143 Sensitivities of Soap Solutions in Leak Detection

Simulating Pressure Effects of High-Flow Volumes

Dynamic test stresses are realized without high-volume pumps.

Marshall Space Flight Center, Alabama

A large flow passage may be tested at high pressure with the aid of a mandrel contoured to simulate the local pressures exerted during actual use. Realistic dynamic tests can thus be conducted without the need for a high-volume pump.

For rocket-combustion-chamber testing, the mandrel is shaped to provide a changing cross-sectional area for flow (see figure). It gradually constricts the flow as it approaches the throat of the chamber, thus increasing the pressure upstream relative to that downstream according to the profile that would prevail during operation. Aft of the throat, the mandrel diffuses the flow so that pressure drops rapidly as it would during firing.

Impractically large and costly pumps are made unnecessary. At the same time, stresses are generated that would not be imposed by static testing.

This work was done by M. S. Kaufman of Rockwell International Corp. for **Marshall Space Flight Center.** *No further documentation is available.*

Inquires concerning rights for the commercial use of this invention should be addressed to the Patent Counsel, Marshall Space Flight Center [see page 29]. *Refer to MFS-19909.*

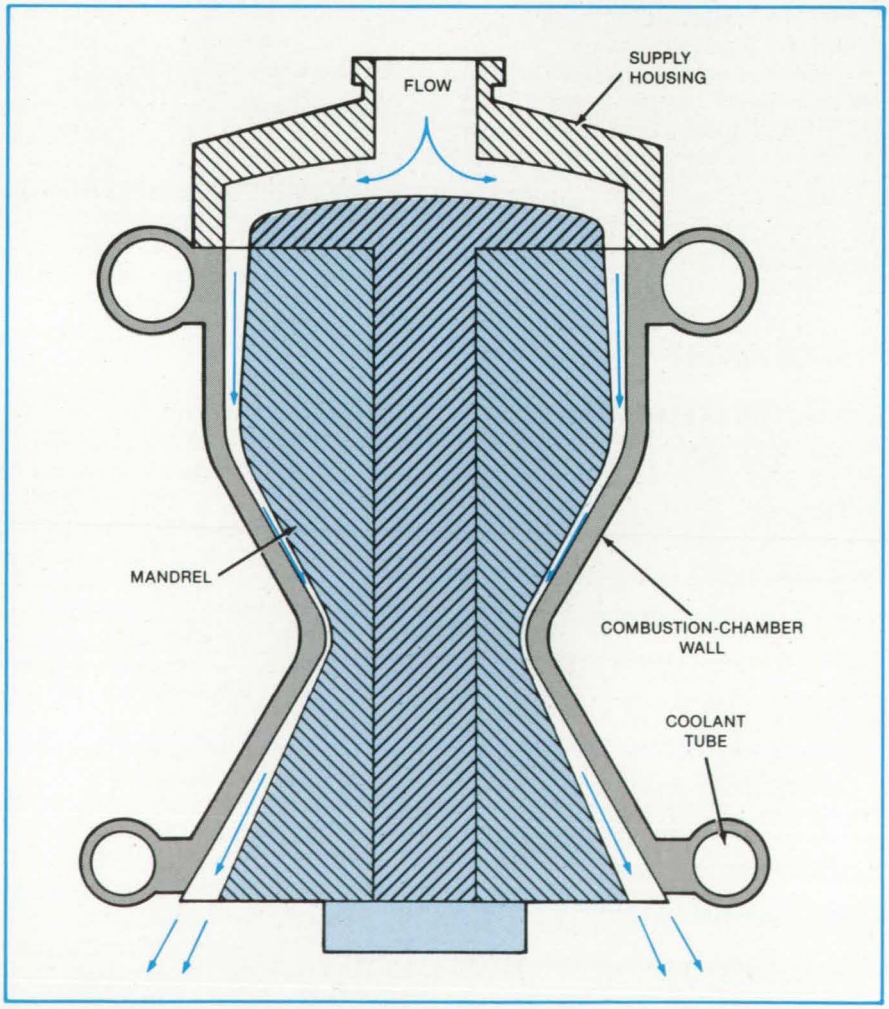

Assembled in Sections in a gas-flow passage, a contoured mandrel restricts the flow rate to a valve convenient for testing and spatially varies the pressure on the passage walls to simulate the operating-pressure profile. Realistic test pressures are thereby achieved without extremely high flow volumes.

Low-Loss Fuel and Oxidizer Injector

Pressure losses may be reduced without degrading combustion stability.

Marshall Space Flight Center, Alabama

A proposed injector for a rocket engine would inject fuel and oxidizer into the combustion chamber with lower pressure loss while maintaining stable combustion. Ordinarily, the stabilization of a combustion process requires a high pressure loss in the injector and its feed lines so that flow fluctuations are kept low even when the pressure oscillates. However, high pressure losses are uneconomical because they limit engine thrust, which in turn limits the weight of the payload.

The low-loss injector consists of an array of posts, each composed of a concentric shroud, separator, and plug (see figure). Fuel in the form of hot gas is fed through the space between posts and enters an annular cavity around the separator through holes in the shroud. Oxygen is fed through a central tube in the post and enters an annular cavity between the separator and plug through holes in the central plug wall. Fuel and oxygen emerge from their respective cavities at the tip of the post, where they burn. A small amount of oxygen leaks through an orifice at the tip of the plug to cool it.

The inside and outside surfaces of the separator are both rough to induce downstream turbulence to enhance mixing of the fuel and oxidizer. Pockets etched into the inner and outer surfaces of the separator further induce turbulence and damp flow fluctuations. As a result of these provisions, the flow into the combustion chamber should be well mixed and steady, and combustion should be stable.

The diameter of the posts is considerably larger than that in previous injectors. The fuel and oxygen outlets, therefore, have a relatively large area. Transverse acoustic waves should be readily attenuated, and the exposed area of the primary faceplate is minimized. At the same time, the larger size of the outlets reduces the pressure drop. The larger diameter makes the post stronger, reduces bending and vibration stresses, relaxes dimensional tolerances, and reduces the number of posts required.

The injector is designed for improved assembly and maintenance. The posts are accessible from the primary combustion chamber side and can be changed for flow adjustment.

This work was done by George Livon Pragemau of **Marshall Space Flight Center.** *For further information, Circle 41 on the TSP Request Card.*

Inquires concerning rights for the commercial use of this invention should be addressed to the Patent Counsel, Marshall Space Flight Center *[see page 29].* *Refer to MFS-25989.*

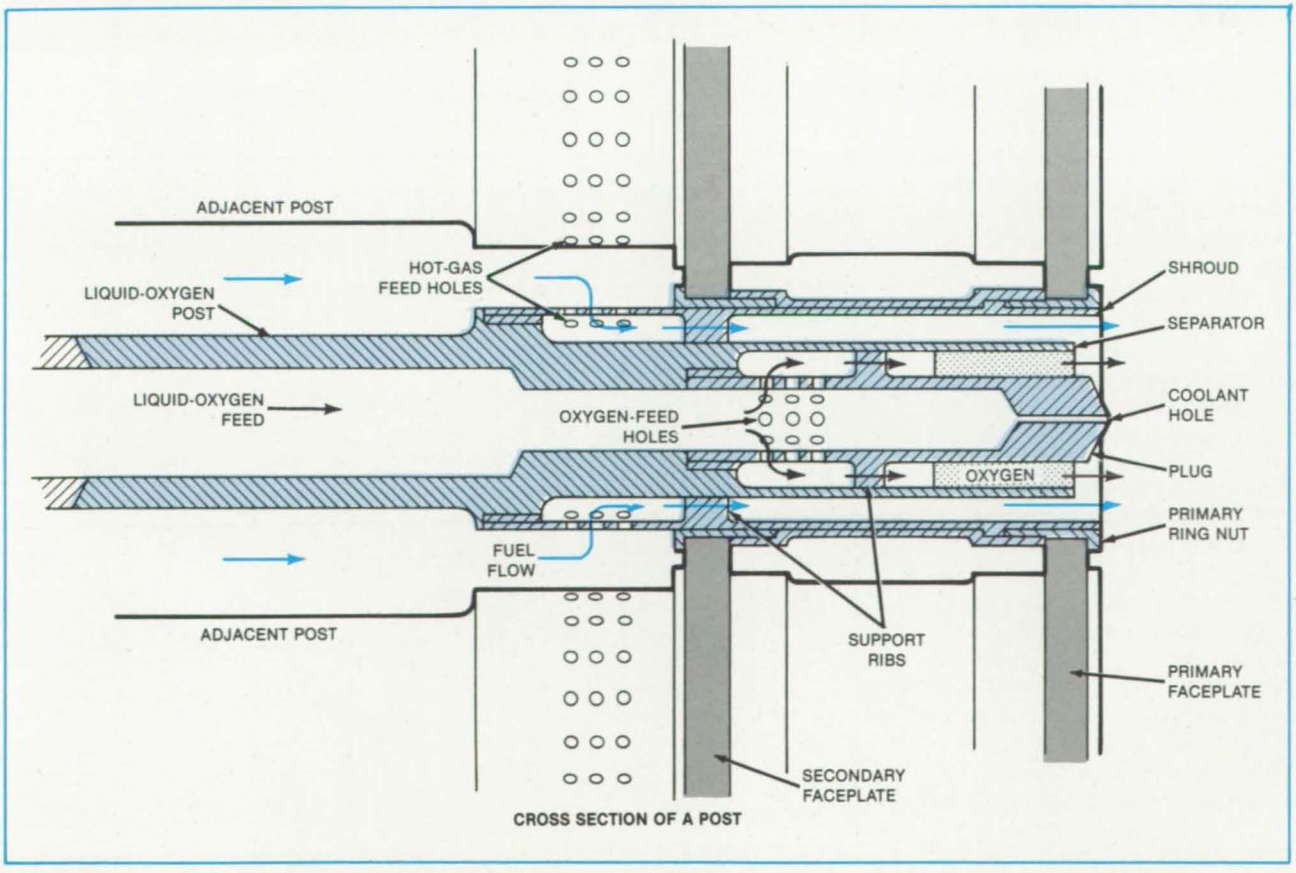

Injection Posts form a forest in the cavity between the oxygen manifold and the secondary faceplate. This cavity is the fuel manifold; fuel floods the post forest and enters each post through side holes in the shroud.

Continuously Variable Transmission

A chain slides along two cones, in a novel transmission concept.

Langley Research Center, Hampton, Virginia

A transmission proposed at Langley Research Center includes a chain drive between two splined shafts. The chain sprockets follow the surfaces of two cones. As one chain sprocket moves toward the smaller diameter, the other chain sprocket moves toward the larger diameter, thereby changing the "gear" ratio. The movement is initiated by tension applied to the chain by a planetary gear mechanism.

The speed ratio between drive and driven shafts is a function of the position of the chain with respect to the conical surfaces. For example, if the plane of rotation of the chain is at the end of the axes of the cones, as shown in Figure 1, then the speed ratio (output speed/input speed) is at its minimum value. However, if the chain is positioned at the opposite ends of the cone axes, the speed ratio between the shafts is at its maximum.

Positioning the chain along the surfaces of the cones is accomplished by the movement of the hubs along the splined inner shafts of the cones. This movement of the hubs is transmitted to the chain through gear trains that move up or down cogs that radiate from the hubs. Movement of the gear assembly up and down the cogs, as shown in Figure 2, causes a simultaneous rotation of the pinion on the rack. This rotation of the pinion produces a rotation of the worm, which in turn causes a rotation of the worm wheel and chain sprocket. Thus, the rotation of the chain sprocket is synchronized with the change in circumference of the chain so that a constant tension is maintained in the chain as the chain and gear assembly move parallel to the cone surface.

Previous devices such as spur gears, belt and chain-link drives, and conventional hydraulic and mechanical automobile transmissions do not provide a simple, compact, or efficient method for continuously varying the speed ratio between driving and driven components. This device is positive, simple, and efficient over a wide range of speed ratios.

This work was done by David C. Grana of **Langley Research Center.** *No further documentation is available.*
LAR-12844

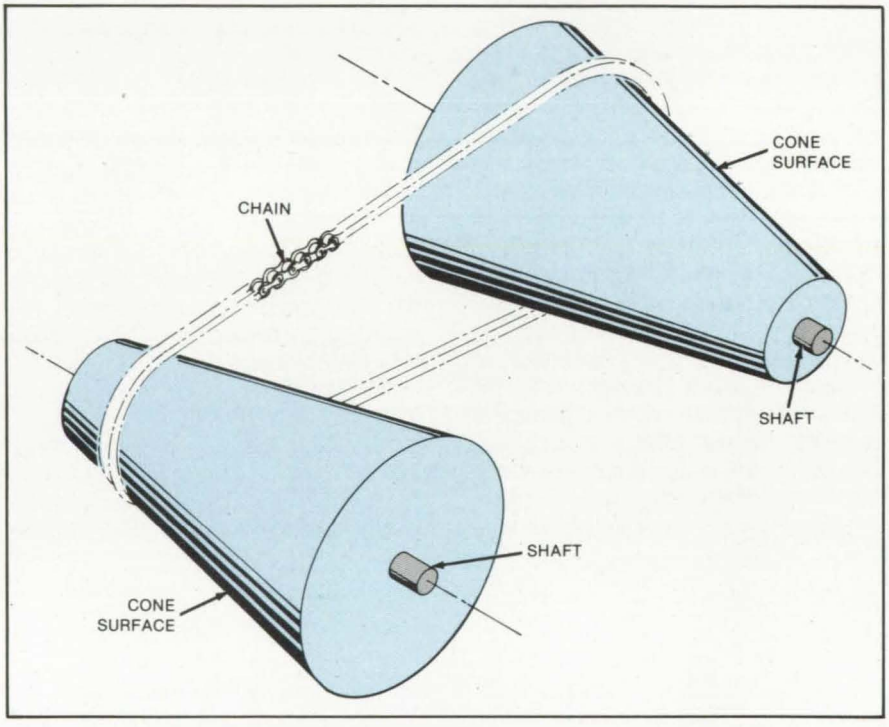

Figure 1. **The Speed Ratio** between driving and driven shafts is a function of the position of the chain with respect to the conical surfaces.

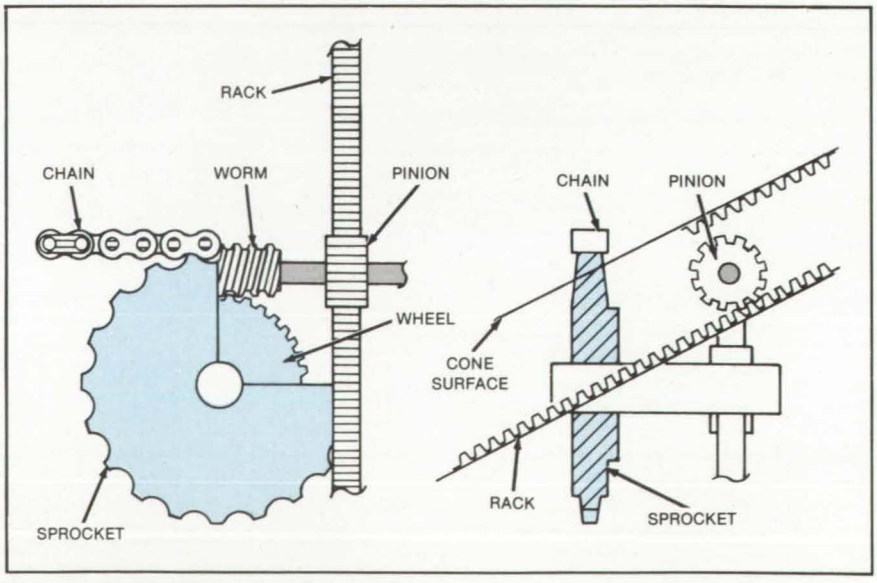

Figure 2. **Movement of the Gear Assembly** up and down the cogs causes a simultaneous rotation of the pinion on the rack.

Spill-Detector-and-Shutoff Device

Overflow in liquid chromatography systems is rapidly detected and stopped.

Lyndon B. Johnson Space Center, Houston, Texas

The system shown in the figure minimizes the amount of liquid spilled from a liquid-chromatography system. It can also be adapted to other systems that transfer electrically conductive liquids.

During normal operation, liquid is pumped through a pliable tube into the chemical-component detector of the chromatography apparatus (see figure). The detector sends signals to the fractionator, which rotates sample tubes into position under the liquid-output nozzle to receive the liquid fractions. If a sample tube overflows or if a malfunction prevents the placement of a tube under the nozzle, the liquid will spill onto the liquid sensor that is placed under the tubeholder.

The liquid sensor consists of two sets of interdigitated wires, each set of wires being electrically connected together and electrically insulated from the other set by insulating spacers. A small voltage is applied between the two sets. When a conductive liquid is present, current flows between the sets. This current is amplified; and the amplified, inverted signal is used to trip a set of relays. One relay then shuts off power to the pump and solenoid while the other relay turns on an audible or visible alarm.

When the power is on, the plunger is held by the solenoid against the spring. When the relays trip and the power goes off, the plunger is released, allowing the spring to force the plunger to the left, thereby pinching the pliable tube between the plunger and the anvil. This shuts off the liquid passage, thus saving the liquid that is already in the tube on the way to the detection and fractionation subsystems.

The power relay for the pump and solenoid is of the normally-off, self-holding-on type, so that once the system shuts off, it must be reset manually with a momentary-contact button switch. This insures against accidental turn-on after a power failure and helps to remind the operator to make nec-

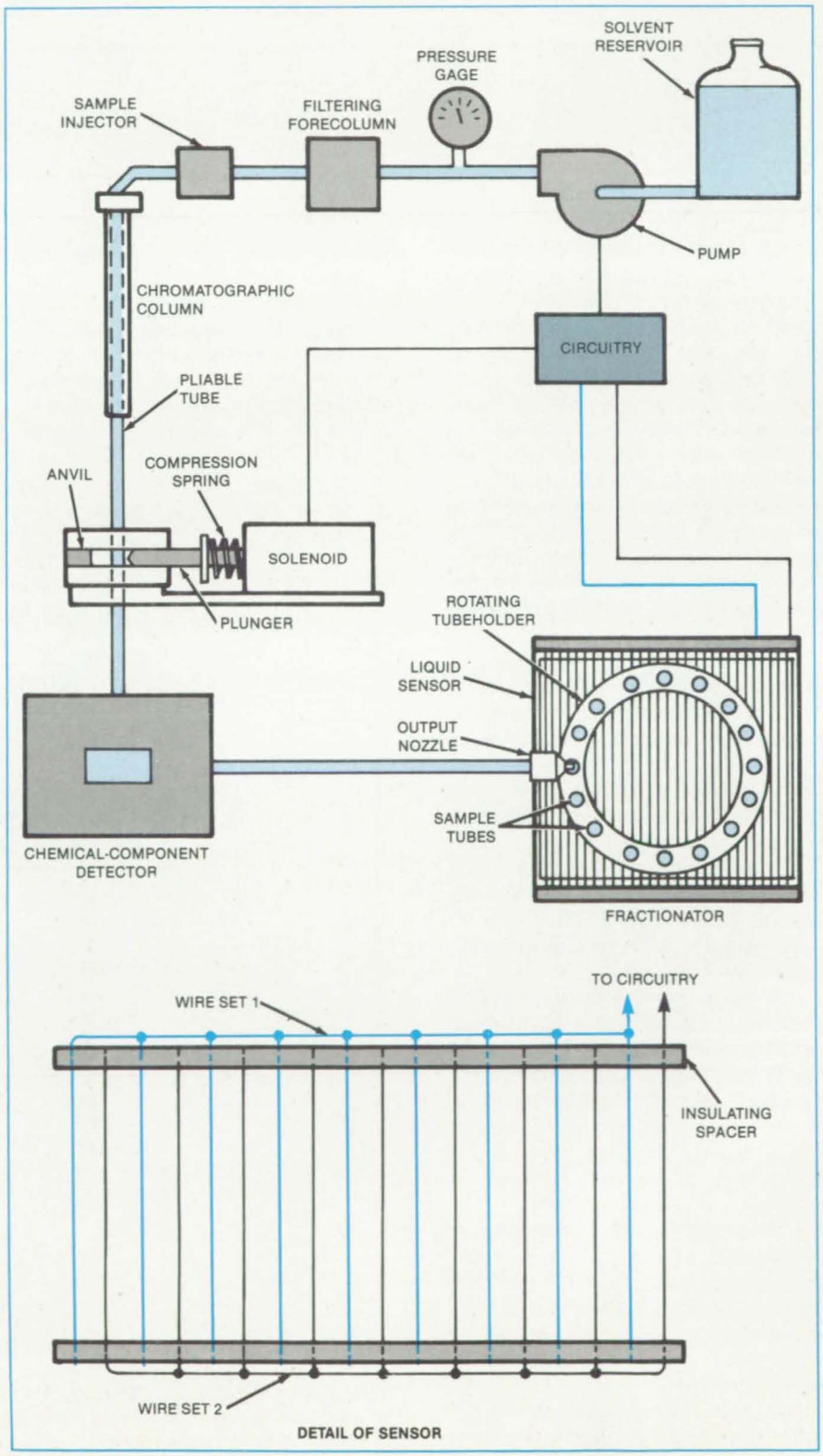

The **Spill-Detector-and-Shutoff Device** is incorporated into a liquid-chromatography system. When liquid from the output nozzle spills on the liquid sensor, the device automatically shuts off the pump and releases the solenoid to pinch off the flow in the tube. The device uses a common type of alarm circuit that must be reset manually before normal operation can resume.

essary repairs or adjustments before resuming normal operation.

This work was done by Michael R. Jarvis and Donald S. Fulton of the University of Illinois for **Johnson Space Center.**

For further information, Circle 35 on the TSP Request Card.

This invention is owned by NASA, and a patent application has been filed. Inquiries concerning nonexclusive or exclusive license for its commercial development should be addressed to the Patent Counsel, Johnson Space Center [see page 29]. Refer to MSC-20206.

Reciprocating Magnetic Refrigerator

Unit cools to 4 K by adiabatic demagnetization.

NASA's Jet Propulsion Laboratory, Pasadena, California

A reciprocating closed-cycle refrigerator cools objects to 4 K, exhausting the heat to another refrigerator at 15 K. Unlike earlier designs, this magnetic refrigerator provides continuous rather than "one-shot" cooling.

The figure shows the refrigerator in simplified form. Two porous matrices of the paramagnetic material gadolinium/gallium/garnet are held in a long piston called the displacer, which is machined out of Micarta (a phenol formaldehyde polymer). Holes in the side of the displacer allow the heat-exchange fluid to flow to and through the matrices within. Piston seals on the displacer prevent substantial mixing of the fluid in the two loops.

The heat-exchange fluid is helium gas and is circulated in two loops by reciprocating, linear-displacement, magnetically driven pumps. The displacer is slowly reciprocated along the axis of the stainless-steel cylinder, thereby alternately placing one matrix and then the other in the field of a superconducting magnet. The magnetically soft material surrounding the magnet helps to confine the magnetic field so that the displacer stroke required to bring each matrix into and out of the field will be as short as possible.

As the displacer moves to one end of the stroke, the matrix that was in the magnetic field in the "warm" (15 K) loop moves out of the magnetic field and away from the warm-loop circulation port. Thus thermally isolated, the matrix cools as it demagnetizes. (This is the adiabatic cooling step and is analogous to the adiabatic expansion of conventional refrigeration cycles.)

At the end of the stroke, the matrix is in the cold-loop circulation port. The helium gas is then pumped around the cold loop, absorbing heat from the stage that is to be cooled and transferring the heat to the matrix, which has been cooled by adiabatic demagnetization.

Meanwhile, the matrix that was in the "cold" loop moves to the center of the magnet. The matrix is thermally isolated as it moves into the magnetic field and warms as the matrix becomes magnetized. (This is analogous to the compression step in conventional refrigeration.) At the end of the stroke, the heat the matrix carried along from the cold loop is removed by the flowing helium in the "warm" loop and is transferred to the stage at 15 K.

This work was done by Dean L. Johnson of Caltech for **NASA's Jet Propulsion Laboratory.** *For further information, Circle 47 on the TSP Request Card.*

NPO-16257

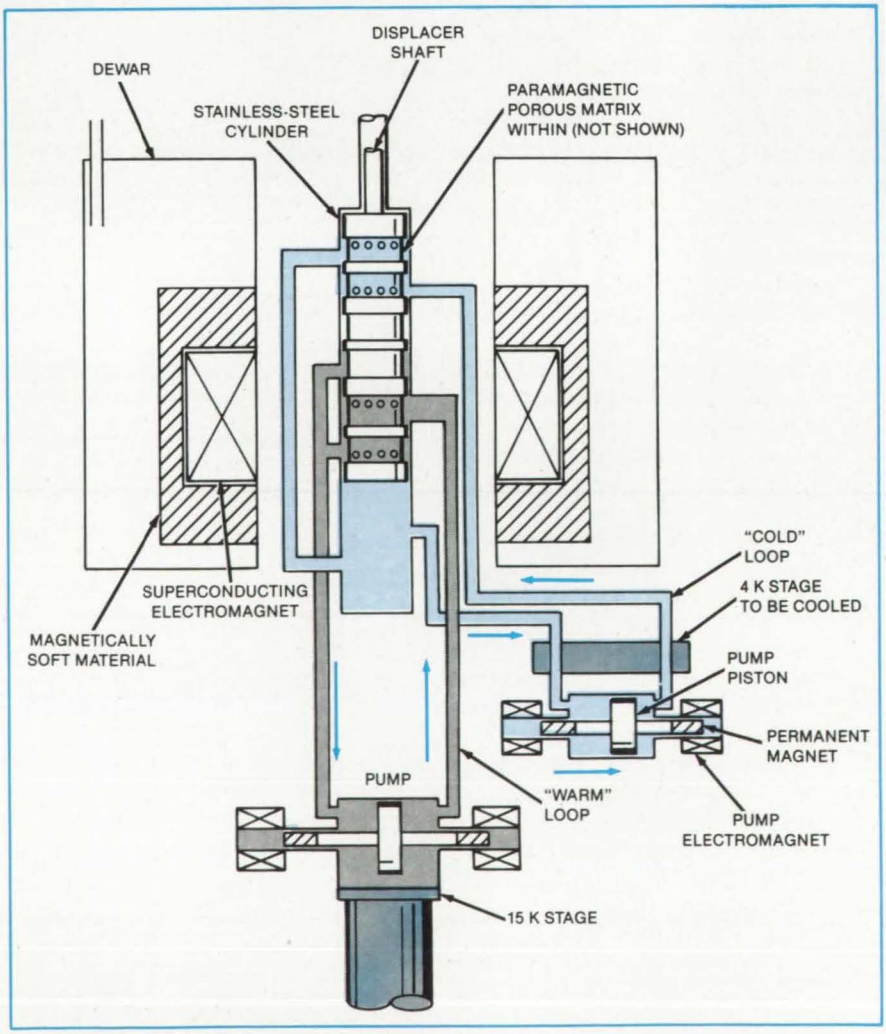

The **Reciprocating Magnetic Refrigerator** is depicted here at the upper end of the stroke. The lower matrix in the 15 K loop will subsequently be cooled by adiabatic demagnetization during the downward stroke.

Flushing Ring for EDM

Removing debris more quickly lowers the cutting time.

Marshall Space Flight Center, Alabama

The speed of electrical-discharge machining (EDM) was increased in a NASA application by increasing the flushing rate at the cutting face. Reductions in machining time of up to 30 percent are possible.

The flushing problem arose in an EDM application in which 600 fuel-injector posts had to be cut on a plate. Originally, the cutting rate was reduced by debris on the workpiece.

To remove the debris, an oil agitator was constructed. Tubing of 1/2-inch (1.27-centimeter) outside diameter was formed into a ring (see figure). Small holes were drilled in the tube facing the center of the ring, and inlets for air and oil were attached to the ring at diametrically opposite points.

In operation, cutting oil and pressurized air are supplied to the ring, which is placed around the workpiece. The air forces the oil through the small holes and agitates the oil as it flows over the workpiece. The high flow rate and agitation dislodge and remove debris. The electrical discharge can then remove material from the workpiece faster. One indication of the greater effectiveness was a jump in EDM current from 25 to 40 amperes when the flushing ring was installed.

This work was done by L. G. Earwood of Rockwell International Corp. for **Marshall Space Flight Center.** *No further documentation is available.*
MFS-19876

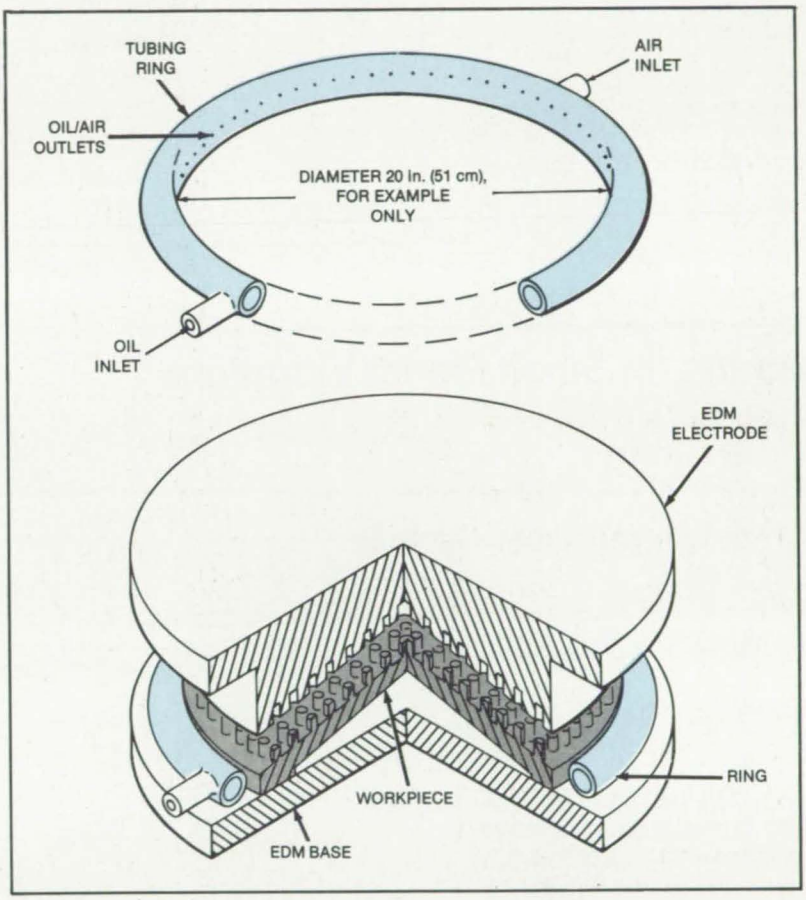

The **Flushing Ring** is placed around a workpiece for electrical-discharge machining. The flushing ring is inexpensive and easily fabricated.

Back-Pressure Regulator for Large Gas Flows

Cost is reduced, and safety is enhanced.

Lyndon B. Johnson Space Center, Houston, Texas

An automatic control system maintains a back pressure of a few psi in the gas flowing from a pipe about 8 in. (20 cm) in diameter. The system, which replaces a pneumatically actuated valve, makes it unnecessary for an operator to set a valve or flow restrictor. The principal applications of the system lie in environmental testing or production facilities requiring large gas flows at low pressures.

As shown in the figure, a conical throat plug partially blocks the flow of gas out of the end of the pipe, thus establishing the back pressure inside the pipe. This pressure is sensed by a commercially-available pressure-control unit and compared with a preset reference pressure.

The pressure-control unit takes gas from a gas supply and sends it at a reduced control pressure to a pneumatically-operated pressure-control actuator (also a com-

mercial unit). The control pressure varies in response to the sensed back pressure: This causes the actuator to change the axial position of the plug, thereby changing the amount of obstruction to flow and adjusting the back pressure to reduce the deviation from the desired value.

This work was done by Eugene A. Theodore and Floyd Chin of Rockwell International Corp. for **Johnson Space Center.** *For further information, Circle 20 on the TSP Request Card.*
MSC-20536

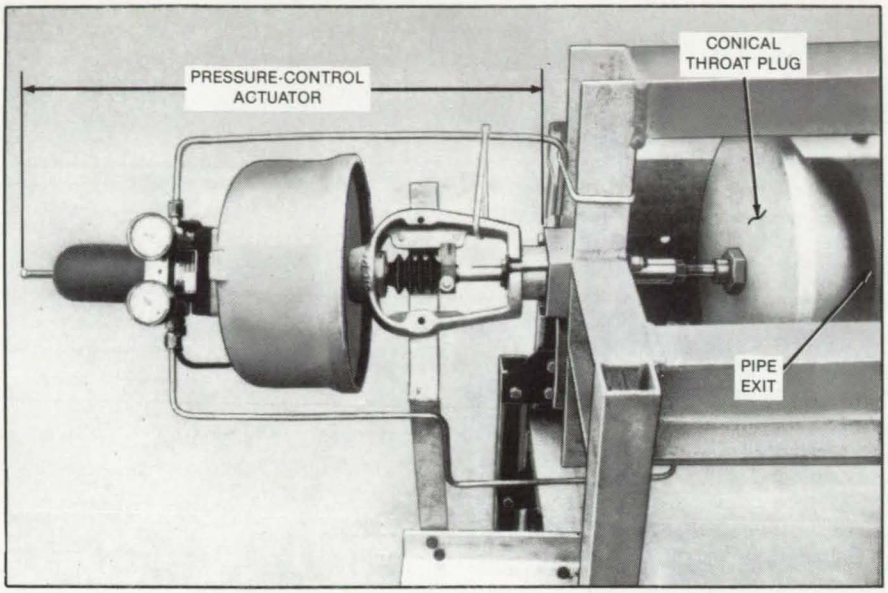

A **Pipe Exit is Partially Obstructed** by a conical throat plug. When the pressure in the pipe falls below (or rises above) the desired back pressure, the plug is automatically moved in (or out).

Air Bearing for Small Planar Vibrations

Air-cushion device provides vibrations along axes 90° apart.

Marshall Space Flight Center, Alabama

An air bearing allows small linear displacements in any direction in a horizontal plane as well as rotation about a vertical axis. It can support a large mass at the end of a long arm, yet it transmits no microphonic or other vibrations to the mass. The bearing was originally developed for stirring crystal-growth liquids in containers.

The bearing includes a movable slide (see figure) sandwiched between two fixed support plates. The separation between the plates is adjusted to standard air-bearing tolerances. Pressurized air is supplied to the slide so that it floats between the plates on a cushion of air. The air exhausts on the top and bottom surfaces of the three arms of the slide.

The object to be oscillated — a crucible in the case of crystal growth — is secured to the movable plate at the center. The crucible projects through a hole in the upper support plate. The crucible can be oscillated with a displacement of up to ±0.125 inch (±3.18 millimeters) at frequencies up to 100 hertz. The crucible can be supported at a distance of 1 meter or more from the oscillators.

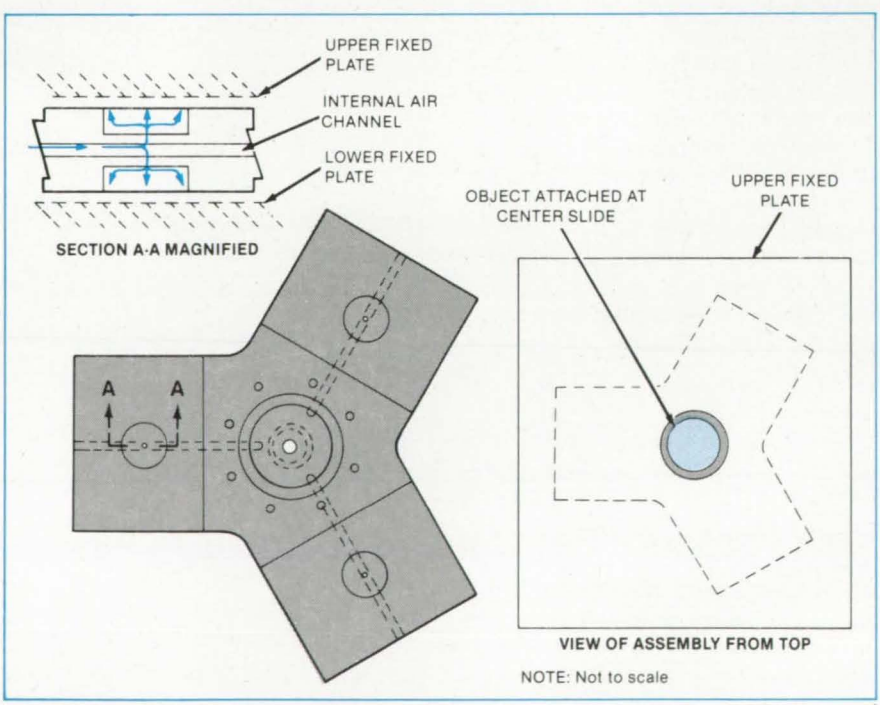

A **Y-Shaped Plate** supports an object to be oscillated linearly or rotationally in a plane. Pressurized air forms a cushion above and below the plate.

This work was done by Martin F. Wolf of Stanford University for **Marshall Space Flight Center.** *For further information, Circle 94 on the TSP Request Card.*

Inquires concerning rights for the commercial use of this invention should be addressed to the Patent Counsel, Marshall Space Flight Center [see page 29]. Refer to MFS-26003.

Quasi-Porous Plug With Vortex Chamber

Pressure letdown would be controllable.

NASA's Jet Propulsion Laboratory, Pasadena, California

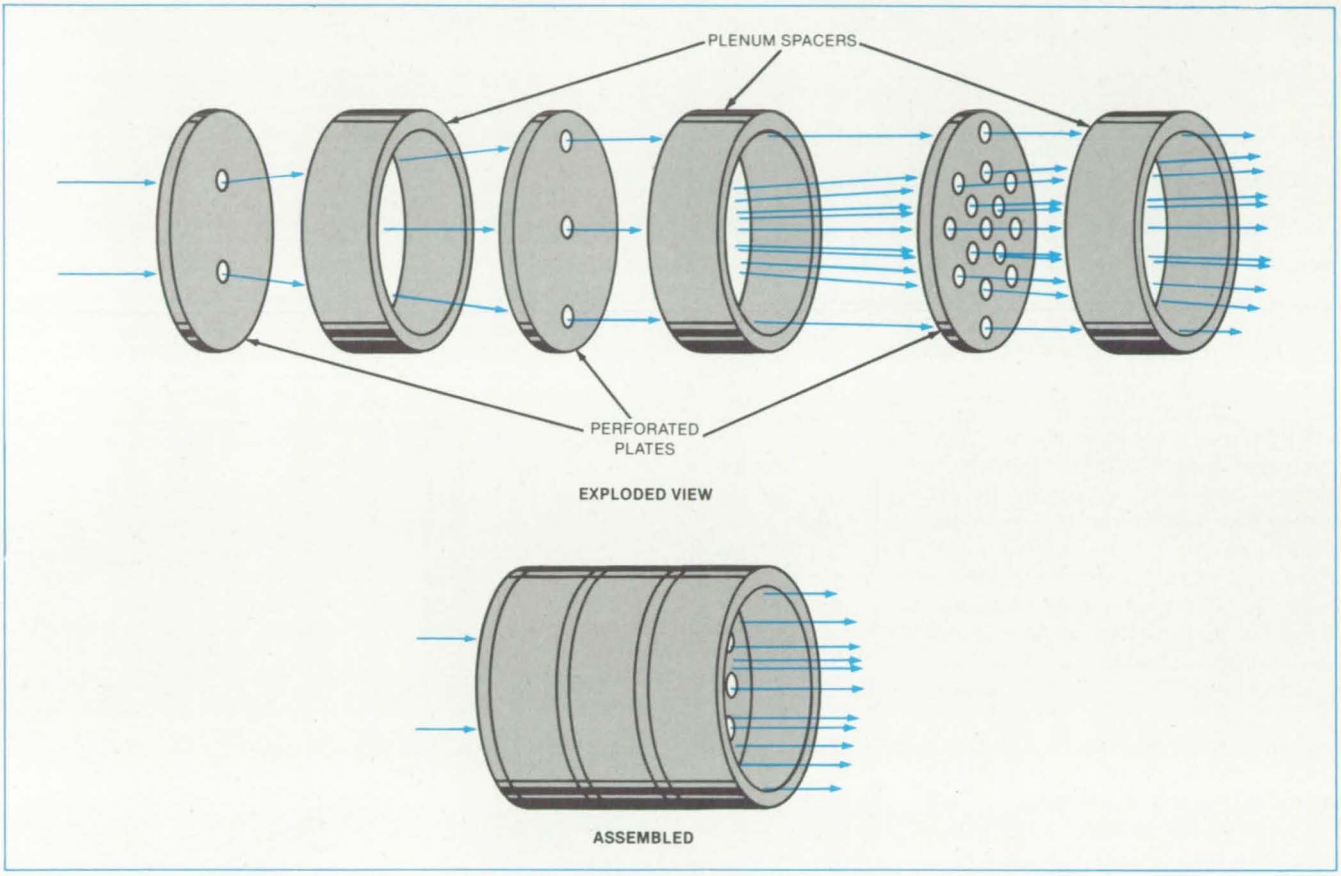

Figure 1. A **Quasi-Porous Plug** consists of plenums separated by perforated plates. The number or size of perforations increases with each succeeding stage to compensate for expansion.

A proposed pressure-letdown valve would combine a quasi-porous-plug and a vortex-chamber in one controllable unit. Such a valve would be useful in fossil-energy plants for reducing pressures in such erosive two-phase process streams as steam/water, coal slurries, or combustion gases with entrained particles.

The principle of the quasi-porous plug was discussed in "Pressure Reducer for Coal Gasifiers" (NPO-15100), *NASA Tech Briefs*, Vol. 7, No. 3, p. 322. This type of valve reduces the pressure of a fluid by allowing the fluid to expand through a series of plenums and perforated plates separating the plenums (see Figure 1).

To compensate for the increase in flow volume, the number and size of perforations increase with each stage so that the flow velocity and the consequent erosive effect of particles or droplets do not exceed the maximum allowable at any stage. For example, the plates may be designed so that the flow velocity through the per-

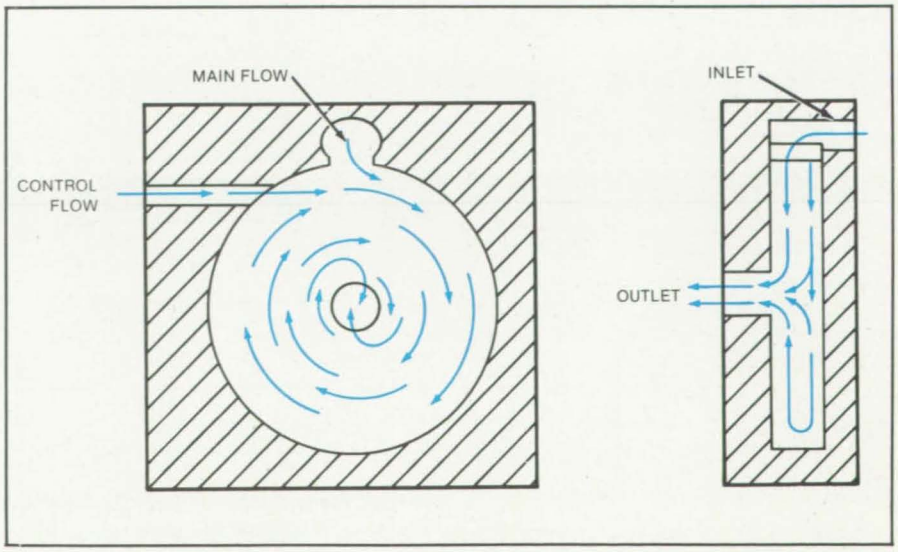

Figure 2. In a **Vortex Chamber**, the control flow can be varied to control the swirl and therefore the difference between inlet and outlet pressures.

forations is the same at all stages. In the case of two-phase evaporative flow (as with water flashing to steam), the designer must also consider the increase in flow volume due to the phase change.

In the new valve, the flow or pressure is not controlled by reducing the flow area as in conventional valves. Instead, the flow is controlled by generating a vortex to vary the back pressure in one of the plenums. As shown in Figure 2, the fluid flow to be controlled enters at the periphery and leaves at the center. An azimuthally-injected control flow creates a swirl, the centrifugal effect of which creates a radial pressure gradient. Thus, the pressure at the outlet is less than the pressure at the inlet. A turn-down ratio of 2:1 is obtainable in one such vortex stage; higher ratios are possible with multiple stages.

This work was done by John V. Walsh of Caltech for **NASA's Jet Propulsion Laboratory.** *For further information, Circle 22 on the TSP Request Card.*
NPO-16076

Hinged-Blade, Vertical-Shaft Windmill

The blade profile is reduced when moving against the wind.

Marshall Space Flight Center, Alabama

A vertical-shaft windmill concept calls for hinged, flapping blades to increase energy-conversion efficiency by reducing the wind-energy loss. When a blade is moving on the downwind half cycle, the wind pressure forces the blade halves to unfold from each other and present a larger cross section to the wind, thereby capturing more wind energy (see figure). When a blade is moving on the upwind half cycle, the wind folds the blade halves together, thereby reducing the cross section to wind and therefore the wind resistance.

Of course, the windmill design must be made resistant to the vibrations caused by the flapping of the blades. The sound of the flapping may also be a consideration.

This work was done by Bennie Shultz, Jr., of **Marshall Space Flight Center.** *No further documentation is available.*
MFS-25980

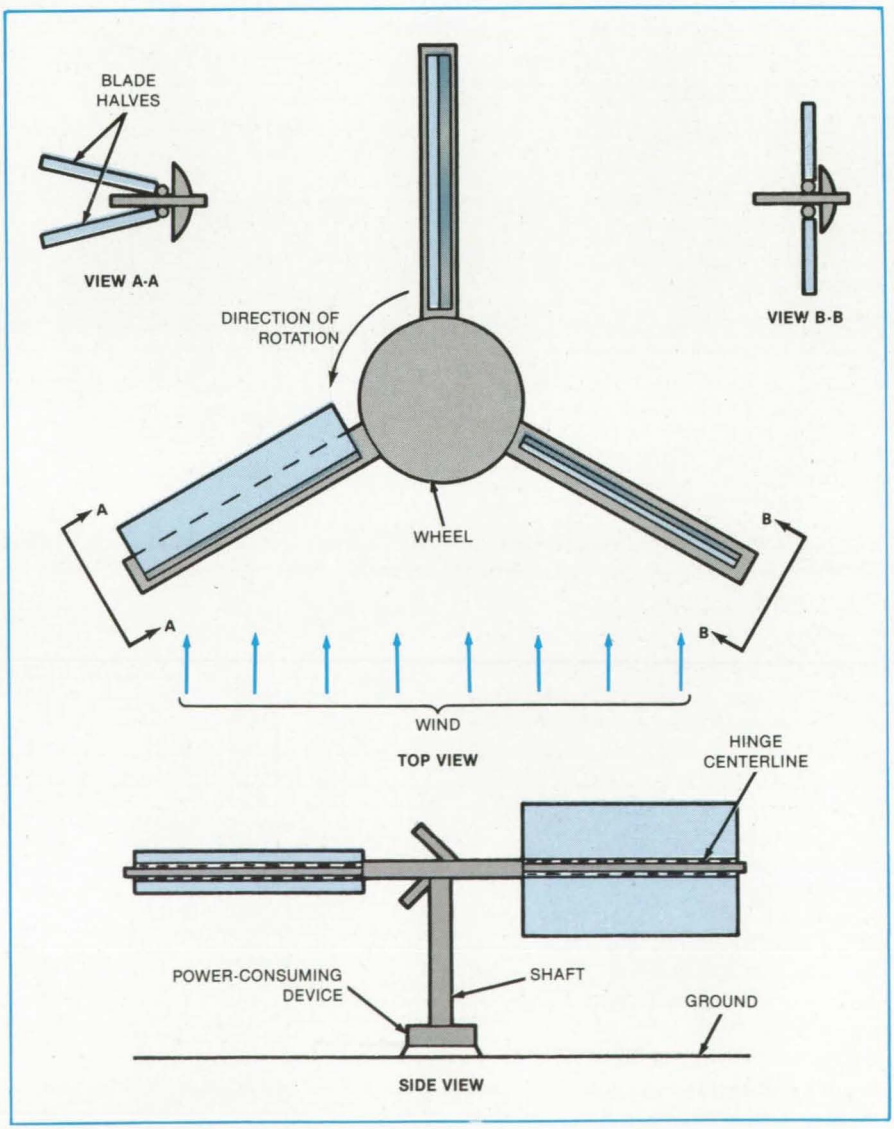

Hinged Blade Halves unfold to catch the wind when moving with it, then fold away from the wind when moving against it.

"Page missing from available version"

"Page missing from available version"

Fastening Parts Having Mismatched Thermal Coefficients

Fastener eliminates thermal stresses and maintains snug fit.

Langley Research Center, Hampton, Virginia

A fastener developed at Langley Research Center is used where the material to be fastened has a thermal-expansion coefficient very different from that of the fastener. Conventional metal fasteners require a snug-fitting shank to transmit shear effectively. When heated, the shank tends to expand considerably more than the hole in a material with a much lower coefficient of thermal expansion. Consequently, the material attempts to restrain the growth of the fastener, which is the source of large thermal stresses. Moreover, the clamping force of the fastener is lost at elevated temperature as the fastener grows in length more than the material being fastened increases in thickness.

This problem is solved through the application of conically-configured metal fasteners. There are only two restrictions on the use of conical fasteners. First, the theoretical apex of the cone(s) must reside within the boundaries of the material; and second, if the fastener employs a double conic, one for the "bolt" and one for the "nut," the theoretical apex of each must be coincident. Any cone angle may be employed, and either single or double conic may be used to configure bolts or rivets in either accessible or blind applications.

A snug fit exists between the parts being joined and the fastener at all temperatures. The amount of bearing force, or snugness of fit, may be controlled by adjusting the torque on the fastener.

The DAZE [Differential-Alpha, Zero-Strain (ε)] metal fastener expands thermally without restraint by the material while simultaneously maintaining continuous contact over sufficient area to permit shear transmission through the joint at an acceptable bearing stress in the material. The fastener (see figure) consists of conical heads that have coincident vertexes and mate with countersunk holes in the material. As the joint is heated, the metal expands radially from the point of coincident vertexes. Where the metal fastener contacts the material, the snug-fitting conical heads slide without interference. Since the fastener is free to expand, no thermal stress is produced in either the fastener or the material.

The DAZE fastener can be modified to meet different fastening configurations.

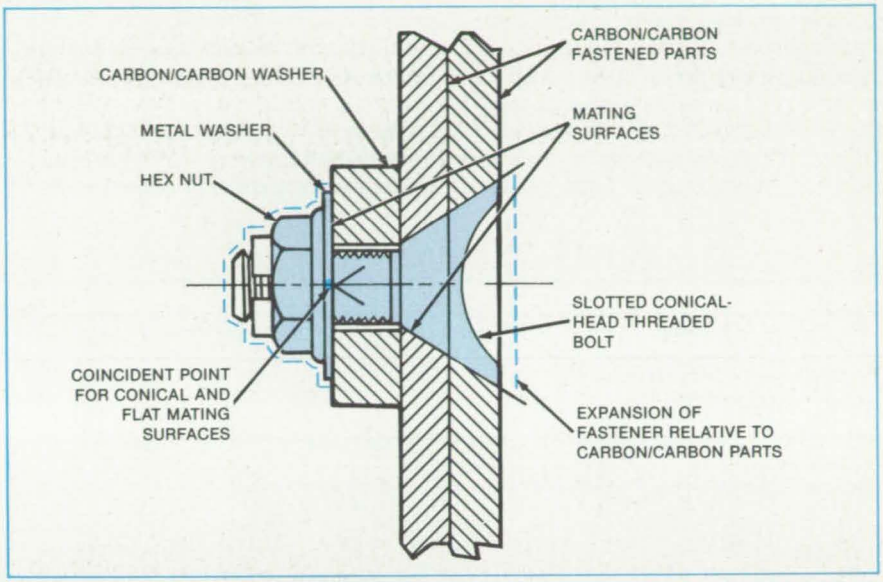

A **Conical-Head Bolt and Metal Washer** are the main components of the fastener that keeps constant tension on the carbon/carbon parts regardless of thermal stress. This fastener, also shown in the photograph on the bottom, is used in cases where the fastened parts have unmatched thermal-expansion coefficients. It does not become looser or tighter as conventional bolts and nuts or rivets do at elevated temperatures.

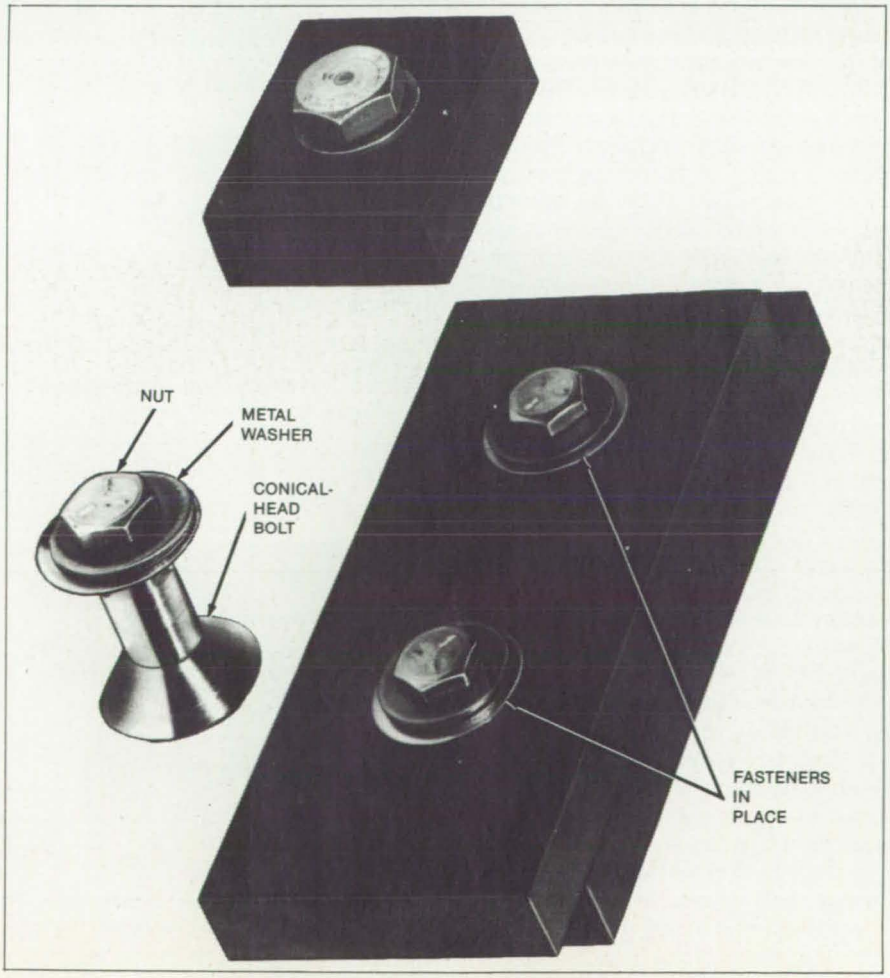

For example, threaded inserts can be made when access to only one side of a structure is available. Bushings used to distribute the load from a pin or shaft can be customized to produce acceptable bearing stresses in the joined members. The basic characteristic of all DAZE fasteners, inserts, and bushings is the coincident vertexes of the surfaces that contact mating surfaces of the structure. These contacting and mating surfaces can be cones, pyramids, disks, or their combinations.

Metals and some varieties of carbon/carbon (three-dimensional weave) have the same coefficient of thermal expansion in all directions, but some carbon/carbon materials (two-dimensional cloth layups) have a greater coefficient of thermal expansion through the thickness of the sheet than in the plane of the sheet. When the through-the-thickness coefficient of thermal expansion is not much greater than that in the plane, the thermal stresses using basic DAZE fasteners will be low. Alternative configuration of DAZE fasteners, however, have been designed for use with nonisotropic materials where these differences are large. These configurations employ either an offset between vertexes or curved mating surfaces.

This work was done by L. Robert Jackson, Randall C. Davis, Allan H. Taylor, Robert R. McWithey, and Max L. Blosser of **Langley Research Center.** *For further information, Circle 86 on the TSP Request Card.*

This invention is owned by NASA, and a patent application has been filed. Inquiries concerning nonexclusive or exclusive license for its commercial development should be addressed to the Patent Counsel, Langley Research Center [see page 29]. Refer to LAR-13009.

Performance Improvement for Nonaxisymmetric Nozzles

Internal flow separation is eliminated during reverse thrust.

Langley Research Center, Hampton, Virginia

The rotating-drum thrust reverser and boundary-layer control device improves the performance of nonaxisymmetric nozzles in three ways: (1) It controls the thrust-reverser exhaust port area by elimination of internal flow separation in the reverser exhaust port; (2) it provides control of reverse-thrust flow direction (exhaust angle); and (3) it eliminates external flow separation over the nozzle boattail. Current nonaxisymmetric-nozzle thrust-reverser designs are either of the integral nozzle/reverser type or the cascade (upstream) type and have exhibited, among other limitations, a significant detrimental effect of thrust-reverser operation on nozzle discharge coefficient, or the ratio of actual mass flow to ideal mass flow. The new device eliminates the large variations in nozzle discharge coefficient and provides additional benefits to jet-engine thrust operation during cruise and reverse-thrust modes.

The major components of the device are two rotating drums (one on top and one on the bottom), mounted spanwise across the nonaxisymmetric nozzle (see figures). During the cruise operating mode, the drums rotate such that the exposed outside surfaces of the drums move in the direction of the external flow. At the same time, bleed slots direct high-pressure exhaust flow externally down the nonaxisymmetric nozzle boattail. During the reverse-thrust operating mode, the nozzle convergent and divergent flaps rotate to form the blocker and simultaneously open reverser exhaust ports on the nozzle upper and lower surfaces. In this mode, the rotating drums form the forward

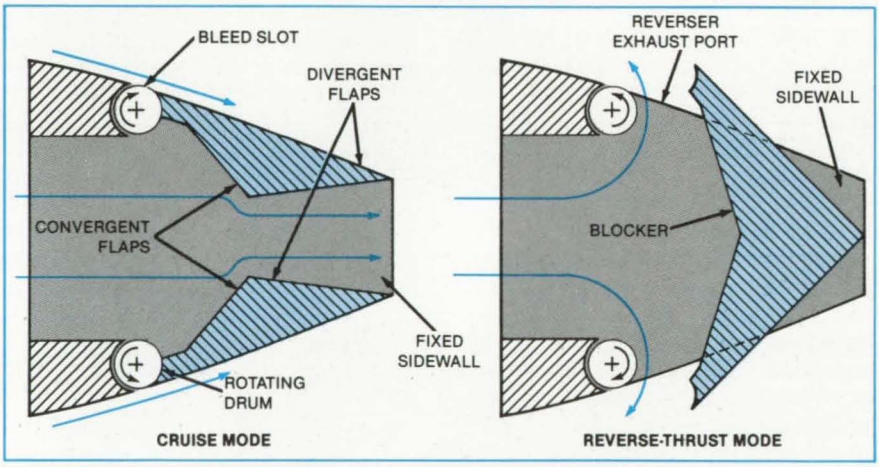

Figure 1. The **Convergent and Divergent Nozzle Flaps** rotate to form the reverser blocker for reverse-thrust operation (right).

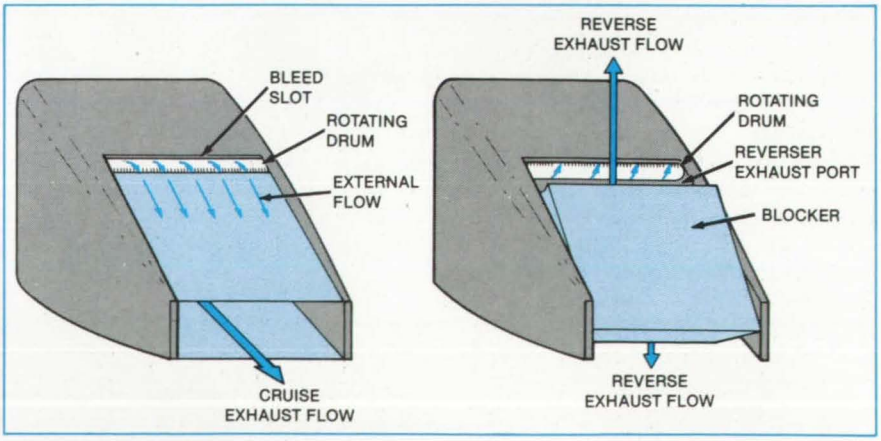

Figure 2. **During Cruise Operation**, the drums rotate in the direction of the external flow. During reverse-thrust operation, the drums rotate in the direction of the internal flow.

reverser exhaust-port surface and rotate in such a direction that the inside surface of each drum moves in the same direction as the internal flow.

By use of the rotating drums, internal flow separation at the reverser-port entrance lip is eliminated, and large variations in discharge coefficient are avoided when the operating mode changes from cruise to reverse thrust. By controlling the discharge coefficient, engine stalls during reverse-thrust operation can be avoided, the need for additional port-area control can be eliminated, and nozzle weight and complexity can be reduced.

The same rotating drums can be used to provide a variable reverse-flow exit angle, and thus reverse-thrust magnitude, when the blocker is deployed. This reverse-thrust modulation is obtained by varying the rotational speed of the drums, with reverse-flow angle and reverse-thrust magnitude increasing as a function of the increasing rotational speed of the drums. Different rotational speeds of the upper and lower drums would result in unequal amounts of reverse thrust from the upper and lower ports and would provide a normal force and pitching moment that could be useful for airplane control augmentation during low-dynamic-pressure flight regimes such as in landing.

The rotating drums, whether used alone or in conjunction with the bleed slots, energize the nozzle boattail boundary layer and delay external flow separation on the nozzle boattail, thus reducing nozzle drag. This effect would permit nozzle designs of shorter length with steeper boattail angles. Such nozzles would be of lighter weight than current nozzles having similar levels of nozzle drag.

In addition to the configuration shown in the figure, this device would work equally well on multiengine installations with other nozzle or reverser designs and with reverser ports located on all four sides of the nozzle. Also, if control of the reverser exhaust angle is not required, a fixed drum rotation speed could be used for control of internal flow separation and discharge coefficient during reverse-thrust operation. If control of the external boundary layer is not required, the bleed slots could be eliminated.

This work was done by Bobby L. Berrier of **Langley Research Center.** *No further documentation is available.*

Inquiries concerning rights for the commercial use of this invention should be addressed to the Patent Counsel, Langley Research Center [see page 29]. Refer to LAR-13036.

Automatic Erection System for Antenna Masts

A telescoping mast does not require the payout of guy wires under tension.

Langley Research Center, Hampton, Virginia

A proposed mechanism for erecting and retracting an antenna mast is totally contained within the mast. Locking systems automatically secure the mast elements, allowing the guy wires to be tensioned after the element to which they are attached is extended and locked. Thus, only a relatively short length of the mast is unrestrained at any time during the erection process, and the guy wires do not have to be payed out while they are under tension.

The mast elements can be either tubular or open-truss. The new device is a separate component built into the stack of telescoping elements.

The figure shows the essential components of the mast and its erection system. A seven-element mast is shown, but the principle can be applied to a much larger number of elements [e.g., twenty 50-ft (15-m) elements for a 1,000-ft (305-m) mast]. The bottom element is rigidly connected to the base support, leaving six elements to be raised. If N is the total number of elements in the mast, there will always be N-1 elements to be raised.

The erection mechanism, or "erector column," is represented by the grey shaded area at the center of the stack of telescoping mast tubes shown in the figure. It contains four shuttles that move up and down the length of the erector column. These shuttles are guided by tracks and are pulled

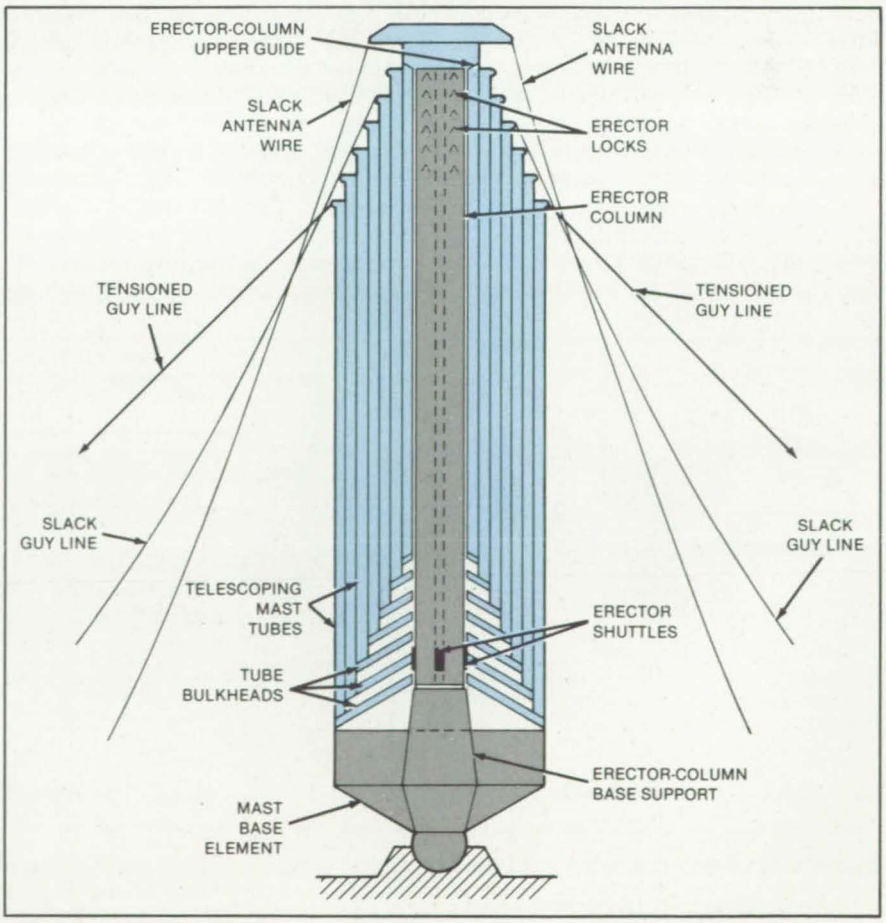

The **Erection System** is built into the stack of telescoping mast elements and is thereby protected from the weather.

by roller chains passing over sprockets at the top and bottom of the column. The shuttles are individually driven by electric motors at the base of the column. Four sets of locking devices are mounted at the upper end of the column. They automatically engage their mating parts, which are mounted on the tube bulkhead flanges. Unlocking is either mechanically or electrically controlled by an automatic selector.

The system can retract the column by simply reversing the extension process. Although this concept is based on a telescoping tube mast, it is also applicable to an open truss with only minor modifications. However, the open truss would not protect the system against the weather.

This work was done by Ronald Dayle Dotson and Georges Guy Jacquemin of Lockheed Missiles & Space Co., Inc., for **Langley Research Center.** *For further information, Circle 109 on the TSP Request Card.*
LAR-13115

Long-Life Cryogenic Cooler

Magnetic bearings and noncontacting seals would let a cooler operate unattended at 65 K for more than 3 years.

Goddard Space Flight Center, Greenbelt, Maryland

A Stirling cycle cryogenic cooler would operate unattended for more than 3 years to cool infrared detectors and other scientific instruments. Its target operating temperature is 65 K with 5 watts of refrigeration load. The new cooler uses magnetic bearings, small piston/cylinder clearance seals, and linear motors. [Details of the magnetic bearings appear in *NASA Tech Briefs* articles "Magnetic Bearing Consumes Low Power" (GSC-12517) and "Magnetic Bearing With Active Control" (GSC-12582) on pages 200 and 201 of Vol. 6, No. 2].

As the figure shows, the cooler consists of compression and expansion sections connected end-to-end. The compression section houses a reciprocating hollow piston driven by a linear motor [as described in "Reciprocating Linear Electric Motor" (GSC-12773), *NASA Tech Briefs*, page 108 of Vol. 8, No. 1]. The piston compresses the helium working fluid; the interior of the piston is vented to the motor housing to prevent a pressure differential. To minimize the power needed to run the cooler, the piston bounces off gas springs and is driven at its resonant frequency. The expansion section houses another linear motor (smaller and less complex than the first) that moves the displacer piston. The linear motors are driven in response to the sensed outputs of position sensors to sinusoidally reciprocate the piston and the displacer in sequence.

Electronic circuits control the cooling cycle. The circuits energize the magnetic bearings and control the stroke amplitude and the relative phase angle between the compression piston and displacer. Control is accomplished through feedback signals generated by position sensors coupled to the piston and displacer. Each bearing contains four orthogonally positioned electromagnets, and the bearings are selectively energized, depending upon the outputs of radial-position sensors. If the piston or displacer goes to one side, the sensors cause power to be applied to the electromagnet on the opposite side to pull it back to a central position. Vibration of the cooler is minimized by a spring-coupled mass that moves in the opposite direction to counterbalance the disturbance.

This work was done by Allan Sherman, Max G. Gasser, and Philip Studer of **Goddard Space Flight Center** *and Alex Daniels and M. Goldowsky of North American Philips Corp. For further information, Circle 106 on the TSP Request Card.*

This invention is owned by NASA, and a patent application has been filed. Inquiries concerning nonexclusive or exclusive license for its commercial development should be addressed to the Patent Counsel, Goddard Space Flight Center [see page 29]. Refer to GSC-12697.

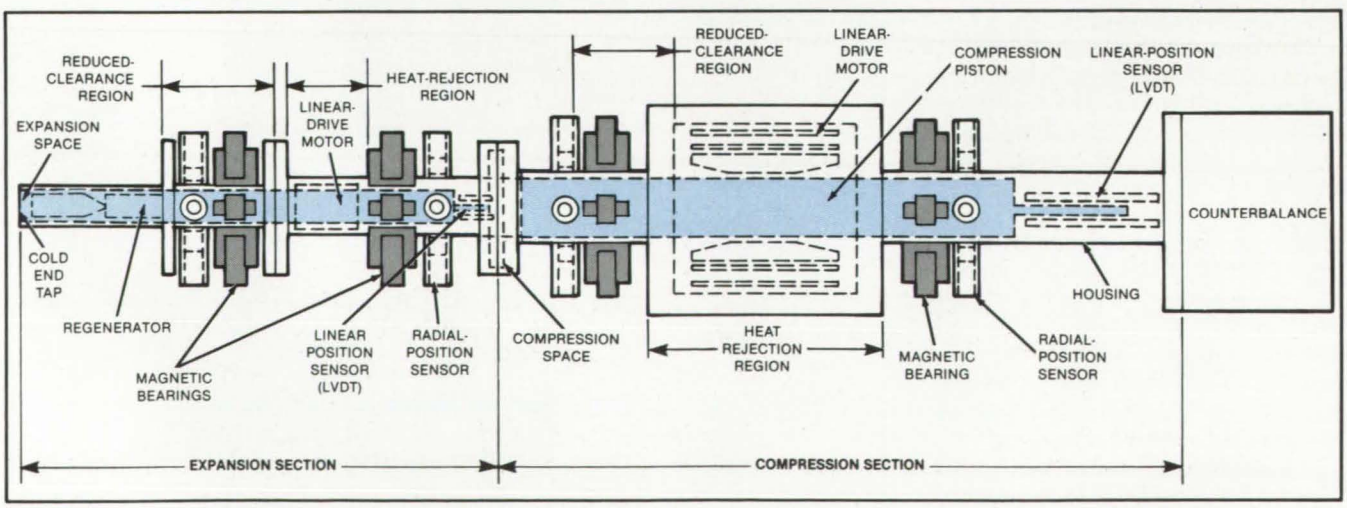

Magnetic Bearings Keep Piston and Displacer radially centered while preventing wear on cooler parts. On each end of the piston, between the piston and its housing, is a clearance seal — a reduced-clearance region. Located in the same area as the seals are position sensors and magnetic bearings. The clearance seal for the displacer, located in the forward bearing area, causes most of the working fluid to go through the regenerator. In the clearance-seal length, flow is through the center of the displacer. After the seal, radial flow passages direct the fluid around the linear motor through heat-exchanger tubes, where heat is transferred to a cooling jacket.

Mechanical Mixer for Rudder/Braking Wedge

Right and left rudder panels are moved separately.

Lyndon B. Johnson Space Center, Houston, Texas

A mechanical mixer enables the panels of a two-panel rudder to be rotated in the same direction for steering or in opposite directions for dynamic braking (see figure). The steering and braking inputs are separate so that any combination of steering and braking motions can be executed simultaneously.

Each panel is connected to the output of a separate differential. The braking input is applied to the sun gears of the two differentials through two large gears that mesh with each other, each of which is connected to one of the sun gears. Since they mesh, the two sun gears and the two differential output shafts rotate by equal amounts in opposite directions in response to a braking input. The panels are rotated toward each other to decrease braking or away from each other to increase braking.

The steering input is fed to the ring gears of the differentials. The two ring gears are coupled through two large gears with an idler gear between them. Because of the idler, the ring gears and the differential output shafts rotate in the same direction by equal amounts in response to a steering input.

Developed for aerodynamic braking of the Space Shuttle orbiter, this kind of steering/braking drive train and rudder arrangement might be used for similar purposes on aircraft, thereby reducing the sizes of thrust reversers.

This work was done by Duane Grimm of Sundstrand Energy Systems for **Johnson Space Center.** *No further documentation is available.*

Inquires concerning rights for the commercial use of this invention should be addressed to the Patent Counsel, Johnson Space Center [see page 29]. Refer to MSC-20759.

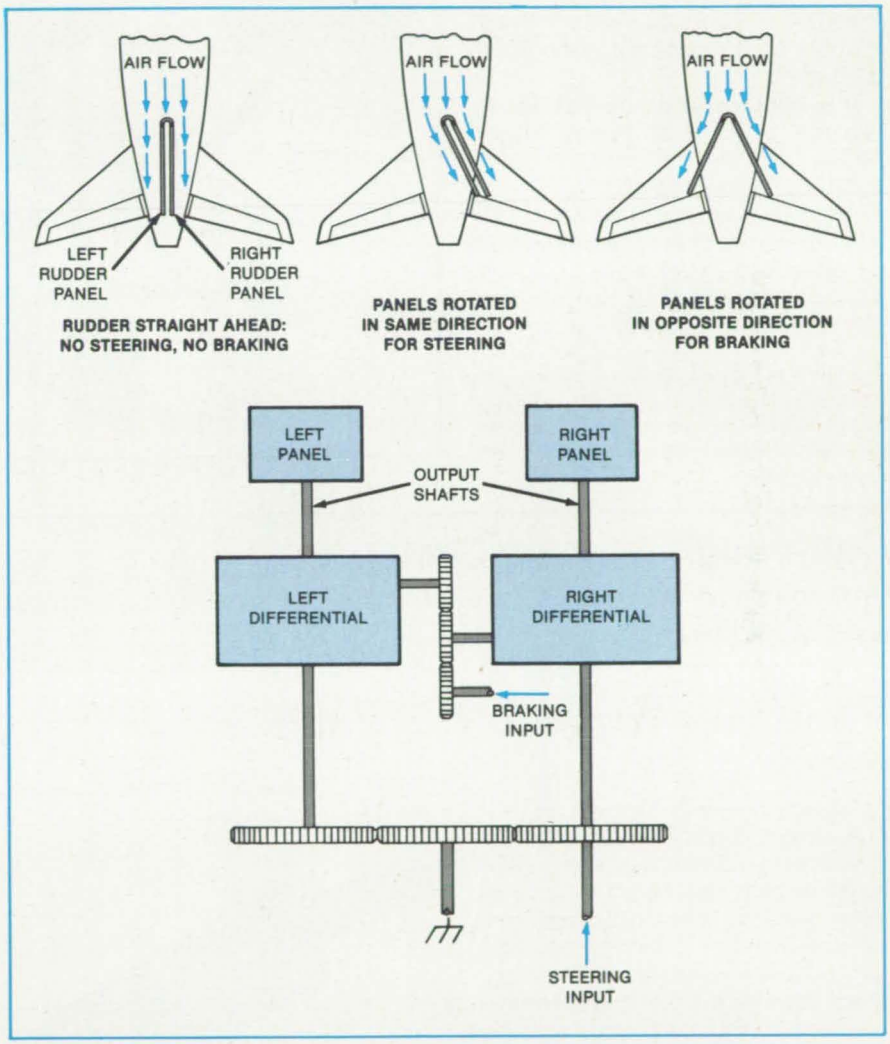

Rudder Panels are rotated in the same direction for steering or in the opposite direction to vary the degree of dynamic braking. The drive-train representation is schematic only to illustrate the principle of operation.

Wide-Grasp Latching Mechanism

Fingers capture and clamp without accurate positioning.

Marshall Space Flight Center, Alabama

A latching mechanism grasps a bar located within a relatively wide envelope of possible positions, retains the object, and releases it on command. The large acceptance envelope reduces the accuracy with which the object must be positioned for capture by the latch.

Fingers move out of the body of the mechanism. When fully extended, the

fingers accommodate a cubic capture envelope measuring approximately 5 inches (12.7 centimeters) on a side. As the fingers retract, they capture and clamp a bar located anywhere in that envelope and move it to a precise locked position. In releasing the bar, which is usually a trunnion attached to a large object, the fingers return to their fully extended position, retaining and controlling the bar before finally freeing it.

A rack and pinion drive the fingers. A worm/spur gear, powered by a worm gear at a 90° angle, drives the rack and pinion. The movement of the fingers can be halted at any point in the latching and unlatching sequence.

This work was done by Malcolm F. Nesmith of **Marshall Space Flight Center.** *For further information, Circle 67 on the TSP Request Card.*

Inquiries concerning rights for the commercial use of this invention should be addressed to the Patent Counsel, Marshall Space Flight Center [see page 29]. Refer to MFS-28002.

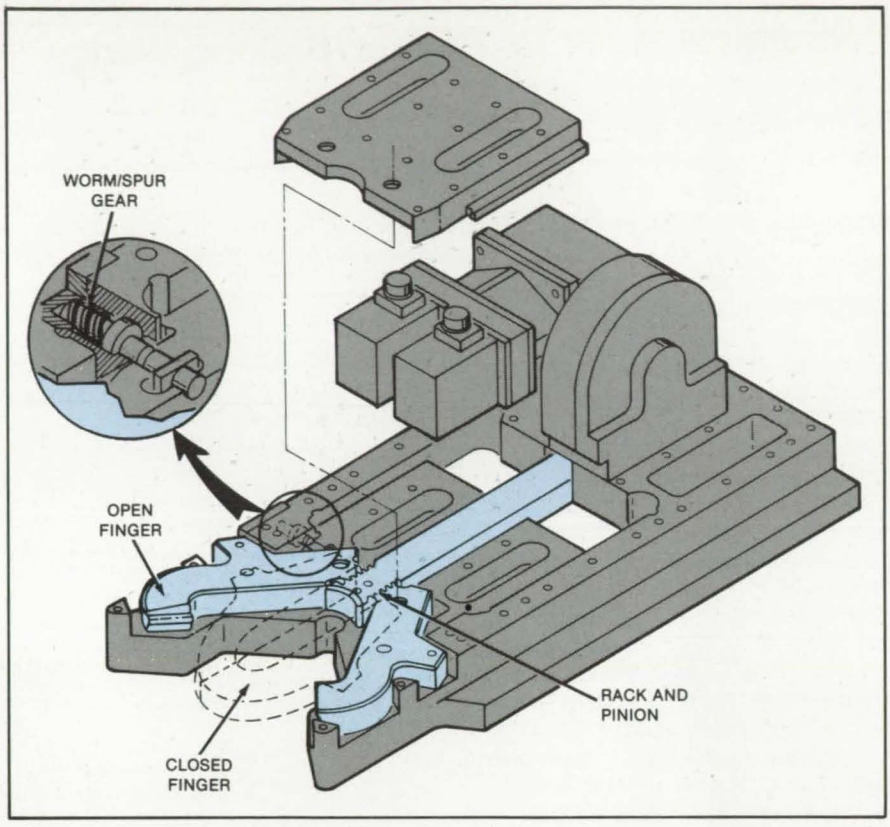

In their **Fully Open Position**, fingers encompass a large envelope. When activated by the rack and pinion, the fingertips move together, thereby grasping an object within the envelope.

Cutthrough Warning Circuit

Damage to an underlying layer is averted.

Marshall Space Flight Center, Alabama

A simple, inexpensive electrical circuit prevents overcutting when one of two close parts must be cut away; for example, when a liner must be removed from the wall of a chamber. The circuit can be used where there is enough space between the liner and the wall for the insertion of a shim before machining.

The shim is made of metal coated with polytetrafluoroethylene or other suitable insulator. The shim metal is connected through an insulated wire to a 6-volt battery, a warning light, and a metal part of the air motor that drives the liner cutter (see figure). This dc series circuit is normally open.

When an operator cuts through the liner and a polytetrafluoroethylene layer on the shim, the cutter blade contacts the interior metal of the shim and completes the circuit. The warning light is thereby turned on, alerting the operator that the liner has been penetrated, and cutting should stop. The operator is warned against damaging the chamber wall.

This work was done by R. D. McKown of Rockwell International Corp. for **Marshall Space Flight Center.** *No further documentation is available. MFS-19900*

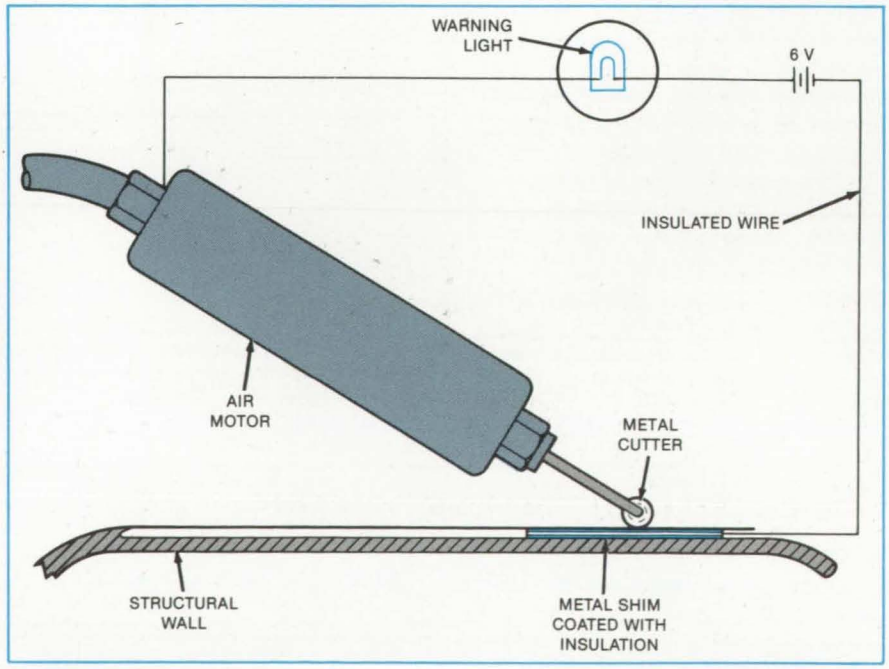

The **Contact of the Cutter Blade** with the metal shim completes a circuit that warns the cutting-tool operator to stop. The tool is thus prevented from cutting into the structural wall.

Books and Reports

These reports, studies, and handbooks are available from NASA as Technical Support Packages (TSP's) when a Request Card number is cited; otherwise they are available from the National Technical Information Service.

Remotely Piloted Aircraft for Research

Controlled from the ground, these vehicles allow new concepts to be tried without subjecting pilots to danger.

A NASA Technical Memorandum presents an overview of remotely-piloted research vehicle (RPRV) activities. RPRV's are aircraft controlled via a radio link by a pilot on the ground. Unlike military drones, an RPRV is intended to explore unknown engineering areas that cannot be explored by autopilots or preprogramed control systems. The pilot's job is to establish the appropriate flight conditions for maneuvers and to recover from them; the pilot has complete responsibility for determining emergency options and evaluating vehicle performance and handling qualities.

The paper is primarily concerned with RPRV's for testing relatively-untried, high-performance aircraft. The history of RPRV's is reviewed, the development of RPRV's as flight-test tools is discussed, and system configurations are presented. Solutions derived from human factors experience with RPRV's are summarized. Visual displays, which are a critical feature of successful RPRV flights, are also discussed.

The nucleus of the RPRV test facility described in the paper is a laboratory containing several computers for preflight, checkout, and flight support. Also in the laboratory are telemetry equipment, ultra-high-frequency and very-high-frequency communications, and control cockpits augmented with graphical displays, x-y plotters, and input/output devices. Television cameras on the RPRV's provide the ground pilots with the necessary visual cues. Analog control signals from the cockpit are sent, along with feedback signals from the RPRV, to one of the computers. These signals are processed according to control laws programed in the computer. The processed control signals are encoded and transmitted to the RPRV.

Since 1969, RPRV's as flight-test tools have evolved continuously. The systems now in regular use are sophisticated and adaptable. They are capable of emulating a variety of aircraft in a broad range of flight regimes using a number of control and display systems. The critical role of the pilot in flight testing with RPRV's has been demonstrated repeatedly, and many system anomalies have been uncovered with no risk to human life.

This work was done by Terrence W. Rezek of **Ames Research Center.** *Further information may be found in NASA TM-84913 [N83-27978/NSP], "Unmanned Vehicle Systems Experiences at the Dryden Flight Research Facility" [$7]. A copy may be purchased [prepayment required] from the National Technical Information Service, Springfield, Virginia 22161.*

Inquiries concerning rights for the commercial use of the technology described in this report should be addressed to the Patent Counsel. Ames Research Center [see page 29]. Refer to ARC-11498.

Sensitivities of Soap Solutions in Leak Detection

Bubbles are formed at smaller leak rates than were previously assumed.

A document describes a method for determining the minimum leak rate to which soap-solution leak detectors are sensitive. Previously, the minimum rate was assumed to be 0.25 stdin.^{3}/min (7×10^{-2} stdcm^3/s). The method shows that the minimum is actually less than one-tenth that value.

Soap-solution leak testing is widely used in aerospace and commercial products. The solution is brushed on the joint to be tested while the vessel in question contains helium under pressure. If no bubbles appear, it is assumed that the leakage through the joint is acceptably low. Precisely how low has not been quantified until now, however. A variety of pressurized systems should benefit as a result, including natural-gas pipelines, refrigeration units, welding-gas manifolds, and hospital/oxygen systems.

The document is based on tests of six flange-type connectors ranging in diameter from 0.8 to 9.15 in. (2.03 to 23.24 cm). Each seal was intentionally damaged by making a single small mark across the seal tip with a knife. The leak rate was varied by adjusting the torque on the connector bolts. During a test, a joint was placed in an enclosure from which a tube directed leaked helium to a water-displacement measuring device that indicated the leak rate.

Measurements were made at two helium-pressure levels [25 and 40 psig (172 and 276 kPa gage)], with two types of soap solution and in two joint orientations (horizontal and vertical). These tests yielded data on the minimum leakage rate that could be indicated by soap bubbles. Additional measurements at increments of pressure up to the maximum pressure rating [6,800 psig (47 mPa)] of the cells under test yielded data on leakage rate as a function of pressure.

With specific values dependent on joint type and orientation, minimum leakage rates for producing soap bubbles range from 0.0007 to 0.015 stdin.^{3}/min (2×10^{-4} to 41×10^{-4} stdcm^3/s) measured at 25 psig pressure. For 40 psig pressure, the range for the same joint conditions was 0.002 to 0.029 stdin.^{3}/min (5×10^{-4} to 79×10^{-4} stdcm^3/s). In the leakage-vs. -pressure tests, maximum leakage occurred at the 2,000 to 4,000 psig (14 to 28 MPa) range. In addition to presenting test results, the document discusses the effects of joint-flange configurations, the properties of soap solutions, and correlation of the test results with earlier data.

This work was done by D. E. Stuck, D. Q. Lam, and C. M. Daniels of Rockwell International Corp. for **Marshall Space Flight Center.** *To obtain a copy of the document, "Quantifying Leak Test Soap Solution Flowrate Sensitivity Thresholds," Circle 87 on the TSP Request Card.*
MFS-19864

Fabrication Technology

Hardware, Techniques, and Processes

144 Hybrid Contactless Heating and Levitation
145 Photovoltaic-Panel Laminator
145 Series Connection of Solar Cells
146 Perforating Thin Metal Sheets
146 Precise Fabrication of Electromagnetic-Levitation Coils
148 Screw-Retaining Allen Wrench
148 Making Stronger Twine With Matched Strands
149 Universal Cable Brackets
150 Bonded and Bolted Graphite/Polyimide Composite Joints
150 Spray Application of Rapidly Solidified Metals
151 Cutting Guide for Fibrous Sheets
152 Copyboard Quickly Makes Clean Printing Plates

Hybrid Contactless Heating and Levitation

Acoustic and electromagnetic fields would be applied.

NASA's Jet Propulsion Laboratory, Pasadena, California

A contactless material-processing concept involves the levitation, heating, and cooling of a sample of material through the coordinated use of electromagnetic and acoustic fields. The electromagnetic field would be used for both levitation and heating, while the acoustic field would be turned on to levitate the sample whenever the electromagnetic field must be weakened below the minimum strength required for levitation.

Radio-frequency (RF) power is applied to a coil in the levitation apparatus. Eddy currents induced in the sample by the RF field heat the sample and interact with the RF field to levitate the sample. The acoustic field can be applied simultaneously to increase the levitation stability, or the amplitude of both fields can be adjusted incrementally to provide various combinations of levitating, heating, and cooling effects.

The steps of a representative alloying process might be as follows (see figure):

1. The ingredients are placed in the electromagnetic levitating/heating field for initial contactless alloying.
2. After the alloy is formed, the RF power is reduced to lower the temperature.
3. When the RF power reaches the minimum required for levitation, the acoustic levitator is turned on and the RF power is further reduced until the desired lower temperature is reached. (For rapid cooling, the RF power might be turned off altogether and the coil removed from the acoustic field.)

Many variations are possible; for example, heating and cooling gradually or in specified increments, maintaining a specified temperature for a preset interval, and alternating cycles of heating and cooling. The apparatus could provide rapid heating and cooling or slow heating and cooling for such processes as nucleation, crystallization, incubation, deep undercooling, and heterogeneity control.

This work was done by Mark C. Lee of Caltech for **NASA's Jet Propulsion Laboratory.** *For further information, Circle 30 on the TSP Request Card.*
NPO-15657

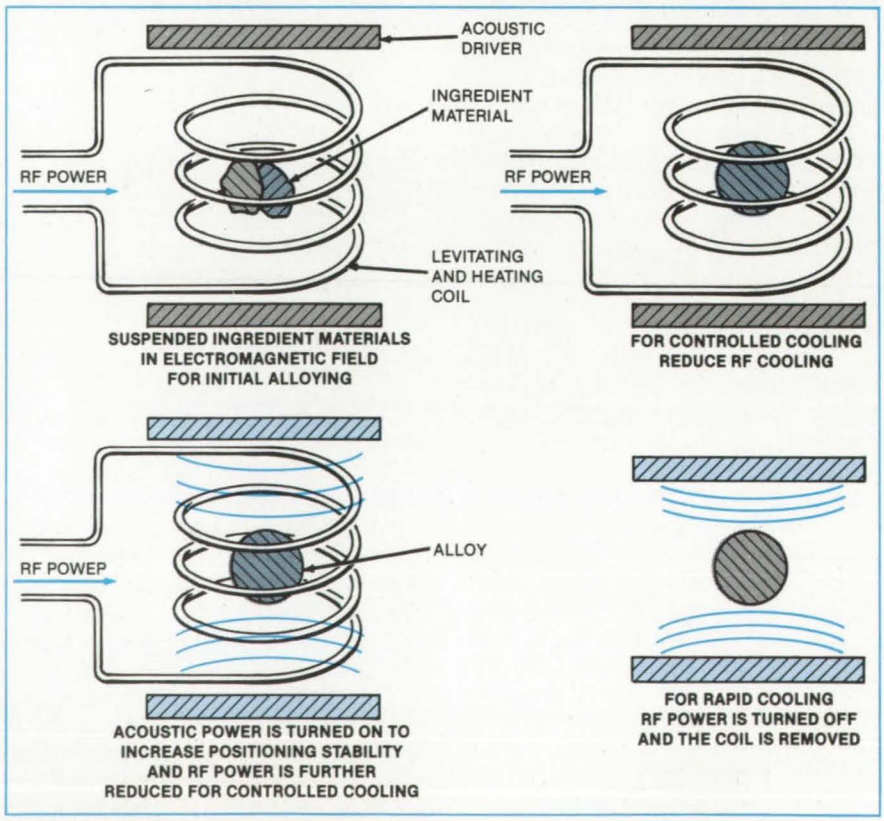

In this **Contactless Processing Apparatus**, acoustic and electromagnetic levitating fields are employed alternately or simultaneously with the amplitude of each controlled to produce various combinations of heating, cooling, and levitation.

Photovoltaic-Panel Laminator

A two-piece unit heats and presses protective layers to form a laminate.

NASA's Jet Propulsion Laboratory, Pasadena, California

A two-chamber laminator encapsulates strings of solar cells to form panels for photovoltaic arrays. The encapsulation helps to protect the cells from the environment and to ensure long panel life while allowing efficient generation of electricity from Sunlight.

The two chambers are separated by a rubber diaphragm (see figure) that serves as a gasket to maintain a pressure difference between the chambers or, with the chambers at the same pressure, between them and the atmosphere. The solar cells and their interconnections are placed on a grating in the lower chamber, between two layers of polyvinyl butyral that in turn are sandwiched between a layer of glass on the bottom and Tedlar (or equivalent) on the top.

The upper chamber is placed on the lower one, and the lower chamber is evacuated. Atmospheric pressure in the upper chamber presses the diaphragm against the solar-cell assembly. The upper chamber is then evacuated so that the diaphragm returns to its neutral position, and the infrared heater is energized. The heater warms the assembly so that the plastic layers soften and bond to the glass, the solar cells, and each other.

Next, the heater is turned off. The upper chamber is returned to atmospheric pressure, thereby causing the diaphragm to press the assembly together into a laminate while it cools. Finally, the lower chamber is returned to atmospheric pressure, and the completed solar-cell panel is removed.

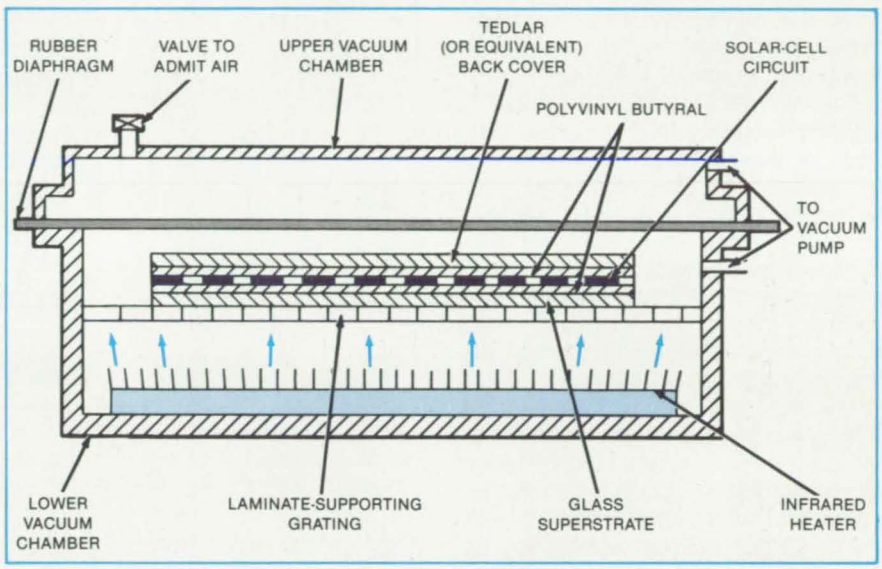

The **Rubber Diaphragm Between the Upper and Lower Vacuum Chambers** alternates between a neutral position and one that presses against a solar-cell array, supplying the distributed force necessary to press the layers of the laminate together.

This work was done by Richard Keenan of Arco Solar, Inc., for **NASA's Jet Propulsion Laboratory.** *For further information, Circle 26 on the TSP Request Card.*
NPO-16092

Series Connection of Solar Cells

Roll soldering forms a continuous string of cells.

NASA's Jet Propulsion Laboratory, Pasadena, California

An automatic, continuous process attaches interconnecting strips to a series string of silicon solar cells. The manufacturing process attaches each conductor from the positive side of one cell to the negative side of the next. For reliability, 22 contacts are soldered on each side of each cell.

Solder paste is applied to the cell, and the copper interconnecting ribbons are placed on the cells. The cells are heated by an infrared lamp to a temperature of 220 ± 20° C. The heat melts the solder. Compliant rollers press the ribbons against the top and bottom of the cell. As each cell passes through the rollers, it cools; the molten solder solidifies, bonding the ribbons securely to the wafer.

This work was done by Richard Keenan of Arco Solar, Inc., for **NASA's Jet Propulsion Laboratory.** *For further information, Circle 10 on the TSP Request Card.*
NPO-16091

Perforating Thin Metal Sheets

Sheets only a few mils thick are bonded together, punched, then debonded.

Ames Research Center, Moffett Field, California

Metal sheets and foils as thin as 0.003 inch (0.076 mm), are perforated by a mechanical punch with the aid of a new technique. Previously, such foils were perforated while they were 10 times thicker, and excess material was then removed by chemical milling.

The perforation technique was developed for fabricating a conductive layer on blankets that collect and remove ions; however, perforated foils have other applications — as conductive surfaces on insulating materials; stiffeners and conductors in plastic laminates; reflectors in antenna dishes; supports for thermal blankets; lightweight grille cover materials; and material for the mockup of components.

The new technique is performed in three steps (see figure). Many sheets — 10 or more — of the foil are bonded with a heat-degradable adhesive, so that the composite is thick enough to withstand the perforation process without tearing or crumpling. The laminated foil is then perforated in a punch press. Finally, the bonding adhesive is removed by baking in an oven, yielding individual perforated sheets of the requisite thickness.

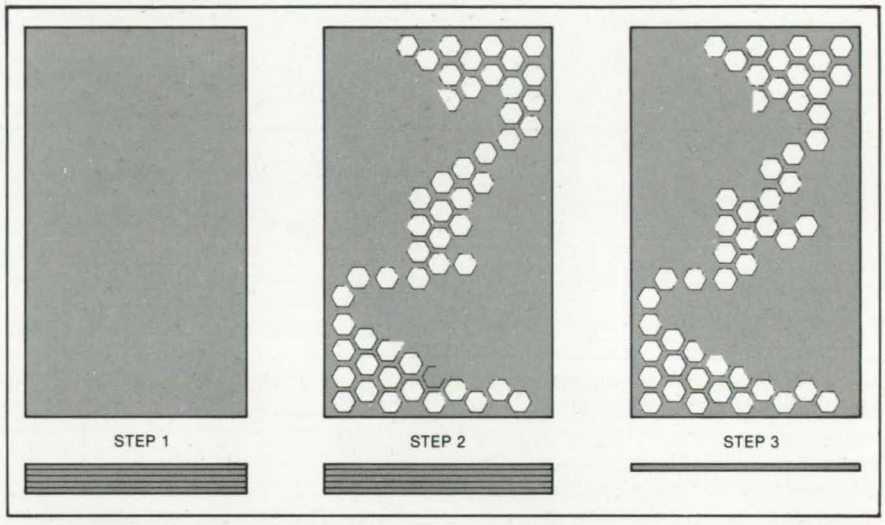

A **Three-Step Process** yields perforated sheets of metal. Step 1: Individual sheets are bonded together to form a laminate. Step 2: The laminate is perforated in the desired geometric pattern. Step 3: After baking, the laminate separates into individual sheets.

This work was done by Milton E. Davidson of Hughes Aircraft Co. for **Ames Research Center.** *No further documentation is available.*

Inquires concerning rights for the commercial use of this invention should be addressed to the Patent Counsel, Ames Research Center [see page 29]. Refer to ARC-11280.

Precise Fabrication of Electromagnetic-Levitation Coils

Winding copper tubing on a jig ensures reproducible performance.

Marshall Space Flight Center, Alabama

A method for winding induction coils for electromagnetic levitation is both fast and consistent. The previous method of manual freehand winding required a full day to fabricate one coil and half of all coils performed unsatisfactorily. The new method, in contrast enables a technician to produce eight coils per day, and 95 percent of them are acceptable. The new method employs a precise step-by-step procedure on a specially-designed wrapping and winding jig.

The coils are used for containerless processing of metals. A multikilowatt induction generator operating at a frequency of 400 kilohertz furnishes power to a coil. The coil induces eddy currents in a metal specimen. The interaction between the eddy currents and the coil current produces magnetic forces that levitate the specimen within the coil. At the same time, heat from the eddy currents melts the specimen. The molten globule can then be manipulated and processed without coming into contact with tools or vessels.

Efficient inductive coupling between the coil and the specimen is essential. Coupling is affected by the total length of the coil, the diameter of the turns, the tightness of the turns, and the spacing of the turns. Not surprisingly, fabrication of coils has been something of an art; an operator trying to wind several "identical" coils would find that not all coils performed in the same way. A few coils might efficiently levitate and melt a specimen, while others might levitate the specimen but not melt it.

The new method eliminates these vagaries. A 36-inch (91.4-centimeter) length of precision-bore copper capillary tubing is cut, placed on the jig, and subjected to the sequence of bending operations shown in the figure. After the bends have been made, the mandrel is disassembled so that the coil can be removed. The coil is finished by soldering to its ends connectors for insertion in the induction-furnace receptacles. The tube is then cut flush with the ends of the connectors.

The coils made by this method have levitated and melted a variety of metals and alloys including copper, silver, silver/nickel, copper/iron, iron/carbon, and niobium/germanium. The highest melting temperature attained was 2,400° C (with Nb/Ge).

This work was done by E. C. Ethridge,

P. A. Curreri, and J. Theiss of **Marshall Space Flight Center** *and G. J. Abbaschian of the University of Florida. For further information, Circle 42 on the TSP Request Card.*

Inquires concerning rights for the commercial use of this invention should be addressed to the Patent Counsel, Marshall Space Flight Center [see page 29]. Refer to MFS-25986.

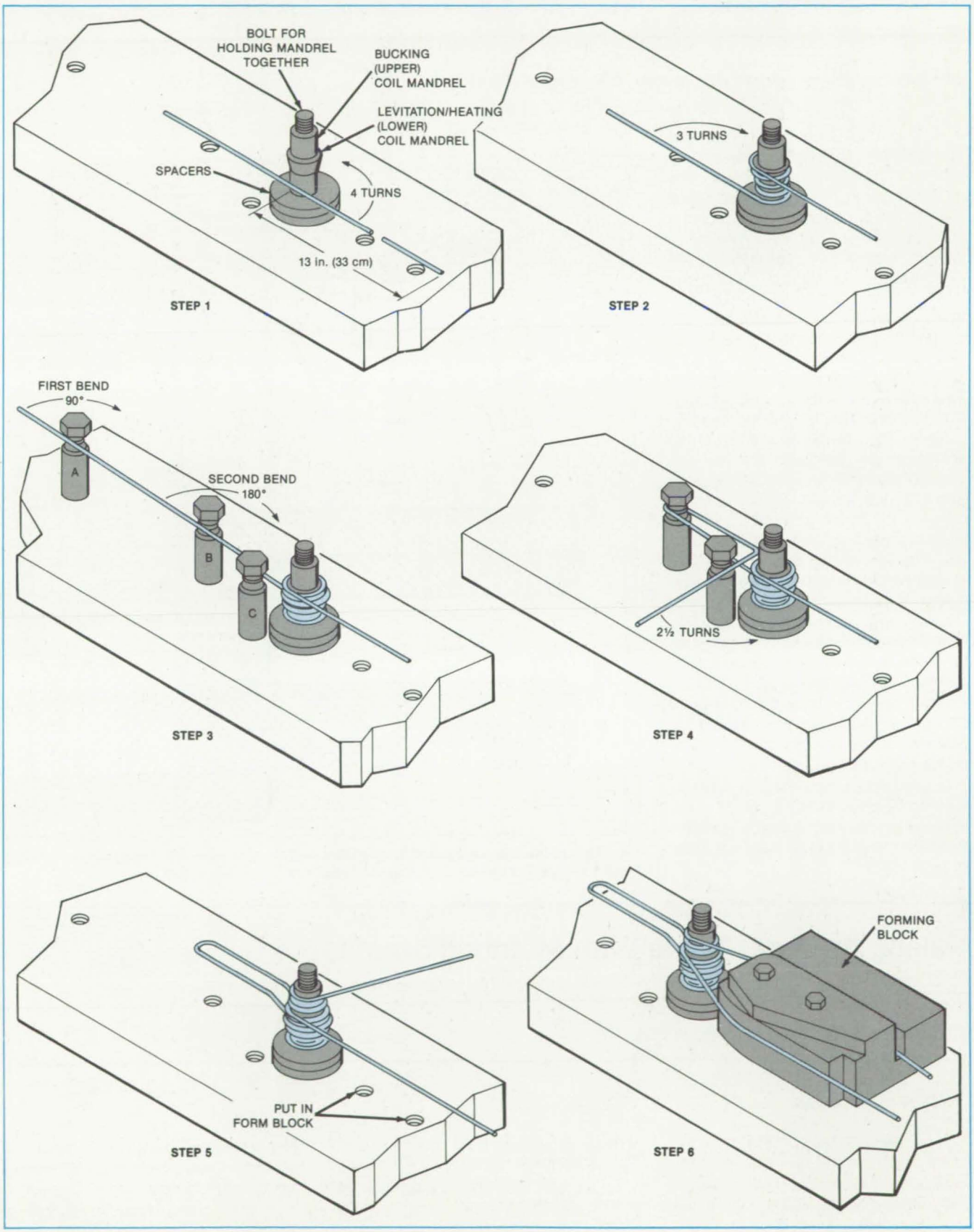

This **Sequence of Steps** insures the consistent fabrication of levitation-and-melting coils. Step 1: forming inner part of lower coil. Step 2: forming outer part of lower coil. Step 3: beginning loop between upper and lower coils. Step 4: completing loop. Step 5: winding upper coil. Step 6: positioning ends of coil for attachment of connectors.

Screw-Retaining Allen Wrench

Steadying screws with
the fingers is unnecessary.

NASA's Jet Propulsion Laboratory, Pasadena, California

A wire spring at the end of an Allen wrench holds a screw while it is inserted or removed. The tool can be used with Allen-head screws in cramped spaces where there is little or no room for the fingers to hold the fastener while it is turned by the wrench. A tool of the same function but different design is described in "Padded Allen Wrench Grips Fasteners," *NASA Tech Briefs*, Vol. 7, No. 2 (Winter, 1982), p. 191.

The spring lies in a groove in the wrench (see figure). A crimp near the end of the spring protrudes slightly from the groove. The opposite end of the spring is anchored in a transverse hole through the wrench.

When the wrench is inserted in the socket of a screwhead, the crimp is pressed into the groove and thus exerts a force on the socket wall. The force prevents the screw from sliding off the wrench, regardless of the wrench orientation. The spring thus retains the screw while the screw is started into a threaded hole or while it is extracted from the hole. The wrench is separated from the screw by pulling it axially from the socket while the screw is held by the threaded hole or by the user's fingers.

This work was done by Dan Granett of Caltech for **NASA's Jet Propulsion Laboratory.** *For further information, Circle 78 on the TSP Request Card.*

Inquires concerning rights for the commercial use of this invention should be addressed to the Patent Counsel, NASA Resident Office-JPL [see page 29].Refer to NPO-16275.

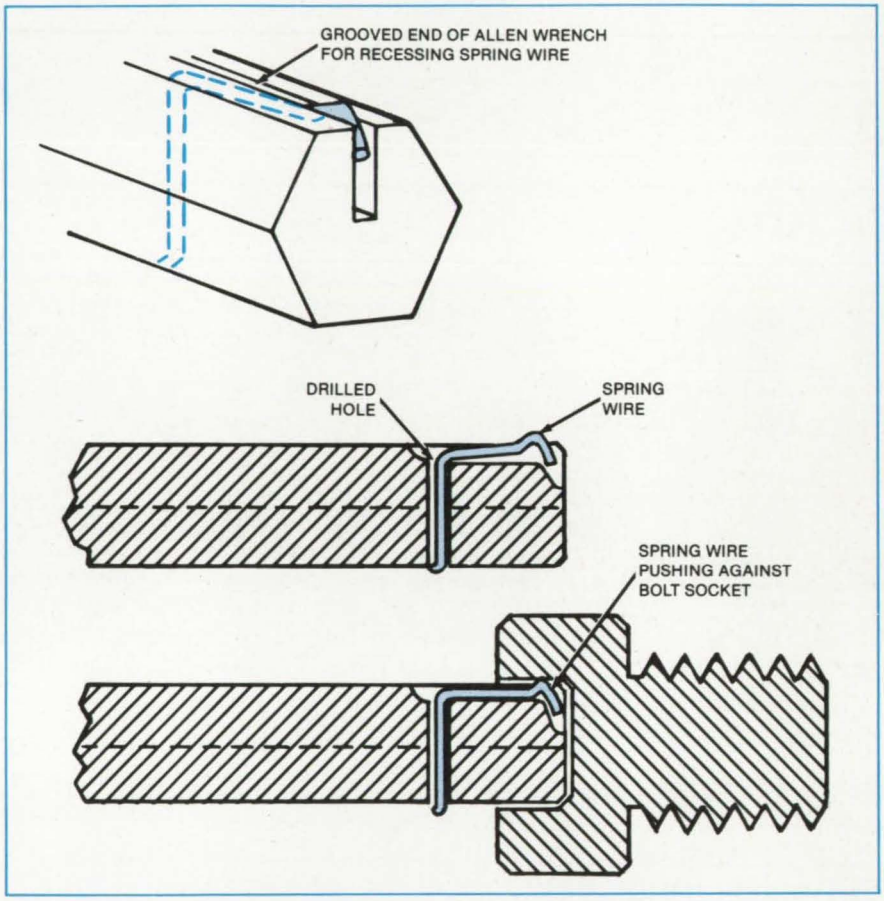

A **Crimp in the Uncompressed Spring Wire** slightly protrudes from one facet of an Allen wrench (top). Compressed, the spring retains an Allen screw (bottom).

Making Stronger Twine With Matched Strands

Higher tensile strength is achieved
with the same production equipment.

Lyndon B. Johnson Space Center, Houston, Texas

Strong twine is made by using matched spools in the second step of a two-step manufacturing process. The technique has been used successfully in the manufacture of safety netting with 600- to 700-lb (2,700-to 3,100-N) tensile strength and a 60-ton (54 x 10^3 kg) tuna seine with an area of 86 acres (3.5 x 10^5 m^2). The safety net is part of the ground support equipment at the Space Shuttle launch complex.

In the first manufacturing step, single filaments are twisted together at high speed to form a primary strand that is wound onto a spool. Several primary stranding machines are usually operating at the same time, each producing a primary strand that differs slightly from the others in tension and twist because of slight mechanical differences among the machines.

In the second stage, three primary strands are twisted together in the opposite direction to form a three-ply twine. Normally, the three primary spools that feed the secondary twisting machine are selected at

random. The process improvement consists of selecting three spools from the same primary twisting machine.

The increase in strength of the finished twine is due to a change in the way the fibers break. In conventional twine, the individual fibers in the three strands are under slightly different tensions. Under a severe load, the tightest fibers break first, transferring the load to the second tightest fibers, which then break, and so on: The twine thus ruptures in a sort of chain reaction.

With matched primary strands, all the fibers lie next to each other under more nearly the same initial tension. Consequently, all fibers bear more nearly the same tensile load, and all approach the breaking tension together at a higher overall load. The increase in the tensile strength of the completed twine was found experimentally to be 10 to 12 percent.

This work was done by William L. Kirkland of West Coast Netting, Inc., for **Johnson Space Center.** *For further information, Circle 102 on the TSP Request Card.*
MSC-20444

Universal Cable Brackets

Concept would allow routing to be easily changed.

Marshall Space Flight Center, Alabama

A concept for "universal" cable brackets would make it easy to route electrical cable around and through virtually any structure. No custom hardware is required in the concept. Instead, standard brackets are cut to length and installed at selected locations along the cable route. If a cable route is changed, then the brackets are simply moved to the new locations.

The bracket, made of extruded aluminum, would be cut to lengths corresponding to distances between structural members. Holes would be drilled or punched to accommodate fasteners for attachment to the structure (see figure). Keylike appendages on cable clamps would fit in channels on the brackets. The brackets would be stackable so that the cables could cross.

The scheme makes it unnecessary to design brackets specifically for a cable route, to generate separate drawings and documentation for each bracket, and to make modifications on part drawings and layouts. Instead, only a single set of bracket drawings would be needed. All documentation and tabulation for a cable route would appear on the assembly-level drawing. Modification of a cable route would require changing the assembly drawing only.

This work was done by Charles Vanvalkenburgh of Essex Corp. for **Marshall Space Flight Center.** *For further information, Circle 40 on the TSP Request Card.*

Inquiries concerning rights for the commercial use of this invention should be addressed to the Patent Counsel, Marshall Space Flight Center *[see page 29].*
Refer to MFS-26001.

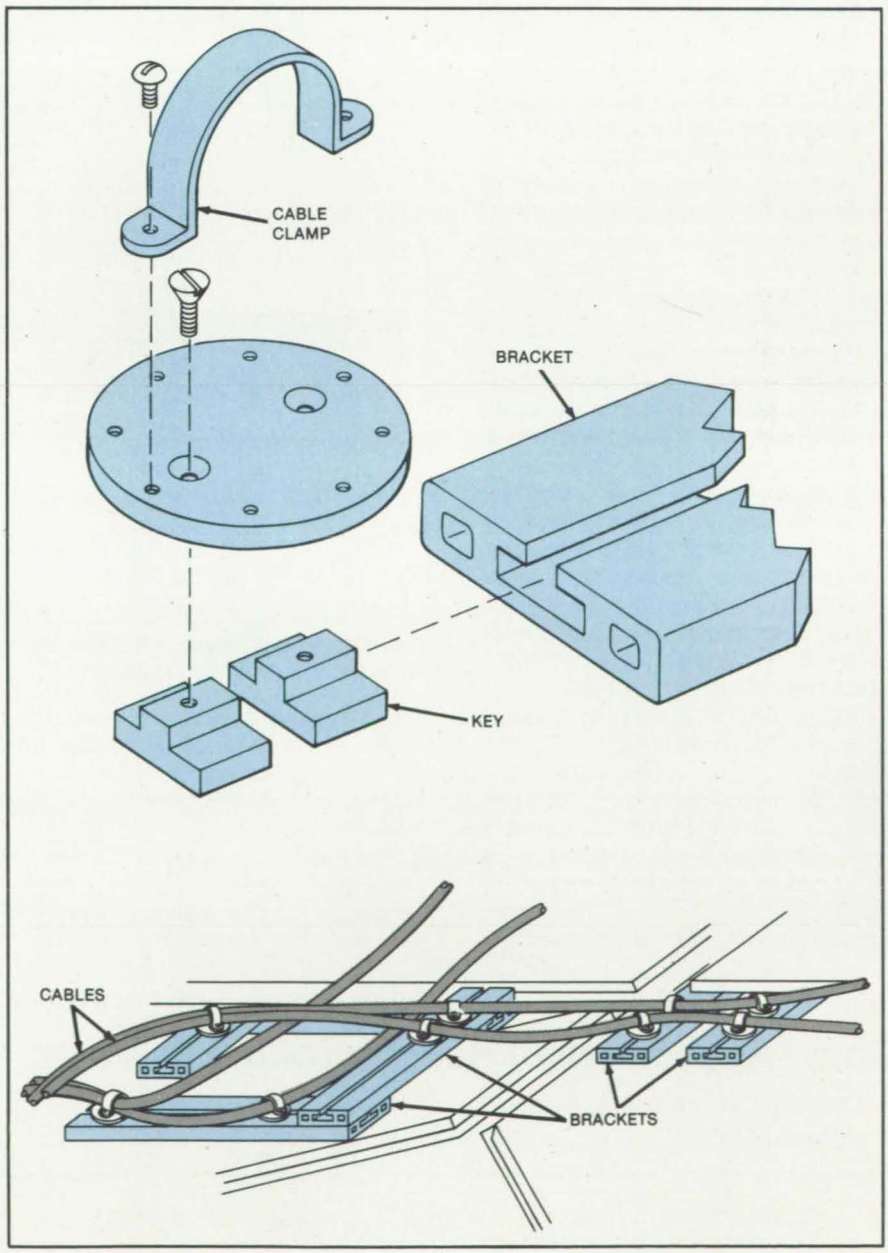

This **Clamp Assembly** illustrates one of several possible configurations, all based on keys in bracket channels. Like the brackets, the clamps would be in standard sizes to accommodate a variety of cable thicknesses.

Bonded and Bolted Graphite/Polyimide Composite Joints

Four types of high-temperature joints are designed for control surfaces.

Langley Research Center, Hampton, Virginia

Advanced designs for high-speed aircraft and space transportation systems require efficient structures for operation in the 500° to 600° F (260° to 316° C) temperature range. Design concepts and data for bonded and/or bolted composite joints are needed to support advanced structural development.

Design, analysis, and testing were performed to develop four types of graphite/polyimide bonded and bolted composite joints for lightly loaded control surfaces on advanced transportation systems that operate at temperatures up to 550° F (288° C). Approximately 10 concepts were analyzed for each of the 4 generic attachment types shown in the figure.

The Type 1 attachment is typical of an attachment in the sandwich shell at a rib or spar interface of an aerodynamic surface such as a wing or control surface. The Type 2 attachment is typical of the attachment occurring at an unloaded edge of a wing or aerodynamic surface. The Type 3 attachment is typical of a localized attachment of a metallic plate to a composite sandwich structure: The attachment is subjected to relatively large in-plane forces that must be distributed to the sandwich face sheets. The Type 4 attachment is similar to the Type 1 attachment in that it connects members that are perpendicular; however, the cover panels are not spliced in the Type 4 attachment, and the applied load levels are well below those required for the Type 1 attachments.

Tests of the final joint concepts demonstrated that both bonded and bolted graphite/polyimide joints can be designed and fabricated to carry loads up to 3,200 lb/in. (560 kN/m) at 550° F (288° C). Further, a bolted design (not shown) attaching graphite composite to titanium carried nearly 12,000 lb/in. (2,100 kN/m). The bonded joints demonstrated fabrication advantages over bolted joints. Bonding proved to be faster and thus less costly than the procedures required for a bolted joint. However, bolted joints offer advantages in reliability and repairability.

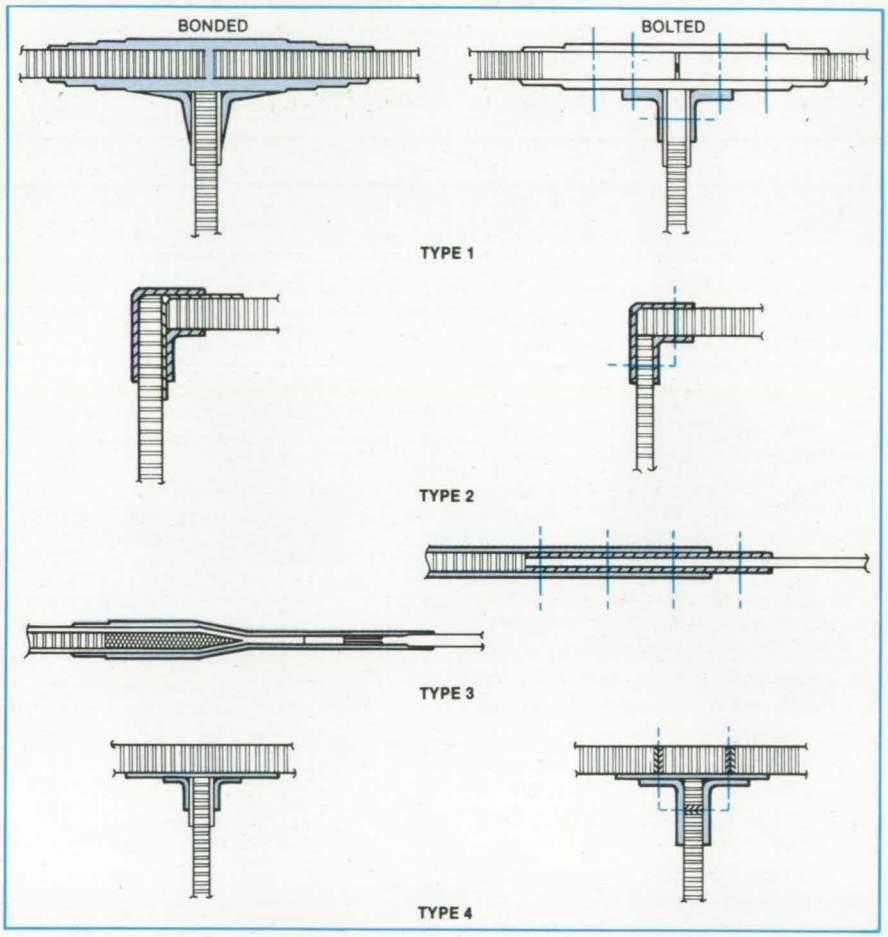

Four Attachment Types are representative of joints of lightly loaded control surfaces of advanced transportation systems.

This work was done by Donald E. Skoumal and James B. Cushman of Boeing Aerospace Co. for **Langley Research Center.** *Further information may be found in NASA CR-3601 [N83-16786/NSP], "Design, Fabrication and Test of Graphite/Polyimide Composite Joints and Attachments" [$11.50]. A copy may be purchased [prepayment required] from the National Technical Information Service, Springfield, Virginia 22161.*

LAR-13090

Spray Application of Rapidly Solidified Metals

A fast and economical process is now available.

Goddard Space Flight Center, Greenbelt, Maryland

A new process applies rapidly solidified (RS) metal coatings to substrates. RS metals are made directly from molten material. They have amorphous or microcrystalline structures and yield coatings having superior wear and corrosion

resistance.

Previous methods of applying RS metals as coatings for large areas have been expensive or difficult. Such methods include ion plating, laser glazing, and ion implantation. The new process, which employs shot peening, is safe, fast, and inexpensive. A mixture of RS metal powder and peening particles is sprayed from a nozzle against the surface to be coated. The powder and peening particles strike the surface simultaneously, and the impact bonds the powder to the surface as a uniform coating.

The process may be carried out in a peening apparatus. The powder and particles can be mixed in a hopper before spraying. Glass beads make good peening particles.

The RS metal may be aluminum, titanium, nickel, iron, and other alloys. New RS powders are continually being developed. The powder size required in a specific application depends on the speed of the process and the intended thickness of the coating. However, the metal-particle size should be no larger than half that of the peening particles.

A variety of materials may be used as substrates. Examples include such metals as copper, steel, magnesium, and aluminum; Two or more different RS powders may be introduced into the peening particle stream simultaneously or alternately.

The process can precondition the substrate surface by spraying with peening particles alone before the powder is introduced into the stream. For example, the substrate may be cleaned by a gentle, stream of peening particles to remove rust, scale, or paint to improve adhesion of the coating. Or the surface may be peened by a forceful jet of particles to create beneficial compressive stresses in the substrate, thereby improving its resistance to fatigue and stress corrosion.

The substrate may be moved automatically into the spray paths of several nozzles in sequence. A variety of surface preparations can thus be performed and a sequence of layers deposited.

This work was done by Huai-Pu Chu and Charles L. Staugaitis of **Goddard Space Flight Center.** *For further information, Circle 18 on the TSP Request Card.*

This invention is owned by NASA, and a patent application has been filed. Inquiries concerning nonexclusive or exclusive license for its commercial development should be addressed to the Patent Counsel, Goddard Space Flight Center [see page 29]. Refer to GSC-12880.

Cutting Guide for Fibrous Sheets

Tool facilitates repetitive cutting of fibrous sheets.

Lyndon B. Johnson Space Center, Houston, Texas

Strips can be cut from rolls of fibrous materials easily and accurately with the aid of a new tool. Previously, such hard-to-handle material had to be measured, marked, and cut one strip at a time. With the new tool, many strips can be cut in one setup, and total job time is reduced by two-thirds. Developed for cutting strips of alumina-fiber matting, the tool can also be used on such materials as felts, textiles, and sheet metals.

The tool consists of a flat plate of stainless steel to which a series of stainless-steel strips are attached by aluminum tape. Each steel strip is as wide as the strip to be cut. The user simply runs the cutter along the length of the outer strip to sever a strip of material. The user then turns back the steel strip to the top of the adjacent steel strip and makes another cut (see figure). In this way, the user can cut the material into strips of uniform width in quick succession.

The tool has been used to cut rolls of alumina fiber matting 50 ft long, 2 ft wide, and 1.5 in. thick (1,524 by 61.0 by 3.8 cm). For this purpose, the tool base was 4 by 32 in. and was 0.32 in. thick (10.2 by 81.3 by 0.08 cm). The tool had sixteen strips, each 0.25 in. (0.6 cm) wide. Thus, 0.25-inch-wide strips can be cut from the matting. Alternatively, the user can fold back two, three, or more strips at a time and cut the matting in widths of 0.5 in. (1.3 cm), 0.75 in. (1.9 cm) or more.

This work was done by Aubrey D. Warren of Rockwell International Corp. for **Johnson Space Center.** *No further documentation is available.*
MSC-20798

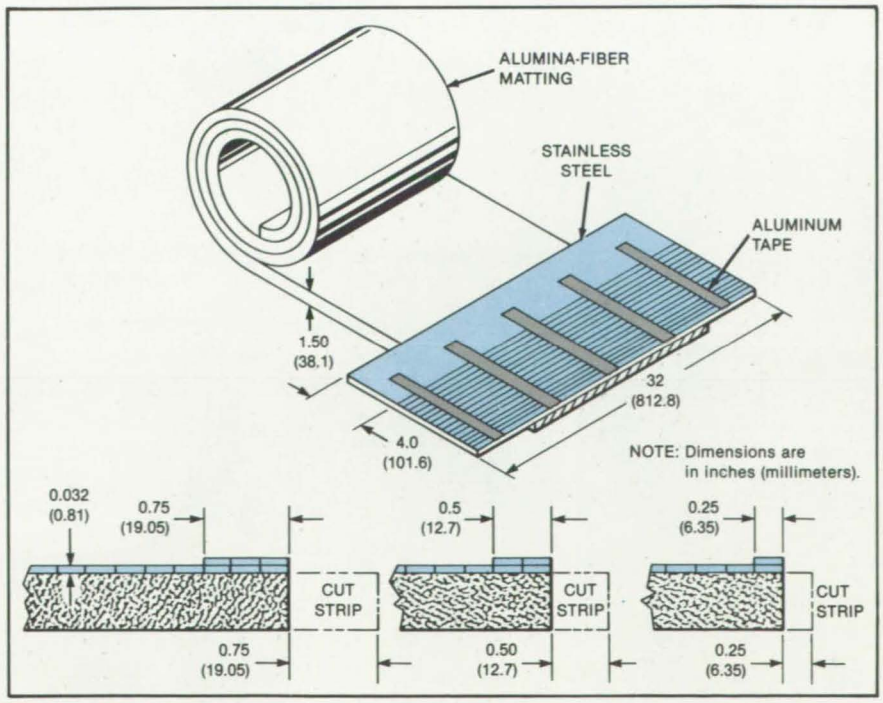

Flexible Aluminum Tape allows metal strips to be folded back on themselves, exposing fresh material for cutting. More than one strip may be folded back, and the cutting width can therefore be increased in multiples of the strip width.

Copyboard Quickly Makes Clean Printing Plates

Vacuum-chuck eliminates glass and sponge artwork support.

Ames Research Center, Moffett Field, California

A copyboard for printing shops keeps a camera-ready original clean and in the proper position for making plates. The copyboard is intended for use on an electrostatic platemaker consisting of a lighttight plate container, processing tank and dryer, lamps to illuminate the copyboard, and a camera lens focused on the copyboard.

The camera-ready original — a drawing, photograph, or page of text — is placed face up on the copyboard, illuminated by the lamps, and photographed by the camera. After developing, the plate made by the camera is used directly on a printing press.

With the previous copyboard, the original is placed on a white spongy mat containing light-blue positioning lines. A glass plate is swung down over the original, pressing it against the mat. The original is then photographed through the glass. Three surfaces — the two sides of the glass plate and the mat — must be kept scrupulously clean so that specks and smudges do not appear on the photographic plate.

The original tends to jump out of place when the glass is lowered or raised, and the calibration lines on the mat are easily obliterated. Because of these difficulties, the image alinement often must be corrected, and the plate must be cleaned up while it is on the press. With the new copyboard, these time-consuming and costly procedures are unnecessary.

The new copyboard consists of a box having a clear plastic top and white bottom (see figure). The camera-ready original is placed face up on the clear top plate, which contains holes of 1/32-in. (0.80-mm) diameter [the hole size is optional — 1/16-in. (1.59-mm) may be more suitable for some operations] spaced about 1 inch (2.54 centimeters) apart. The interior of the box is connected by a hose to a vacuum pump. When the pump is turned on, via a convenient foot switch, the original is drawn against the top plate. A bleed valve allows adjustment of the partial vacuum in the box. Posts within the box prevent the top plate from sagging toward the base, ensuring a level, distortion-free surface for photography. Posts and holes are precisely located to accommodate standard paper sizes.

Calibration lines are scribed lightly in the top plate so that the original can be positioned for the proper reduction or enlargement. The calibration lines are fine enough so that they do not appear on the finished plate.

This work was done by William D. Balandis of **Ames Research Center**. *No further documentation is available.*
ARC-11365

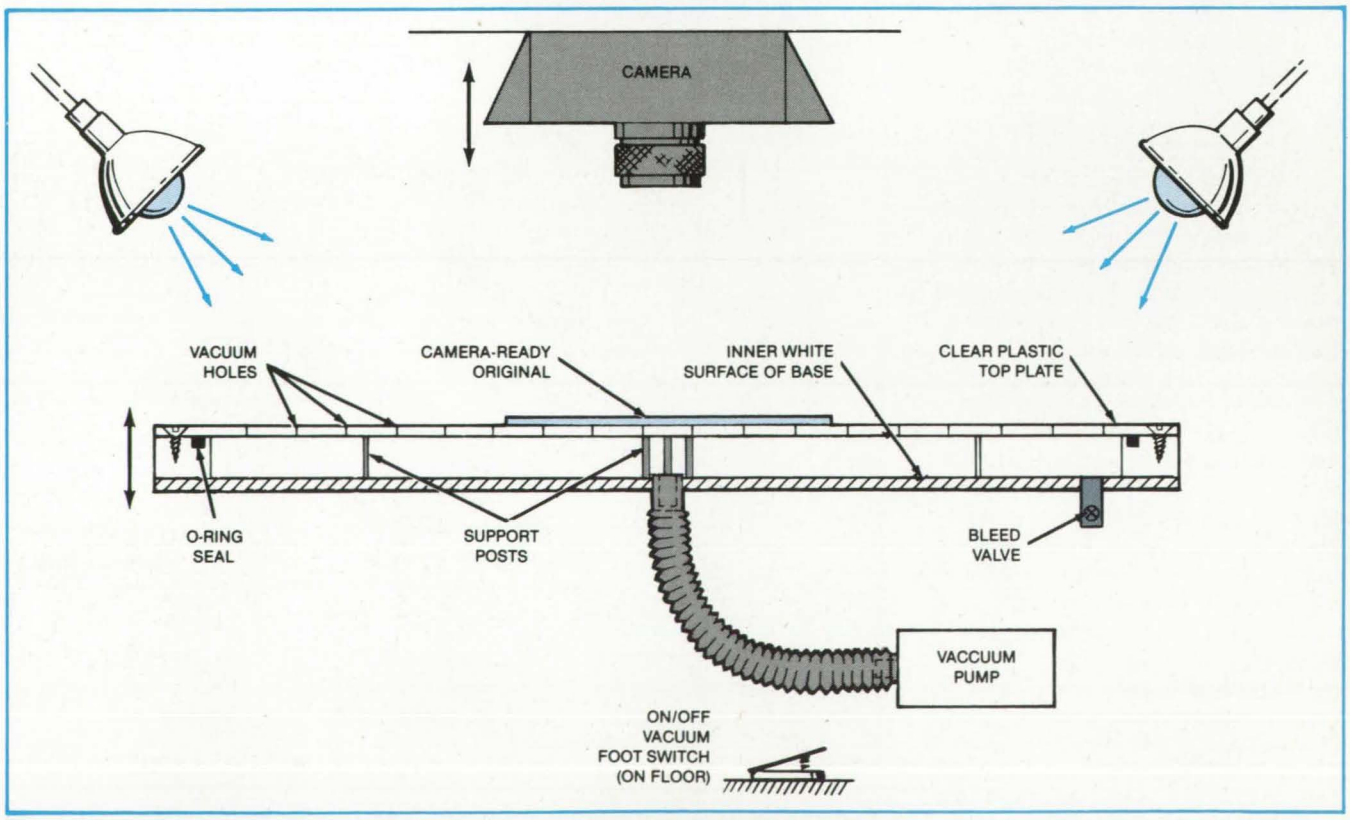

Vacuum Copyboard allows a camera-ready original to be slid on the top plate for proper positioning, then holds it securely for photography. The bleed valve allows the vacuum in the copyboard box to be adjusted for small or large originals.

SCIENCE/SCOPE

Two communications satellites rescued by NASA's space shuttle in November are being refurbished to be launched again. The spacecraft were brought back to Earth after shooting into wayward orbits nine months earlier when their rocket motors misfired. Spacecraft controllers at Hughes Aircraft Company spent months taming the satellites and bringing them into orbits low enough that they could be reached by the shuttle. Their efforts were the most sophisticated series of orbital maneuvers ever attempted. In addition, Hughes and NASA engineers worked tirelessly to develop hardware that permitted the actual recovery. The satellites emerged in good condition. Most of the electronics were never turned on, but certain items—batteries, thermal blankets, and thrusters—are being replaced.

Pilots of future aircraft may rely on artificial intelligence systems to help them assess combat situations and take appropriate offensive or defensive actions. Hughes engineers are conducting studies for the U.S. Air Force on potential uses of artificial intelligence for fire control and battle management. One focus is how to identify targets automatically and present this information for a pilot's use. Another aspect involves tactical analysis, including decision-making that advises a pilot whether to attack, flee, apply electronic countermeasures, or fly low-altitude routes. New automation techniques may be necessary for pilots to cope with the fire control systems now being designed for the next generation of military aircraft.

The feasibility of turning sea water into electricity is being studied in fusion energy experiments at Kyoto University in Japan. The studies involve a Hughes gyrotron, a microwave tube that uses a spiraling stream of electrons to produce extremely high power microwave frequencies. Fusion energy holds tremendous potential because its source of fuel (hydrogen) can be extracted from sea water. It could produce large amounts of power with little or no radioactive waste and no threat of meltdown or explosion. In fusion energy research, the gyrotron's high-power radio waves heat hydrogen particles (plasma) to temperatures of tens of millions of degrees. These particles fuse under pressure, causing a thermonuclear reaction that provides energy for driving steam turbines.

A new 5-volt-only, 256-bit nonvolatile random access memory combines the data retention capabilities of an EEPROM with the convenience of a CMOS RAM. The Hughes circuit, designated H13500, is designed for such applications as reconfigurable systems and fault protection without battery back-up. It is organized as 64x4 bits. Both the read and write operations are performed as in a standard CMOS RAM. A single store operation transfers all data in the RAM cells in parallel to the background EEPROM array. The recall operation restores data in parallel to foreground RAM cells.

A broad spectrum of technologies, many of which grew up within the past five years, are represented in the products of Hughes Industrial Electronics Group. Six divisions and two subsidiaries, each operated like a small high-tech company but backed by resources of its multibillion-dollar parent, offer career benefits to qualified engineers and scientists. Advancing technologies such as microwave and millimeter-wave communications, silicon and GaAs solid-state circuitry, fiber optics, and image processing equipment are pursued in facilities located in many of Southern California's most desirable coastal communities. Send your resume to B.E. Price, Hughes Industrial Electronics Group, Dept. S3, P.O. Box 2999, Torrance, CA 90509. Equal opportunity employer. U.S. citizenship required.

For more information write to: P.O. Box 11205, Dept. 67-8, Marina del Rey, CA 90295

HUGHES
AIRCRAFT COMPANY

Mathematics and Information Sciences

Hardware, Techniques, and Processes

154 Algorithms for Software Development
155 Simplified Worst-Case Analysis of Complex Systems
156 Compensating for Range Migration in Synthetic-Aperture Radar
156 Residue-Measure Model-Reduction Technique
157 Encoding Scheme Reduces Hardware Requirements

Books and Reports

158 Vector Lyapunov Functions for Stochastic Interconnected Systems

Algorithms for Software Development

A management aid makes changes obvious.

NASA's Jet Propulsion Laboratory, Pasadena, California

A set of algorithms aids in controlling software development and maintenance. With the algorithms, the people responsible for making changes in programs can easily spot differences between a current version and previous ones. When they are given a new release of a large program, for example, they can readily identify new features without rereading the entire document. Moreover, managers can determine the rate of development and the amounts of new code, modified code, and reused unmodified code. In addition, managers can control the issuance of new versions, ensuring that only the prescribed form is released to customers.

The algorithms can be applied whenever it is possible to attach a six-character code to each record of the source files. (The code is placed within delimiters that cause a compiler to ignore the code field.) The code contains two characters for a check sum of the record, two for the record number in the file, and two for the date on which the encoding took place. Once the source file has been coded in this way, it is possible to detect the following transactions:

- Addition of new records,
- Modification of existing records,
- Deletion of records,
- Movement and duplication of existing records, and
- Modification and duplication of records.

In addition, it is possible to extract a history of record creation and modification by date. A file-listing program prints the file records without showing the six-character version codes, but places a "change bar" at the right margin whenever a change is detected. The program also lists changed pages.

The programer uses a text editor to build and modify program and documentation source files (see figure). At regular intervals, these source files are submitted to the encoding program, which checks each line for the correct check sum. When the check sum is correct — that is it matches the check sum in the code supplied in an earlier run — the date is not changed. If the check sum is in error, the current date is inserted in the date code. Thus, after each run of the encoding program, the source file has a correct check sum code, correct sequence number code, and a date for each line in the file.

Subsequent editing of the file may create new lines, delete old ones, modify characters, move lines, or copy (reuse) existing lines. The combination of the three elements of the line code permits all of these transactions to be detected.

This work was done by Robert C. Tausworthe of Caltech for **NASA's Jet Propulsion Laboratory.** *For further information, Circle 23 on the TSP Request Card.*

NPO-16079

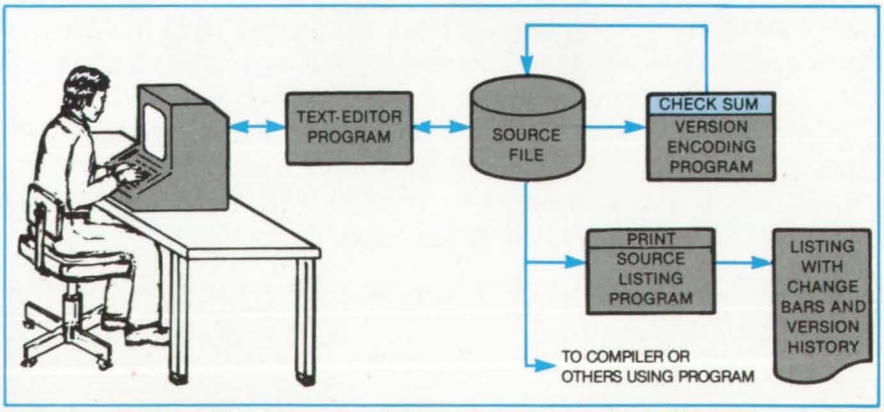

One **Key Element in This Scheme for Software Development Control** is check summing. If the check sum for a given line in a source file is different from that of the previous version, it is evident that a change has been made.

Simplified Worst-Case Analysis of Complex Systems

Statisical method avoids excessive computer time.

Lyndon B. Johnson Space Center, Houston, Texas

In nonlinear systems comprised of many subcomponents, each subcomponent has an ideal operating point and an allowed tolerance for deviations around that ideal. Part of the analysis of such a system involves determining whether or not the deviations could combine to drive the system as a whole out of tolerance. This might happen, for example, if all deviations are near their maximum limits and they add in phase.

Such an analysis requires a certain amount of intuition on the part of the designer and involves invoking probability theory to determine the chances that at any given instant the subcomponent deviations will add up to an out-of-tolerance condition. For a complex system, this analysis can be quite difficult.

A new technique reduces the complexity and expense of worst-case analysis of nonlinear systems having many components. The technique involves a simplified Monte Carlo simulation of the system with randomly chosen parameters and a comparison of the tolerance extremes of several of worst-case situations found. The resulting combination of tolerance extremes is then used in a detailed analysis — one that makes use of a full complex nonlinear model capable of accurate simulations.

The technique has been used in an evaluation of a complex nonlinear system — the quadruply-redundant actuator system of the Space Shuttle — to prevent erroneous isolation of good channels. The complexity of the system prevented an intuitive assignment of the polarities of the worst-case combinations. Moreover, the nonlinear behavior of the system precluded an analytical statistical approach. A sufficient number of Monte Carlo runs with a complex, high-accuracy model would have been prohibitively expensive. The new technique permitted the design objective to be met with a simple and cheap model for the Monte Carlo runs and a few runs on the high-accuracy model.

The procedure is as follows:

- Calculate the probability functions for the maximum tolerable, nominal, and minimum tolerable values of each operating parameter (for example, see table).
- Run the required number of randomly chosen cases on the Monte Carlo simulation using the three-valued tolerance distributions. The required number of cases depends on the situation, but good results were obtained for the Space Shuttle actuator system with 1,000 cases.
- Among the simulations, choose the 5 to 10 with the lowest design margins.
- For each random parameter, compare the tolerance polarities among the 5 or 10 worst cases to determine whether that tolerance is in the same direction in most cases. If so, that direction is considered the worst-case polarity.
- Set the worst-case parameters to the worst-case polarity.
- Rerun the Monte Carlo simulation. Parameters found to have the same tolerance polarity as the 5 or 10 worst cases constitute a second generation of worst-case parameters. The combination of first- and second-generation parameters becomes a new generation of worst-case parameters.
- After two or three generations of worst-case parameters are found, those that still appear randomly distributed are probably not contributors to the worst-case situation. These parameters can be set to their nominal values. The worst-case polarities found thus far are considered to represent the worst-case combination of tolerances.
- Substitute the worst-case combination into the complex design model for a high-accuracy analysis.

If worst-case conditions for additional design requirements are needed, the procedure is repeated for each requirement.

This work was done by Charles L. Pond of Rockwell International Corp. for **Johnson Space Center.** *For further information, Circle 6 on the TSP Request Card.*

MSC-20232

Parameter	Nominal Value	Tolerance
Servo-Valve Null Offset	0	±0.60 mA
ASA and MDM Null Offset	0	±0.078 V
Position Transducer Offset	0	±0.064 V
Secondary Pressure Transducer Offset	0	±180. psi
Secondary Pressure Transducer Hysteresis	0	0
MDM Scale-Factor Error	0	0
Command/Position Summing Ratio Error	0	±2.1%
Transducer-Excitation Supply Voltage Error	0	±2.3%
Command/Position Scale Factor	0.181 V/°	0
Servoamplifier Gain	13.5 mA/V	±1.3%
Servo-Valve Pressure Gain	500 psi/mA	±100 psi/mA
Equalization Feedback Gain	0.0124 V/psi	±3.5%
Equalization Lag Time Constant	1.7 s	±6.24%
Equalization Authority	44.8 psi	±10.1%
Equalization Dead Band, Low Side	−1,250 psi	±3.1%
Equalization Dead Band, High Side	1,250 psi	±3.1%
ASA Driver Current Limiter	9.4 mA	±0.9%
Fault Monitor Threshold Level	2,025 psi	±5.0%
Fault Monitor Trip Time	0.12 s	±0.02 s

Parameters and Tolerances representative of a multicomponent nonlinear system are those for the Space Shuttle rudder-actuator system. The simplified Monte Carlo method enables relatively quick identification of the likely worst-case combinations of individual parameters.

Compensating for Range Migration in Synthetic-Aperture Radar

A correlation algorithm sharpens radar imagery.

NASA's Jet Propulsion Laboratory, Pasadena, California

An algorithm compensates for excessive range migration in synthetic-aperture-radar (SAR) imagery. Range migration is not a serious problem in terrestrial and airborne radars, but can be significant in satellites, where the orbital speed or the rotation of the Earth causes perceptible target movement between resolution elements. Because vehicle speed poses a similar problem with regard to sonar, the algorithm may have terrestrial applications in this field.

The first step in developing the algorithm is to model the response of a point target. This response takes the form of a two-dimensional convolution in the azimuth and range coordinates, weighted by the radar amplitude and phase modulation and by the azimuthal antenna pattern. The round-trip path length is approximated to second order in the azimuth coordinate.

It is assumed that the transmitted radar pulse is a linear frequency-modulated pulse of constant amplitude, so that range pulse compression would yield an impulse response of the familiar form (sin x)/x. With this and the other assumptions, the range-correlated point-target response is dispersed along the azimuth axis to a degree determined by the radar-beam width, and along the range axis by the variation in the range distance between the target and the radar set.

The azimuthal correlation of the point-target response is performed in the frequency domain by fast Fourier transforms, which are relatively efficient in arithmetic operations. The frequency-domain azimuthal response has a simple form that enables the correction for the range migration to be made simultaneously and over a wide area, thereby providing many picture elements.

The SAR echo response of an extended target of spatially varying reflectivity is treated as a superposition of the responses of many point targets. This is expressible as a two-dimensional convolution. A reconstructed target image is obtained by a correlation algorithm as follows:

- A secondary range compression is performed as a range correlation of the range-correlated echo signal with a weighting function that depends on the bandwidth and on the Doppler quantities.
- An azimuth two-dimensional correlation is performed by taking the inverse Fourier transform of the composite spectrum obtained by extracting data along the range-migration curve in the azimuth spectral domain and then multiplying by the ratio of the range-correlated point-target response to the azimuthal antenna pattern.

This work was done by Michael Y. Jin and Chialin Wu of Caltech for **NASA's Jet Propulsion Laboratory.** *For further information, Circle 8 on the TSP Request Card. NPO-15954*

Residue-Measure Model-Reduction Technique

A dynamic model is simplified by eliminating modes with small residues.

Lyndon B. Johnson Space Center, Houston, Texas

A new residue-measure criterion simplifies mathematical models of feedback-control systems. Although originally developed for flight control, this approach can be applied to any flexible structural system involving dominantly linear dynamics.

The design and analysis of a control system require high fidelity in plant representation. When the plant is a flexible structure, a model with a finite number of terms must be chosen to represent the infinite dimensionality of the system. First, a representation of the vibrational modes of the structure is generated. Next, the series of modes must be truncated in such a way that the model is susceptible to numerical analysis yet adequately predicts the behavior of the system.

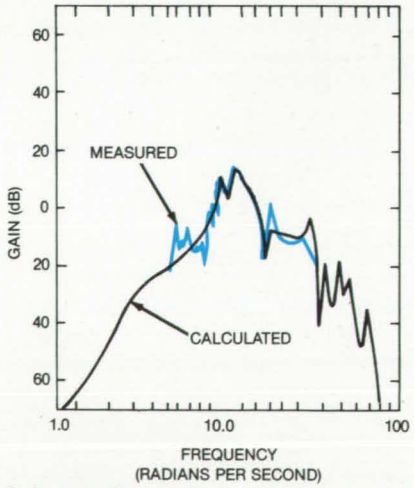

Roll-Loop Response as calculated (black line) and measured (color line) are shown here.

The dynamics of many systems of interest can be described by linear second-order matrix equations. The size of the matrices increases with each additional oscillation mode included. The computing time required to solve the equations increases much faster than linearly in the size of the matrices. However, the effect of some modes on system response is much less than that of others. Thus at some point the inclusion of additional modes of ever lesser importance affects the cost of the analysis far beyond their value in improving the knowledge of system response.

The new residue-measure criterion is based on identifying poles of the open-loop system transfer function and ranking their importance according to the magnitudes of their residues. Some en-

gineering judgment is required for this task. The criterion is justified by the fact that the residue is a direct measure of the controllability and observability of each mode. Phasing is not considered directly. It is assumed that unless the magnitude of a mode is large, it will not significantly affect the gain and/or phase of the complex open-loop system and that a sufficient number of modes is retained to ensure that, cumulatively, the discarded modes have insignificant residues.

The technique was applied to the Space Shuttle attitude-control system. The free/free modes of the vehicle were generated using a Rayleigh-Ritz procedure. A total of 31 mode frequencies and their roll, yaw, and pitch residues were calculated. Fifteen modes were selected for the pitch-axis model. Since the lateral axis involved both roll and yaw residues, modes with large residues in both axes were included first. Where only one axis had a large residue and the physical characteristics of the mode (for example, wing motion or tail bending) suggested that the mode might be important in the axis with the smaller residue, it was included in the lateral mode set.

Following this mode-selection process, system-response tests were performed. Sweep-frequency and step-command excitations were applied to the control surfaces while the Shuttle was sitting in a building supported on its tires. As shown in the figure, a comparison of the experimental and calculated responses for the roll loop showed fairly good agreement.

This work was done by David P. Gluch of Honeywell Inc. for **Johnson Space Center.** *For further information, Circle 69 on the TSP Request Card.*
MSC-20369

Encoding Scheme Reduces Hardware Requirements

A shift register is time-shared in a proposed error-correcting code for tape-storage systems.

Lyndon B. Johnson Space Center, Houston, Texas

A proposed encoding/decoding system would correct random burst errors of up to 80 consecutive bits within a block of 4,096 information bits. While designed primarily to compensate for data dropouts caused by oxide loss from magnetic tape, the scheme could improve the error-correcting capability of any serial data stream subject to burst errors.

The high error-correcting capability of the system is due to the combination of 16-level interleaving with a Fire code of 270-bit (14-check-bit and 256-data-bit) code words. Without interleaving, the Fire code corrects burst errors of up to 5 bits in each word. With interleaving, an 80-bit burst error is distributed over 16 code words in 5-bit errors per word. Thus, the 80-bit error can be corrected.

The encoded data are transmitted in blocks of 4,320 bits comprising 4,096 information bits plus 224 parity-check bits for the Fire code. To prepare the data for transmission, they are entered in a random-access memory (RAM). Bits from the input serial stream are placed in RAM locations that are addressed by a modified 13-bit up counter. Interleaving is accomplished by addressing the memory locations sequentially in the input-bit order, modulo 16. The carry logic of the counter is alterable under switch control, so that interleaving and deinterleaving are accomplished by the same circuit.

The interleaved data in the RAM are initially arranged in 16 code words of 256 information bits each and expanded

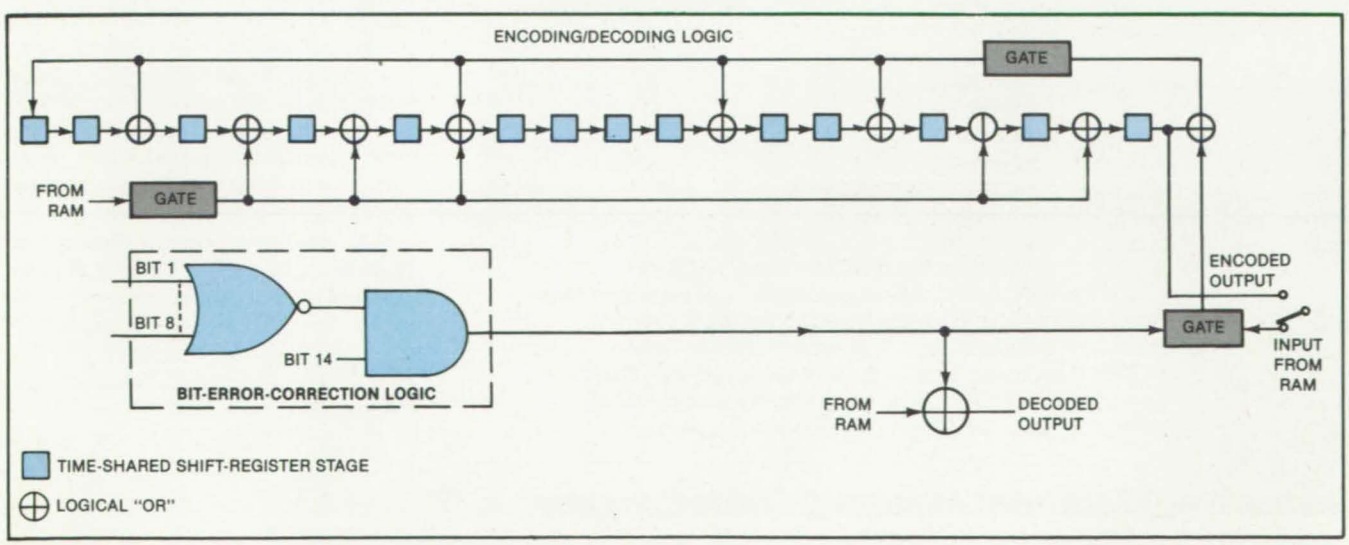

Error-Correcting Code logic for blocks of 256-bit data words is implemented by a 14-stage time-shared shift register, two 4,096-bit RAM's, and logic gates. Encoding and decoding logic implement a generator polynomial that defines the error-correcting code, and error correction is based on an algorithm also implemented by the logic.

during processing to 270 bits each with the addition of 14 check bits to each word. In the encoder logic a single 14-bit time-shared shift register located in the feedback loop of the RAM acts in place of 16 shift registers that would ordinarily be used if the scheme were to be implemented with conventional logic circuitry. As the interleaving and encoding progress, data and parity-check bits are taken from the RAM, passed through the shift register, and placed back in the RAM in the proper Fire-code sequence to form the 270-bit code words. Decoding is performed by the same logic, and error correction is performed by circuitry that implements the error-correcting algorithm.

The proposed system (see figure) requires less hardware than a previous design. Only two 4,320-bit RAM's are needed. The logic circuit is adaptable to other data-stream word formats by modifying the logic to implement a generator polynomial that defines the data-encoding and error-correction algorithms.

This work was done by Harold Sasnowitz of IBM Corp. for **Johnson Space Center.** *For further information, Circle 36 on the TSP Request Card.*
MSC-20044

Books and Reports

These reports, studies, and handbooks are available from NASA as Technical Support Packages (TSP's) when a Request Card number is cited; otherwise they are available from the National Technical Information Service.

Vector Lyapunov Functions for Stochastic Interconnected Systems

A stability criterion is developed for composite systems.

A theoretical paper presents a set of sufficient conditions for asymptotic and exponential stability with probability 1 for a class of stochastic interconnected systems. The theory is applicable to complicated, large-scale mechanical or electrical systems, and, for several design problems, it reduces the computational difficulty by relating the stability criteria to the fundamental structural features of the system.

First, subsystem Lyapunov functions are used to construct a vector Lyapunov function for the composite system.

Then a system of linear or nonlinear stochastic differential inequalities satisfied by the vector Lyapunov function is formed, depending upon the isolated-subsystem models, the interconnecting structure, and a constant parameter vector, the optima selection of which widens the domain of systems to which the method is applied.

A linear comparison system is obtained by replacing the inequalities with equalities. It is shown that for a class of stochastic interconnected subsystems, the stability of the linear comparison system is sufficient to assure the asymptotic or exponential stability of the stochastic interconnected system with probability 1.

The new stability criterion has been applied to an experimental pointing and tracking system with one degree of freedom. The system consists of an optical tracker and gyroscope mounted on a platform driven by a brushless dc torque motor, which in turn is mounted on an air-bearing rotating table. A nonlinear five-dimensional system of equations provides a simplified model of the motor, the air-bearing table, the gyroscope, and their interconnections.

This work was done by Dhemetrios Boussalis of Caltech for **NASA's Jet Propulsion Laboratory.** *To obtain a copy of the paper, "Vector Lyapunov Functions for a Class of Stochastic Interconnected Systems," Circle 13 on the TSP Request Card.*
NPO-16170

SATELLITE OPERATIONS

Discover the challenges in the field of Satellite Operations that will place you in the forefront of America's most advanced technological environment.

We have immediate career opportunities in Sunnyvale, CA for individuals with NASA Shuttle Flight Operations experience in one or more of the following:

- Satellite Operations
- Orbits
- DSM
- Communications
- Network
- Command and Control
- Simulation
- Telemetry
- Support Planning & Readiness Activities

If you have a BS or advanced degree in an applicable field or equivalent experience, Lockheed invites you to join the team. Send your resume to Professional Staffing, Dept. 512CF27, Lockheed Missiles & Space Company, P.O. Box 3504, Sunnyvale, CA 94088-3504. We are an equal opportunity, affirmative action employer. U.S. citizenship is required.

Lockheed Missiles & Space Company
Giving shape to imagination.

Circle Reader Action No. 12

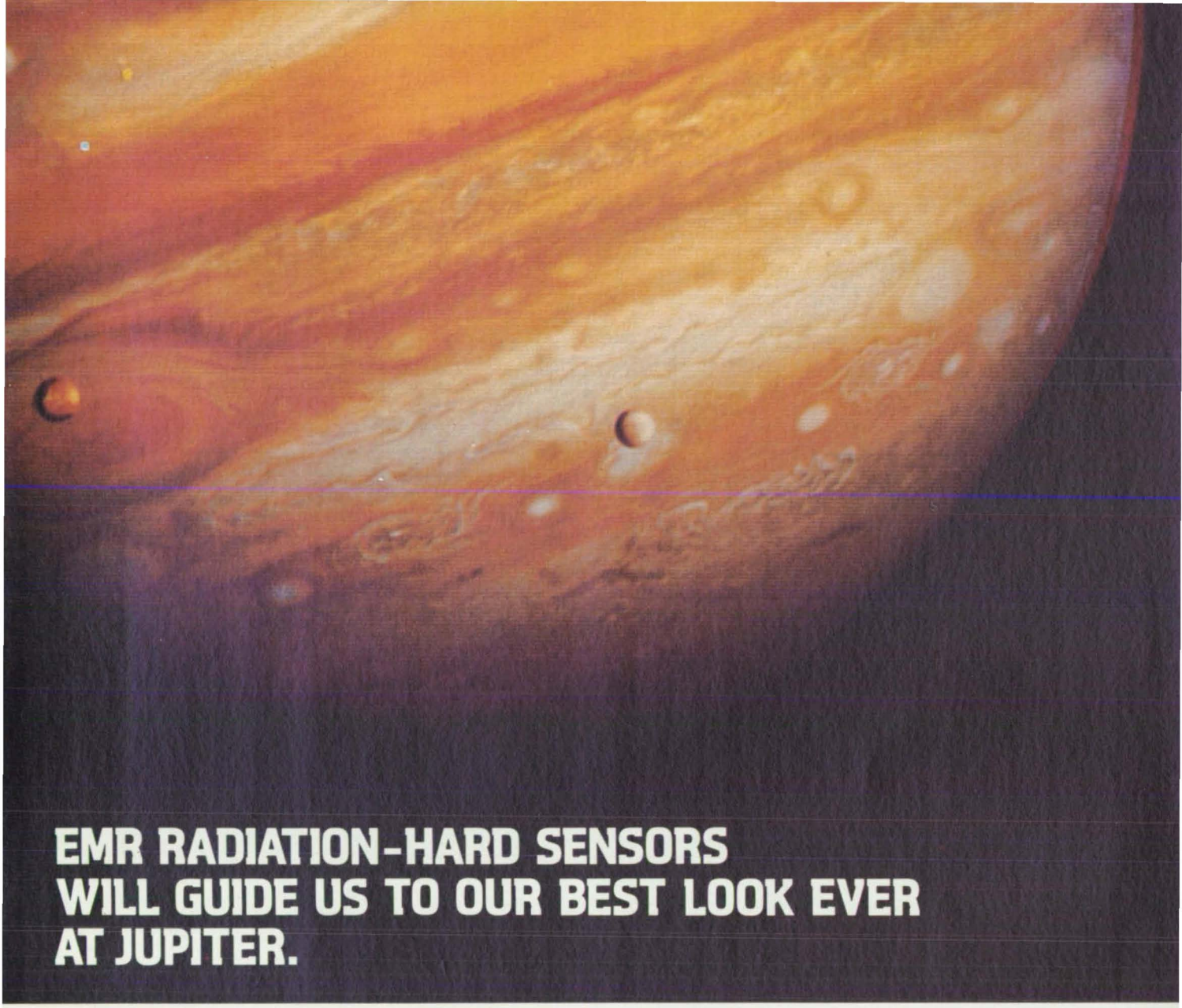

EMR RADIATION-HARD SENSORS WILL GUIDE US TO OUR BEST LOOK EVER AT JUPITER.

The Jovian radiation belts can wreak havoc with traditional photoelectronic sensors. The high-energy electron flux — more than 10^9 e/cm²/sec — can cause false signals and a reduction in detector efficiency, problems unacceptable in NASA's most important mission to Jupiter yet.

So a team of scientists and engineers at EMR and JPL designed a radiation-hard photomultiplier tube especially for the Galileo Star Tracker.

The result? A lightweight, five-inch-long PMT with a special radiation-resistant window and ceramic body. Continuous exposure to a cobalt 60 Jupiter simulation environment proves the new tube to be *40 times less sensitive* to radiation-induced noise than conventional glass-envelope PMTs.*

The same tube is available now, here on earth, for military or industrial assignments from EMR, the world's leader in the application of technology to tough environmental problems of photoelectronic sensors.

*M.M. Birnbaum, R.L. Bunker, J. Roderick, K. Stephenson; Development of Radiation Hard Photomultiplier Tube; AIAA Guidance and Control Conference, August 20-22, 1984. AIAA-84-1852.

EMR MODEL 730N-01-12, a radiation-hard photomultiplier tube, will stabilize the Galileo spacecraft when it orbits Jupiter. The ceramic-envelope tube — with its thin, small-diameter glass window and special electron-focusing design — minimizes fluorescence and Cerenkov emissions caused by high-energy electron and proton emissions.

For more information call or write:

EMR Schlumberger EMR PHOTOELECTRIC

P.O. Box 44, Princeton, NJ 08542 • 609-799-1000

Circle Reader Action No. 25

Subject Index

A

ACCELEROMETERS
Superconducting-cavity accelerometer
page 120 GSC-12797

ACCESS CONTROL
Synchronizing data-bus messages
page 66 MSC-20640

ACOUSTIC LEVITATION
Hybrid contactless heating and levitation
page 144 NPO-15657

AEROEMBOLISM
Effect of hydration on nitrogen washout in humans
page 113 MSC-20686

AEROSOLS
Laser-assisted analysis of aerosol particles
page 86 NPO-15308

AIRCRAFT CONTROL
Aircraft control-position indicator
page 54 LAR-12984

ALGORITHMS
Compensating for range migration in synthetic-aperture radar
page 156 NPO-15954

Algorithms for software development
page 154 NPO-16079

ALIGNMENT
Out-of-focus alinement of solar concentrators
page 75 NPO-15563

ALUMINUM
Purifying aluminum by vacuum distillation
page 96 NPO-16114

AMMETERS
Lowering ammeter input impedance
page 55 NPO-16067

ANASTIGMATISM
Nearly anastigmatic X-ray telescope
page 77 MFS-25984

ANTENNAS
Dual-mode horn antenna for millimeter wavelengths
page 42 NPO-16297

Automatic erection system for antenna masts
page 139 LAR-13115

AUDITORY DEFECTS
Telephone instrument for the deaf
page 48 KSC-11303

AUTOMATIC CONTROL
Back-pressure regulator for large gas flows
page 131 MSC-20536

B

BACKUPS
Double light-emitting diode
page 49 GSC-12832

BACTERIA
Coculture production of butinol by clostridium bacteria
page 113 NPO-16203

BAFFLES
Telescope with reflecting baffle
page 74 ARC-11502

BALANCING
Microprocessor-controlled laser balancing system
page 118 LEW-13294

BALL BEARINGS
Further tests of 38 ball-bearing greases
page 111 MFS-27043

BATTERY CHARGERS
Flux coupling for wheelchair battery chargers
page 43 NPO-16269

BEAMS (SUPPORTS)
Deployable M-braced truss
page 123 LAR-13081

BEARINGS
Air bearing for small planar vibrations
page 132 MFS-26003

BIOCONVERSION
Coculture production of butinol by clostridium bacteria
page 113 NPO-16203

BOLTS
Fastening parts having mismatched thermal coefficients
page 137 LAR-13009

BONDING
Bonded and bolted graphite/polyimide composite joints
page 150 LAR-13090

BOOSTER RECOVERY
Rocket-booster towing simulation
page 125 KSC-11289

BOUNDARY LAYER CONTROL
Performance improvement for nonaxisymmetric nozzles
page 138 LAR-13036

BRACKETS
Universal cable brackets
page 149 MFS-26001

BRAKING
Mechanical mixer for rudder/braking wedge
page 141 MSC-20759

BRIGHTNESS DISCRIMINATION
Finding bright-spot coordinates in television images
page 65 MFS-25999

BUFFER STORAGE
FIFO buffer for asynchronous data streams
page 67 MSC-20403

BUTYRIC ACID
Coculture production of butinol by clostridium bacteria
page 113 NPO-16203

C

CANOPIES
Aircraft canopy lock
page 114 FRC-11065

CAVITY RESONATORS
Superconducting-cavity accelerometer
page 120 GSC-12797

CERAMIC COATINGS
Ceramic coatings for engine parts
page 94 NPO-16228

CERAMICS
Improving emittance of high-temperature insulating tile
page 108 MSC-20714

CHARGE COUPLED DEVICES
Hybrid fiber-optic/CCD chip
page 38 NPO-16030

CHARGE EFFICIENCY
Battery-charge-state model
page 87 NPO-16158

CHIPS
Designing test chips for custom integrated circuits
page 64 NPO-15988

CIRCUIT PROTECTION
Protective cover for IC packages
page 46 NPO-15537

CLAMPS
Universal cable brackets
page 149 MFS-26001

Wide-grasp latching mechanism
page 141 MFS-28002

CLEANLINESS
Copyboard quickly makes clean printing plates
page 152 ARC-11365

CLOCKS
Satellite time- and frequency-transfer system
page 68 MFS-28010

Fast clock recovery for digital communications
page 53 NPO-16083

Synchronization for optical PPM signals
page 68 NPO-16256

CLOUDS
Measuring clouds with microwaves and infrared
page 75 NPO-16265

Estimates of latent heat in clouds
page 85 MFS-25977

CMOS
Dynamic-RAM data-storage unit
page 62 LEW-14017

FIFO buffer for asynchronous data streams
page 67 MSC-20403

CODING
Algorithms for software development
page 154 NPO-16079

COLOR PHOTOGRAPHY
Vision screening by color photography
page 112 MFS-25800

COLUMNS
Inflatable column structure
page 116 NPO-16216

COMBUSTION CHAMBERS
Low-loss fuel and oxidizer injector
page 127 MFS-25989

COMPOSITE MATERIALS
Resin characterization in cured composite materials
page 103 LAR-13172

Strength of graphite/metal composite lap joints
page 110 MFS-27030

COMPUTER PROGRAMS
Algorithms for software development
page 154 NPO-16079

CONCENTRATORS
Out-of-focus alinement of solar concentrators
page 75 NPO-15563

CONTAINERLESS MELTS
Hybrid contactless heating and levitation
page 144 NPO-15657

CONTROL EQUIPMENT
Power-factor controllers: How safe?
page 57 MFS-27016

COOLERS
Long-life cryogenic cooler
page 140 GSC-12697

COORDINATES
Finding bright-spot coordinates in television images
page 65 MFS-25999

COUPLINGS
Flux coupling for wheelchair battery chargers
page 43 NPO-16269

CRYOGENIC COOLING
Long-life cryogenic cooler
page 140 GSC-12697

CRYOGENIC EQUIPMENT
Foam insulation for cryogenic flowlines
page 96 MSC-20552

CRYSTAL GROWTH
Preparation and characterization of $Hg_xCd_{1-x}Te$
page 110 MFS-27037

Efficient process for making polycrystalline silicon
page 104 NPO-16121

Variable-temperature-gradient device for solidification research
page 73 MFS-26008

CUSHIONS
Air bearing for small planar vibrations
page 132 MFS-26003

CUTTERS
Cutthrough warning circuit
page 142 MFS-19900

Cutting guide for fibrous sheets
page 151 MSC-20798

CYANIDES
Solar-assisted oxidation of toxic cyanide
page 106 LAR-13171

D

DAMPERS (VALVES)
Quasi-porous plug with vortex chamber
page 133 NPO-16076

DATA BUSSES
Synchronizing data-bus messages
page 66 MSC-20640

DATA STORAGE
Dynamic-RAM data-storage unit
page 62 LEW-14017

DECODING
Telephone instrument for the deaf
page 48 KSC-11303

DECOMPRESSION SICKNESS
Effect of hydration on nitrogen washout in humans
page 113 MSC-20686

DEGRADATION
Environmental degradation of solar reflectors
page 88 NPO-16053

DETECTION
Sensitivities of soap solutions in leak detection
page 143 MFS-19864

DIFFERENTIAL THERMAL ANALYSIS
Preparation and characterization of $Hg_xCd_{1-x}Te$
page 110 MFS-27037

DIGITAL COMMUNICATION
Fast clock recovery for digital communications
page 53 NPO-16083

DIGITAL DATA
FIFO buffer for asynchronous data streams
page 67 MSC-20403

Storing data and video on one tape
page 59 MSC-20705

DIODES
Fast-recovery high-voltage power diode
page 49 LEW-14036

Damping relaxation oscillations in laser diodes
page 45 NPO-15980

DISCRIMINATORS
Segmented detector for cosmic gamma rays
page 82 NPO-16245

DISPLAY DEVICES
Digital high-current monitor
page 39 LAR-13072

High-visibility data display
page 58 MFS-19925

DISTILLATION
Purifying aluminum by vacuum distillation
page 96 NPO-16114

DROPS (LIQUIDS)
Calibrating-droplet generator for pressurized testing vessel
page 119 MFS-25992

DUCTS
Foam insulation for cryogenic flowlines
page 96 MSC-20552

DYNAMIC MODELS
Residue-measure model-reduction technique
page 156 MSC-20369

E

ELECTRIC BRIDGES
Tiltmeter indicates sense of slope
page 40 NPO-16153

ELECTRIC COILS
Recovering energy from relays
page 47 NPO-16268

ELECTRIC CURRENT
Digital high-current monitor
page 39 LAR-13072

ELECTRIC DISCHARGES
Flushing ring for EDM
page 131 MFS-19876

ELECTRIC EQUIPMENT
Power-factor controllers: How safe?
page 57 MFS-27016

ELECTRIC POWER PLANTS
Photovoltaics in Japan
page 57 NPO-16330

ELECTRIC RELAYS
Recovering energy from relays
page 47 NPO-16268

ELECTROCHEMICAL CELLS
Thermally-rechargeable electrochemical cell
page 78 NPO-16273

ELECTRON MICROSCOPES
Measuring recombination velocities in solar cells
page 36 NPO-16243

ELECTRONIC PACKAGING
Protective cover for IC packages
page 46 NPO-15537

ELECTROSTATIC SHIELDING
High-voltage isolation transformer
page 52 GSC-12817

EMITTANCE
Improving emittance of high-temperature insulating tile
page 108 MSC-20714

ENCODING
Encoding scheme reduces hardware requirements
page 157 MSC-20044

ENERGY CONVERSION EFFICIENCY
Hinged-blade, vertical-shaft windmill
page 134 MFS-25980

Solar cells with multiple small junctions
page 55 NPO-16126

ENGINE PARTS
Ceramic coatings for engine parts
page 94 NPO-16228

EPOXY RESINS
Increasing fire safety of epoxies
page 94 ARC-11506

ERECTION
Automatic erection system for antenna masts
page 139 LAR-13115

ERROR ANALYSIS
Complementary-logic fault detector
page 51 NPO-15410

ERROR CORRECTING CODES
Encoding scheme reduces hardware requirements
page 157 MSC-20044

ESTERS
Ethynyl-terminated ester oligomers and polymers
page 107 LAR-13118

EXPLOSIVES
Predicting effects of impacts on confined explosives
page 111 NPO-16258

EYE EXAMINATIONS
Vision screening by color photography
page 112 MFS-25800

F

FABRICATION
Precise fabrication of electromagnetic-levitation coils
page 146 MFS-25986

G

FASTENERS
Aircraft canopy lock
page 114 FRC-11065

Fastening parts having mismatched thermal coefficients
page 137 LAR-13009

FAULT TOLERANCE
Complementary-logic fault detector
page 51 NPO-15410

FERMENTATION
Coculture production of butinol by clostridium bacteria
page 113 NPO-16203

FIBER OPTICS
Hybrid fiber-optic/CCD chip
page 38 NPO-16030

FIBERS
Making stronger twine with matched strands
page 148 MSC-20444

FIBROUS MATERIALS
Cutting guide for fibrous sheets
page 151 MSC-20798

FILLETS
High-performance filleting and channel sealants
page 95 ARC-11408

FINGERS
Wide-grasp latching mechanism
page 141 MFS-28002

FIRE PROOFING
Increasing fire safety of epoxies
page 94 ARC-11506

FLAME RETARDANTS
Rubberized, brominated epoxies
page 109 ARC-11427

FLASH LAMPS
Altering flashlamp output for realistic solar simulation
page 82 NPO-16167

FLIGHT CONDITIONS
Remotely piloted aircraft for research
page 143 ARC-11498

FLIGHT INSTRUMENTS
Aircraft control-position indicator
page 54 LAR-12984

FLOW VISUALIZATION
Continuous laminar-smoke generator
page 116 LAR-13014

FLUID BOUNDARIES
Spill-detector-and-shutoff device
page 129 MSC-20206

FLUID PRESSURE
Contact heat exchanger
page 117 MSC-20419

FLUIDIZED BED PROCESSORS
High-purity silicon seeds for fluidized bed silane pyrolysis
page 90 NPO-16287

FLUSHING
Flushing ring for EDM
page 131 MFS-19876

FOLDING STRUCTURES
Hinged-blade, vertical-shaft windmill
page 134 MFS-25980

FRAMES
Deployable M-braced truss
page 123 LAR-13081

FREQUENCY MODULATION
Damping relaxation oscillations in laser diodes
page 45 NPO-15980

FUEL CELLS
Methanol fuel cell
page 79 NPO-15823

FUEL INJECTION
Low-loss fuel and oxidizer injector
page 127 MFS-25989

FURNACES
High-temperature Hall-effect apparatus
page 69 NPO-16279

GAMMA RAYS
Protective package for a gamma-ray detector
page 72 NPO-16019

Segmented detector for cosmic gamma rays
page 82 NPO-16245

GAS FLOW
Simulating pressure effects of high-flow volumes
page 126 MFS-19909

Back-pressure regulator for large gas flows
page 131 MSC-20536

GLASS
Reversing glass wettability
page 100 MFS-26006

GLOBAL POSITIONING SYSTEM
Doubly-differenced measurements for orbit determinations
page 71 NPO-16111

GRAPHITE-EPOXY COMPOSITES
Rubberized, brominated epoxies
page 109 ARC-11427

GRAPHITE-POLYIMIDE COMPOSITES
Bonded and bolted graphite/polyimide composite joints
page 150 LAR-13090

GRAZING INCIDENCE
Nearly anastigmatic X-ray telescope
page 77 MFS-25984

GREASES
Further tests of 38 ball-bearing greases
page 111 MFS-27043

H

HALL EFFECT
High-temperature Hall-effect apparatus
page 69 NPO-16279

HEAT
Estimates of latent heat in clouds
page 85 MFS-25977

HEAT EXCHANGERS
Contact heat exchanger
page 117 MSC-20419

Reciprocating magnetic refrigerator
page 130 NPO-16257

HEATING EQUIPMENT
Differential temperature control of electrical heaters
page 123 LAR-13047

HIGH TEMPERATURE
High-temperature Hall-effect apparatus
page 69 NPO-16279

HIGH VOLTAGES
Fast-recovery high-voltage power diode
page 49 LEW-14036

HOLDERS
Ultrahigh-vacuum sample-transfer system
page 86 LAR-12993

Manipulator for heating and cooling in ultrahigh vacuum
page 80 LAR-13040

Spring-loaded transducer holder
page 122 LAR-13048

Cutting guide for fibrous sheets
page 151 MSC-20798

HORN ANTENNAS
Dual-mode horn antenna for millimeter wavelengths
page 42 NPO-16297

HYBRID CIRCUITS
Hybrid fiber-optic/CCD chip
page 38 NPO-16030

HYDRATION
Effect of hydration on nitrogen washout in humans
page 113 MSC-20686

HYDROGEN PRODUCTION
Methanol fuel cell
page 79 NPO-15823

I

IMAGERY
SAW-modulated image device
page 44 LAR-12633

Imaging spectrometer for geophysical surveys
page 76 NPO-16072

IMAGING TECHNIQUES
Finding bright-spot coordinates in television images
page 65 MFS-25999

Wide-angle, wide-band camera for remote imaging
page 81 NPO-15799

IMIDES
Synthesizing metal phthalocyanine imide polymers
page 105 ARC-11413

IMPACT PRESSURES
Predicting effects of impacts on confined explosives
page 111 NPO-16258

IMPACT RESISTANCE
Rubberized, brominated epoxies
page 109 ARC-11427

IMPEDANCE
Lowering ammeter input impedance
page 55 NPO-16067

INDUCTORS
Precise fabrication of electromagnetic-levitation coils
page 146 MFS-25986

INDUSTRIAL WASTES
Solar-assisted oxidation of toxic cyanide
page 106 LAR-13171

INFRARED DETECTORS
Preparation and characterization of $Hg_xCd_{1-x}Te$
page 110 MFS-27037

INFRARED IMAGERY
Infrared linear imaging array
page 56 NPO-15805

INFRARED RADIATION
Measuring clouds with microwaves and infrared
page 75 NPO-16265

INTEGRATED CIRCUITS
Protective cover for IC packages
page 46 NPO-15537

Designing test chips for custom integrated circuits
page 64 NPO-15988

INTERPROCESSOR COMMUNICATION
Synchronizing data-bus messages
page 66 MSC-20640

INTERROGATION
Self-identifying reflecting targets
page 65 NPO-16106

ISOLATORS
High-voltage isolation transformer
page 52 GSC-12817

J

JOINTS (JUNCTIONS)
Bonded and bolted graphite/polyimide composite joints
page 150 LAR-13090

L

LAMINAR FLOW
Continuous laminar-smoke generator
page 116 LAR-13014

LAMINATES
Photovoltaic-panel laminator
page 145 NPO-16092

LAMINATING
Perforating thin metal sheets
page 146 ARC-11280

LAP JOINTS
Strength of graphite/metal composite lap joints
page 110 MFS-27030

LASERS
Shielding against intense laser beams
page 97 NPO-16166

Laser-assisted analysis of aerosol particles
page 86 NPO-15308

Microprocessor-controlled laser balancing system
page 118 LEW-13294

Calibrating-droplet generator for pressurized testing vessel
page 119 MFS-25992

LATCHES
Aircraft canopy lock
page 114 FRC-11065

Wide-grasp latching mechanism
page 141 MFS-28002

LEAD ACID BATTERIES
Battery-charge-state model
page 87 NPO-16158

LEAKAGE
Sensitivities of soap solutions in leak detection
page 143 MFS-19864

LEVITATION
Precise fabrication of electromagnetic-levitation coils
page 146 MFS-25986

Hybrid contactless heating and levitation
page 144 NPO-15657

LIAPUNOV FUNCTIONS
Vector Lyapunov functions for stochastic interconnected system
page 158 NPO-16170

LIGHT EMITTING DIODES
Double light-emitting diode
page 49 GSC-12832

LINEAR EQUATIONS
Residue-measure model-reduction technique
page 156 MSC-20369

LINKAGES
Continuously variable transmission
page 128 LAR-12844

LIQUID CHROMATOGRAPHY
Spill-detector-and-shutoff device
page 129 MSC-20206

LOGIC CIRCUITS
Complementary-logic fault detector
page 51 NPO-15410

M

MACHINE TOOLS
Flushing ring for EDM
page 131 MFS-19876

MAGNETIC STORAGE
Recovering energy from relays
page 47 NPO-16268

MAGNETIC TAPES
Encoding scheme reduces hardware requirements
page 157 MSC-20044

MANIPULATORS
Ultrahigh-vacuum sample-transfer system
page 86 LAR-12993

Manipulator for heating and cooling in ultrahigh vacuum
page 80 LAR-13040

MASS SPECTROSCOPY
Laser-assisted analysis of aerosol particles
page 86 NPO-15308

MATHEMATICAL MODELS
Battery-charge-state model
page 87 NPO-16158

MECHANICAL DRIVES
Mechanical mixer for rudder/braking wedge
page 141 MSC-20759

Continuously variable transmission
page 128 LAR-12844

MECHANICAL PROPERTIES
Resin characterization in cured composite materials
page 103 LAR-13172

Strength of graphite/metal composite lap joints
page 110 MFS-27030

MELTS (CRYSTAL GROWTH)
Melt stirring by horizontal crucible vibration
page 98 MFS-26005

MERCURY CADMIUM TELLURIDES
Preparation and characterization of $Hg_xCd_{1-x}Te$
page 110 MFS-27037

METAL COATINGS
Spray application of rapidly solidified metals
page 150 GSC-12880

METAL CUTTING
Cutthrough warning circuit
page 142 MFS-19900

METAL SHEETS
Perforating thin metal sheets
page 146 ARC-11280

METHYL ALCOHOLS
Methanol fuel cell
page 79 NPO-15823

MICROCIRCUITS
Infrared linear imaging array
page 56 NPO-15805

MICROELECTRONICS
Designing test chips for custom integrated circuits
page 64 NPO-15988

MICROPROCESSORS
Redundant asynchronous microprocessor system
page 63 ARC-11348

Microprocessor-controlled laser balancing system
page 118 LEW-13294

MICROWAVE ANTENNAS
Improved thick dichroic reflector for microwave feeds
page 39 NPO-13506

Dual-mode horn antenna for millimeter wavelengths
page 42 NPO-16297

MICROWAVE RADIATION
Measuring clouds with microwaves and infrared
page 75 NPO-16265

MILLIMETER WAVES
Dual-mode horn antenna for millimeter wavelengths
page 42 NPO-16297

MIRRORS
Telescope with reflecting baffle
page 74 ARC-11502

MIXING
Melt stirring by horizontal crucible vibration
page 98 MFS-26005

MONITORS
Digital high-current monitor
page 39 LAR-13072

High-visibility data display
page 58 MFS-19925

MONTE CARLO METHOD
Simplified worst-case analysis of complex systems
page 155 MSC-20232

MOTION STIMULATORS
Rocket-booster towing simulation
page 125 KSC-11289

MULTIPLEXING
Single-frequency multitransmitter telemetry
page 70 LAR-13006

N

NITROGEN
Effect of hydration on nitrogen washout in humans
page 113 MSC-20686

NITROGEN POLYMERS
Synthesizing metal phthalocyanine imide polymers
page 105 ARC-11413

NOZZLE EFFICIENCY
Performance improvement for nonaxisymmetric nozzles
page 138 LAR-13036

NUMERICAL CONTROL
Redundant asynchronous microprocessor system
page 63 ARC-11348

High-speed computer-controlled switch-matrix system
page 60 LEW-14050

O

OPERATIONAL AMPLIFIERS
Lowering ammeter input impedance
page 55 NPO-16067

OPTICAL EQUIPMENT
Wide-angle, wide-band camera for remote imaging
page 81 NPO-15799

OPTICAL FILTERS
Altering flashlamp output for realistic solar simulation
page 82 NPO-16167

OPTICAL WAVEGUIDES
Hybrid fiber-optic/CCD chip
page 38 NPO-16030

OSCILLATIONS
Damping relaxation oscillations in laser diodes
page 45 NPO-15980

OXIDIZERS
Low-loss fuel and oxidizer injector
page 127 MFS-25989

P

PAINTS
Static-suppressing optical paint
page 107 NPO-15992

PARTICLES
Laser-assisted analysis of aerosol particles
page 86 NPO-15308

PERFLUORO COMPOUNDS
Further tests of 38 ball-bearing greases
page 111 MFS-27043

PERFORATING
Perforating thin metal sheets
page 146 ARC-11280

PERFORMANCE TESTS
Remotely piloted aircraft for research
page 143 ARC-11498

PHASE SHIFT CIRCUITS
Signal processor for multirate PSK signals
page 43 MSC-20195

PHOTOCHEMICAL REACTIONS
Nonyellowing polycarbonate for outdoor use
page 99 NPO-15836

PHOTOVOLTAIC CELLS
Spectrophotovoltaic power generation
page 78 MFS-27027

Photovoltaic-panel laminator
page 145 NPO-16092

Photovoltaics in Japan
page 57 NPO-16330

PHTHALOCYANIN
Synthesizing metal phthalocyanine imide polymers
page 105 ARC-11413

Thermosetting phthalocyanine polymers
page 91 ARC-11511

PIPES (TUBES)
Contact heat exchanger
page 117 MSC-20419

Foam insulation for cryogenic flowlines
page 96 MSC-20552

PLASTICS
Nonyellowing polycarbonate for outdoor use
page 99 NPO-15836

PLUGS
Quasi-porous plug with vortex chamber
page 133 NPO-16076

POLYCARBONATES
Nonyellowing polycarbonate for outdoor use
page 99 NPO-15836

POLYCRYSTALS
Efficient process for making polycrystalline silicon
page 104 NPO-16121

POLYESTERS
Ethynyl-terminated ester oligomers and polymers
page 107 LAR-13118

POLYMERIC FILMS
Silicone coating on polyimide sheet
page 98 GSC-12913

POLYMERIZATION
Thermosetting phthalocyanine polymers
page 91 ARC-11511

POSITION INDICATORS
Aircraft control-position indicator
page 54 LAR-12984

POSITIONING
Manipulator for heating and cooling in ultrahigh vacuum
page 80 LAR-13040

POWER CONDITIONING
Power-factor controllers: How safe?
page 57 MFS-27016

POWER LINES
Universal cable brackets
page 149 MFS-26001

PRESSURE
Simulating pressure effects of high-flow volumes
page 126 MFS-19909

PRINTING
Copyboard quickly makes clean printing plates
page 152 ARC-11365

PROPELLERS
Wingtip vortex-augmented turbopusher-propeller thrust
page 119 LAR-13019

PROTECTIVE COATINGS
Silicone coating on polyimide sheet
page 98 GSC-12913

Ceramic coatings for engine parts
page 94 NPO-16228

PULSE POSITION MODULATION
Synchronization for optical PPM signals
page 68 NPO-16256

PUMPS
Simulating pressure effects of high-flow volumes
page 126 MFS-19909

PURIFICATION
Purifying aluminum by vacuum distillation
page 96 NPO-16114

R

RADIATION DETECTORS
Protective package for a gamma-ray detector
page 72 NPO-16019

Segmented detector for cosmic gamma rays
page 82 NPO-16245

RADIATION PROTECTION
Protective package for a gamma-ray detector
page 72 NPO-16019

RANDOM ACCESS MEMORY
Dynamic-RAM data-storage unit
page 62 LEW-14017

RANGE ERRORS
Compensating for range migration in synthetic-aperture radar
page 156 NPO-15954

RAWINSONDES
Estimates of latent heat in clouds
page 85 MFS-25977

RECHARGING
Thermally-rechargeable electrochemical cell
page 78 NPO-16273

RECIPROCATION
Reciprocating magnetic refrigerator
page 130 NPO-16257

RECOVERABLE LAUNCH VEHICLES
Rocket-booster towing simulation
page 125 KSC-11289

REDUNDANT COMPONENTS
Redundant asynchronous microprocessor system
page 63 ARC-11348

REFLECTORS
Improved thick dichroic reflector for microwave feeds
page 39 NPO-13506

Self-identifying reflecting targets
page 65 NPO-16106

REFRIGERATORS
Reciprocating magnetic refrigerator
page 130 NPO-16257

REGULATORS
Back-pressure regulator for large gas flows
page 131 MSC-20536

REMOTE CONTROL
Remotely-controlled docking system
page 121 MSC-18969

Remotely piloted aircraft for research
page 143 ARC-11498

RESIDUES
Residue-measure model-reduction technique
page 156 MSC-20369

RESIN MATRIX COMPOSITES
Resin characterization in cured composite materials
page 103 LAR-13172

RESOLUTION
SAW-modulated image device
page 44 LAR-12633

RESONANT FREQUENCIES
Resistive fine tuning of resonant circuit
page 47 NPO-16276

RETAINING
Screw-retaining Allen wrench
page 148 NPO-16275

RLC CIRCUITS
Resistive fine tuning of resonant circuit
page 47 NPO-16276

RUDDERS
Mechanical mixer for rudder/braking wedge
page 141 MSC-20759

S

SAFETY
Predicting effects of impacts on confined explosives
page 111 NPO-16258

SAMPLES
Ultrahigh-vacuum sample-transfer system
page 86 LAR-12993

SCANNERS
Inspecting hollow parts with a CAT scanner
page 115 MFS-19916

SCHMIDT CAMERAS
Wide-angle, wide-band camera for remote imaging
page 81 NPO-15799

SCREWS
Screw-retaining Allen wrench
page 148 NPO-16275

SEALERS
High-performance filleting and channel sealants
page 95 ARC-1108

SELF ALIGNMENT
Remotely-controlled docking system
page 121 MSC-18969

SEMICONDUCTOR JUNCTIONS
Solar cells with multiple small junctions
page 55 NPO-16126

SEMICONDUCTORS (MATERIALS)
High-purity silicon seeds for fluidized bed silane pyrolysis
page 90 NPO-16287

SHAKING
Multishaker modal testing
page 124 MFS-27052

SHIELDING
Shielding against intense laser beams
page 97 NPO-16166

SHUTDOWNS
Spill-detector-and-shutoff device
page 129 MSC-20206

SIGNAL PROCESSING
Signal processor for multirate PSK signals
page 43 MSC-20195

SILICON
Efficient process for making polycrystalline silicon
page 104 NPO-16121

High-purity silicon seeds for fluidized bed silane pyrolysis
page 90 NPO-16287

SILICON DIOXIDE
Waterproofing agents for silica tiles
page 109 MSC-20364

SLOPES
Tiltmeter indicates sense of slope
page 40 NPO-16153

SMOKE
Continuous laminar-smoke generator
page 116 LAR-13014

SOAPS
Sensitivities of soap solutions in leak detection
page 143 MFS-19864

SODIUM SULFUR BATTERIES
Thermally-rechargeable electrochemical cell
page 78 NPO-16273

SOLAR CELLS
Photovoltaic-panel laminator
page 145 NPO-16092

Series connection of solar cells
page 145 NPO-16091

Efficient process for making polycrystalline silicon
page 104 NPO-16121

Solar cells with multiple small junctions
page 55 NPO-16126

Measuring recombination velocities in solar cells
page 36 NPO-16243

Photovoltaics in Japan
page 57 NPO-16330

SOLAR COLLECTORS
Out-of-focus alinement of solar concentrators
page 75 NPO-15563

SOLAR REFLECTORS
Environmental degradation of solar reflectors
page 88 NPO-16053

SOLAR SIMULATORS
Altering flashlamp output for realistic solar simulation
page 82 NPO-16167

SOLDERING
Series connection of solar cells
page 145 NPO-16091

SOLIDIFICATION
Variable-temperature-gradient device for solidification research
page 73 MFS-26008

SPECTRAL BANDS
Spectrophotovoltaic power generation
page 78 MFS-27027

SPECTRAL ENERGY DISTRIBUTION
Spectrophotovoltaic power generation
page 78 MFS-27027

SPECTROMETERS
Imaging spectrometer for geophysical surveys
page 76 NPO-16072

SPECTROSCOPIC ANALYSIS
Resin characterization in cured composite materials
page 103 LAR-13172

SPRAYED COATINGS
Spray application of rapidly solidified metals
page 150 GSC-12880

Ceramic coatings for engine parts
page 94 NPO-16228

STATIC ELECTRICITY
Static-suppressing optical paint
page 107 NPO-15992

STATISTICAL ANALYSIS
Simplified worst-case analysis of complex systems
page 155 MSC-20232

STIRLING CYCLE
Long-life cryogenic cooler
page 140 GSC-12697

STOCHASTIC PROCESSES
Vector Lyapunov functions for stochastic interconnected system
page 158 NPO-16170

STORAGE BATTERIES
Battery-charge-state model
page 87 NPO-16158

STRANDS
Making stronger twine with matched strands
page 148 MSC-20444

STRUCTURAL MEMBERS
Inflatable column structure
page 116 NPO-16216

STRUCTURAL STABILITY
Vector Lyapunov functions for stochastic interconnected system
page 158 NPO-16170

STRUCTURAL VIBRATION
Multishaker modal testing
page 124 MFS-27052

SUBSTRATES
Spray application of rapidly solidified metals
page 150 GSC-12880

Infrared linear imaging array
page 56 NPO-15805

SUPERCONDUCTIVITY
Superconducting-cavity accelerometer
page 120 GSC-12797

SUPPORTS
Automatic erection system for antenna masts
page 139 LAR-13115

Inflatable column structure
page 116 NPO-16216

SURFACE ACOUSTIC WAVE DEVICES
SAW-modulated image device
page 44 LAR-12633

SURFACE PROPERTIES
Reversing glass wettability
page 100 MFS-26006

SURVEYS
Imaging spectrometer for geophysical surveys
page 76 NPO-16072

SWITCHING CIRCUITS
High-speed computer-controlled switch-matrix system
page 60 LEW-14050

SYNCHRONIZATION
Synchronization for optical PPM signals
page 68 NPO-16256

Fast clock recovery for digital communications
page 53 NPO-16083

SYNTHESIS (CHEMISTRY)
Synthesizing metal phthalocyanine imide polymers
page 105 ARC-11413

SYNTHETIC APERTURE RADAR
Compensating for range migration in synthetic-aperture radar
page 156 NPO-15954

SYSTEMS ANALYSIS
Simplified worst-case analysis of complex systems
page 155 MSC-20232

T

TARGET RECOGNITION
Self-identifying reflecting targets
page 65 NPO-16106

TELECONFERENCING
Low-cost teleconference system
page 61 NPO-16057

TELEMETRY
Single-frequency multitransmitter telemetry
page 70 LAR-13006

TELEPHONES
Telephone instrument for the deaf
page 48 KSC-11303

TELESCOPES
Telescope with reflecting baffle
page 74 ARC-11502

TEMPERATURE CONTROL
Differential temperature control of electrical heaters
page 123 LAR-13047

TEMPERATURE GRADIENTS
Variable-temperature-gradient device for solidification research
page 73 MFS-26008

THERMAL EXPANSION
Fastening parts having mismatched thermal coefficients
page 137 LAR-13009

THERMAL INSULATION
Foam insulation for cryogenic flowlines
page 96 MSC-20552

Improving emittance of high-temperature insulating tile
page 108 MSC-20714

THERMAL STABILITY
Ethynyl-terminated ester oligomers and polymers
page 107 LAR-13118

THERMOCOUPLES
Differential temperature control of electrical heaters
page 123 LAR-13047

THERMOSETTING RESINS
Thermosetting phthalocyanine polymers
page 91 ARC-11511

THRUST
Wingtip vortex-augmented turbopusher-propeller thrust
page 119 LAR-13019

Performance improvement for nonaxisymmetric nozzles
page 138 LAR-13036

TILES
Waterproofing agents for silica tiles
page 109 MSC-20364

Improving emittance of high-temperature insulating tile
page 108 MSC-20714

TILTMETERS
Tiltmeter indicates sense of slope
page 40 NPO-16153

TIME DIVISION MULTIPLE ACCESS
High-speed computer-controlled switch-matrix system
page 60 LEW-14050

TOMOGRAPHY
Inspecting hollow parts with a CAT scanner
page 115 MFS-19916

TOWED BODIES
Rocket-booster towing simulation
page 125 KSC-11289

TOXIC HAZARDS
Solar-assisted oxidation of toxic cyanide
page 106 LAR-13171

TRANSDUCERS
Spring-loaded transducer holder
page 122 LAR-13048

TRANSFORMERS
High-voltage isolation transformer
page 52 GSC-12817

TRANSMISSION
Continuously variable transmission
page 128 LAR-12844

TRANSMITTERS
Single-frequency multitransmitter telemetry
page 70 LAR-13006

TRUSSES
Deployable M-braced truss
page 123 LAR-13081

TUNING
Resistive fine tuning of resonant circuit
page 47 NPO-16276

TURBINE BLADES
Inspecting hollow parts with a CAT scanner
page 115 MFS-19916

TWISTING
Making stronger twine with matched strands
page 148 MSC-20444

U

ULTRAPURE METALS
Purifying aluminum by vacuum distillation
page 96 NPO-16114

ULTRASONIC SCANNERS
Spring-loaded transducer holder
page 122 LAR-13048

V

VACUUM PUMPS
Copyboard quickly makes clean printing plates
page 152 ARC-11365

VALVES
Quasi-porous plug with vortex chamber
page 133 NPO-16076

VECTOR ANALYSIS
Vector Lyapunov functions for stochastic interconnected system
page 158 NPO-16170

VELOCITY
Measuring recombination velocities in solar cells
page 36 NPO-16243

VIBRATION
Melt stirring by horizontal crucible vibration
page 98 MFS-26005

VIBRATION DAMPING
Air bearing for small planar vibrations
page 132 MFS-26003

VIBRATION TESTS
Multishaker modal testing
page 124 MFS-27052

VIDEO DATA
Low-cost teleconference system
page 61 NPO-16057

VIDEO EQUIPMENT
Storing data and video on one tape
page 59 MSC-20705

VISION
Vision screening by color photography
page 112 MFS-25800

VOLT-AMPERE CHARACTERISTICS
Fast-recovery high-voltage power diode
page 49 LEW-14036

VORTICES
Wingtip vortex-augmented turbopusher-propeller thrust
page 119 LAR-13019

W

WARNING SYSTEMS
Cutthrough warning circuit
page 142 MFS-19900

WATERPROOFING
Waterproofing agents for silica tiles
page 109 MSC-20364

WAVEGUIDES
Improved thick dichroic reflector for microwave feeds
page 39 NPO-13506

WEATHERING
Environmental degradation of solar reflectors
page 88 NPO-16053

WETTABILITY
Reversing glass wettability
page 100 MFS-26006

WHEELCHAIRS
Flux coupling for wheelchair battery chargers
page 43 NPO-16269

WIND TUNNEL TESTS
Continuous laminar-smoke generator
page 116 LAR-13014

WINDMILLS (WINDPOWERED MACHINES)
Hinged-blade, vertical-shaft windmill
page 134 MFS-25980

WRENCHES
Screw-retaining Allen wrench
page 148 NPO-16275

X

X RAY TELESCOPES
Nearly anastigmatic X-ray telescope
page 77 MFS-25984

Participate in
Space Station and Related Space Programs with Vitro Corporation

Challenging Career Opportunities Available in:

- Systems Engineering
- Systems Integration
- Maintainability Planning
- Data Management
- Logistics Management
- Test and Evaluation
- Information Systems
- Operational Support

Please call Amon Bridges at (301) 231-1146 or (800) 782-1517 or send resumes to:

Vitro CORPORATION
Vitro Corporation
14000 Georgia Avenue
Silver Spring, MD 20910
AN EQUAL OPPORTUNITY EMPLOYER M/F/H
U.S. CITIZENSHIP REQUIRED

Circle Reader Action No. 36

Are You a Subscriber?

The most relied-upon "intelligence/communications" network serving the aviation/aerospace industry worldwide.

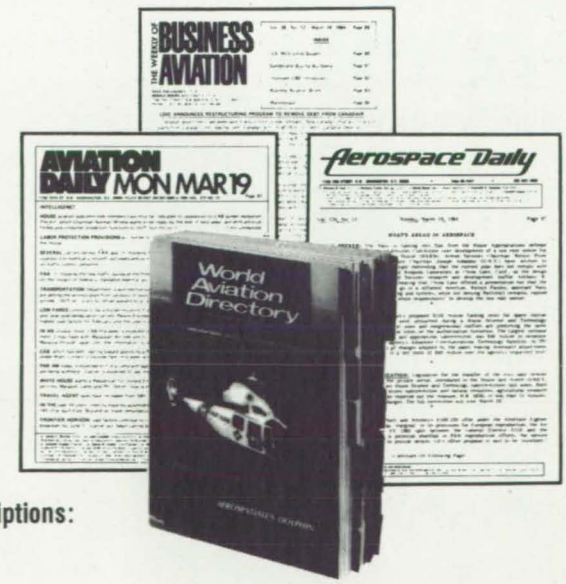

Write on company letterhead or call for FREE trial subscriptions:

- 3 weeks of Aerospace Daily
- 30 day inspection of World Aviation Directory
- 3 weeks of Aviation Daily
- 4 weeks of Business Aviation
- Plus 1 month test of Aerospace Online*

*Aerospace Daily is now on-line as part of a comprehensive network of electronic databases called **Aerospace Online.** Call 202-822-4691 for a one month test at only a nominal cost.

1156 15th St., NW • Washington, DC 20005 • 202-822-4600

Letters

A new feature of *NASA Tech Briefs* is a letters column. The editors would like it to be a wide exchange of ideas among our readers. To start the column we are printing a few of the thousands of requests NASA has received in the last several months. To make it easy we added additional feedback cards in this issue. Use them for comments or to add information to a colleague's request for aid. While we can only print a small number, we will endeavor to select letters for the column that are varied and of wide interest.

ION THRUSTERS

I am seeking information on ion propulsion technology; specifically "ion thrusters" in the 1000-2000 ev energy range. I understand NASA has done this work with Case Western Reserve University.

Archie Woodworth
Program Manager
Travenol Labs
Round Lake, IL

The following publications are available from American Institute of Aeronautics (AIAA), Technical Information Service, 555 W. 57th St., New York, NY 10019:
A83-12511, *Qualification Test Results of IAPS 8 cm Ion Thrusters*; A83-12503, *RFI and ECH Plasma Generator Development For Ion Thrusters*; A82-15438, *Measuring The Spacecraft and Environmental Interactions of the 8-cm Mercury Ion Thrusters on the P80-1 Mission.*

The following documents are available from the National Technical Information Service (NTIS), 5285 Port Royal Road, Springfield, VA 22161:
N84-18322, *Sputtering Phenomena in Ion Thrusters*; N84-10180, *Development of Advanced Inert-Gas Ion Thrusters*; N83-28072, *High Frequency Plasma Generators for Ion Thrusters*; N83- 25779, *Endurance Test of a 30-CM-Diameter Engineering Model Ion Thruster. Task 12: Investigation of Thin-Fill Erosion Monitors for ION Thrusters*; N83-22318, *Design, Fabrication, and Testing of Porous Tungsten Vaporizers for Mercury Ion Thrusters*; N83-14159, *Analysis and Design of Ion Thrusters for Large Space Systems*; N82-12133, *Retrofit and Acceptance Test of 30-cm Ion Thrusters.*

Write to AIAA and NTIS directly to inquire about costs and mailing arrangements. For extensive literature search services in your area of interest, you may wish to contact the NASA Industrial Applications Center nearest you. These Centers offer computerized access to a comprehensive collection of scientific and technical documents produced by NASA, by other government agencies, and by corporate and academic research organizations around the world. Each Center also has a professional staff that can help you evaluate your information needs and assist you with solutions to specific technical problems.

HEAVY METAL REMOVAL

Would like to see items concerning removal of heavy metals from waste streams.

Victor J. Obrig
Foundry Technical Director
American International
Manufacturing Corp.
Fort Worth, TX

NTIS (see above) has the following: N84-17323, *Pilot System for the Purification of Rinse Water and for the Recuperation of Metals in Electroplating Companies. Pilot System Metal Recovery from Waste Water*; N79-17747, *Process for Purification of Waste Water Produced by a Kraft Process Pulp and Paper Mill*; N78-234310, *Application of Activated Coal for the Purification of a Multiple Component Chemical Waste Water*; N74-33858, *Waste-Product Pollution of Bodies of Water and Waste Water Purification*; N74- 21733, *On Waste Product Loading of Waters and Waste Water Purification.*

POWER-FACTOR CONTROLLERS

The TSP's regarding motor power-factor controllers allowed us to evaluate several vendors of these devices. Also, the TSP's helped us to establish that PFC's were a valid energy saving device. We have purchased and installed several, representing considerable savings on over-rated motors.

Tom Miller
Senior Engineer
Allied Bendix Aerospace
Fort Lauderdale, FL

Not only does NASA Tech Briefs appreciate your comments, but we are sure the Department of Energy echoes our sentiments.

PHOTOGRAPHIC & IMAGING TECHNOLOGY

I would like to see articles presented on the following: photographic & imaging technology re: optics, film, chemistry. Also more attention devoted to television signal distribution, video switching & control, TV cameras, scan-conversion techniques, etc. Please send index on this if available. Thanks,

Anthony R. Kaseta
Engineering Staff
Crosspoint Latch Corporation
Clark, NJ

continued on page 167

PRECISION FABRICATED
Ceramics
Aluminum Oxide: 96% 99% 99.5% pure
Aluminum Silicate — Silicon Nitride — Boron Nitride — Corning Macor®
With emphasis on precision; standard tolerances of ± .0025" or ½% (whichever is greater) can be achieved, while closer tolerances of ± .0001" are available through diamond grinding, lapping and polishing.

- INSULATORS
- CRUCIBLES
- COMPONENTS
- FIXTURES
- SEAL RINGS
- NUCLEAR PARTS
- BIOMEDICAL DEVICES
- WIRE GUIDES
- VALVE HOUSINGS
- COIL FORMS
- HEAT SHIELDS
- HEAT SINKS

Consult our Technical Staff for Design and Materials Recommendations

Duramic
PRODUCTS, INC.
P.O. Box 426, 426 Commercial Avenue, Palisades Park, New Jersey 07650 U.S.A. (201) 947-8313
TWX 710-991-9632

Mission Accomplished

NASA and new technology go hand-in-hand. As its projects become increasingly sophisticated, so do its demands for technological innovation. Often, systems, methods and devices pioneered for NASA are re-applied in the private sector, obviating duplicate research and fostering productivity. The "space block," developed for the Space Shuttle program, is one example of NASA technology finding re-application in private industry.

In this age of the computer, it would seem unlikely that models for American automobiles are still made of wood. Yet, by and large, this is the case: based on computer-generated designer specifications, models are hand-made of laminated Cativo wood.

This time-consuming process is currently being revolutionized with the aid of a material developed by Ren Plastics, a subsidiary of CIBA-GEIGY Corporation, East Lansing, Michigan. Ren devised the material in response to Space Shuttle prime contractor Rockwell International's need for a model material with which to test their numerically-controlled (NC) machines—digitally instructed precision cutting machines programmed to fashion the 30,000 individual heat-shield tiles which cover the shuttle.

Rockwell's selection of a polyurethane foam material had been overruled by both NASA and OSHA, who cited the foam's potential combustibility, and the cost of using the actual tile material—a special form of silica—for testing the NC programs was prohibitive. Suggestions from twenty-seven companies for use of existing materials proved unacceptable, and out of that field Ren alone agreed to undertake the necessary research and development to create a new master model material which would meet both safety and design specifications.

The successful material—technically known as the TDT-177-51 Ren Shape™ epoxy model block, and more familiarly as the "space block"—exceeded even Rockwell's expectations by allowing further refining of NC programs, thereby enhancing the machines' productivity.

After its initial success, the Ren Shape, which consists of a newly formulated epoxy resin filled with minute glass globules, began attracting the attention of companies in a number of industries where the high costs of materials and labor inherent in traditional modeling processes were under scrutiny.

In response, Ren developed and marketed the Ren Shape line of master materials—epoxy blocks and boards which can be sawed, sanded, carved or machined for use in commercial applications.

A variety of industries are currently using the Ren Shape line in their precision modeling processes, among them the foundry, toy, vacuum-forming, aerospace and automotive industries.

Visioneering, a Fraser, Michigan company which produces master models for both U.S. and European automobile companies, and a number of U.S. aerospace companies, currently uses the Ren Shape line in place of wood, urethane and other traditional modeling materials. Visioneering has determined that Ren Shape boards take 10 percent less time to machine and finish than wood, and the company is pleased with the material's dimensional stability. (Unlike wood, the epoxy resin does not "grow" when subjected to extreme temperature or humidity.)

Visioneering's clients, particularly European automobile manufacturers who use their models for up to ten years, are pleased with the new modeling material, and American manufacturers, who typically replace their models annually, are exploring the use of epoxy modeling materials in their efforts to streamline production processes.

Now that the time-honored practice of making models out of wood has met its technological match, it's probably safe to say that Ren Plastics has created the shape of things to come.

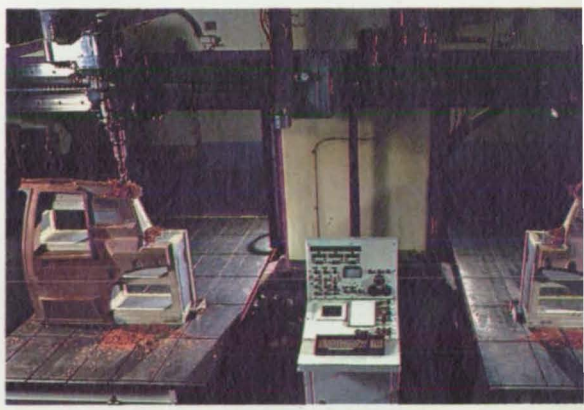

At left, a Visioneering engineer checks tolerances for an autohood model made from Ren epoxy resin model material. The new material was originally developed for modelling Space Shuttle thermal tiles. Above, Visioneering's numerically-controlled Duplex Milling Machine cuts model parts from Ren Shape boards. The Ren Shape line is attracting private sector interest as a replacement for traditional modeling materials used in automobile, aerospace and foundry industries.

ABOUT THE NASA TECHNOLOGY UTILIZATION PROGRAM

Thumb Index

NASA TU Services

New Product Ideas

Electronic Components and Circuits

Electronic Systems

Physical Sciences

Materials

Life Sciences

Mechanics

Machinery

Fabrication Technology

Mathematics and Information Sciences

Subject Index

This document was prepared under the sponsorship of the National Aeronautics and Space Administration. *NASA Tech Briefs* is published quarterly and is free to engineers in U.S. industry and and to other domestic technology transfer agents. It is both a current-awareness medium and a problem-solving tool. Potential products...industrial processes...basic and applied research...shop and lab techniques...computer software...new sources of technical data...concepts...can be found here. The short section on New Product Ideas highlights a few of the potential new products contained in this issue. The remainder of the volume is organized by technical category to help you quickly review new developments in your areas of interest. Finally, a subject index makes each issue a convenient reference file.

Further information on innovations—Although some new technology announcements are complete in themselves, most are backed up by Technical Support Packages (TSP's). TSP's are available without charge and may be ordered by simply completing a TSP Request Card, found at the back of this volume. Further information on some innovations is available for a nominal fee from other sources, as indicated. In addition, Technology Utilization Officers at NASA Field Centers will often be able to lend necessary guidance and assistance.

Patent Licenses—Patents have been issued to NASA on some of the inventions described, and patent applications have been submitted on others. Each announcement indicates patent status and availability of patent licenses if applicable.

Other Technology Utilization Services—To assist engineers, industrial researchers, business executives, Government officials, and other potential users in applying space technology to their problems, NASA sponsors Industrial Applications Centers. Their services are described on pages 28-30. In addition, an extensive library of computer programs is available through COSMIC, the Technology Utilization Program's outlet for NASA-developed software.

Applications Program—NASA conducts applications engineering projects to help solve public-sector problems in such areas as safety, health, transportation, and environmental protection. Two applications teams, staffed by profesionals from a variety of disciplines, assist in this effort by working with Federal agencies and health organizations to identify critical problems amenable to solution by the application of existing NASA technology.

Reader Feedback—We hope you find the information in *NASA Tech Briefs* useful. A reader-feedback card has been included because we want your comments and suggestions on how we can further help you apply NASA innovations and technology to your needs. Please use it; or if you need more space, write to the Manager, Technology Transfer Division, P.O. Box 8757, Baltimore/Washington International Airport, Maryland 21240.

Advertising Reader Service—Reader Action Card (RAC): For further information on the advertisers, please circle the RAC number on the separate Reader Action Card in this issue.

Change of Address—If you wish to have *NASA Tech Briefs* forwarded to your new address, use the Subscription Card enclosed at the back of this volume of *NASA Tech Briefs*. Be sure to check the appropriate box indicating change of address, and also fill in your identification number (T number) in the space indicated.

This document was prepared under the sponsorship of the National Aeronautics and Space Administration. Neither Associated Business Publications, Inc., nor anyone acting on behalf of Associated Business Publications, Inc., nor the United States Government nor any person acting on behalf of the United States Government assumes any liability resulting from the use of the information contained in this document, or warrants that such use will be free from privately owned rights. The U. S. Government does not endorse any commercial product, process, or activity identified in this publication.

Letters continued from page 164

Enclosed are indexes for *NASA Tech Briefs* 1976-1980. If, after looking through the indexes, you wish to order individual Tech Briefs or additional supporting information, you may do so.

SUBSCRIPTIONS

Having borrowed a copy from someone in another division, I would like to receive a subscription to this publication.
W. M. Kelly
Principal Design Engineer
Boeing Aerospace Co.
Seattle, WA

Any engineer, researcher, or person involved in new product development wishing a personal copy of *NASA Tech Briefs* can receive a subscription by returning one of the bound-in cards for new subscriptions. A qualification questionnaire will be sent by return mail. In addition, whenever space is available a copy of the questionaire will be included in copies of *NASA Tech Briefs*.

Classifieds

Classified advertising rates and specifications are as follows: Set in 6 point light type face, with up to five words at beginning of copy in bold caps. Count box numbers as six words.

50 words or less ..... $ 125
100 words ..... $ 175

Check or money order must accompany order to: Classified Advertising Manager, NASA Tech Briefs, Suite 921, 41 East 42nd Street, New York, NY 10017-5391.

HIGH QUALITY DISPLAY MODELS. Reasonably priced, completely finished, solid aerospace models with highly detailed markings. Mounts on beautiful wooden stand. Choose from NASA Space Shuttles, 747's w/orbiter, X-29A, XB-70, X-1, B-1B, SR-71, F-15, B-52, B-17 and many more. Start your collection now! Perfect for your home or office. For brochure send self-addressed, stamped envelope or call Toys and Models Corp., P.O. Box 8, Bergen Field, NJ 07621; (201) 384-4014.

A "LITTLE" KNOWLEDGE is a dangerous thing—in the business world. Obtain profitable monthly information from the publication which monitors the Space Business: *AEROSPACE BUSINESS REVIEW*. Only $95/year. Complimentary copy on request. *Aerospace Business Review*, 76 Larkspur Ave., Merrick, NY 11566.

SPACE
THE NEW FRONTIER

The Equity Research Department of Shearson Lehman/American Express Inc.

and

The Center for Space Policy, Inc.

advisors to the U.S. Government and Industry are pleased to announce

SPACE

the first monthly analysis of commercial investment opportunities in space.

The financial expertise of SHEARSON LEHMAN/AMERICAN EXPRESS and the special knowledge of THE CENTER FOR SPACE POLICY have teamed to offer a totally new investment service, to help investors evaluate these and other opportunities in this New Frontier.

For information contact: James P. Samuels, Shearson Lehman/American Express, 2 World Trade Center, New York, NY 10048, (212) 321-5722 or Brad M. Meslin/David Lippy, CENTER FOR SPACE POLICY, INC. 1972 Massachusetts Avenue, Cambridge, MA 02140, (617) 576-2266/2828

Circle Reader Action No. 37

Advertiser's Index

Amoco Chemical Corporation	(RAC 1*)	16-19
BEI Motion Systems Corp./Digital Products	(RAC 2)	89
Center for Space Policy	(RAC 37)	167
Control Data Corporation	(RAC 4)	27
Data General/Federal Systems	(RAC 38)	41
Du Pont - KAPTON	(RAC 5,21,22)	95,97,99
Duramic Products Inc.	(RAC 24)	164
Emerson & Cuming	(RAC 26)	92-93
EMR Photoelectric	(RAC 25)	159
Fairchild Control Systems	(RAC 6)	25
The Fisher Pen Company	(RAC 7)	37
GAF Corporation	(RAC 8)	15
General Electric Company, Space Systems Division	(RAC 9)	Cov.II-1
Honeywell Inc. Space and Strategic Avionics Division	(RAC 27)	168, Cov.III
Hughes Aircraft Co.		153
IBM/Federal Systems	(RAC 10)	8-9
Interstellar Communications Corp.	(RAC 35)	6
Klinger Scientific Corp.	(RAC 11)	34
Lockheed Missiles & Space Company	(RAC 12)	158
McDonnell Douglas	(RAC 23,15)	33,Cov.IV
Motorola Inc./Government Electric Group	(RAC 14)	12-13
Outer Space Laboratories, Inc.	(RAC 32)	6
Pioneer Electric/Research Corp.	(RAC 16)	167
Pressure Systems Inc.	(RAC 17)	26
Rockwell International Corporation	(RAC 18)	4-5
Rockwell International Corporation/Rocketdyne Division	(RAC 29)	21
Shearson Lehman/American Express	(RAC 37)	167
Space Genetics Research Corporation	(RAC 33)	6
Space Metallurgy, Inc.	(RAC 31)	6
Space Shuttle Cargo Corporation	(RAC 34)	6
Vitro Corporation	(RAC 19,36)	2,163
World Aviation Directory		163
Wyle Laboratories	(RAC 20)	35
Zero Gravity Enterprises, Inc.	(RAC 30)	6

***RAC** stands for **Reader Action Card.** For further information on these advertisers, please circle the RAC number on the Reader Action Card elsewhere in this issue. This index has been compiled as a service to our readers and advertisers. Every precaution is taken to ensure its accuracy, but the publisher assumes no liability for errors or omissions.

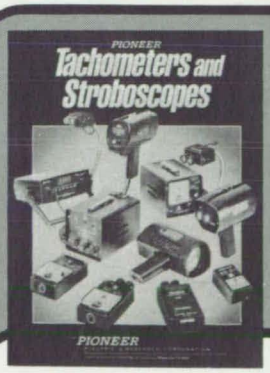

PIONEER PHOTOELECTRIC
Tachometers and Stroboscopes

FREE CATALOG

A fully illustrated catalog details complete line of photoelectric tachometers and stroboscopes. Instruments require no wires or mechanical connections to give touchless rpm measurements accurate to ±1 RPM. Catalog describes portable, battery powered units capable of speeds up to 50,000 rpm, remote reading up to 100 feet away, and ac-powered units for continuous measurement of speeds to 50,000 rpm. Pioneer Stroboscopes can be used to study machine behavior or used as an electronic tachometer. Tachometers and stroboscopes are available with digital or analog readout. Complete line of Pioneer accessories is also described.

Send for your free copy today!

THE **PIONEER**
ELECTRIC & RESEARCH CORPORATION
743 Circle Avenue • Forest Park, Illinois 60130 / Phone 312/771-8242

Circle Reader Action No. 16

Honeywell, Martin Marietta and Orbital to create a new privately financed

Commercial Space

In the early 1960's, Honeywell pioneered Ring Laser Gyro technology. Now we are working together with Orbital Sciences Corporation and Martin Marietta to pioneer the opening of space as a commercial frontier.

Orbital Sciences Corporation (OSC) recognized that something could be done to reduce the high cost of space transportation. So they developed a vehicle with Martin Marietta for the purpose of low cost, highly reliable commercial space transportation.

Reliability

OSC, as the entrepreneurial firm responsible for making this project a success, needed team members who would be able to perform to the extreme demands of technical challenge, fixed cost and on-time delivery with a system that worked the first time. And every time.

That's why OSC and Martin Marietta came to Honeywell. We have demonstrated 25 years of

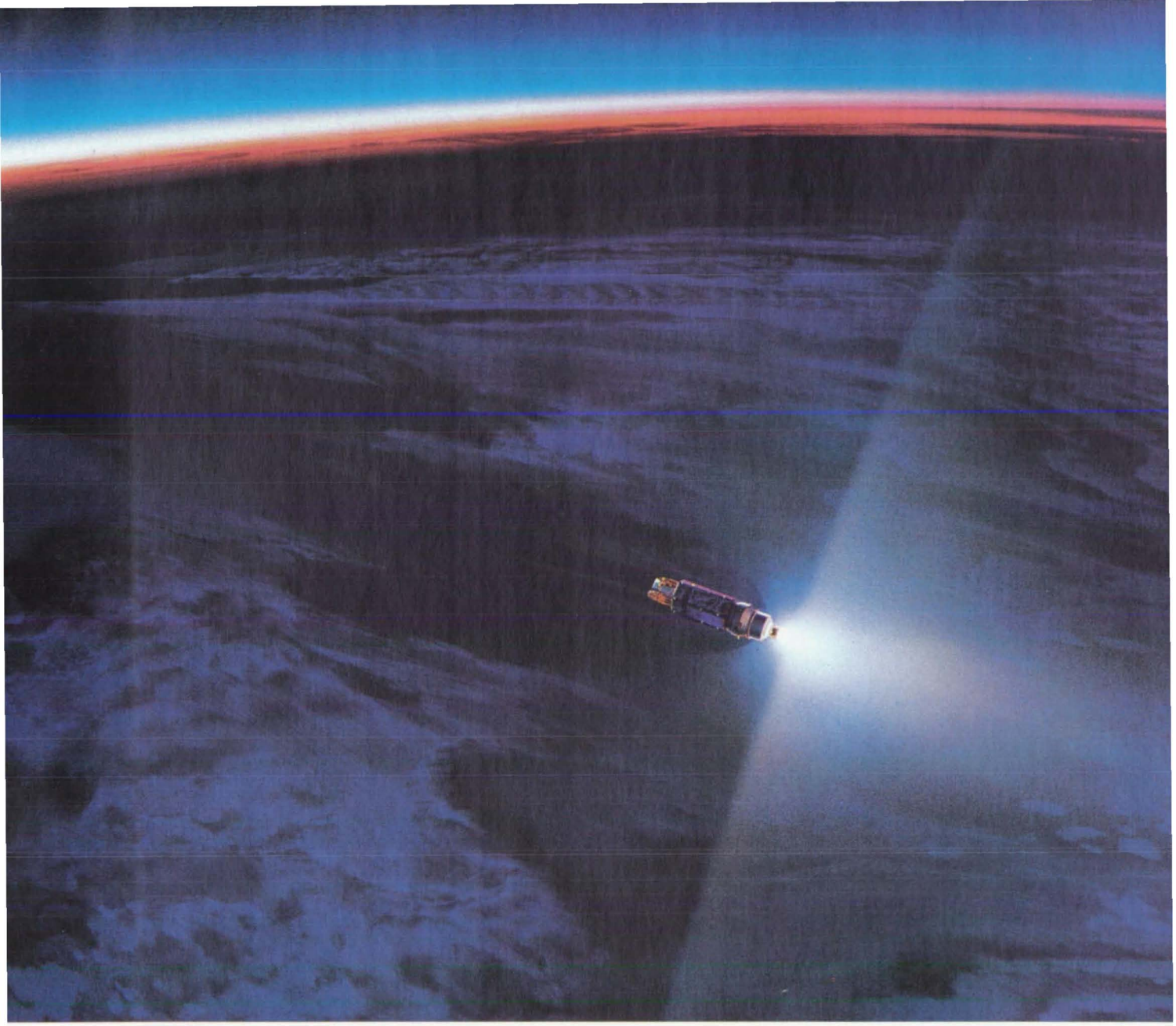

Sciences Corporation are working together commercial space vehicle.

reliable high performance on virtually every major American space program. From Project Mercury to the Space Shuttle, Honeywell reliability has been a part of over 740 flights into space. The selection of Honeywell's Ring Laser Gyro technology was based on its low cost, exceptional performance capabilities, and its highly reliable operation in over 1500 Laser Inertial Navigation Systems (LINS).

Teamwork

If you would like to know more about our work with Orbital Sciences Corporation and Martin Marietta or how we could work with you, contact: Larry N. Speight, Space and Strategic Avionics Division, 13350 U.S. Highway 19 South, Clearwater, Florida 33546. Phone 813/539-5502.

Together, we can find the answers.

Honeywell

©1985 Honeywell Inc.
Above photo used with permission of Orbital Sciences Corporation ©1984 Orbital Sciences Corporation

Circle Reader Action No. 27

THE WORLD NEEDS A PLACE LIKE NO PLACE ON EARTH—NASA SPACE STATION.

A manned space station will offer governments, industries and people opportunities that cannot be matched on Earth.

It will make possible technology advances held back by Earth's limitations. The space environment offers a weightless, vibrationless, moistureless, soundless vacuum in and with which to work; an obstruction-free perspective for scanning our planet and a host of other out-of-this-world advantages.

A manned space station makes good business sense. A space station can revolutionize medicine, metallurgy, communications, energy generation, meteorology and dozens of other sciences and technologies—ones that exist now, and new ones a space station can help create.

A manned space station will help promote understanding. It will offer the people of the world an opportunity to unite in peaceful enterprise.

And a manned space station will help America maintain its momentum in space science and exploration.

An experienced team.

We have teamed with Honeywell, IBM and RCA for a major segment of a NASA contract for definition and preliminary design of the manned space station. And already we're developing the pharmaceutical technologies and the production factories that will find their full potential in the space station environment.

At McDonnell Douglas, our capabilities are focused on making a space station a reality by the next decade—and we offer exciting opportunities to companies and the men and women in them who want to help.

Because the world needs a place like no place on Earth.

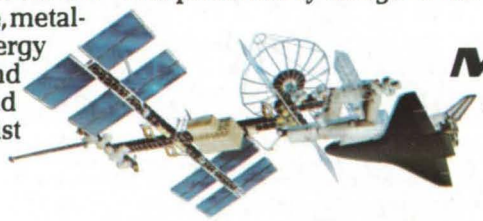

MCDONNELL DOUGLAS

©1984, McDonnell Douglas Corporation